

Novel ACM Mouse Model Derived From a Human Desmoplakin Variant Displays a Cardiac
Phenotype Upon Stress

Dissertation

Presented in Partial Fulfillment of the Requirements for the Degree Doctor of Philosophy
in the Graduate School of The Ohio State University

By

Tyler Lewis Stevens, M.S.

Molecular, Cellular and Developmental Biology

The Ohio State University

2022

Dissertation Committee

Dr. Peter J. Mohler, Advisor

Dr. Federica Accornero

Dr. Brandon Biesiadecki

Dr. Thomas Hund

Dr. Maegen Borzok

Copyrighted by
Tyler Lewis Stevens
2022

Abstract

Arrhythmias account for approximately 250,000 deaths in the U.S annually, with nearly half being associated with heart disease. Arrhythmogenic disorders are broken down into a variety of subcategories, with the vast majority being primarily caused by either activity changes or variants in ion channels/exchangers. Arrhythmogenic cardiomyopathy (ACM) is a unique form of heart disease that is primarily hereditary, where variants in genes encoding structural proteins are the most frequent cause of disease formation. Variants within desmosomal genes are one of the leading predisposing factors to ACM, primarily characterized by fibro-fatty infiltration in the ventricular myocardium with an increased propensity for ventricular arrhythmias. This frequently results in sudden cardiac death, even prior to the detection of any cardiac structural abnormalities. Previous work on a familial ACM variant in desmoplakin (*DSP*) (p.R451G) identified a post-translational degradation of DSP that stemmed from increased sensitivity to the protease calpain, a pattern identified in additional pathogenic variants. Despite these findings, incomplete penetrance within most familial ACM cases complicates understanding of the associated molecular pathways, as well as determining the external factors that contribute to disease development. While the generation of murine models have significantly contributed to the understanding of disease progression, most utilized knock-out or transgenic techniques, limiting the potential translational impact. Our group has developed one of the first mouse models of ACM derived from a human variant by introducing the murine equivalent of the R451G variant into endogenous desmoplakin (*Dsp*^{R451G/+}). Mice homozygous for this variant displayed embryonic lethality. While *Dsp*^{R451G/+} mice were viable with reduced

expression of DSP, no presentable arrhythmogenic phenotype was identified at baseline. Following acute stress through catecholaminergic challenge, *Dsp*^{R451G/+} mice displayed more frequent and prolonged arrhythmias compared to their control littermates. Chronic stress using pressure overload resulted in reduced cardiac performance, increased chamber dilation, and more rapid progression to heart failure in the *Dsp*^{R451G/+} mice. Finally, localization patterns in a key protein associated with DSP, connexin-43, were identified in the *Dsp*^{R451G/+} cardiac tissue. In summary, this model displays a phenotype only following cardiac stress, suggesting this model may be a useful tool for understanding the influences of environmental factors on disease penetrance. Further evaluation of variants of unknown pathogenicity within an N-terminal mutation hotspot of *DSP* determined calpain sensitivity may be a shared mechanism in DSP variants, which can be a predictor model for those of unknown pathogenicity. These studies highlight the need for personalized medicine based on the phenotypic variability among patients with different variants, and even among those in the same family.

Dedication

I dedicate my dissertation work to my loving family. I am eternally grateful to my parents Karen and Daniel Stevens, who have been instrumental in the development of my academic career, and continuously provided emotional support throughout my life. My older brother Eric was my best friend growing up and a strong motivator to continue pursuing my educational goals. His children, Olivia, Eli, and Isabella, as well as my younger sister Jassmine King, were joys that pushed me to better myself, and inspired me to become a better role model and a mentor. I give a special thanks to all my extended family in Kentucky and Illinois that continued to provide me with support.

I would also like to dedicate my dissertation work to my four closest friends, Trevor Dew, Jacob Longenecker, Eric Suttman, and Connor Tyree, as well as my lovely cat Boomer Jr. They each played a tremendous role either inside or outside my academic career that significantly improved my experience during my graduate career.

Finally, I would like to dedicate my scientific growth to two incredible scientists, Dr. Juyle Adams and Dr. Erin Strome, who were essential to the development of my scientific career during my high school and undergraduate years respectively. Without them, and all my friends and family, I would not be the scientist I am today.

Acknowledgments

I would first like to acknowledge my advisors Maegen Ackermann and Peter Mohler, both of who displayed great ability to lead, provide with feedback and direction on my project, and developed my critical thinking skills to improve myself as a scientist. In the Ackermann lab, Maegen and Heather Manring both guided me on my project early on and helped me development into an independent thinker, strengthen my work ethic, and provided many great memories that made me feel wanted.

Upon Maegen's departure from the university, Peter Mohler, who I previously rotated with, showed great kindness in allowing me to continue my project in his lab. He continually motivated me during my graduate career, and pushed me to face through adversity, from job interviews to the global pandemic.

I would like to acknowledge the entirety of the Mohler lab for welcoming me with open arms, both becoming essential for my development as a scientist and assisting with experiments, as well as becoming my closest friends that made graduate school enjoyable. Particular thanks goes to Mona El Refaey and Sara Koenig, who were both mentors I looked up to that were essential for my success, and provided guidance through my years in the lab. I would also like to acknowledge my committee members Federica Accornero Brandon Biesiadecki, and Thomas Hund, each member providing me with appreciated feedback and advice that was necessary in my preparations for my future career goals.

Vita

2013.....Scott County High School, Georgetown KY
2017.....B.S, Biological Sciences at Northern
Kentucky University
2019.....M.S, Biology at The Ohio State University
2017 to Present.....Graduate Research Associate, Department
of Physiology and Cellular Biology, The
Ohio State University

Publications

Ng, R.,[#] Manring, H.R.,[#] Papoutsidakis, N., Albertelli, T., Tsai, N., See, C., Li, X., Park, J., **Stevens, T.L.**, Bobbili, P.J., Riaz, M., Ren, Y., Janssen, P.M.L., Bunch, T.J., Hall, S.P., Lo, Y-C., Jacoby, D.,** Qyang, Y.,** Wright, N.,** Ackermann, M.A.,** Campbell, S.,** “Patient mutations linked to arrhythmogenic cardiomyopathy enhance calpain-mediated desmoplakin degradation.” JCI Insight. 2019.

Stevens TL, Wallace MJ, Refaey ME, Roberts JD, Koenig SN, Mohler PJ. Arrhythmogenic Cardiomyopathy: Molecular Insights for Improved Therapeutic Design. J Cardiovasc Dev Dis. 2020 May 26;7(2):21. doi: 10.3390/jcdd7020021. PMID: 32466575; PMCID: PMC7345706.

Stevens T.L., Adelman S., Sturm.A.C., Hoover C.A., Borzok M.A., El Refaey M., Mohler P.J. (2021) Molecular Pathways and Animal Models of Arrhythmias. In: Rickert-Sperling S., Kelly R., Driscoll D. (eds) Congenital Heart Diseases: The Broken Heart.

El Refaey M, Coles S, Musa H, **Stevens TL**, Wallace MJ, Murphy NP, Antwi-Boasiako S, Young LJ, Manring HR, Curran J, Makara MA, Sas K, Han M, Koenig SN, Skaf M, Kline CF, Janssen PML, Accornero F, Borzok MA, Mohler PJ. Altered Expression of Zonula occludens-1 Affects Cardiac Na⁺ Channels and Increases Susceptibility to Ventricular Arrhythmias. *Cells*. 2022 Feb 14;11(4):665. doi: 10.3390/cells11040665. PMID: 35203314; PMCID: PMC8870063.

Stevens TL, Manring HR, Dew T, Wallace MJ, Papaioannou P, Argall A, Antwi-Boasiako S, Xu X, Campbell SG, Akar FG, Borzok MA, Hund TJ, Mohler PJ, Koenig SN, El Refaey M. Humanized *DSP* ACM Mouse Model Displays Stress-induced Cardiac Electrical and Structural Phenotypes, *frontiers in cardiovascular medicine*. Submitted 6/15/2022; In Revision 7/8/2022

Fields of Study

Major Field: Molecular Cellular and Developmental Biology

Table of Contents

Abstract.....	ii
Dedication.....	iv
Acknowledgments.....	v
Vita.....	vi
List of Tables	x
List of Figures.....	xi
Chapter 1. Introduction	1
1.1 Normal cardiac conduction and the action potential	1
1.2 Disruption of normal electrical signaling and the formation of cardiac arrhythmias	4
1.3 Role of intercalated discs and desmosomes.....	8
1.4 Function of desmoplakin and its connection to arrhythmogenic cardiomyopathy	15
1.5 Cluster of desmoplakin variants display increased sensitivity to the protease calpain.....	23
1.6 Summary.....	27
Chapter 2. Arrhythmogenic Cardiomyopathy: Molecular Insights for Improved Therapeutic Design	30
2.1 Abstract.....	30
2.2 Introduction- Arrhythmogenic Cardiomyopathy	31
2.3 Genetics and Animal Models of Arrhythmogenic Cardiomyopathy	33
2.3.1 Desmosomal Genes	36
2.3.2 Non-Desmosomal Genes.....	47
2.3.3 Additional ACM Models.....	56
2.4 Environmental Factors.....	58
2.4.1 Exercise.....	58
2.4.2 Additional Factors.....	61
2.5 Clinical Management of Arrhythmogenic Cardiomyopathy	61
2.5.1 Risk Stratification for SCD and Implantable Cardioverter–Defibrillator (ICD) Placement	64
2.5.2 Anti-Arrhythmic Medications	66
2.5.3 Catheter Ablation	67
2.5.4 Sympathectomy.....	68
2.5.5 Heart Transplant.....	69
2.6 Future Implications.....	69

Chapter 3. Humanized <i>DSP</i> ACM Mouse Model Displays Stress-induced Cardiac Electrical and Structural Phenotypes	72
3.1 Abstract.....	73
3.2 Introduction	74
3.3 Materials and Methods	76
3.4 Results	81
3.4.1 Homozygous <i>DSP</i> p.R451G knock-in mice display embryonic lethality	81
3.4.2 <i>Dsp</i> ^{R451G/+} mice do not display changes in cardiac structure or function at baseline....	87
3.4.3 <i>Dsp</i> ^{R451G/+} mice do not display electrical abnormalities at baseline.....	89
3.4.4 <i>Dsp</i> ^{R451G/+} mice display accelerated heart failure following pressure overload.....	90
3.4.5 <i>Dsp</i> ^{R451G/+} mice display stress-induced arrhythmias	95
3.4.6 <i>Dsp</i> ^{R451G/+} mice display normal localization of key ID proteins but altered distribution of Cx43.....	97
3.5 Discussion.....	101
Chapter 4. Calpain Sensitivity may be a Predictor of Disease for <i>DSP</i> Variants of Unknown Pathogenicity	106
4.1 Abstract.....	106
4.2 Introduction	107
4.3 Materials and Methods	110
4.4 Results	112
4.4.1 Desmoplakin UP variants surround the calpain target site primarily in the SR4 domain	112
4.4.2 Select UP variants disrupt important interactions within the calpain target site	115
4.4.3 Exposure of the calpain target site is not influenced by most UP variants	118
4.4.4 Calpain sensitivity detected in the majority of UP variants <i>in vitro</i>	120
4.5 Discussion.....	123
Chapter 5. Discussion	127
References.....	139
Appendix A. Chapter 2 Tables.....	174
Appendix B. Chapter 3 Tables.....	176
Appendix C. Chapter 4 Tables.....	179

List of Tables

Table 1: A list of all genes linked to ACM/ARVC.....	174
Table 2: Full list of echocardiographic findings from <i>Dsp</i> ^{R451G/+} mice and control littermates...	176
Table 3: ECG findings from conscious mice without anesthetic or catecholaminergic stimulation.	178
Table 4: DSP variant distance from calpain target site.....	179
Table 5: Calpain targeting prediction values for each pathogenic and UP DSP variants.	180

List of Figures

Figure 1: Cardiac action potential.....	2
Figure 2: Diagram of the different ID components.....	12
Figure 3: N-terminal diagram of DSP and mammalian sequence homology	19
Figure 4: Schematic of ACM-associated proteins	35
Figure 5: ACM-linked variant distribution among desmosomal genes	37
Figure 6: Schematic overview of the R451G mouse model	83
Figure 7: Genotyping analysis of the DSP R451G ⁺ mouse model.....	84
Figure 8: <i>Dsp</i> ^{R451G/+} mice display a reduction in DSP protein expression	86
Figure 9: <i>Dsp</i> ^{R451G/+} mice display a reduction in DSP protein expression at different timepoints	87
Figure 10: <i>Dsp</i> ^{R451G/+} mice display no structural changes at baseline	88
Figure 11: <i>Dsp</i> ^{R451G/+} mice display no significant electrical abnormalities at baseline.....	90
Figure 12: <i>Dsp</i> ^{R451G/+} mice display structural changes post TAC surgery	92
Figure 13: Structural changes in <i>Dsp</i> ^{R451G/+} mice post TAC surgery	93
Figure 14: Surface ECG recordings from <i>Dsp</i> ^{R451G/+} mice and control littermates post-TAC surgery	94
Figure 15: Representative ECG traces following TAC surgery.....	95
Figure 16: <i>Dsp</i> ^{R451G/+} mice display arrhythmias following catecholaminergic challenge.....	96
Figure 17: Electrocardiographic findings following catecholaminergic stimulation in telemeter mice.....	97
Figure 18: <i>Dsp</i> ^{R451G/+} mice display no changes in expression of key ID proteins.....	98
Figure 19: No changes in the expression of additional key ID proteins	99
Figure 20: <i>Dsp</i> ^{R451G/+} mice display changes in ID protein localization.....	100
Figure 21: Stability of SH3/SR4 domains are maintained by the residues many UP variants reside	114
Figure 22: Select UP variants disrupt intra-molecular interactions surrounding the calpain target site.....	117
Figure 23: Core exposure of the calpain target site is uninfluenced by UP variants	119
Figure 24: Increased sensitivity to calpain identified in most UP variants.....	122

Chapter 1. Introduction

1.1 Normal cardiac conduction and the action potential

Heart disease remains as the leading cause of death worldwide, with sudden cardiac death (SCD) resulting in the largest proportion (60%) of all cardiovascular disease related deaths [1]. Ultimately attributing to causing between 180,000 to 300,000 deaths annually in the United States, the vast majority of SCD cases are caused by cardiac arrhythmias, defined as a disruption in proper electrical signaling within the heart [1-2]. Typical cardiac excitation-contraction is initiated by pacemaker cells within the sinoatrial (SA) node, which propagates the electrical signal uniformly throughout the atria. This impulse is then conducted to the atrioventricular (AV) node through the intermodal pathway. Following a slight delay, the electrical impulse conducts through the bundle of His, where the signal propagates into two separate bundle branches (left and right). This signal is then transmitted to the left and right ventricles via the Purkinje system, where the signal is transmitted to ventricular myocytes. Throughout this process, the body maintains homeostatic cardiac function by regulating this conduction through a variety of signaling pathways, particularly the sympathetic and parasympathetic nervous system, which are responsible for the regulation of heart rate and cardiac contractility [3-4].

The Purkinje fibers are essential for proper electrical conduction and cardiac contraction, as they transmit action potentials (AP) faster than ventricular myocardium, and rapidly spreads a uniform impulse through the entire ventricular myocardium [3]. The intercalated disc (ID) is vital for this for this electrical exchange between cardiomyocytes.

The cardiac ID is the junction that joins adjacent cardiomyocytes to exchange both electrical and mechanical signals, and is comprised of multiple protein complexes to both accomplish this signaling and provide structural integrity [5]. ID function is vital for both ventricular and atrial myocytes. As the action potential propagates through one cardiomyocyte that results in a contraction, the ID allows for ion exchange with the neighboring cell, resulting in a rapid, and importantly unidirectional, transmission of the electrical impulse. As each cardiomyocyte contracts, neighboring cardiomyocytes will synchronously contract as the cytoskeleton of each cell is mechanically linked through the ID [5]. Misregulation at any of these steps in cardiac conduction can result in arrhythmias that may trigger SCD.

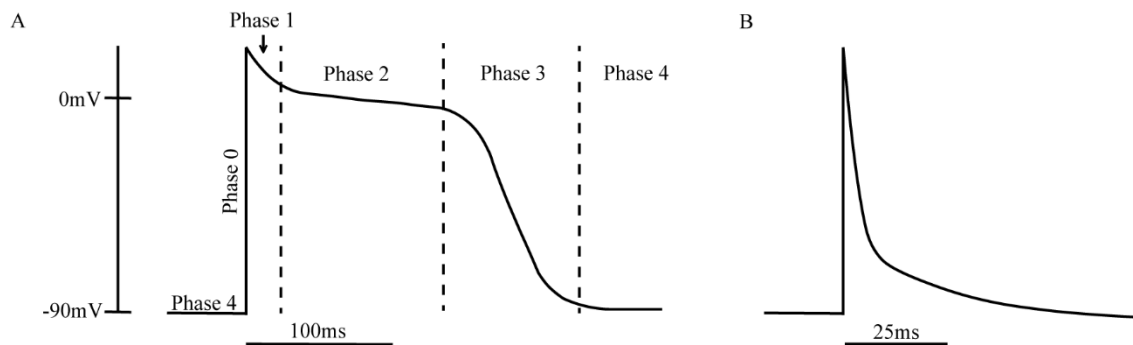


Figure 1: Cardiac action potential

(A) Schematic of the cardiac action potential in humans (scale bar =100ms), (B) and in mice (scale bar =25ms).

Typical (non-pacemaker) cardiac action potentials can be broken into 5 major phases as seen in Figure 1 above. Note the murine action potential has a substantial different morphology where these phases are harder to distinguish (Figure 1B). Known as phase 4, resting membrane potential is between -80mV and -90mV [6]. Following an

external (depolarizing) stimuli, phase 0 is initiated via the opening of voltage gated sodium channels, resulting in the rapid influx of Na^+ (I_{Na}) that causes a rapid cellular depolarization. This is followed by phase 1, an early initial repolarization that is primarily acts through the transient outward potassium current (I_{to}), but inward Cl^- (I_{Cl}) contributes as well. In phase 2, the rapid depolarization results in Ca^{2+} influx ($I_{\text{Ca,L}}$) via L-type calcium channels [6-7]. Ultimately this results in cardiac contraction, as Ca^{2+} influx results in the opening of the cardiac ryanodine receptor (RyR2), resulting in the release of calcium from the sarcoplasmic reticulum (SR) into the cytoplasm that triggers actin-myosin crossbridge formation. This is known as calcium-induced calcium release (CICR) [8]. Phase 2 is known as the plateau phase, as the inward calcium current offsets the outward potassium current, leading to a relatively stable membrane potential [6]. At phase 3, the L-type calcium channels close, allowing for potassium currents to begin rapid repolarization. This is primarily initiated through the opening of the delayed rectifier channels ($I_{\text{Kr/Ks}}$), that is later taken over by the inward rectifier current (I_{K1}) [6-7]. As the resting membrane potential returns to baseline (-80mV to 90mV) at phase 4, I_{K1} remains active early on, and multiple exchangers and ATP-dependent channels return ion concentrations to basal levels. These include the sodium-calcium exchanger (NCX) and the sodium-potassium pump (NKA) [6]. As each of these channels, exchangers, and pumps are necessary for proper cardiac AP propagation, variants or misregulation in any of these proteins can alter AP properties that may result in arrhythmias and impaired cardiac contractions.

1.2 Disruption of normal electrical signaling and the formation of cardiac arrhythmias

Arrhythmias can be classified into two major subgroups, atrial and ventricular arrhythmias. The most common types of atrial arrhythmias are supraventricular tachycardia, which include atrial fibrillation (AF) and atrial flutter (AFL). Atrial fibrillation is the most common cardiac arrhythmia with nearly 33 million cases worldwide, and is associated with an increased mortality linked to cardiomyopathy, heart failure, and stroke [9-10]. Overall AF is a multi-faceted disease with a variety of factors contributing to the phenotype, including changes in ion channel activity, alterations to calcium handling, atrial fibrosis and dilation [9]. Generally AF is induced by reentry pathways (single or multiple, frequently from the pulmonary veins), where perturbed AP conduction may result in premature firing of atrial myocardium prior to a second signal from the SA node, leading to rapid and irregular electrical activity [9-10]. The atria are at particular risk for this disrupted signaling due to shortened AP propagation and refractory periods [9]. Atrial flutter has a milder impact on atrial function, where atrial conduction and heart rhythm are more stable and uniform compared to AF [11]. While less severe, AFL still poses multiple health complications, including an increased risk of stroke and other thromboembolic events [11]. While these conditions may lead to palpitations and play a role in ventricular tissue, they often times only impact the atria [9-11].

Ventricular arrhythmias are generally considered more severe than atrial arrhythmias. The most frequent arrhythmic trigger of SCD is ventricular fibrillation (VF) [2, 12], identified in approximately 70% of cardiac arrest patients [13]. Defined as a wide complex tachycardia, VF has a notable irregular rhythm with abnormal QRS morphology,

ultimately an extreme risk for disrupting cardiac output and resulting in SCD [13]. Ischemic heart disease and myocardial scarring is a common trigger for this [12], but can develop in the absence of structural defects through a variety of arrhythmic disorders.

Brugada syndrome is a ventricular disorder characterized by abnormal ST segment elevation, ultimately resulting in syncope, VF, and SCD [14]. The disease has a prevalence of ~1:2000, and while traditionally being inherited autosomal dominantly, Brugada syndrome is known to have a low penetrance level. This risk for SCD is low in asymptomatic cases, which comprises of approximately two-thirds of all cases [14]. Despite this, men are nearly eight times more likely to be diagnosed. While more than 25 genes have been linked to the pathogenicity of Brugada syndrome, nearly 20% of Brugada syndrome patients have an identified loss-of-function variant in *SCN5A*. This gene encodes the alpha subunit of $\text{Na}_v1.5$ [15-16], the predominant channel responsible for the I_{Na} current [17]. Genetic variants are also commonly found in targets responsible for proper trafficking of $\text{Na}_v1.5$, thus reducing I_{Na} . Examples include genes related to the β -subunit of $\text{Na}_v1.5$ (*SCN1B*, *SCN2B*, and *SCN3B*) [18-20], glycerol-3-phosphate dehydrogenase 1 (*GPD1L*) [21-22], and sarcolemmal membrane associated protein (*SLMAP*) [23]. Outside of sodium current, loss-of-function variants that decrease $I_{\text{Ca,L}}$ (*CACNB2b*, *CACNA2D1*, *CACNA1C*, each components of the L-type calcium channel $\text{Cav}1.2$) [22, 24-25], or gain of function variants that increase potassium currents I_{to} and I_{K1} (*KCND2*, *KCND3*, *KCNE3*, *KCNE5*, *KCNJ8*, and *KCNH2*) [22, 26-30] also contribute toward Brugada syndrome development.

Early repolarization syndrome (ERS) has a similar phenotype to Brugada syndrome, with differences in diagnosis being determined by the primary region of the

heart being affected [31-32]. While occasionally phenotypically indistinguishable from Brugada syndrome, ERS is diagnosed based on the identified genetic variant [31]. There are at least six ERS associated genes, with variants frequently resulting in reduced $I_{Ca,L}$ or I_{Na} current activity, or increased I_{to} , ATP-sensitive K^+ current (I_{KATP}) or acetylcholine-regulated K^+ current ($I_{K,Ach}$) [31-32].

Long QT (LQTS) and short QT syndromes (SQTS), as the names suggest, are characterized by abnormal repolarization, resulting in morphological changes in T wave structure, and prolonged or shortened QTc intervals, that can attribute towards syncope, ventricular arrhythmias, and SCD [33-34]. While both LQTS and SQTS have different subgroupings based on ECG parameters, symptoms, and genetic cause, the downstream alterations in ion channel activity lead to disrupted AP propagation. Due to the delay in appropriate repolarization in LQTS, the most frequent causes are loss-of-function variants in potassium channel-linked genes, or gain-of-function in either I_{Na} or $I_{Ca,L}$ [35]. LQTS has frequently reduced responsiveness to β -adrenergic signaling or altered channel gating that leads to a prolonged AP propagation/QTc intervals, ultimately triggering arrhythmogenesis [36-37]. In contrast, SQTS is typically associated with gain-of-function variants in potassium channels, or loss-of-function variants in calcium voltage-gated channels [38]. Despite having near opposite changes in ion activity, the reduction in AP duration and refractory periods pose a risk in the development of arrhythmias such as VT/VF that can result in SCD [38-39].

Catecholaminergic polymorphic ventricular tachycardia (CPVT) is a disorder linked to episodic syncope that occurs during stress, particularly physical or emotional

stress, without the presence of a structural phenotype. These syncope events are triggered by VT events, that ultimately may develop into VF and SCD [40]. While idiopathic forms exist, nearly all CVPT cases are linked to calcium handling proteins outside of the L-type calcium channel. Most cases are linked to autosomal dominant variants in *RYR2*, and while around 70 variants have been identified, mechanistically most of these variants impact *RYR2* luminal sensitivity of Ca^{2+} , binding to associated proteins, the SR Ca^{2+} load, and initiation threshold [15]. Other genes linked to CPVT include triadin (*TRDN*), calsequestrin (*CASQ2*), and calmodulin (*CALM1/3*), each responsible for producing calcium regulatory proteins [40]. While a variety of variants and mechanisms have been linked to each of these proteins, they share downstream molecular consequences including abnormal SR calcium load and calcium leak, resulting in calcium sparks that may trigger ventricular arrhythmias including VT. β -adrenergic activity has been shown to have a strong connection with the formation of arrhythmias [41].

While there are exceptions, the vast majority of disease-causing variants in each of these arrhythmogenic disorders is primarily electrical, typically by altering the activity or regulations of either ion channels or calcium-handling proteins. However, arrhythmogenic cardiomyopathy (ACM) is an arrhythmic disorder that is primarily linked to genetic variants in structural genes that lie within the ID [42]. There is a structural component to ACM, particularly in late stages of disease development. However, a hallmark of ACM is an arrhythmogenic ‘concealed phase’, where patients may be at risk for the development of life threatening arrhythmias prior to the onset of a structural phenotype [43-44]. Despite recent work, the molecular mechanisms of disease development, and how they are

influenced by external stress factors, remain largely unknown. This gap of knowledge on how structural proteins can result in an arrhythmogenic disorder prevents optimal treatment of ACM patients. A more thorough description of the genetic background, environmental factors, and treatments for ACM is provided in chapter 2 [45].

1.3 Role of intercalated discs and desmosomes

As previously stated, the ID is the junction between adjacent cardiomyocytes that not only provides structural integrity to withstand contractile forces, but transmits electrical and mechanical signals between cardiomyocytes to allow for synchronized and unidirectional AP conduction [5]. This structure is drastically different from the lateral membrane, which is responsible for stabilizing portions of the cytoskeleton and sarcomeres to the extracellular matrix [5]. The ID plays an important role in both atrial and ventricular cardiomyocytes, but there are differences in protein expression [46]. Recent studies have suggested there is significant heterogeneity among different ID structures within the ventricular tissue, as well as between atria and ventricular discs. [47-49]. This may explain why select diseases linked to the ID may only affect ventricular (ACM) or atrial (AF) portions of the heart [47, 50].

Despite the variability between different discs, there are three major protein complexes that compose all ID structure. These include the adherens junction (AJ), gap junction (GJ), and the desmosome [5, 51]. The AJ links the actin cytoskeleton of adjacent cardiomyocytes, anchors myofibrils, and senses mechanical forces. As it links the actin cytoskeleton, mechanical forces and signals related to actin and contractions are

transmitted between cells through AJs [5]. The major contributor towards AJ structure and function is the transmembrane protein N-cadherin (N-Cad). N-Cad extends into the extracellular space of the ID and homodimerizes with N-Cad from adjacent cells, allowing cardiomyocytes specificity when forming extracellular interactions [5]. This homodimerization occurs in a calcium-dependent manner, as the extracellular domains have multiple calcium binding domains. While its expression is essential for fully developed heart, N-Cad also plays an extremely important role in the developing heart as the primary cadherin expressed in the myocardium [52]. The intracellular portion of N-cad primarily interacts with β -catenin, but is also capable of interacting with α -catenin, γ -catenin, p120-catenin and vinculin [51, 53]. Among these proteins, α -catenin and vinculin are primarily responsible for forming interactions with actin [5]. These proteins, practically N-Cad, α -catenin, and vinculin, play a role in mechano-sensing, where increased force detected by N-cad leads to a cascade of protein recruitment and phosphorylation that ultimately leads to changes in sarcomeric organization and cell stiffness [5, 54-56]. Alterations in expression patterns or variants in these proteins have been frequently linked to dilated cardiomyopathy (DCM) or hypertrophic cardiomyopathy (HCM) like phenotypes [51, 57-58]. Overexpression or inducible knock-out (KO) of *N-cadherin* results in a DCM phenotype in adult mice [59-60], with the haploinsufficient KO model displaying increased susceptibility to arrhythmias and disrupted localization of connexin 43 (Cx43), an essential GJ protein [59, 61].

Gap junctions are regions of multiple intercellular channels that allow the passage of small molecules (<1 kD) between adjacent cells. Ion exchange occurs frequently via

these channels during AP propagation. Different connexin proteins dimerize to form these channels, where six connexin molecules form a hexameric hemichannel in the membrane, then dimerize with another hemichannel in the opposite cell to produce a function channel that links the adjacent cells [51]. In ventricular tissue the primarily expressed connexin is Cx43, where atrial tissue has expression of both Cx43 and Cx40 [5, 62]. Key proteins within AJs, as well as the desmosome, are vital for proper localization and expression of Cx43 at the ID. Zonula occludens-1 (ZO-1) is a scaffolding protein expressed at the ID that interacts with α -catenin, and provides structural support by connecting with the actin cytoskeleton [63-64]. ZO-1 also directly binds to Cx43, establishing a physical link between AJ and GJ, and has been suggested to modulate turnover rates of Cx43 [65]. One study examining a ZO-1 haploinsufficient model indeed showed loss of ZO-1 results in altered localization of Cx43 within the cardiomyocyte with increased aggresome formation, as well as increased Cx43 expression [66].

The final major protein complex at the ID is the desmosome. Acting as a cellular anchor that links cardiomyocytes at the ID, the desmosome is essential for providing support to cells to protect their structural integrity from the mechanical forces generated during contractions [5]. Desmosomes also stabilize epithelial tissue as well. While AJs do provide some structural stability at the ID, desmosomes are considered significantly more robust, as they form interactions with more mechanically resilient, yet flexible portions of the cytoskeleton in the intermediate filaments [67]. In the cardiomyocyte, the intermediate filaments primarily linked to the ID is desmin [5]. There are 5 major desmosomal proteins essential for ID stability. Desmoglein-2 (DSG2) and desmocollin-2 (DSC2) are cadherins,

like N-Cad, that extends extracellularly to form intercellular interactions [5]. These cadherins are regulated by calcium to control adhesive strength, which provides the ability for desmosomes to be flexible during wound healing or embryogenesis [68]. Misregulation of this flexibility, or diminished mechanical strength of these cadherins through reduced adhesion, results in ACM pathology including ventricular arrhythmias and infiltration of fibrotic tissue [69]. Beyond DSC2 and DSG2, two essential armadillo proteins in plakoglobin (PKG) and plakophilin-2 (PKP2) bind to the cytosolic portion of these desmosomal cadherins. Of note, PKG is also known as γ -catenin, and PKP2 is homologous to p120 catenin, both key members of the AJ. This provides a physical link between desmosomes and AJs via interactions with N-Cad, α -catenin and β -catenin [5]. Indeed, PKG appears to have particular importance in not only organizing and recruiting DSP to the ID, but for organization of the ID by separating desmosomes from AJs. Referred to as both PKG and γ -catenin, this protein plays an essential role in both of these protein complexes. However, binding experiments have shown PKG, while bound to DSG-2, cannot interact with α -catenin, separating the two protein complexes [70]. The last major component of the desmosome is desmoplakin (DSP). A member of the plakin family that directly links to the intermediate filament desmin, DSP connects the remainder of the desmosome with this cytoskeletal network [67]. A transmission electron microscopy (TEM) diagram pointing out the different ID components can be found in figure 2.

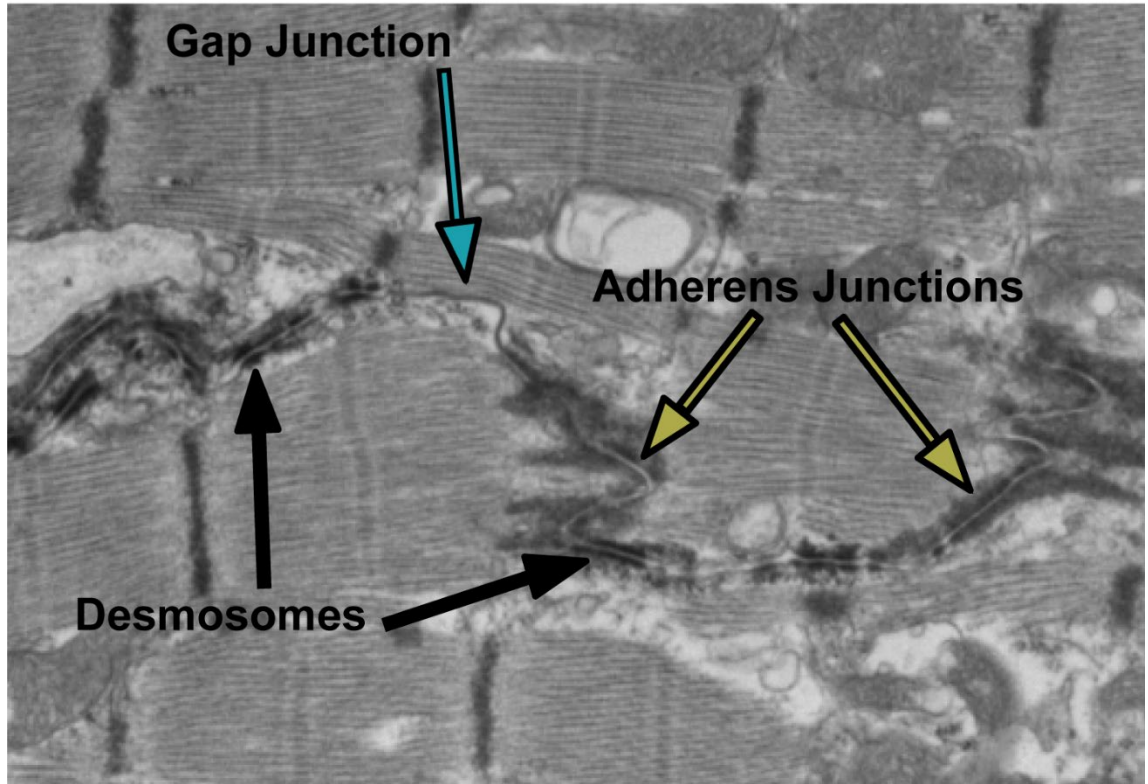


Figure 2: Diagram of the different ID components

Arrows point to the three major components of the ID, including the desmosome (black) the adherens junction (yellow), and the gap junction (blue). The desmosomes are defined by regions where the membranes between two cells can be seen, with a very dark, electron dense shell surrounding the region. Adherens junctions are identified by a separation between the two membranes with a light density. Gap junctions are tight lines where the membrane of the two cells cannot be distinguished.

As with AJs, desmosomes are also capable of interacting and recruiting GJ proteins. Evidence has supported that DSP plays a role in the recruitment of Cx43 to the ID through interactions with microtubule end binding protein 1 (EB1), and essential protein that regulates microtubule formation and promotes stability during cell growth. ACM-linked DSP genetic variants can disrupt Cx43 recruitment via reduced binding to EB1 [71]. Additionally, loss of DSP triggers the lysosomal-mediated degradation of Cx43 through a RAS dependent mechanism [72]. *Pkp2* inducible KO mice show an increased propensity

for inducible arrhythmias, linked to the disruption of both calcium handling proteins and ID structure [73-74]. Furthermore, increased hemichannel Cx43 was also identified, displaying leaky behavior with increased cellular permeability [75]. Multiple diseases linked to disrupted desmosome integrity, including ACM [75-76], Naxos disease [77], and Carvajal syndrome [78], frequently exhibit disrupted Cx43 expression and localization.

While each of these three ID components have unique and complex functions towards proper transmission of electrical and mechanical signals, functionally each portion of the ID relies on each other, and forms many structural connections. They each have their own subdomains in the ID, making the structure of the disc non-uniform with significant heterogeneity between each ID. However, select regions of the ID have tight interactions of different combinations of these three complexes [5]. These provide unique physiological functions including regulation of the localization of different compartments, recruitment of select ion channels, and for building interactions with the SR. The connexome is defined as regions with closely interacting Cx43 and Na_v1.5 to the desmosome, particularly through PKP2 [5, 79]. Super-resolution fluorescent microscopy is required to identify these regions, believed to play a role in regulating excitability, intercellular communication, and cell-cell adhesion [79]. Evidence suggests Cx43 plays a vital role in the recruitment of Na_v1.5 as well as appropriate sodium signaling [80-82].

Additionally, the perinexus is defined by the region on the edge of functional gap junction plaques, where individual Cx43 hexamers interact with ZO-1. This interaction prevents the formation of intercellular connexin channels, indicating ZO-1 may play a role in Cx43 recruitment to the ID, but may also regulate the size of GJ plaques [5]. Loss of

ZO1 in mice results in increased Cx43 expression, mislocalization, and extended GJ plaque size [66, 83].

Ankyrin G (AnkG) is scaffolding protein that plays an imperative role in ion channel recruitment and organization at the ID. AnkG is involved in both connexome and perinexus organization, particularly through direct interactions with Cx43. For perinexus structure, AnkG-Cx43 interactions occur away from the GJ beyond ZO-1-Cx43 interactions, suggesting AnkG plays a role in recruitment of Cx43 to gap junctions, and plays a regulatory role in the size of these plaques [5]. Additionally interactions between AnkG and Nav1.5 are vital for proper ion exchange at the connexome, [81, 84], which are facilitated through EB1 [5]. NCX, Na⁺/K⁺-ATPase, and Nav1.5 have also been connected to regulation via AnkG, where variants have been associated with electrical dysfunction and reduced cellular adhesion [5].

Being essential for both AP propagation between cardiomyocytes through the passage of appropriate ions, as well as ensuring a synchronous contraction between cells, it is not surprising dysfunction of the ID leads to the phenotypic progression in many diseases. ACM is of particular interest in relation to the ID, specifically the desmosome. While the vast majority of arrhythmic disorders stem from variants or dysfunction in either ion channels or proteins that regulate them, as many as 90% of ACM cases (with an identified genetic culprit) arise from variants in ID proteins, with the vast majority being among desmosomal proteins [45]. Among the desmosomal genes, *DSP*, *PKP2*, and *DSG2* are the most frequently affected [45, 85]. *DSP* is of particular interest for a variety of reasons. Based on affected protein region the variant disrupts, can result in either an ACM

or DCM phenotype [45, 85-87]. Additionally, while many ACM patients experience a more severe phenotype in the right ventricle (RV), *DSP*-linked ACM cases are often biventricular or LV dominant [76, 88-89].

1.4 Function of desmoplakin and its connection to arrhythmogenic cardiomyopathy

Desmoplakin is one of the largest desmosomal proteins and is a member of the plakin family. DSP is expressed primarily in cardiac, vascular, and epithelial tissue, tissues that experience significant mechanical stress [5, 90-91]. Regardless of cell type, plakin proteins are responsible for linking intermediate filaments to desmosomal targets in order to provide mechanical strength to the desmosome [91]. Variants in *DSP* have been linked to a variety of diseases, including ACM, DCM, and a variety of epithelial/skin disorders [78, 87]. There are three major domains in DSP, an N-terminal spectrin repeat (SR) domain, a central coiled-coil domain, and a C-terminal plakin repeat domain (PRD) [91]. A single *DSP* gene encodes for two separate isoforms, DSP I (~320kD) and DSP II (~260kD). DSP II lacks a portion of the coiled-coil domain, and is not expressed in cardiac tissue [91]. Overall the expression of DSP is vital for proper embryonic development of both epithelial and cardiac tissue as seen from *Dsp* KO mouse models. Whole body KO of *Dsp* results in embryonic lethality at ~E6.5 due to disruption of epidermal sheet formation, whereas cardiac specific restriction results in delayed lethality at approximately E10.5-E15.5 [90, 92].

There are a total of six α -helical SRs encompassing the N-terminal region of the protein (SR3-SR6, SR7-SR8) [76]. Between the SR4-SR5 domains is a Src homology 3

(SH3) domain, where the majority of ACM-linked variants in the ‘hotspot’ lie [45, 76, 85, 93]. To date, while the structure of SR and SH3 domains are known, there are gaps of knowledge in terms of function of this region. This N-terminal domain is responsible for forming interactions with the armadillo proteins PKP2 and PKG, ultimately connecting the desmosome to the intermediate filaments [70, 94]. However, despite having similar structures, the regions of these proteins that interact with DSP are different. While PKG interacts with DSP through the armadillo repeats [70], PKP1/2 are shown to interact with DSP through its N-terminal head domain region [94]. The role these proteins seem to play on DSP/desmosomal interactions also appear to drastically differ. Using epithelial cell culture and Co-IP experiments, PKP1 was shown to interact very strongly with DSP, but only interacts weakly with the desmosomal cadherins [94]. Contrarily, PKG interacts strongly with both DSP as well as the cadherins [70], ultimately suggesting PKG plays a stronger role in linking DSP to the desmosomal cadherins, while PKP1 is more essential for DSP’s stability at the ID and enhancing the ability to form homodimers [94]. PKP1 is capable of recruiting DSP to the desmosome alone, whereas PKG requires the assistance of desmosomal cadherin to perform this task. While PKP2 is more capable of interacting with the desmosomal cadherins than PKP1, this suggests these armadillo proteins each plays a unique role in recruitment and organization of DSP at the desmosome [94]. This is essential as DSP is unable to directly from interactions with DSG2 [70].

Beyond protein interactions, *in silico* and *in vitro* studies have proposed this SR region, specifically the SH3 domain, plays a vital role in directly providing DSP and the desmosome with structural stability, as well as having a mechano-sensing role [93, 95].

When the SH3 domain is removed from DSP (also tested in another plakin member, plectin), the amount of force required to rupture the protein is drastically reduced via molecular dynamics (MD) simulations [93]. These results were verified in another SH3-containing plakin protein, plectin. Additionally, as force is applied to the N-terminus of DSP, unfolding occurs at the SR domains that restrict exposure of the SH3 to the surrounding environment, potentially opening up interactions downstream mechano-sensing signaling pathways [93]. In a separate study, multiple ACM-linked variants were introduced into DSP using MD-force studies that are within or interact with the SH3 domain [95]. Select variants in this region appear to result in an increase in DSP flexibility/buckling, ultimately reducing the force required to rupture the protein. Interestingly, variants buried in the protein, and therefore more likely to form intramolecular interactions, had a more severe impact on SH3/SR4-5 stability [95]. Outside of these MD-studies, others have linked N-terminal variants to ACM via perturbed recruitment and stability of the key GJ protein Cx43 as previously described [71-72]. Select variants within DSP were unable or had reduced interactions with EB1, which ultimately restricted the recruitment of Cx43 to the cellular membrane. Indeed loss of Cx43 is frequently reported in ACM models [73, 75, 96], as well as ACM patients with *DSP* variants [76, 96]. Additionally, others have supported that select variants result in increased sensitivity to the protease calpain [76, 97], which will be described in more detail in chapter 1.5. It is possible all of these mechanisms may be responsible for ACM development, and may just depend on the variant's role in protein-protein interactions and SR-SH3 stability. Regardless of the mechanism, dysfunction of the SR/SH3 domain is strongly correlated

with ACM, as 16 of the 25 known disease causing variants lie within this region, 9 of which surrounding or directly in the SH3 domain [93]. Models of the N-terminus of DSP, as well as the localization of the ACM-linked variants within DSP, can be found in figure 3. While the sequence of *DSP* is conserved among mammals, the region associated with the mutational ‘hotspot’ displays extreme conservation at >99% for most mammals (Figure 3B).

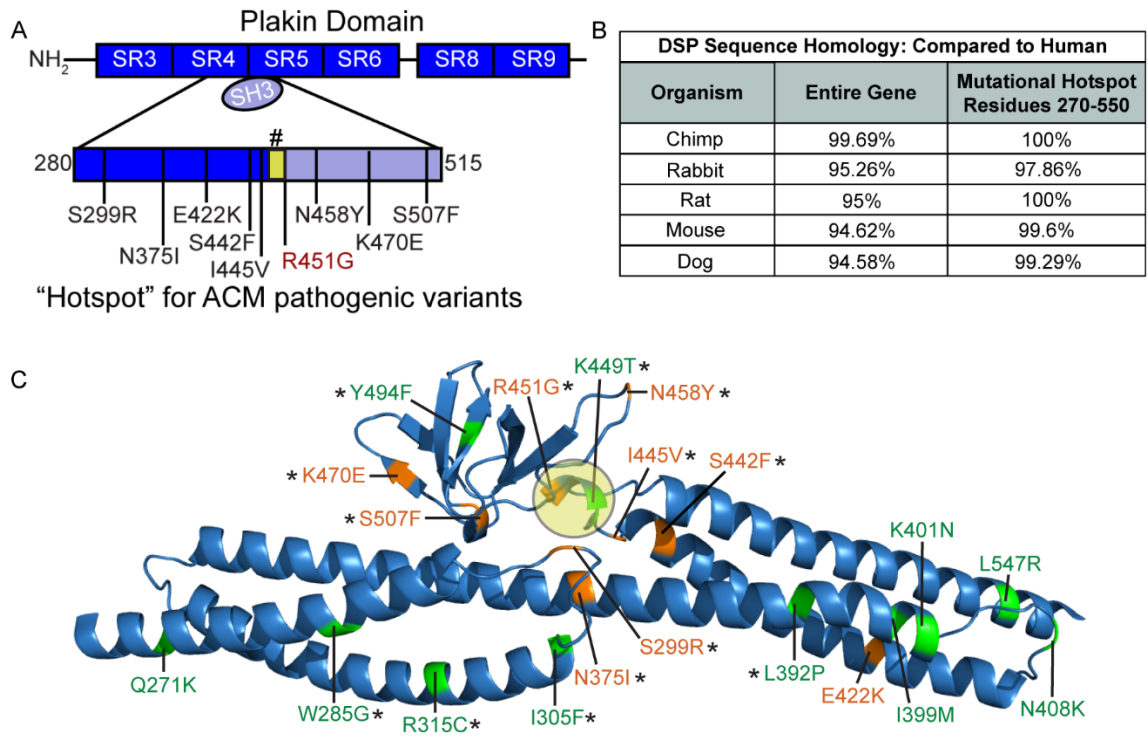


Figure 3: N-terminal diagram of DSP and mammalian sequence homology

(A) Two dimensional diagram of the N-terminus of DSP, showing the relation of the SH3 domain to the spectrin repeats. A zoom in of the mutation hotspot (residues 280-515) of pathogenic variants is included. # indicates the calpain target site (residues 447-451). (B) Sequence homology examining the conservation of the mutational hot spot, as well as DSP's entire sequence through mammals. (C) Three dimensional model of the N-terminus of DSP (residues 265-554) showing the proximity of each variant to the calpain target site (yellow circle). Pathogenic variants are labeled in orange, variants of unknown pathogenicity are labeled in green. *Indicates the variant is within 30 angstroms of the central piece of the target site (residue 448).

The central coiled-coil domain and the C-terminal plakin repeat domains, while not as strongly associated with ACM, still play an intrinsic role in desmosomal/DSP function. Homodimerization is essential for proper DSP function and stability [98-99]. Coiled-coil domains are responsible for not only providing significant structural support, but assist in protein-protein interactions [100]. This coiled-coil domain is found in many proteins

including desmin, where region often prominent of variants for diseases such as ACM [101]. Despite this, no significant disruption of this region in DSP has been linked to ACM. The C-terminus of DSP is comprised of three PRDs (PRDa-PRDc), with the role to recruit and bind directly to the desmin network [91, 98, 102]. Variants in this region are not commonly linked to ACM, but instead to skin disorders and DCM [84, 103-104]. While all three of these repeats are essential for interactions with desmin, the most C-terminal PRDc region is the most important in forming these interactions, being comprised of a 68 residue repeat of glycine-serine-arginine [104]. Nearly 50% of the residues within these PRDs are target sites for phosphorylation, and misregulation of phosphorylation patterns have been associated with broken DSP-desmin interactions and disease formation. Ultimately glycogen synthase kinase 3 (GSK3) and protein arginine methyl transferase 1 (PRMT-1) are responsible for the post-translational modifications that maintain the integrity of DSP to desmin [104]. The most well characterized variant that perturbs this interaction is the S2849G that ultimately drastically increases the binding affinity of DSP to the intermediate filament network by nearly tenfold. While this may seem like an increase in stability, it was shown to greatly delay desmosomal assembly [104]. A variant within this region was introduced into mice, R2834H, which impacted desmosomal formation and phosphorylation of the C-terminal of DSP [104-105]. This mouse model displayed cardiac dysfunction of the LV and RV, chamber enlargement, and increased fatty development within the cardiomyocyte [105].

The connection between DSP and ACM development has been significantly enlightened from the development of two heterozygous *Dsp* KO mouse models [90, 96].

These two separate models differed in severity and identified disrupted molecular targets, but this may be attributed to differences in the genetic background of mice, as well as the type of induced stress. Garcia-Gras et al. developed a *Dsp* haploinsufficient model, where homozygous deletion of *Dsp* lead to high levels of embryonic lethality. This model displayed increased chamber dilation, decreased cardiac output, increased fibrotic buildup, and increased propensity for both spontaneous and inducible arrhythmias. Ultimately this was attributed to the mislocalization of PKG from the ID to the nucleus, which was shown to suppress Wnt/ β -catenin signaling [90]. This triggered increased protein levels of targets related to adipogenic, including PPAR γ , CCAAT enhancer-binding protein- α (C/EBP- α), as well as upregulation of fibrotic genes including *Colla1*, *Colla2*, and *Col3a1* [90]. Overall Wnt/ β -catenin signaling in ACM is one of the most well studied pathways that is linked to the development of fibro-fatty infiltration. Briefly, nuclear localization of β -catenin acts as an activator for the transcription factors TCF/LEF, ultimately leading to a downstream cascade of gene activation, including cMyc, cyclinD, Axin2, WISP1, etc. Wnt activation allows this to occur by sequestering GSK3 β and Axin to the cell membrane at the Frizzled receptor. A lack of Wnt signaling releases Axin and GSK3 β to colocalize to the cytosol, where it can form a complex with APC and CK1, ultimately leading to β -catenin degradation to control gene expression [106]. In a zebrafish *Dsp* KO model, the suppression of this signaling pathway can be alleviated via genetic and pharmacological intervention, partially rescuing the phenotype [107]. While loss of β -catenin, or disrupted trafficking from the ER to the membrane has been noted in ACM models [106, 108-109], PKG plays a strong role as a repressor for this pathway. It acts as an antagonist of β -catenin

due to high homology of the structures [5]. Disruption of desmosomal/ID integrity can result in PKG translocating to the nucleus, preventing the appropriate β -catenin/TCF transcription factor activation [90, 106]. Downstream consequences include the activation of genes responsible for fibrosis, adipogenesis, and apoptosis [90, 110]. On the contrary, excessive β -catenin signaling has been linked to hypertrophy and ACM like symptoms [106, 111], so a physiological balance of this signaling pathway is essential for normal cardiac function [106].

In the following years, Gomes et al. established a similar *Dsp* genetic KO, with a less severe phenotype. These mice failed to display baseline arrhythmias, but following induction were vulnerable to VT [96]. While there was no significant signs of chamber dilation or reduced output, increased levels of fibro-fatty accumulation were noted at a later age. These mice did display a mild reduction of PKG after 6 months, but Cx43 had reduced signal at the ID through immunofluorescence staining, and increased aggregation was noted within the cytosol [96]. Multiple studies have connected DSP to Cx43, where disease causing DSP variants interfere with EB1 dependent recruitment of Cx43 to the ID [71], and loss of DSP expression resulted in enhanced degradation of Cx43 from the ID [72]. This can result in leaky hemichannels that can result in arrhythmias as seen in a *Pkp2* inducible KO model [73, 75], and ultimately loss/mislocalization of Cx43 has been identified in ACM and other related diseases [76, 78, 112].

1.5 Cluster of desmoplakin variants display increased sensitivity to the protease calpain

As stated previously, the N-terminus has a significant mutational ‘hotspot’ for ACM variants that is a clear overrepresentation, as 27.2% of disease-causing variants lie in this region despite only making up 8.6% of the total gene [85, 113]. These have been characterized by multiple groups suggesting potential influences in Cx43 recruitment or decrease in structural stability as force is administered [71, 93, 95]. A recent study by our group has identified these variants surround a calpain target site that is buried within the SH3 domain at residues 447-451 [76]. Despite these variants being spread out over 100s of residues, structurally these residues are in close proximity to each other, with all but two pathogenic variants localizing within 15 angstroms of the central region of the SH3 domain (residue 448) [76]. An additional group of variants of unknown pathogenicity lie in this region within close proximity of the SH3 domain as well (Figure 3C).

Calpain is a group of ubiquitously expressed calcium-dependent cysteine proteinases, which are essential for a variety of functions including normal protein turnover [114-116]. *In vitro* studies showed WT DSP was capable of being degraded via calpain [76]. Using *in silico* analysis through MD simulations, no major protein unfolding occurred following introduction of any pathogenic DSP variant. One specific variant, DSP p.R451G, was examined in depth because of its localization within the calpain target site, as well as it being associated with a large family with clinical signs of ACM and SCD [76]. *In silico*, introduction of the R451G variant resulted in a disruption in the interactions that maintain the structural integrity of the calpain target site, ultimately increasing the exposure of this cleavage site to the external environment. *In vitro*, recombinant R451G DSP displays

increased degradation following calpain incubation. When all N-terminal variants were examined on their influences, 44.4% of the variants displayed decreased molecular stability as determined by MD simulations, which correlated with reduced protein stability following calpain incubation [76]. While not commonly identified in other ACM cases, select variants in PKP-2 have shown loss of protein expression linked to calpain mediated degradation [114].

Calpain contributes to a significant amount of physiological functions, including remodeling of the cytoskeleton for cellular motility and contractility, proteolytic modifications in signaling pathways, regulation of the cell cycle and gene expression, and involvement in apoptotic pathways [115-116]. There are two major forms of calpain arising from separate genes, m-calpain and μ -calpain. While m-calpain and μ -calpain share similar size and structure, each sharing 4 essential domains, they differ in the level of calcium required for activation (micromolar for μ -calpain, millimolar for m-calpain) [115, 117]. A separate gene produces a smaller regulatory subunit shared by both forms of calpain to form a heterodimer [115, 118]. While traditionally inactive without the presence of calcium, autolysis of calpain occurs once sufficient levels of calcium are present, leading to the activation of the proteolytic portion of the protein, however cleavage activity has been reported even without this autolysis [115, 117]. Misregulation of calpain, or indiscriminate targeting of calpain, has been linked to a variety conditions including Alzheimer's and heart disease [97, 119-120]. Indeed calpain is vital for appropriate function and regulation of cardiac sarcomeres [116], so the potential connection to ACM [76, 97] or other forms of heart disease are not unexpected. Although linked to a variety of

diseases when either not properly regulated, loss of calpain is detrimental to physiological function, as its regulation of a variety of enzymes and transcription is essential for cellular maturation and health [120].

Typically, calpain is disbursed in the cytosol with minimal catalytic activity. Upon increased levels of calcium, calpain activates, and localizes to the cell membrane/ID, the Golgi apparatus and the endoplasmic reticulum [121-122]. Overall, this activation helps promote normal cardiac function, but also assists with wound healing and sarcomere function [116, 118]. Regulation of calpain is essential for proper physiological function and can result in disease formation if not tightly regulated. Calpastatin is a physiological inhibitor of calpain, where the subunit of both forms of calpain shares similar homology to select portions of calpastatin [115, 123-124]. Calpain expression levels remain relatively unchanged within the cell, but regulation of calpastatin expression is essential for the maintenance of calpain activity in the cell [125]. Calpastatin normally localizes in the cytoplasm at low calcium levels to ensure inhibition of calpain, but transfers into the nucleus following prolonged exposure to calcium [125]. Phosphorylation of calpastatin through protein kinase A and C (PKA/PKC) has been shown to regulate activity, suggesting a variety of mechanisms influences calpastatin ability's to inhibit calpain [126]. Calpain can also be directly regulated through calmodulin-dependent protein kinase II (CaMKII) [127-128], suggesting β -adrenergic signaling may play a vital role in the maintenance of the calpain-calpastatin activity [127, 129]. Upon interactions with calcium and calmodulin, CaMKII autophosphorylates, resulting in activation of the CaMKII. This also allows for the interaction between calpain-CaMKII that allowed for translocation to

the cell membrane, but was restricted upon the introduction of phospho-restrictive CaMKII variant (T287A) [127].

While calpain is related to a variety of cardiac disorders, it has essential physiological function in a multitude of pathways, making it less than ideal for therapeutic targeting [97, 120-121, 130]. Additionally, while there have been physiological benefits after injury by reducing calpain activity via CaMKII inhibition [127-128], this controls essential pathways including calcium signaling, increased contractility, etc. [129]. This important physiological role played by calpain makes it less than suitable for therapeutic targeting, but there are still promising approaches to either targeting calpain post-translational modifications [127], or protecting targets of calpain with small molecule approaches [97]. In regards to the N-terminal DSP variants, a ‘protective’ L518Y variant was introduced that helps block the calpain target site from the environment. Through molecular dynamic stimulations, this L518Y variant was able to interact with the calpain target site, and stabilized the interactions that hold this region together among proteins also containing a pathogenic variant. Indeed, by introducing the L518Y variant in recombinant DSP that also contained pathogenic, calpain sensitive variants, the levels of protein degradation via calpain was diminished [97]. While these approaches are promising, additional studies are required to determine potential safe approaches and therapeutics that can protect DSP without off target effects, or those that might significantly impact the physiological role of calpain.

1.6 Summary

Overall, ACM is an extremely dangerous disease, as life threatening arrhythmias may develop in the absence of a structural phenotype or identifiable risk factors [43-44]. In nearly half of probands, SCD is the first clinical manifestation of ACM [131]. The current approach to treatments and therapeutics is severely limited, as they generally only mitigate the symptoms without preventing disease progression. Typical approaches focus on minimizing the risk of ventricular arrhythmias through medications, catheter ablation, or implantable defibrillators [132-133], so the need for improved therapeutics is vital. Posing even more of a challenge is the incomplete penetrance commonly associated with familial ACM [88, 134]. Within our previous study of the familial ACM R451G variant, two experienced SCD within a year each other. However, of the 21 records of genotype positive individuals, only 15 displayed cardiac symptoms. Symptoms varied greatly between these 15 phenotype positive individuals, where many patients showed no structural phenotype, or variable arrhythmic symptoms [76]. There are additional family members positive with the variant that lacked a phenotype within this study that did not have records to share, and there was significant variation in the age of onset within patients with a phenotype [76]. While significant work was done to determine the DSP R451G variant, as well as neighboring variants, were vulnerable to degradation via DSP, the downstream consequences remain poorly characterized [76]. Additionally, this variability in phenotype from patient to patient suggests external or environmental factors may be playing a major role in the onset of symptoms, but the molecular pathways triggered by these stressors also remains unsolved. While exercise frequently can trigger arrhythmias that result in SCD, as

seen in the R451G family, there are other members that still develop a phenotype despite not regularly physically exerting [135-137].

These gaps in knowledge for disease development must be solved to better facilitate treatments for ACM patients. The need for a suitable model is apparent to understand the role between genetics and external stress on disease manifestation and progression. Murine models of ACM have been fundamental in enhancing our understanding the role desmosomal and other ID proteins play for proper cardiomyocyte health and disease progression [73, 75, 90, 96, 138-139]. However, many of these models utilize transgenic, overexpression, or KOs of essential genes, circumstances not generally relevant to humans. These models are beneficial for understanding molecular pathways and binding partners of the target of interest, but are limited in understanding the progression of ACM in relations to humans. These models are also not ideal in evaluating the influences of different cardiac stressors due to the lack of genetic relevance. To improve the translatable impact of mouse to human ACM research, improved mouse models derived from human variants need to be developed. Our group has successfully developed one of the first humanize mouse models that expresses the endogenous equivalent of the human R451G DSP variant to enlighten our understanding of genetic and environmental triggers for ACM. Future studies can evaluate potential therapeutic approaches based on the phenotypic progression of the model.

Approximately 50% of the N-terminal variants previously studied showed heightened sensitivity to calpain mediated degradation, suggesting multiple families may share a similar mechanism of disease onset [76]. Finding potential ways to protect these

calpain sensitive variants is ongoing [97], but many additional *DSP* variants within this region have been identified [113]. Many of these *DSP* variants lie within the mutational hotspot, but because of insufficient clinical data, are considered to have unknown or no known pathogenicity. Identifying a sensitivity to calpain in these variants may be beneficial for proper clinical management of these familial cases, and may contribute to the development of therapeutic approaches that can protect DSP.

Chapter 2. Arrhythmogenic Cardiomyopathy: Molecular Insights for Improved Therapeutic Design

Tyler L. Stevens¹, **Michael J. Wallace**^{1,2}, **Mona El Refaey**^{1,2}, **Jason D. Roberts**³, **Sara N. Koenig**¹ and **Peter J. Mohler**^{1,2,*}

¹ Departments of Physiology and Cell Biology and Internal Medicine, Division of Cardiovascular Medicine, The Ohio State University College of Medicine and Wexner Medical Center, Columbus, Ohio, 43210, USA.; tyler.stevens@osumc.edu (T.L.S.); sara.koenig@osumc.edu (S.N.K.)

² Dorothy M. Davis Heart and Lung Research Institute, The Ohio State University Wexner Medical Center, Columbus, Ohio, 43210, USA; michael.wallace@osumc.edu (M.J.W.); mona.elrefaey@osumc (M.E.R.)

³ Section of Cardiac Electrophysiology, Division of Cardiology, Department of Medicine, Western University, London, N6A 5A5, Ontario, Canada; jason.roberts@lhsc.on.ca

* Correspondence: peter.mohler@osumc.edu; Tel.: +1-614-247-8610
Academic Editor: James Smyth

Received: 27 April 2020; Accepted: 20 May 2020; Published: date

2.1 Abstract

Arrhythmogenic cardiomyopathy (ACM) is an inherited disorder characterized by structural and electrical cardiac abnormalities, including myocardial fibro-fatty replacement. Its pathological ventricular substrate predisposes subjects to an increased risk of sudden cardiac death (SCD). ACM is a notorious cause of SCD in young athletes, and exercise has been documented to accelerate its progression. Although the genetic culprits are not exclusively limited to the intercalated disc, the majority of ACM-linked variants reside within desmosomal genes and are transmitted via Mendelian inheritance patterns; however, penetrance is highly variable. Its natural history features an initial “concealed phase” that results in patients being vulnerable to malignant arrhythmias prior to the onset

of structural changes. Lack of effective therapies that target its pathophysiology renders management of patients challenging due to its progressive nature, and has highlighted a critical need to improve our understanding of its underlying mechanistic basis. In vitro and in vivo studies have begun to unravel the molecular consequences associated with disease causing variants, including altered Wnt/ β -catenin signaling. Characterization of ACM mouse models has facilitated the evaluation of new therapeutic approaches. Improved molecular insight into the condition promises to usher in novel forms of therapy that will lead to improved care at the clinical bedside.

Keywords: arrhythmogenic cardiomyopathy; desmosome; genetic diseases; sudden cardiac death

2.2 Introduction- Arrhythmogenic Cardiomyopathy

Arrhythmogenic cardiomyopathy (ACM) is a rare form of heart disease characterized by fibro-fatty replacement of ventricular myocardium [140]. ACM prevalence varies considerably by geographic location with a range that extends from 1:2000 to 1:5000 people worldwide. Italy has one of the highest prevalences of the condition, and males are more commonly affected at a ratio of 3:1 [88, 141-142]. Studies have shown that ACM is responsible for 3–10% of sudden cardiac deaths (SCD) worldwide among individuals less than 40 years of age, with studies in Italy attributing over 20% of SCD cases to ACM in young athletes [142-144]. Although the risk of SCD is exacerbated by exercise, many malignant arrhythmic ACM events are not exercise related [131, 145].

Average age of onset of the disease is approximately 30 years of age. Disease onset prior to adolescence is relatively rare, and most individuals destined to manifest a positive phenotype will do so prior to 65 years of age [146]. Electrical abnormalities generally precede structural defects, commonly referred to as the “concealed phase” [43-44]. ACM families are initially identified via an SCD event in 7–23% of cases [131], with some studies estimating SCD as the first clinical manifestation of ACM in 50% of probands [147-148]. Encompassing cardiomyopathies associated with a high risk of ventricular arrhythmias, ACM is a general term that includes multiple subtypes. The most common subtype of ACM is arrhythmogenic right ventricular cardiomyopathy (ARVC); however, left and biventricular dominant forms of the disease are well documented [88, 149-151], including lamin types A/C (*LMNA*) and phospholamban (*PLN*) cardiomyopathies [152-153]. Notably, autopsy reports have suggested that as many as 76% of ACM cases possess left ventricular (LV) abnormalities [151, 154].

Due to the absence of a single test that can confirm the condition, its diagnosis can be challenging. This has necessitated the development of task force criteria in an effort to standardize ACM diagnosis. Originally introduced in 1994 and subsequently modified in 2010, the task force criteria are a composite of clinical, structural, electrocardiographic, and genetic features that allow for clinical cases to be categorized as definite, borderline, and possible [140]. Following an ACM diagnosis, clinical management most often consists of some degree of exercise restriction and β -blockade. Among ACM patients deemed to be at significant risk for SCD, insertion of an implantable cardioverter device (ICD) should be considered. Among patients that experience ventricular arrhythmias, anti-arrhythmic

drug therapy and catheter ablation are relied upon to suppress further episodes and avoid painful ICD shocks [132, 155-157].

This review focuses on our current knowledge of the genetics underlying ACM and the mechanisms leading to disease onset and progression. Current disease models of ACM and environmental factors shown to contribute to disease development and progression will also be discussed, followed by a review of recent studies examining promising future therapeutics.

2.3 Genetics and Animal Models of Arrhythmogenic Cardiomyopathy

An underlying genetic culprit is identified in approximately 30–60% of ACM cases [44, 158-159]. Although viewed as a monogenic disorder, 30–40% of ACM cases are sporadic, suggesting oligogenic and environmental contributions [44, 158-159]. Notably, de novo and somatic mutations are not anticipated to account for significant proportions of sporadic cases given findings from a large study involving 209 genotype positive ACM probands, in whom only 1.4% had de novo variants [160]. Males are more likely to develop ACM and develop a more severe arrhythmogenic phenotype at an early age [146, 159], possibly secondary to hormonal differences, as high testosterone levels are linked to more severe arrhythmogenic events [161]. The primary mode of transmission of desmosomal variants is considered autosomal dominant; however, autosomal recessive forms of ACM have been documented, most notably the cardio-cutaneous forms, including Naxos disease (*JUP*) and Carvajal syndrome (*DSP*) [162]. While autosomal dominant inheritance is the primary method of transmission, penetrance is quite variable in patients. Additional

undiscovered genetic variants are likely attributed strongly to disease penetrance and the formation of genetic subtypes [163].

Putative genetic ACM culprits are quite diverse, as highlighted by the presence of 16 potential disease-causing genes (Table 1). ACM is commonly referred to as a disease of the desmosome and, indeed, reports document that 85–90% of all ACM-linked variants reside within desmosomal genes [160, 164]. Outside the desmosome, additional ACM-linked genes encode proteins that are associated with the intercalated disc (ID), including α -T-catenin (*CTNNA3*), desmin (*DES*), N-cadherin (*CDH2*), tight junction protein-1 (*TJPI*), voltage-gated sodium channel alpha subunit 5 (*SCN5A*), and transmembrane protein 43 (*TMEM43*) [42, 158, 165]. Although the full array of genetic variants have been reported in ACM, the majority are truncating. One report indicated that 83% were nonsense, frameshift, or splice site mutations, while 14% were missense variants [88]. While the genetic cause, subtype, and incomplete penetrance results in significant variance in disease characteristics between individuals, features including fatty infiltration and increased prevalence of ventricular arrhythmias are common among ACM cases [163]. While the pathophysiology of ACM, particularly for fatty infiltration, is not completely understood, alterations to adipogenic pathways including the Wnt/ β -catenin signaling and the Hippo pathway are commonly reported [111, 166-167].

Although identification of an underlying genetic culprit for ACM can be helpful for guiding proper clinical diagnosis and treatment, several variables make this challenging. Incomplete penetrance is commonly seen among familial cases of ACM. Multiple disease-causing variants have been identified in ACM, with variants in select genetic subtypes,

such as TMEM43-p.S358L, *PLN*, *LMNA*, and filamin-C (*FLNC*), posing additional challenges due to association with severe or unique forms of ACM [158, 168-171]. In addition, recent reports have suggested desmoplakin (DSP) related myopathies may be distinct from other ACM cases [172]. One of the most difficult challenges is determining if variants in these ACM-associated genes are disease causing or incidental noise. Within the ARVC database, the majority of variants listed (~70%) are classified as unknown or no known pathogenesis [113, 173]. Figure 4 shows the localization of known ACM-associated proteins within cardiomyocytes.

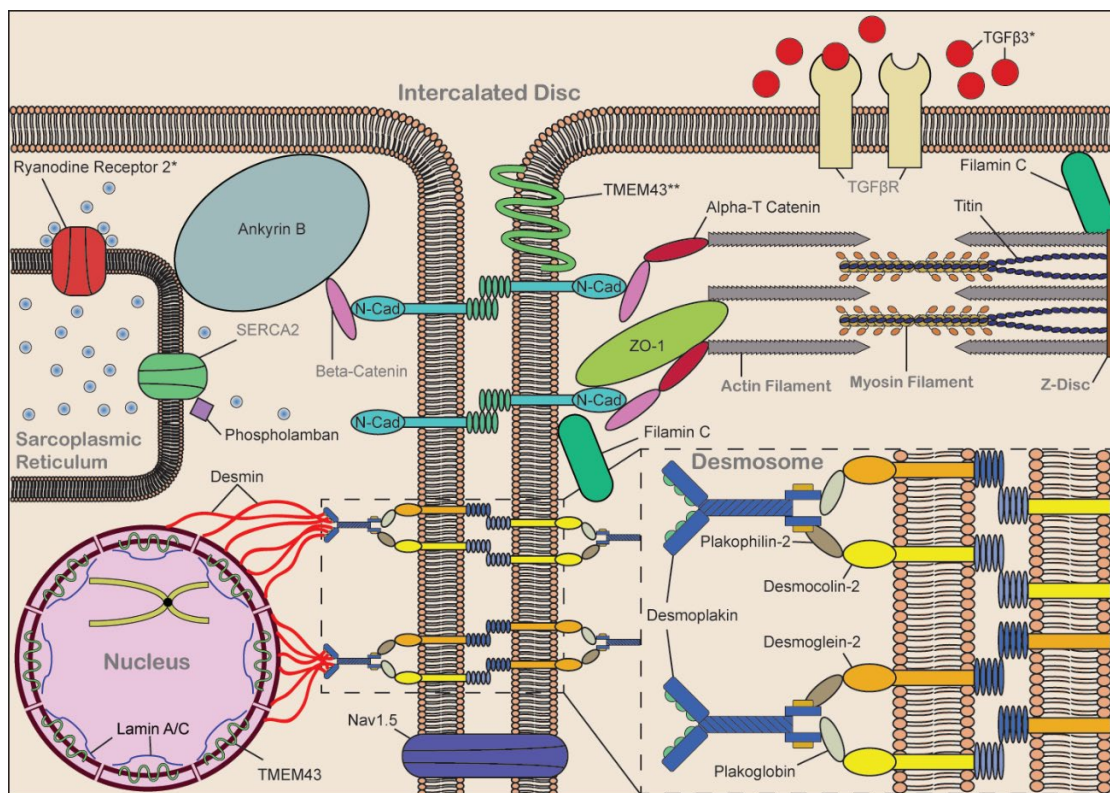


Figure 4: Schematic of ACM-associated proteins

Schematic of adjacent cardiomyocytes with key organelles and protein complexes labeled in grey bold text. Localization of the ACM-linked proteins provided, written in black text. Zoom in of the desmosome provided. *RYR2 and TGFβ3 considered borderline ACM genes. **Conflicting results over TMEM43 localization. Figure reused from a previous open access publication [45].

2.3.1 Desmosomal Genes

The desmosome is one of three major protein complexes that comprises the cardiac ID, where it links desmin between adjacent cardiomyocytes and acts as a cellular anchor to maintain cardiac tissue integrity following force generation [5] (Figure 4). The first gene linked to ACM was the desmosomal gene junctional plakoglobin (*JUP*) [174]. Desmosomes also play a key role in intracellular signaling and gap junction function [5, 131]. Associated genes plakophilin-2 (*PKP2*), *DSP*, desmoglein-2 (*DSG2*), desmocolin-2 (*DSC2*), and *JUP* comprise the majority of known ACM-causing variants, which are present in nearly 90% of cases with an identified genetic cause [42, 131, 165]. Desmosomal variants from the ARVC database are listed in Figure 5.

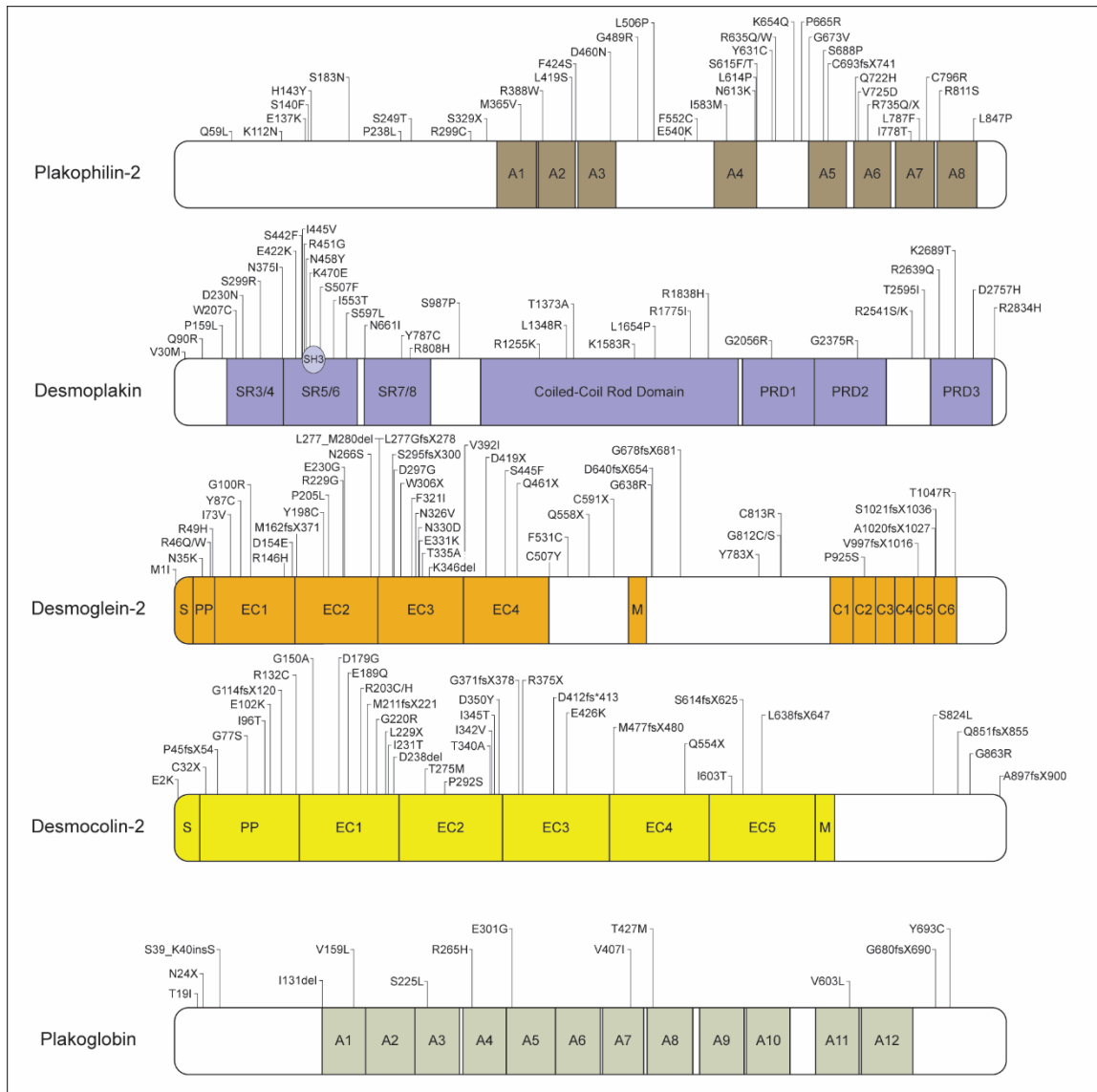


Figure 5: ACM-linked variant distribution among desmosomal genes

Linear diagram of the 5 desmosomal genes with labeled domains and the distribution of pathogenic ACM-variants. Variants of plakophilin-2 and desmoplakin limited to those mentioned throughout the review and missense variants among the ARVC database. Domain abbreviations: A, arm domain; SR, spectrin repeat; PRD, plakin repeat domain; S, signal peptide; PP, propeptide; EC, extracellular cadherin; M, membrane; C, cytoplasmic repeat. Figure reused from previous open access publication [45].

2.3.1.1 *Plakophilin-2*

Genetics: Variants in PKP2 are the most common cause of ACM, accounting for 32–81% of ACM cases with an identified causative variant [85, 159-160, 164, 175-177]. ACM-linked PKP2 variants frequently appear in highly conserved regions of the protein when compared to PKP2 variants in control populations [85]. Outside of its central structural role, PKP2 has been suggested to have a key role in recruitment of other ID proteins and may regulate expression of a variety of cardiac genes such as calcium handling genes, including ankyrin-B (ANK2), ryanodine receptor-2 (RYR2), and calsequestrin-2 [73, 75]. Additionally, PKP2 has been shown to interact with PKC [178] and β -catenin [179], both suggested players in fibrosis and adipogenesis. Most disease-causing PKP2 variants result in expression of a truncated protein secondary to frameshift, nonsense, and splice site mutations [173]. Fortunately, PKP2 variant carriers are spared from cardiac-cutaneous disease because PKP2 is not expressed in stratified epithelium [68]. Generally, PKP2 linked ACM cases have a traditional ARVC like phenotype with minimal LV involvement, although mild LV dilation and dysfunction has been noted in later stages [73, 131, 158-159]. Insight into disease development secondary to PKP2 variants is gradually emerging. Characterization of a pathogenic variant, Q62K, revealed increased protein turnover, along with an inability to initiate desmosome formation [180]. Evaluation of the pathogenic variant C796R revealed decreased protein stability, mislocalization to the cytoplasm, and disrupted binding with DSP. The mechanism of increased protein turnover in this variant, along with additional pathogenic missense/frameshift variants (S615F,

K654Q, and C693fsX741), was shown to be via increased calpain protease-mediated degradation [114].

Animal Models: With the majority of ACM-linked variants within desmosomal genes, the majority of ACM animal models have been designed to evaluate alterations in these genes. Whole body plakophilin-2 knockout (KO) mice were developed and were embryonically lethal at approximately embryonic day 11.5 (E11.5). Cardiac evaluation at E10.75 revealed multiple cardiac abnormalities, including atrial thinning, abnormal blood distribution, reduced ventricular trabeculation, abnormal ID structure with decreased adherens junction (AJ) heterogeneity, and disrupted DSP and DSG2 localization, resulting in DSP aggregate formation. Heterozygous (Het) KO mice were born healthy with no apparent cardiac phenotype [181]; however, further characterization revealed altered ID structure with sporadic or absent desmosomes, along with sodium current dysfunction [74].

A cardiac-specific and inducible (tamoxifen) KO mouse model was developed, aiming to evaluate the consequences at adult stages. Increased fibrosis, impaired wall movement, and dilation were observed in the right and left ventricle at 21 and 28 days post injection, respectively, and no animals survived 50 days post-injection [73]. This inducible model has a strong ACM phenotype with LV involvement, showing many traits of the human phenotype, including a concealed phase with altered connexin-43 (Cx43) and RYR2 function [75]. In addition, models with transgenic expression of truncated PKP2 (S329X, R735X) also result in cardiac remodeling that is exacerbated following exercise [182-183]. Truncated PKP2 has shown expression in cardiac tissue, and increased

transgenic dose is correlated with increased severity of disease progression. Overall, loss of full length PKP2 results in major cardiac defects leading to ACM.

2.3.1.2 *Desmoplakin*

Genetics: As a member of the plakin family, DSP directly interacts with the intermediate filament desmin to link the cytoskeleton to the remainder of the desmosome [5, 71]. DSP is essential for recruitment of plakoglobin (PKG) and DSG for proper desmosome formation [70] and is involved with trafficking the key gap junction protein Cx43 [71]. Loss of DSP leads to decreased Cx43 at the ID, as well as increased Cx43 degradation caused by increased phosphorylation levels via RAS signaling [71-72], a key kinase pathway essential for proper cellular proliferation and differentiation found to be improperly regulated in many diseases. This ultimately results in slowed conduction velocity that may be a substrate for ventricular arrhythmias (VA) [96]. *DSP* is ubiquitously expressed in desmosomal containing cells, and consequently, pathogenic variants are associated with cutaneous/cardiac–cutaneous disorders, including woolly hair disease, palmoplantar keratoderma, and Carvajal syndrome. Variants in *DSP* result in a variety of cardiac phenotypes, including left, right, and biventricular dominant ACM and dilated cardiomyopathy (DCM), and they are associated with LV dysfunction, heart failure, and SCD [86].

A variant “hot spot” has been identified in an evolutionary conserved SH3 domain surrounded by multiple spectrin repeats in the N-terminal portion of the protein [85, 93]. Molecular dynamic simulations show these structures are important for mechano-

stabilization that prevents rupture upon force generation, shown to be disrupted by multiple pathogenic variants. Similar to variants within PKP2, select DSP N-terminal variants display increased sensitivity to calpain [76], while others variants show an inability to interact with PKG [105]. Outside the N-terminal region, DSP variants are thought to be pathogenic through loss of proper homodimerization or disrupted interactions with desmin.

Animal Models: Whole body KO of DSP also shows embryonic lethality at ~E6–E6.5 due to defects in desmosome rich extra-embryonic tissues, resulting in a failure of egg cylinder formation within the ectoderm [92]. Cardiac specific KO of DSP was analyzed via Cre-recombinase expression under an MLC2v promotor (activated ~E9 [184]). Mice were born at normal Mendelian ratios, but showed 50% lethality by two months of age. Fibro-fatty infiltration was apparent, and through use of lineage labeling, showed adipose tissue of both cardiac and non-cardiac origin [185]. Interestingly, although Cx43, Cx40, DSC2, DSG2, and PKP2 displayed altered expression or localization, PKG was unaltered [185] despite being commonly altered in ACM cases [90, 186].

Two additional groups have generated het KO models using a α MHC-Cre system. Homozygous KO mice typically experienced embryonic lethality, although some survived until approximately two weeks of age with small hearts and unorganized chambers, with the presence of adipocyte-like cells. Het KO mice displayed a classic ACM like phenotype with altered Wnt/ β -catenin signaling, fibro-fatty infiltration, moderate ventricular dilation with reduced ejection fraction (EF%), and more frequent ventricular arrhythmias with or without exogenous stressors [90]. Years later, Gomes et al. examined a similar haploinsufficient model with a similar phenotype, with exception to a lack of functional

changes identified via echocardiography [96]. Interestingly, consistent with the mouse model, data from human hearts with ACM secondary to pathogenic *DSP* variants showed reduced PKG, Nav1.5, and Cx43 from the ID, and aggregates of Cx43 were also noted. Yang et al. established multiple transgenic variant models of DSP, identifying embryonic lethality in two variants (V30M, Q90R), and ID remodeling via disrupted desmin interactions [105].

2.3.1.3 Desoglein-2

Genetics: Two extracellular cadherin-like proteins, DSG2 and DSC2, stabilize the desmosome between adjacent cardiomyocytes. Along with *PKP2* and *DSP*, *DSG2* variants are found in a significant amount of ACM patients [85, 159-160, 164, 175-177]. *DSG2* variants occur in evolutionary conserved residues and cluster at an N-terminal mutational “hot spot” containing the first three N-terminal cadherin domains, along with a prosequence region [85]. These extracellular cadherin (EC) domains are vital for dimerization and mechanically stabilizing desmosomes, which have been shown to be disrupted by variants D154E and V392I [187]. Outside of the cadherin repeats, a noncoding variant in the 5' untranslated region (UTR), -317G>A, results in a loss of binding affinity with transcription factors. Evaluation of human tissue and ECG recordings revealed a borderline ARVC phenotype in patients with this noncoding variant [188]. N-terminal variants often prevent proper *DSG2* processing before protein maturation [86]. Pathogenic variants within the intracellular portion of *DSG2* can potentially dissociate interactions with PKG [86]. Although the majority of *DSG2* variants are autosomal dominant, gene

dosage is likely important, as cases of homozygous or multiple disease causing variants have been identified, often associated with a more severe phenotype [168, 189-191]. Homozygous variant F531C results in biventricular ACM with impaired ID ultra-structures [192]. Overall, variants in *DSG2* appear to generate a more severe form of ACM with more severe ventricular dysfunction, associated with a higher risk of heart failure in comparison to PKP2-linked ACM [193].

Animal Models: Complete KO of *DSG2* has been analyzed by multiple groups. Removal of exons 7–8 in previous mouse models resulted in complete embryonic lethality [194], while models with a lack of exons 4 and 5 were capable of surviving with increased rates of lethality [195]. These mice had low expression levels of a truncated protein capable of ID localization. *DSG2* KO mice displayed increased ventricular volume, diastolic dysfunction, reduced EF%, and fibrotic lesions. ECG traces following norepinephrine stimulation resulted in ventricular and atrial arrhythmias [195]. Increased ID heterogeneity and decreased desmosome formation was also observed [196]. Chelko et al. treated these mice with the glycogen synthase kinase-3 β (GSK3 β) inhibitor, SB-216763, and reported an improved cardiac function, decreased fibrosis, and normalized Cx43/PKG localization [197]. Overall, this model has an extreme, although variable, phenotype with many ACM features, including fibro-fatty infiltration and ID structural abnormalities.

A transgenic overexpression (α MHC) model of the ACM linked *DSG2* variant N271S (N266S in humans) was generated and displayed 30% lethality by 3.6 weeks. A severe biventricular phenotype was observed with chamber dilation and reduced systolic function at 12 weeks, along with signs of ventricular wall thinning and increased necrosis.

Conduction velocity was delayed along with multiple ventricular and atrial arrhythmias by six weeks. Fibrosis and calcification were noted as well; however, fatty infiltration was never observed [198]. Additional characterization in a later study showed reduced action potential (AP) upstroke velocity and sodium current, providing a unique potential arrhythmogenic mechanism associated with DSG2 variants [199].

2.3.1.4 *Desocolin-2*

Genetics: Although DSC2 structure and function is similar to that of DSG2, variants within DSC2 make up a smaller percentage of total ACM cases [85, 159-160, 164, 175-177]. Like DSG2, multiple ACM linked variants cluster within DSC2's N-terminus prosequence region at the N-terminus of the gene, shown to influence proper protein localization to the ID [86, 200-201]. Multiple variants have been reported that impact the EC1 and EC2 domains, key for dimerization and stabilizing intramolecular interactions between adjacent EC domains [86]. Variants within the EC1 domain potentially destabilize DSC2 and its extracellular interactions [200, 202-203]. Multiple variants within EC2 have also been reported, including a D350Y variant that alters interactions with calcium, key for stabilizing EC3 interactions [86, 191, 204]. Select variants have also been shown to cause mislocalization of DSC2 to the cytoplasm (E102K, I345T). In addition, multiple variants have been reported to alter binding affinity to PKP2/PKG, including truncated or non-expressed proteins (L229X, G371fsX378), loss of binding residues (A897fsX900), or improper protein maturation via impaired proteolytic processing (R203C, T275M) [205].

Outside of the traditional ARVC phenotype, LV and bi-ventricular dominant forms have been reported.

Animal Models: DSC2 overexpression in mice resulted in enlarged hearts with biventricular dysfunction, patchy areas of fibrosis, necrosis, and calcification by nine weeks of age, and prolonged QRS/QTc interval [206]. This was linked to extreme desmosome dysfunction, partially observed in fibrotic regions. While not representative of any known ACM-linked variants, overexpression of DSC2 did generate a rapid ACM-like phenotype producing focal regions of disrupted myocardium [206]. A unique Zebrafish model was generated based on a splice acceptor mutation (c.631-2A→G) resulting in a premature stop codon that led to decreased desmosome stability and a traditional ARVC phenotype caused DSC2 haploinsufficiency [207].

2.3.1.5 Plakoglobin

Genetics: Variants in *JUP* account for the smallest number of ACM cases among desmosomal genes. Similar to PKP2, PKG is an armadillo protein that is key for linking DSP to DSG2 and DSC2. Despite structural similarities, the binding domains that PKG and PKP2 use to interact with DSP are not identical [70, 94], possibly explaining the discrepancy in ACM cases between the two armadillo proteins. Additionally known as γ -catenin, PKG plays a pivotal role in both desmosome and AJ function [5], and protein recruitment (i.e., Cx43) [77].

Despite the rarity of ACM-associated *JUP* variants, alterations of PKG expression and localization are commonly seen in ACM cases and are believed to influence Wnt/ β -

catenin signaling, where increased nuclear PKG leads to decreased canonical signaling [90, 166, 186, 208-210]. Due to structural and functional similarities, γ -catenin is capable of competing with β -catenin and ultimately results in suppression of canonical Wnt/ β -catenin signaling [5, 90]. Suppression of canonical Wnt/ β -catenin signaling has been shown to promote adipogenesis, fibrosis, and apoptosis, and is believed to be one of the major drivers of fibro-fatty infiltration in ACM [5].

Animal Models: Multiple groups have established mouse models focusing on PKG alterations. Ruiz et al. developed a PKG KO mouse model that was lethal around E12–E16. Desmosomal and ID structural abnormalities, along with DSP mislocalization, were seen as early as E8, resulting in reduced contractility and tachycardia at E11.5 [211]. To avoid embryonic lethality, an inducible cardiac specific KO (α MHC/MerCreMer) with tamoxifen injections at six to eight weeks of age was developed. An ACM-like phenotype manifested at five months post injection with regional myocyte loss and fibrosis, along with right ventricular (RV) wall thinning, dilation, and increased cardiomyocyte size. Despite a lack of an arrhythmogenic phenotype, ID disorganization and increased SCD rates were observed as early as three months post injection [111].

Li et al. successfully generated a non-lethal KO model using α MHC-Cre system. A similar, more rapid overt cardiac phenotype was observed, including dilation, wall thinning, and fibrosis without fatty infiltration. This mouse model displayed SCD as early as one month, with an average lifespan of 4.6 months. Uniquely, electrical abnormalities including ventricular arrhythmias and conduction velocity defects were observed at

baseline that were exacerbated after induction [212]. This phenotype was more severe when generated in conjunction with a β -catenin KO model [213].

The PKG 2157del2 variant, associated with both ARVC and Naxos disease, was also studied in murine models [174]. Transgenic overexpression of either (wild type) WT or the truncated protein (shown to mislocalize to the cytoplasm and nucleus) resulted in decreased LV fractional shortening, diastolic dysfunction, electrical abnormalities, and fibro-fatty infiltration, with a more severe phenotype in the truncated model [110, 197]. Treatment of PKG 2157del2 mice with the GSK3 β inhibitor, SB-216763, resulted in an improved cardiac phenotype, as seen in DSG2 KO mice [197].

2.3.2 Non-Desmosomal Genes

Despite the frequency of variants in desmosomal genes, variants among genes outside the desmosome still contribute to a significant portion of ACM cases. Many of these additional genes are within the ID or interact with the desmosome; however, additional nuclear, sarcoplasmic reticulum (SR), and calcium handling proteins have also been implicated. Variants in the UTR region of transforming growth factor 3 (*TGF3 β*) were associated with an ACM phenotype in one study [214]; however, minimal studies since initial correlation make it unclear if *TGF3 β* is an ACM causing gene. Variants in *RYR2* are known to be a common cause of catecholaminergic polymorphic ventricular tachycardia (CPVT), a primarily electrical cardiac defect [215]. However, structural remodeling and ACM cases caused by *RYR2* variants have been reported [215-217]. Outside of *TGF3 β* and *RYR2*, multiple non-desmosomal genes have been connected to ACM.

2.3.2.1 *α-T-Catenin*

α-T-catenin is responsible for cellular adhesion within the ID via interactions with N-cadherin (N-Cad), PKP2, and *β*-catenin, and is an uncommon cause of ACM with only two reported disease-causing variants at highly conserved residues (V94D and L765del). Each variant has been suggested to cause a traditional ARVC-like phenotype with mild LV involvement. The V94D variant results in abnormal localization to the cytoplasm, along with reduced binding affinity for *β*-catenin and PKG. In contrast, the L765del variant protein has increased homodimerization with either wild type (WT) or variant *α*-T-catenin, resulting in aggresome formation [218], a common defect seen in variants of other non-desmosomal proteins linked to ACM [152, 219-221].

2.3.2.2 *Desmin*

DES is the cytoskeletal intermediate filament that interacts with the desmosome via desmoplakin interactions, and is responsible for cellular organization and connections to other protein complexes, including the Z disc [219]. Cardiac disease caused by *DES* variants are often reported with skeletal muscle involvement, referred to as desmin-related myopathy (DRM) or desminopathy [219, 222-223]. Variants associated with DRM or ACM result in altered desmin filament formation and localization, forming aggregates that can disrupt mechanical/chemical signaling and protein interactions [101, 219-220, 222, 224]. Desmin variants have been reported to result in severe right-sided heart failure, and biventricular forms of disease have also been observed [219-220, 224-226]. These variants

are diverse in their localization within *DES*, ranging from the head domain (S13F), to multiple central rod domains (N116S, N342D). It remains unknown how different variants result in separate cardiac disorders, along with how families with a single variant display significant phenotypic variability.

2.3.2.3 *Lamin A/C*

Variants in lamin A/C cause a unique LMNA cardiomyopathy, a subtype of ACM with significant LV involvement, and are one of the more common non-desmosomal causes of ACM [176, 227]. Lamins are ubiquitously expressed intermediate filament proteins that form scaffolding structures around the nuclear periphery, key for gene regulation, genomic stability, and nuclear integrity [228]. Multiple diseases have been linked to LMNA due its ubiquitous expression, including ACM and DCM (independent or co-segregates with non-cardiac abnormalities), muscular dystrophy, peripheral neuropathy, and lipodystrophy [176, 228]. Many variants commonly occur in conserved residues of the central rod domain (R190W, R72C, and G382V) or globular head of the protein (R644C), all of which are predicted to impact protein structure from in silico analysis [176], with select variants resulting in aggregate formation [152]. *LMNA* based ACM cases compared to desmosomal cases have shown significantly higher instances of bradycardia, a potentially unique feature to other forms of ACM [229].

2.3.2.4 *Phospholamban*

Variants in the non-desmosomal protein PLN makes up a considerable amount of ACM cases among non desmosomal genes [164]. Key for proper regulation of cellular calcium, PLN acts as the natural inhibitor of sarco/endoplasmic reticulum Ca^{2+} -ATPase (SERCA), the SR protein responsible for SR calcium reuptake following contraction [153]. Variants in PLN often result in phospholamban cardiomyopathy, a distinct form of cardiomyopathy with SERCA2 dysfunction that has an overlap of clinical features of ACM and may be considered a form of ACM itself. Generally, PLN-based ACM cases occur at an older age, but have more frequent LV involvement and increased risk of heart failure [159]. Cardiac phenotypes associated with the common R14del variant show extreme variability, including DCM and ACM of biventricular dominance [230]. Further characterization of the R14del variant revealed a potential pathogenic mechanism via aggresome formation [221]. When combined with WT PLN, this R14del variant results in extreme inhibition of SERCA1 [231]. Additional PLN variants have been identified in ACM cases [173], but have yet to be characterized in sufficient detail.

A PLN-p.R14del mouse model was established due to its being a prominent cause of cardiomyopathy within the Netherlands [153, 230, 232]. These mice showed a DCM like phenotype with ventricular dilation, myocyte disarray, and fibrosis along with increased propensity for SCD [231]. Human studies show R14del ACM cases typically have an additional variant to drive an ACM phenotype as opposed to DCM, so additional variants or stressors may make this a useful unexplored ACM model.

2.3.2.5 Transmembrane Protein 43

Reports have established the TMEM43-p.S358L variant as a rare cause of a highly penetrant form of ACM. Like LMNA, TMEM43 is associated with the internal nuclear membrane and plays a role in nuclear organization and stabilization via interactions with lamin and emerin. Controversy concerning TMEM43 function and localization in cardiac tissue remains, as reports have suggested expression is absent from the nucleus and instead locates to the ID [233]. TMEM43-p.S358L is the only variant associated with ACM, but with significant supporting evidence that it alters homodimerization and protein interactions [234-235] and results in a severe form of ACM that is frequently biventricular and confers a high risk of SCD. Catheter ablation is frequently ineffective at suppressing ventricular arrhythmias, and mainstays of therapy are β -blockade, exercise restriction, and ICD insertion. Unlike desmosomal forms of ACM, experts have advocated for primary prevention ICD insertion based on sex-specific age cutoffs, even in the absence of a positive clinical phenotype [235-237].

The TMEM43-p.S358L variant results in an extreme ACM phenotype in humans, and a cardiac specific (α MHC) mouse model expressing human TMEM43 S358L showed a similar severe phenotype [234]. This model displayed extremely high rates of SCD starting before 20 weeks, with nearly no survivors by 30 weeks. These mice were treated with a GSK3 β inhibitor via overexpression of a CnA β 1 splice variant, resulting in downstream activation of AKT, leading to phosphorylation and inactivation of GSK3. Treatment resulted in extended survival and partially improved cardiac structure and function in S358L positive TMEM43 mice [234].

2.3.2.6 *Titin*

As the largest protein in mammalian cells, titin (*TTN*) variants are very difficult to study, with the majority of variants resulting in *TTN* truncation. Variants within *TTN* are tightly correlated with DCM, and are also involved with muscular dystrophy, hypertrophic cardiomyopathy (HCM), and ACM, with the mechanisms of how variants result in a variety of phenotypes remains unknown [238-240]. Although primarily linked to DCM, specific genomic backgrounds or additional factors may promote an ACM phenotype to develop [238, 241-242]. One study sequenced *TTN* in eight ACM families and identified seven rare *TTN* variants characterized by classic signs of ACM with LV involvement and fibro-fatty infiltration, one of which (T2896I) was evaluated in further detail due to complete segregation of the disease with the variant. This variant occurs inside an immunoglobulin (IG) domain required for generating passive cardiomyocyte tension, unrelated to protein interactions [238]. Phenotypically, *TTN*-ACM cases are less severe compared to desmosomal based cases, but more so than ACM cases caused by non-desmosomal variants [239].

2.3.2.7 *Filamin C*

FLNC is a structural protein responsible for linking the sarcomere to the plasma membrane and extracellular matrix in skeletal and cardiac muscle, and is involved in maintaining ID integrity [171, 243-244]. Variants in *FLNC* have been shown to cause restrictive cardiomyopathy, DCM, and ACM with predominant LV involvement [171, 245-246]. A recent study identified two ACM-linked variants in *FLNC* (59_62DLQRdel,

K2260R), along with multiple null variants following genetic screening of ACM patients negative for variants in clinically examined genes. Further evaluation of tissue from SCD victims with *FLNC* null variants revealed reduced protein levels at the ID within the LV, but not the RV compared to controls. In addition Cx43 and DSP ID levels were reduced [171], potentially disrupting both ID stability and electrical signaling [71-72]. Interestingly, minimal changes to PKG and no alteration to GSK3 β levels were examined, common features in classic ARVC [171]. Additional studies have shown similar unique trends in ID protein localization [247], suggesting disease development may be unique in *FLNC* cases compared to others.

2.3.2.8 Voltage-Gated Sodium Channel Alpha Subunit 5

Nav1.5, transcribed via the *SCN5A* gene, is the primary voltage gated sodium channel in cardiomyocytes linked to a variety of arrhythmogenic disorders as well as DCM [248-250]. Similar to *TTN*, variants in *SCN5A* are more closely linked to DCM, but specific genomic backgrounds may promote ACM development [249-251]. Reports have suggested that PKP2 and Nav1.5 co-localize to the ID, and that *SCN5A* loss-of-function variants may contribute to a classic ARVC phenotype. A recent novel variant I137M was identified in an ACM patient with a variety of ventricular arrhythmias, although mild RV dysfunction and dilation were noted as well, which was not unexpected, as variants in ion channels have resulted in myocardial structural abnormalities. Additionally, another novel variant R1898H resulted in a similar phenotype with an identified decreased in sodium current [250]. Finally, a severe splice variant (C3840 + 1G > A) led to a loss of function of the

Nav1.5 channel, resulting in a severe electrical dysfunction with mild RV dysfunction. Although fibrosis was noted, fatty tissue was not discovered, suggesting this may be a unique form of ACM or ACM-like cardiomyopathy [252].

2.3.2.9 Tight Junction Protein 1/Zonula Occludens 1

Rare variants within *TJPI*, encoding tight junction protein-1 (TJP1), have recently been identified as a potential rare cause of ACM through whole exome sequencing [253]. TJP1, also known as ZO1, is a scaffolding protein that has been shown to interact with the ID through a variety of proteins, including Cx43, N-Cad, and α -T-catenin. Although an intriguing finding, further validation of TJP1 as a genetic culprit of ACM should likely be pursued prior to its incorporation of clinical genetic testing panels.

2.3.2.10 N-Cadherin

The extracellular cadherin of the adherens junctions of the ID, N-cadherin, is vital for proper ID formation, stability, and protein recruitment to mechanically link cardiomyocytes via interactions with multiple catenins. Similar to DSG2 and DSC2, variants have been reported within the extracellular domains that are key for protein dimerization and cellular adhesion. One variant that causes a traditional ARVC phenotype with mild wall thinning and fibro-fatty infiltration, D407N, occurs in a highly conserved residue from humans to zebrafish and is predicted to be damaging via in silico analysis [254]. The Q229P variant, which strongly segregates within the affected family, was also

predicted to be damaging and resulted in a similar phenotype, with the exception of lack of fibro-fatty infiltration [255].

2.3.2.11 *Ankyrin-B (ANK2)*

A recent study connected *ANK2* to ACM. Ankyrin-B is responsible for the localization and stabilization of key ion channels, transporters, and ion exchangers to the cell membrane and t-tubules, such as the sodium–calcium exchanger (NCX) and sodium–potassium ATPase. Previously, variants in *ANK2* have been linked to a variety of arrhythmogenic disorders including ankyrin-B syndrome [256], atrial fibrillation [257], and sinus node disease [258]. The AnkB–ACM study evaluated a proband with an identified E1458G variant, revealing biventricular dysfunction, sustained VA, and baseline bradycardia. Additional families with a genotype-negative ARVC diagnosis were reevaluated, and an additional M1988T AnkB variant was discovered that segregated within a family, although likely benign variants within *DSG2* and *DSC2* were identified as well. This family displayed a similar phenotype to AnkB cardiac specific KO mice, with reduced AnkB and NCX expression, along with abnormal Z-line targeting.

The cardiac specific KO of ankyrin-B in mice exhibited both electrical and structural cardiac abnormalities. This mouse model displayed baseline ECG abnormalities at baseline (bradycardia, QT prolongation) and developed sustained VA following epinephrine stimulation, resulting in multiple cases of sudden death. Although adipogenesis was not observed in this model, biventricular dilation with wall thinning, biventricular systolic dysfunction, and widespread fibrosis were findings that mirrored

those observed in other ACM models. Abnormal heterogeneous expression of β -catenin was also observed. GSK3 β inhibition, when administered either before or after the presence of cardiac dysfunction, resulted in an improved phenotype similar to that of control mice [109].

2.3.3 Additional ACM Models

A unique mouse model of a mutant laminin receptor-1 (LAMR1) resulted in a severe ARVC phenotype that was identified by chance. This transgenic model was established from a retroposon insertion, resulting in a 13-amino acid mutation, causing severe fibrosis and calcification of the RV free wall, which never extended to the LV despite equal expression level. Altered gene expression via disrupted histone protein-1 interactions were observed [259]. Despite the lack of major electrical abnormalities, this model may be useful in identifying fundamental differences between the LV and RV, and evaluating why select protein variants have a more severe effect on one ventricle over another.

Zebrafish studies do not have the ideal physiological relevance to humans as mice do, but are still capable of producing unique ACM models. The previously mentioned zebrafish model of the DSC2 variant c.631-2A \rightarrow G was able to reveal not only a reduced expression of DSC2, but disrupted desmosome and cardiac structure [207]. Additional zebrafish models examining alterations to PKG (2057del2) and DSP knockdown revealed multiple ACM phenotypic characteristics, partially restored following SB-216763 treatment [107, 260].

Canine and feline models of ACM have also been studied, which might be a more accurate representation of the human disease. Basso et al. used a boxer dog model to examine ventricular arrhythmias using holter monitors, where 23 genetic candidates for ARVC were identified. All dogs displayed fatty/fibro-fatty infiltration within the RV, with RV dilation and LV lesions seen in about half these animals. Ventricular arrhythmias were common among these animals and SCD was reported in nine dogs [261]. Another study reexamined feline models with congestive heart failure of RV origin. A traditional ARVC phenotype was seen with RV and RA dilation, along with fibrosis, arrhythmic events and/or fatty infiltration seen in all cats, some of which affected the LV [262]. Although the genetic culprits for ACM in the boxer dog model have not been identified, the similar human like phenotype may make evolved mammals more effective for analysis of therapeutic approaches.

Although not as effective at studying organ level cardiac physiology or arrhythmias when compared to animal models, cell models have contributed significantly towards variant protein analysis and their biochemical properties [263]. Isolation of human-induced pluripotent stem cells (iPSCs) allows for quick and efficient analysis of genetic variants by differentiation of iPSCs into cardiomyocytes (iPSC-CMs) [263], and this has been utilized to form engineered heart tissue [76]. HL-1 atrial cells have been utilized for evaluation of the cellular consequences associated with ACM linked variants, as well as evaluating the consequences of gene silencing [90, 114, 263]. Desmosome containing cell lines, including buccal mucosa cells, have significant value for evaluating structural and adhesive consequences associated with desmosomal variants [263].

2.4 Environmental Factors

One of the hallmarks of ACM is incomplete penetrance, even among a family with the same genetic variant. Some carriers may be asymptomatic for most of their life, while others may experience SCD at a young age, making it clear that in addition to the genetic background of these patient, additional environmental factors play a major role in the progression of the disease, as seen in a study of two sisters with drastically different phenotypes despite having the same PKP2 variant. Studying twins with ACM has shown significant diversity in phenotypic development as well [264]. Exercise is understood to be a major driver of ACM progression, and patients are advised to restrict any physical activity to minimize the risk for VA/SCD, as well as to prevent further cardiac remodeling. Additional environmental factors that increase cardiac stress, such as emotions, habitat conditions, and pregnancy may also contribute towards phenotypic progression.

2.4.1 Exercise

Depending on the genetic background and current disease progression, treatment and therapeutic options may vary significantly between individuals. However, exercise restriction is highly recommended for all carriers of an ACM-linked variant, and is considered for variant carriers without a phenotype [155]. One study in Italy analyzing 1642 competitive athletes identified 6% as possessing ARVC. Strikingly, 25% of SCD cases among athletes have been deemed secondary to ARVC in Italy [265]. This

overrepresentation of SCD, along with the majority of cases occurring during athletic activity, strongly suggests exercise is potentially detrimental to ACM/ARVC patients [265-266]. High cardiac strain has been linked to impaired myocyte cell–cell adhesion, resulting in premature cardiomyocyte death that may induce cardiac remodeling [155]. When ARVC patients or genotype positive individuals were studied for six years, a significant correlation was identified between exercise and both reduced RVEF% and increased rates of SCD [267]. Loss of cellular adhesion is a popular mechanism studied in many models of ACM [268], with multiple cell models showing reduced cell–cell adhesion following overexpression or reduction of desmosomal proteins [269-270]. Desmosomal dysfunction may be enhanced via volume overload and mechanical stress, providing additional evidence connecting ACM disease progression and vigorous exercise [142].

One study focused on exercise changes on ACM phenotype progression in patients with desmosomal variants. Of 87 studied individuals, endurance athletes were more likely to meet task force criteria (TFC) for ARVC diagnosis, and were more likely to develop ventricular tachycardia (VT) and ventricular flutter (VF), along with heart failure. Interestingly, only endurance athletes developed heart failure. These athletes were categorized by hours exercised per year, and those who exercised the most have the highest risk compared to more casual athletes. In fact, those who reduced exercise (≤ 515 h/yr.) showed improved survival following an initial sustained VT/VF event [271]. Finocchiaro et al. examined over 400 cases of SCD among athletes, including 48 cases of ACM. The majority (61%) of SCD cases occurred during exertion, including 91% of those diagnosed

with ARVC. Interestingly, LV involvement was a common feature among ARVC athletes, with 35% of cases showing LV fibro-fatty infiltration and 85% with LV fibrosis [272].

Two ACM mouse models described previously, a PKG heterozygous KO [273] and truncated PKP2 (R735X) overexpression model [182], both underwent swim training to accelerate disease progression. Trained mice displayed an increased incidence of spontaneous VT at an earlier age than untrained mice and developed a more severe ACM phenotype [273]. Factors affecting oxygen availability and air quality, such as high elevation, high levels of pollution, or being underwater may enhance cardiac stress during exercise. In addition, extreme temperatures or high humidity can lead to increased workload of the myocardium compared to normal conditions while exercising [274].

Among non-athletes, sudden death occurs less frequently during exercise or exertion. Over 75% of cases of death resulted during daily activities at “rest”, including at home, work, or walking on the street, with only about 3.5% occurred during some sort of sport or exercise. The remaining percentage died during unique events not considered a normal daily activity, including surgery or car accidents, or childbirth [136]. Further complexity is added to the role of exercise among ACM development in genotype negative individuals, or those without a variant in a known ACM-associated gene. La Gerche et al. observed that athletes without genetic variants still developed an ACM phenotype with ventricular arrhythmias and systolic dysfunction. However, athletes without an identified mutation were less likely to develop severe RV dysfunction (33% to 3%) when compared to those with a mutation. Interestingly, no fibro-fatty infiltration was noted [137], further indicating a separate phenotype among those without a mutation. While it has been

proposed that a separate exercise-induced RV cardiomyopathy may explain an ACM like phenotype with select differences, studies have challenged this, suggesting the phenotype is identical between the two groups [164].

2.4.2 Additional Factors

Beyond exercise, additional external factors are proposed to be potential drivers for either arrhythmias or disease progression through additional cardiac stress. Multiple emotional triggers, including anger and stress, may increase sympathetic drive via β -adrenergic signaling, causing increased oxygen demand to maintain increased myocardial contractility and heart rate [274-275]. Therefore, competitive sports, even those among low cardiac stress, could be a stimulus for arrhythmias and SCD. Indeed, analysis of SCD among athletes identified two individuals who experienced lethal arrhythmias while playing golf [272], categorized under the least cardiac strenuous section of exercise [274]. Multiple arrhythmogenic conditions have been previously associated with increased prevalence of arrhythmias following emotional distress, including atrial fibrillation, CPVT, and long QT syndrome. Among non-athletes with ACM, stressful situations including minor car accidents, falls without apparent injuries, car theft, or child birth have all been stimuli resulting in SCD (~20% of deaths among non-athlete ACM patients).

2.5 Clinical Management of Arrhythmogenic Cardiomyopathy

Although ARVC is most commonly an autosomal dominant, genetically inherited disease, only up to 50% of patients have an identifiable desmosomal variant, leaving the cause of remaining ACM cases due to less common or unknown variants [276]. ARVC should not be considered a monogenic disease, but rather an oligogenic or polygenic disease. Many ARVC associated alleles have low pathogenicity, and a family member harboring just one variant might not display the ARVC phenotype [277]. Xu et al. found digenic and compound heterozygous variants to compile a significant portion of ARVC probands [191], which emphasizes the potential role of the gene dosing effect of ARVC penetrance [277]. Further, incomplete penetrance creates variation in the severity of symptoms across a family, potentially complicating recognition of familial disease, particularly if thorough cascade screening is not performed [278]. Unfortunately, diagnosis of ACM remains challenging, resulting in SCD as the first symptom of the disease in some cases [279]. In 2010, updated task force criteria gave clinicians further guidance to diagnose the disease with testing modalities including 2D echocardiogram, cardiac magnetic resonance (CMR), and ECG measurements [140].

The most concerning clinical symptom that clinicians screen for is effort-induced syncope. Other common clinical findings upon testing include T-wave inversion in leads V1–V4 of the ECG, ventricular arrhythmias, such as isolated premature ventricular contractions and non-sustained ventricular tachycardia on Holter monitoring, and right ventricular dilation on imaging studies [278].

Although specific International Task Force guidelines are in place for proper ARVC diagnosis, limitations still exist. Over-diagnosis from genetic screening,

misinterpretation of ECG and echocardiogram recordings, and underutilization of CMR can all lead to misdiagnosis, especially considering the symptom overlap with other cardiomyopathies [280]. Since publication of the updated task force guidelines, more advanced imaging techniques have become more prominent in diagnosis. With 3D echocardiogram, accurate measurements of RV volume and RVEF% can be made, providing a useful tool for RV systolic function quantification. Further, CMR with late gadolinium enhancement can help with ACM diagnosis when only the left ventricle is involved. CMR ultimately provides the best measurement for RV wall abnormalities, RV volumes, and RV-EF. CMR abnormalities alone are unusual unless the ACM variant resides in the left ventricle alone [281].

Depending on the severity of symptoms, among individuals that have a positive clinical phenotype, management usually starts with restriction of physical exercise and β -blockade [271]. ICD insertion is recommended for patients deemed at significant risk for SCD following appropriate risk stratification. Additional pharmacological intervention with anti-arrhythmic drugs may also be advised to minimize the incidence of sustained VAs, which can result in painful and distressing ICD shocks [282]. Similarly, catheter ablation can also be used to suppress VAs, and a combined endocardial–epicardial approach is often necessary, given that the disease originates in the epicardium and migrates inwards. Heart transplant is the last option and may be required for refractory ventricular arrhythmias or heart failure [278, 283]. With the wide range of ACM symptoms and therapeutic options, treatment is best individualized through risk stratification tools and expert clinical care.

2.5.1 Risk Stratification for SCD and Implantable Cardioverter–Defibrillator (ICD) Placement

Prior to the initiation of treatment strategies for ACM patients, particularly ICD insertion, effective risk stratification is crucial. Clearly, the most concerning consequence of ACM is SCD. The best prevention method for known SCD risk is an ICD, so predictions for risk of SCD are essential in targeting patients that require ICD treatment [282]. Identifiable variables for proper risk stratification include sex, age, cardiac syncope events in the prior six months, frequency of non-sustained VT, frequency of premature ventricular contractions (PVCs) within 24 h, number of leads with T-wave inversions, and RVEF%. A recently developed risk calculator showed particular promise by providing VA risk projections across 528 definite ARVC patients with no history of sustained VA, which decreased inappropriate ICD implantation compared to the 2015 task force model. This updated model is currently awaiting additional validation with external, more diverse cohorts [284]. The more common model, the 2015 International Task Force Consensus Statement Risk Stratification Algorithm of ICD placement, uses similar variables and places patients into class indications based on risk factors. Class 1 patients have the greatest risk, and placement in this class requires prior VT or VF, severe RV dysfunction, or severe LV dysfunction. The greater the symptom, the higher the class indication for a patient. This model has been shown to work well clinically, but class 1 and class 2a patients had indistinguishable ventricular fibrillation/flutter events, and the model is limited in its ability to help in primary prevention [285]. As more information surfaces about left ventricular

involvement in ACM, the ability of CMR to identify left ventricular subtypes may be critical in future risk stratification models. A 2019 publication by Miles and colleagues found that the vast majority of SCD cases in ACM patients had left ventricular involvement [150]. Beyond risk assessment from clinical phenotype, certain genotypes are also associated with an increased risk of future major arrhythmic events. ACM subtypes associated with PLN, LMNA, FLNC, TMEM43-pS358L, and DSP have unique features that have separate reported guidelines/suggestions for treatment options [172, 280, 282, 286]. While the 2010 guidelines for ARVC diagnosis have been an improvement, they fail to properly evaluate the genetic background of the disease and account for ACM subtypes outside of ARVC, including left dominant forms [280]. Regardless of risk assessment, exercise restriction is a precautionary measure every ACM patient should take. Should an ACM patient be asymptomatic under proper therapy, noncompetitive and low strain activities are acceptable. Unfortunately, exercise restriction is not sufficient in isolation, as made evident by a study by Wang and colleagues, which showed 58% of athletes still experienced VA after severe reduction in exercise (>80%) [287].

Patients with high risk for SCD from risk stratification should swiftly receive ICD therapy, or if antiarrhythmic drugs and lifestyle changes fail to manage ARVC symptoms. In 2003, Corrado and colleagues evaluated the impact of ICD implantation on SCD prevention in 132 ARVC patients. About 48% of patients who received appropriate ICD intervention did not experience episodes of VT [288]. Males were shown to have a much higher survival rate (95% vs. 65% five-year survival rate) than controls when ICD was used as a primary therapy for cardiomyopathy management, but this same trend did not

translate as strongly to females (97% vs. 85% five-year survival rate) [289]. Unfortunately, inappropriate ICD shocks can be discharged by sinus tachycardia or atrial tachycardia, which adds morbidity to the patient and poses a risk to cardiac health. Proper ICD intervention, however, can be further controlled with other therapeutic options like drug therapy or ablation [155].

2.5.2 Anti-Arrhythmic Medications

Antiarrhythmic medications represent a critical therapeutic approach for ARVC patients. After insertion of an ICD, many ARVC patients continue to require antiarrhythmic medications to reduce the frequency of ICD shocks. Marcus et al. showed that amiodarone significantly decreased the risk of clinically relevant VA (ICD shock or sustained VT) in ARVC patients undergoing ICD therapy [157]. In another study, a combination of flecainide with sotalol/metoprolol was shown to terminate arrhythmias in six of eight patients with diverse ARVC symptoms and variants. Overall, flecainide with sotalol/metoprolol could be a combination therapy for patients refractory to a single-agent therapy or ablation [290], but larger studies are urgently needed. Importantly, a CAST (cardiac arrhythmia suppression trial) study showed higher incidence of death due to arrhythmia and shock in patients who previously suffered myocardial infarction and took flecainide compared to the placebo group, suggesting patients with ventricular scarring should avoid flecainide [291]. A randomized drug study with flecainide and ARVC patients is currently underway (Pilot Randomized Trial With Flecainide in ARVC Patients, NCT03685149, currently ongoing) to provide more insight into the efficacy of flecainide

[292]. Overall, there are no published randomized trials of ARVC patients using various anti-arrhythmic drugs, so drug therapy is often left to the clinician's discretion based on personal history. Importantly, there is no clear consensus on the best anti-arrhythmic drug; therefore, it likely depends on the individual patient.

2.5.3 Catheter Ablation

Catheter ablation is frequently used as a tertiary treatment option for ARVC patients after pharmaceutical intervention and ICDs. Anti-arrhythmic drugs are initially considered to reduce the frequency of VA to prevent painful ICD discharges. However, ablation procedures can often more effectively reduce the risk of recurrent arrhythmias. Although ablation procedures are considered palliative rather than curative, combined endocardial–epicardial ablation procedures have been shown to be remarkably effective [278]. Mahida and colleagues compared the effectiveness of anti-arrhythmic drugs (AAD) and beta blockers (BB) to VT ablation in ARVC patients with a minimum of three VT episodes. A single ablation procedure (both epicardial/endocardial and endocardial only) left 35% of patients free of VT for three years, while 28% of AAD/BB patients were VT free after three years, forcing many patients to require subsequent ablations. However, following a total of 75 patients after the last ablation, 71% of endocardial/epicardial ablation patients were VT-free after three years compared to 47% of patients who underwent endocardial ablation only [293]. Another study with an average follow-up of over four years reported a cumulative VT-free survival rate of 71% across 62 ARVC patients after endocardial only or epicardial/endocardial ablations, which again displayed

the heightened success rate afforded by epicardial ablation [294]. In contrast, Christiansen and colleagues found that although ablation procedures decreased the burden of VA in ARVC patients, recurrence of arrhythmias was evident in 74% of cases just five years after the first ablation procedure [295]. The low percentage of patients that underwent epicardial ablation procedures (16%) may have contributed to the high recurrence rate, which again highlights the importance of epicardial ablation when necessary. Although not completely exempt from surgical complications or need for multiple procedures, catheter ablation remains a good therapeutic option after ICD and anti-arrhythmic drug treatment if ventricular arrhythmias still endure.

2.5.4 Sympathectomy

The autonomic nervous system has long been known to modulate heart rate and cardiac output via the sympathetic and parasympathetic nervous systems via innervation from the right/left stellate ganglia and medulla to the heart, respectively. Reducing sympathetic output via neuraxial modulation by left cardiac sympathetic denervation (CSD) (surgical dissection and resection of the stellate ganglion) protected against various refractory VA in five of nine patients with structural heart disease when all other therapies failed [296]. Preliminary ARVC-specific studies suggest bilateral CSD could be a valuable tool when anti-arrhythmic drugs, in combination with ICD and catheter ablation, fail to stop recurrent VT [297-298]. Although larger ARVC patient sample groups should be studied, ARVC CSD data agrees with more general studies showing the ability of bilateral CSD to decrease recurrent VT (and therefore ICD shock intervention) in patients with

structural heart disease, particularly when drug therapy and epicardial/endocardial ablation have failed to treat the arrhythmias [299-302].

2.5.5 Heart Transplant

Heart transplant remains the last option for ARVC therapy. If refractory ventricular arrhythmias remain after exploring all other therapeutic options, or if the disease has progressed to left or right ventricular heart failure, or more rarely, diffuse biventricular heart failure, heart transplant is required [283]. Overall, survival rates in ARVC patients who received heart transplants are better compared to patients with other cardiomyopathies such as restrictive, ischemic, dilated, and hypertrophic over a follow up period of 10 years. Although severe heart failure in ARVC is rare, carriers for a *PKP2* variant alongside a second ARVC variant were the most likely to suffer severe RV dysfunction and require heart transplant.

2.6 Future Implications

Successful management of ACM must address the three major components of the disease: myocardial damage (fibrosis and myocyte apoptosis), electrophysiological abnormalities (action potential remodeling and ventricular arrhythmias), and inflammation [303]. Garcia-Gras et al. previously identified that loss of desmoplakin resulted in a reduction of Wnt/ β -catenin signaling [90]. SB-216763 was initially discovered to inhibit GSK-3 β , therefore activating glycogen synthesis and expression of β -catenin [304].

Further, SB-216763 successfully rescued the ACM phenotype in a zebrafish model for ACM, which expressed a human 2057del2 variant in the plakoglobin (PKG) encoding gene. Interestingly, SB-216763 was also able to rescue and restore the reduction in I_{Na} and I_{K1} in the zebrafish model of ACM [260]. A second zebrafish model, deficient in desmoplakin by knockdown of *dspa* and *dspb* genes, was also rescued via pharmacological treatment with SB-216763 [107]. Even in rare forms of ACM (a rare *ANK2* variant), Wnt/ β -catenin activation therapy prevented and partially reversed the development of the ACM phenotype in an AnkB cKO murine model [109]. The ability of Wnt/ β -catenin pathway activation to rescue various forms of ACM from different gene variants suggests that the Wnt/ β -catenin may be a common underlying pathway disrupted in ACM development. Future studies should explore other GSK-3 β inhibitors as potential therapies for ACM to gain further insight into the specific mechanism of protection provided by GSK-3 β inhibition, allowing these drug trials to move to clinical trials.

Gene therapy can allow for the mutant gene to be replaced, or potentially even repaired, and has been explored as a potential treatment for genetic muscular dystrophies and associated cardiomyopathies [305]. Although few studies have explored gene therapy for ARVC, gene therapy has been shown to delay onset of familial HCM if treatment begins shortly after birth in a transgenic mouse line. HCM is an autosomal dominant genetic disorder, like many forms of ACM, and is linked specifically to variants in the sarcomeric proteins, causing SCD in young adults [306]. In preliminary gene therapy research for ACM, the loss of cardiac Wnt signaling due to DSP deficiency was restored by genetic manipulation of DSP expression in a ACM type 8 zebrafish model [107], giving hope that

future genetic intervention could reverse the ACM phenotype in well documented variants. While gene therapy shows great promise, the use of gene silencing may be problematic for many ACM cases, as many ACM associated genes, including desmosomal genes, do not show tolerance for haploinsufficiency [73-74, 92, 171].

In summary, ACM is an inherited disease that results from fibro-fatty remodeling of the myocardium and subsequently predisposes subjects to life-threatening ventricular arrhythmias. The complexity of this cardiac disorder is partially attributed to the diversity of genetic abnormalities. At the moment, there is no widely-available therapeutic option that targets the patho-physiologic course of the disease; rather, clinical management of ACM patients is restricted to the treatment of symptoms. Understanding the role of genetics and environmental factors that contribute to disease progression and its underlying pathophysiological mechanisms is crucial to developing new treatment strategies for this complex, life threatening disorder.

Chapter 3. Humanized *Dsp* ACM Mouse Model Displays Stress-induced Cardiac Electrical and Structural Phenotypes

Tyler L. Stevens^{1,2}, Heather R. Manring³, Trevor Dew^{1,2}, Michael J. Wallace^{1,2}, Peter Papaioannou^{1,4}, Aaron Argall^{1,2}, Steve Antwi-Boasiako¹, Xianyao Xu¹, Stuart G. Campbell^{5,6}, Fadi G. Akar^{5,7}, Maegen A. Borzok⁸, Thomas J. Hund^{1,9,10}, Peter J. Mohler^{1,2,10}, Sara N. Koenig^{1,10,*}, Mona El Refaey^{1,4,*}

¹Frick Center for Heart Failure and Arrhythmia Research, The Dorothy M. Davis Heart and Lung Research Institute, The Ohio State University Wexner Medical Center, Columbus, OH 43210, USA.

²Department of Physiology and Cellular Biology, The Ohio State University College of Medicine and Wexner Medical Center, Columbus, OH, 43210, USA

³Comprehensive Cancer Center, The Ohio State University College of Medicine and Wexner Medical Center, Columbus, OH 43210, USA.

⁴Department of Surgery, Division of Cardiac Surgery, The Ohio State University College of Medicine and Wexner Medical Center, Columbus, OH 43210, USA

⁵Department of Biomedical Engineering, Yale University, New Haven, CT 06520, USA.

⁶Department of Cellular and Molecular Physiology, Yale School of Medicine, New Haven, CT 06520, USA.

⁷Department of Internal Medicine, Section of Cardiovascular Medicine, Yale School of Medicine, New Haven, CT 06520, USA.

⁹Department of Natural Sciences, Mansfield University of Pennsylvania, Mansfield, PA 16933, USA.

⁸Department of Biomedical Engineering, The Ohio State University, Columbus, OH 43210, USA.

¹⁰Department of Internal Medicine, Division of Cardiovascular Medicine, The Ohio State University College of Medicine and Wexner Medical Center, Columbus, OH 43210, USA

***Correspondence**

Mona El Refaey
Mona.ElRefaey@osumc.edu
Phone: 6143662748

Sara N. Koenig
Sara.Koenig@osumc.edu
Phone: 6143660510

Key Words: Desmoplakin, Arrhythmogenic Cardiomyopathy, Arrhythmia, Mouse Model, Intercalated Disc, Cardiac Stress.

3.1 Abstract

Arrhythmogenic cardiomyopathy (ACM) is an inherited disorder characterized by fibro-fatty infiltration with an increased propensity for ventricular arrhythmias and sudden death. Genetic variants in desmosomal genes are associated with ACM. However, incomplete penetrance is a common feature in ACM families, particularly those affected by missense variants. This complicates the understanding of how external stressors contribute towards disease development, as well as understanding the molecular pathways responsible for ultimate phenotypes. To better understand the pathways underlying incomplete penetrance associated with specific DSP variants, we developed one of the first mouse models of ACM that recapitulates a human variant by introducing the murine equivalent of the human R451G variant into endogenous desmoplakin ($Dsp^{R451G/+}$). The desmoplakin (DSP) variant (p.R451G) is linked with post-translational degradation due to increased sensitivity to the protease calpain. Mice homozygous for this variant displayed embryonic lethality. While $Dsp^{R451G/+}$ mice were viable with reduced expression of DSP, no presentable arrhythmogenic or structural phenotypes were identified at baseline. However, increased afterload resulted in reduced cardiac performance, increased chamber dilation, and accelerated progression to heart failure. In addition, following

catecholaminergic challenge, *Dsp*^{R451G/+} mice displayed frequent and prolonged arrhythmic events. Finally, aberrant localization of connexin-43 was noted in the *Dsp*^{R451G/+} mice. In summary, cardiovascular stress is a key trigger for unmasking both electrical and structural phenotypes in an ACM model.

3.2 Introduction

Arrhythmogenic cardiomyopathy (ACM) is characterized by fibro-fatty replacement of ventricular myocardium and increased propensity to fatal arrhythmias [140, 307]. In an early pre-symptomatic “concealed phase”, structural hallmarks of ACM are unidentifiable, yet the risk for life threatening ventricular arrhythmias and sudden cardiac death (SCD) is apparent, with up to 50% of index cases experiencing SCD as the first clinical manifestation [43-44, 147]. Incomplete penetrance further complicates the disease progression, as individuals with the same disease-causing variant may experience significant differences in disease symptoms and severity [142].

Despite the large variance in genetic causes and environmental factors, the majority of ACM cases with a disease-causing variant (~85-90%) are linked to variants in desmosomal genes [160, 164, 268]. Desmoplakin (*DSP*) has an N-terminal mutational ‘hotspot’ for ACM variants [85]. Indeed, previous work identified select variants in this region have sensitivity to calpain-mediated degradation [76]. We further focused our work on one calpain-sensitive DSP variant (p.R451G) and using induced pluripotent stem cells (iPSCs) from ACM patients within a single kindred, identified reduced post-translational expression of the full length protein [76]. While this was important in identifying how

multiple DSP variants share a specific mechanism of pathogenicity, a major limitation of these models is understanding phenotypic progression. Furthermore, incomplete penetrance is frequently observed in ACM families, and multiple carriers of the R451G variant fail to display any ACM phenotype.

Nearly every ACM animal model relies on a knock-out or transgenic knock-in system [75, 90, 96, 105, 138, 212, 308], with most models failing to explain phenotypic discrepancies between individuals carrying the same variant. Here, we report the generation of one of the first ACM disease models endogenously expressing the human equivalent of a point variant in *DSP* using CRISPR/Cas9 gene editing. *Dsp*^{R451G/+} mice displayed decreased full length DSP protein level with no differences at the transcript level. Attempted generation of a homozygous variant model (*Dsp*^{R451G/R451G}) led to the discovery of embryonic lethality prior to E10, supporting severe detrimental effects associated with the variant. *Dsp*^{R451G/+} mice displayed no changes in cardiac structure or function throughout adulthood in the absence of stress. Additionally, *Dsp*^{R451G/+} mice did not show baseline arrhythmias or other electrical abnormalities at baseline. However, *Dsp*^{R451G/+} mice progressed to heart failure at an earlier timepoint following pressure overload with increased chamber dilation and reduced fractional shortening. Moreover, *Dsp*^{R451G/+} mice displayed increased prevalence and severity of prolonged arrhythmias following catecholaminergic challenge. At the molecular level, altered localization of connexin-43 (Cx43) was noted in *Dsp*^{R451G/+} hearts. These findings highlight the role of cardiac stress in ACM disease phenotypes and severity.

3.3 Materials and Methods

Animal studies: The R464G (murine equivalent of human R451G) variant was introduced into endogenous *DSP* (whole body) in a C57BL/6J background using a CRISPR/Cas9 system guided by single-stranded oligodeoxynucleotides. The incorporation of this variant introduced a restriction enzyme site for BstNI. Sanger sequencing was used to identify founders capable of starting the R451G. All experimental mice were backcrossed into a pure C57BL/6 background and wildtype littermates were used as controls throughout the manuscript. Genotypes were confirmed using PCR with restriction enzyme digest and Sanger sequencing. Age-matched male and female mice were used throughout the studies to analyze potential sex-based differences (not observed in this study, so male and female findings were combined). Adult mice were studied between the ages of 12-16 weeks of age, with older mice characterized at 22-28 weeks of age. All animal experiments were conducted in accordance with the Ohio State University Institutional Animal Care and Use Committee guidelines.

Embryo isolations: $Dsp^{R451G/+} \times Dsp^{R451G/+}$ crosses we set up for <16 hour to identify the timepoint of $Dsp^{R451G/R451G}$ embryonic lethality. Females were examined for a vaginal plug, and males were immediately removed from the breeding cage. Female mice were aged for appropriate embryonic stage development prior to isolation (E4, E6, E8, E9.5, E11.5, E13, and E16). Embryos were isolated, separated from the placenta, and imaged to identify any abnormalities. Tissue samples/yolk sacs were digested and sent for sequencing to verify genotypes.

Transverse aortic constriction (TAC) surgeries: All mice used for surgery were aged between 12-15 weeks, weighing between 22-25g. Surgeries were conducted as previously described [309]. The surgeon was blinded to genotype. TAC mice had baseline measurements recorded within 48 hours of surgery. Measurements were recorded at two, four, six, eight, ten, and twelve weeks post-surgery.

Telemetry Surgeries: Telemetry implantation procedures were performed as described [309].

Echocardiography: All mice were anesthetized using 2.0% isoflurane in 95% O₂ and 5% CO₂ at ~0.8 L/min. Oxygen administration was continued with ~1% isoflurane throughout the recording process. Following hair removal, recordings were collected of the left ventricle (LV) in a long axis view, with contractile parameters and chamber dimensions being recorded using M-mode function in the short axis view. Parameters analyzed in short axis M-mode include: left ventricular internal diameter at systole and diastole (LVIDs/d), interventricular septal end systole and diastole (IVSs/d), end systolic volume (ESV), end diastolic volume (EDV), left ventricular posterior wall end systole and diastole (LVPWs/d) ejection fraction (EF%), fractional shortening (FS%), and heart rate (HR-BPM). Heart rate was monitored throughout imaging and any recordings associated with a heart rate <400 bpm were excluded.

Electrocardiograms: Telemeter ECG recordings were conducted using Ponemah acquisition software ten minutes prior, and 30 minutes after 2mg/kg intraperitoneal epinephrine injections. All ECG files were analyzed using LabChart (8) software. Intervals analyzed include RR interval, PR interval, P duration, QRS interval, QT/QTc interval

(Mitchell et al. normalization [310]), T_{peak-Tend} interval, and heart rate. Surface ECG analysis was only conducted on mice post-TAC surgery, with ten minute recordings being conducted at baseline, four, eight, and twelve weeks post-surgery. Arrhythmic events analyzed include premature ventricular contractions (PVC), atrioventricular (AV) block, non-sustained ventricular tachycardia (NSVT- minimum of 3 consecutive PVC events lasting <1 second [311]), ventricular tachycardia (VT, >1 second event), and bigeminy (regular sinus beat followed by PVC, at least 3 consecutive occurrences [312]).

Immunoblotting: All murine hearts were washed in cold PBS to remove blood, and immediately placed in either chilled 1% SDS-1% BME lysis buffer with protease inhibitor (PI) for standard protein isolation, or PhosphoSafe extraction reagent (Millipore-71296) with PI for evaluating phosphorylated targets (pCx43). Samples were homogenized using bead homogenization (Precellys 24, Bertin technologies). Following protein quantification, 40ug of protein was used to prepare each sample. Samples were electrophoresed on either a NuPAGE 3-8% Tris-Acetate gel for >250kD proteins (DSP), or Blot 4-12% Bis-Tris Plus gel for <250kD proteins. Membranes were blocked in 5% NFDM or Casein (Thermo Scientific) for one hour, depending on the protein of interest. Following blocking, membranes were incubated with a primary antibody overnight at 4°C and then incubated with secondary antibody for two hours at room temperature. Densitometry was performed using Image J software.

Immunofluorescence: Whole hearts were isolated from either 16-18 week old (Plakoglobin and Connexin-43 staining), or 26-28 week old (DSP staining) *Dsp*^{R451G/+} mice and control littermates. All hearts were submerged in OCT, oriented for four chamber view

sectioning, and frozen using liquid nitrogen vapors. Hearts were sectioned at The Ohio State University's murine pathology core laboratory. Adult ventricular cardiomyocytes were prepared as previously described [313-314]. Isolated cells were fixed and stored in 70% EtOH at -20°C. Both isolated cardiomyocytes and cryosections were blocked for two hours in fish blocking solution (3% fish gel, 0.75% Triton X100 [10%], and 1% DMSO), followed by overnight incubation in primary antibody at 4°C. Samples were washed the following day and incubated in secondary antibody at room temperature for two hours. For negative controls, replicate sections/cells were only incubated with secondary antibodies for two hours. Sections and isolated cells were covered with Vectashield imaging medium with DAPI (Vector Laboratories), and coverslips were applied and sealed. Images were obtained using a confocal microscope (510 Meta, Carl Zeiss, Inc.) Images were collected using identical confocal protocols settings at room temperature, and the observer was blinded to the genotype.

Transcript analysis: Total RNA was isolated from 12-16 week old hearts. Hearts were immediately placed in Trizol and bead homogenized at 4°C. RNA concentrations and purity were analyzed using a Nanodrop (ND1000). Purified mRNA (2µg) underwent reverse transcription using the SuperScript IV VILO Master Mix with ezDNAase enzyme protocol. qPCR was performed on cDNA examining *Dsp* levels, using *Hrpt* as a comparable control.

Tissue histology and staining: Whole hearts were isolated from 24-28 week old *Dsp*^{R451G/+} and control littermates, as well at end timepoints of ~16 week old mice following telemetry surgery and recordings. Hearts were rinsed in cold PBS, rocked in Krebs–

Henseleit solution for 30 minutes, fixed in 10% formalin overnight, and moved into 70% EtOH until paraffin embedding. Heart sections at 5µm thickness were obtained for four chamber views. Heart processing, sectioning, and H&E staining were performed at the Ohio State University's Wexner Medical Center human pathology/histology core. Trichrome staining was performed on sections using a Masson's Trichrome 2000 Stain Kit (KTMTR2) by American Mastertech Scientific. Fibrosis analysis of trichrome images was modified from Gratz et al. as previously described [315].

Antibodies: A list of all primary and secondary antibodies used are provided below:

Antibody Target	Manufacturer	Reference	Host	Class	Application	Concentration
Desmoplakin	Abcam	ab16434	Mouse	Monoclonal	IB/IF	1:500/1:100
Desmoplakin	Abcam	ab71690	Rabbit	Polyclonal	IF	1:100
Plakoglobin	Abcam	ab15153	Rabbit	Polyclonal	IB/IF	1:2500/1:100
Plakophilin-2	Fitzgerald	10R-G109A	Mouse	Monoclonal	IB/IF	1:1000/1:100
N-Cadherin	Invitrogen	33-3900	Mouse	Monoclonal	IB/IF	1:1000/1:200
N-Cadherin	Invitrogen	PA5-19486	Rabbit	Polyclonal	IF	1:200
GAPDH	Fitzgerald	10R-G109A	Mouse	Monoclonal	IB	1:10000
Connexin-43	Abcam	ab11370	Rabbit	Polyclonal	IB/IF	1:2000/1:200
pConnexin-43 (Ser 368)	Sigma-Aldrich	AB3841	Rabbit	Polyclonal	IB	1:1000
Desmin	Invitrogen	PA5-16705	Rabbit	Polyclonal	IB/IF	1:2000/1:200
Integrin β1D	Abcam	ab8991	Mouse	Monoclonal	IB	1:1000
β-Catenin	Invitrogen	MA1-300	Mouse	Monoclonal	IB	1:1000
Nav1.5	Custom-Covance	[316]	Rabbit	Polyclonal	IB/IF	1:500/1:100
Calnexin	Abcam	ab22595	Rabbit	Polyclonal	IF	1:100
Actin	Sigma-Aldrich	A2066	Rabbit	Polyclonal	IB	1:2500
Donkey Anti-mouse HRP (2°)	Jackson Immunology	715-035-150	Donkey	Polyclonal	IB	1:5000
Donkey Anti-Rabbit HRP (2°)	Jackson Immunology	711-035-152	Donkey	Polyclonal	IB	1:10000
Donkey Anti-Mouse IgG Fluro 488	ThermoFisher Scientific	A21202	Donkey IgG	Polyclonal	IF	1:400
Donkey Anti-Mouse IgG Fluro 568	ThermoFisher Scientific	A10037	Donkey IgG	Polyclonal	IF	1:400

Donkey Anti-Rabbit IgG Fluro 488	ThermoFisher Scientific	A21206	Donkey IgG	Polyclonal	IF	1:400
Donkey Anti-Rabbit IgG Fluro 568	ThermoFisher Scientific	A10042	Donkey IgG	Polyclonal	IF	1:400

Primers: A list of all primers utilized are provided below.

Primer Name	Primer Sequence 5'-3'	Use
Genotyping F	5'-GCACTCGTGTTAAAGGCAGAC	Mouse Genotyping
Genotyping R	5'-CCTGGTCTTGTTTGTAGTCGC	Mouse Genotyping
<i>Dsp</i> qPCR F	5'-CACTCTTCAGACGCAGGTGGA	qPCR
<i>Dsp</i> qPCR R	5'-GCCCTTCAGGTAGGCTTCAG	qPCR
Hprt qPCR F	5'-TGCTGACCTGCTGGATTACA	qPCR
Hprt qPCR R	5'-TTATGTCCCCCGTTGACTGA	qPCR

Statistics: Data are presented as mean \pm S.E.M. For the comparison of two groups, we performed unpaired two-tailed Student's t-test when data passed normality test (Shapiro-Wilk normality test). When data failed this normality test, a Mann-Whitney test was performed to compare the groups, and box and whisker plots were used to display this data. When comparing differences in a categorical variable between genotypes, a Fisher's exact test was used. Differences were considered significant at a $p < 0.05$. Statistical analysis was performed using GraphPad Prism (version 7.01 for Windows, GraphPad Software).

3.4 Results

3.4.1 Homozygous DSP p.R451G knock-in mice display embryonic lethality

The N-terminus of DSP is the location of multiple human ACM variants [85]. The R451G variant in this region is of interest due to its presence and variable phenotype in a large kindred, as well as the linkage of this variant to calpain-dependent proteolysis *in vitro*

[76]. To assess this phenotypic variability, we generated a mouse model expressing endogenous DSP^{R451G} (Figure 6A). Mice heterozygous for the DSP p.R451G variant (*Dsp*^{R451G/+}) were bred to study *Dsp*^{R451G/R451G} mice in comparison to control littermates (Figure 6B). *Dsp*^{R451G/R451G} mice were embryonic lethal, and the ratio of *Dsp*^{R451G/+} to control littermates was approximately 2:1, the expected Mendelian ratio of offspring assuming *Dsp*^{R451G/R451G} mice were not viable. Embryonic isolations were performed from *Dsp*^{R451G/+} X *Dsp*^{R451G/+} breeding pairs, and viable *Dsp*^{R451G/R451G} embryos were identified prior to E10, including E4 and E8 (Figure 6C). Verification of genotyping was performed utilizing Sanger sequencing to confirm the nucleotide change at the mutation site as well as the PAM sequence (Figure 7). After E10, no viable *Dsp*^{R451G/R451G} embryos were detected (Figure 6D). Thus, *Dsp*^{R451G/R451G} mice are embryonic lethal prior to E10. As a result of this lethality, only *Dsp*^{R451G/+} mice were evaluated for cardiac phenotypes. These heterozygotes mirror the autosomal dominant inheritance pattern observed in the original R451G patient family [76].

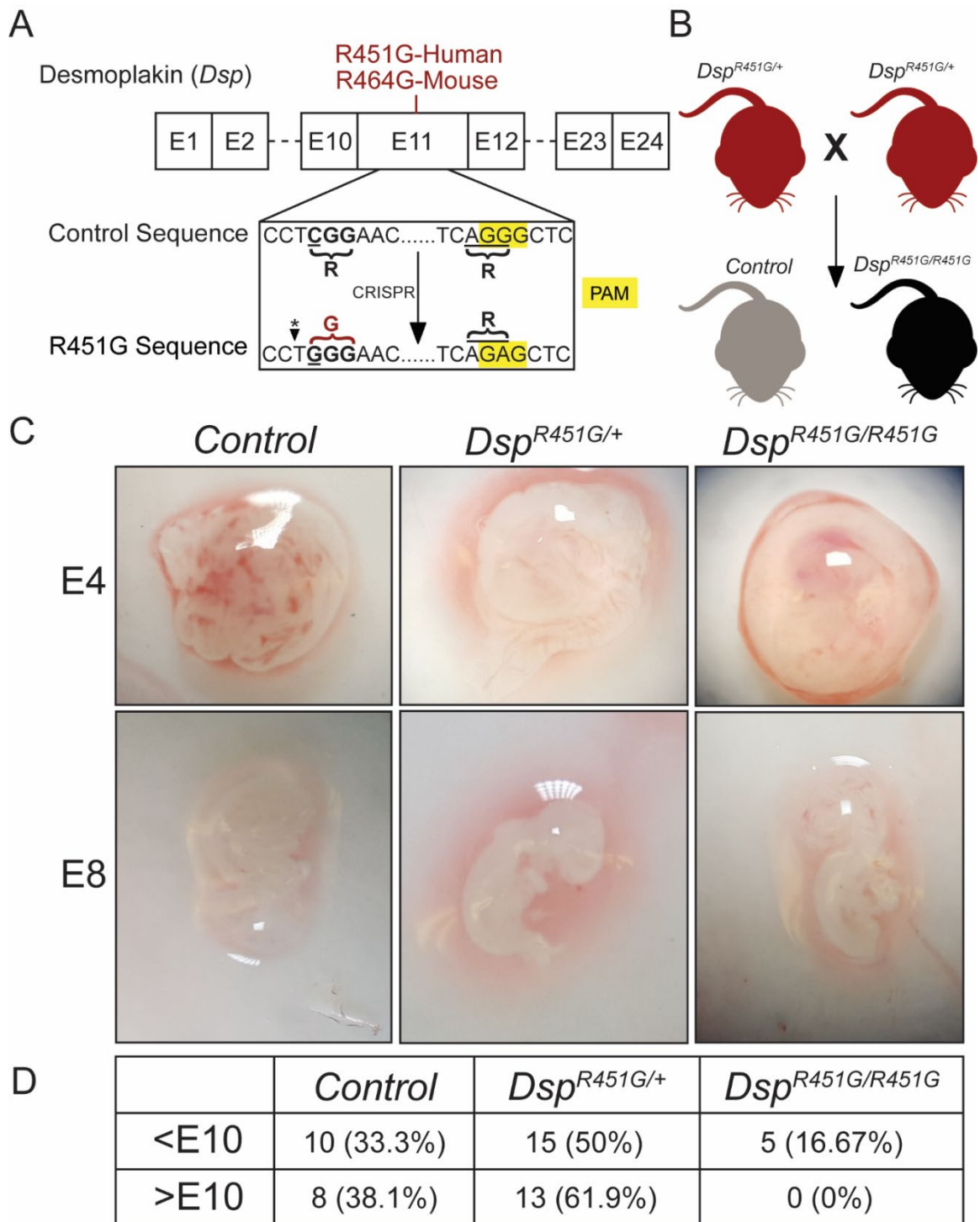


Figure 6: Schematic overview of the R451G mouse model

(A) Amino acid substitution occurs at residue R464, the murine equivalent of the human R451G variant. Alteration at the PAM site results in no changes within the coding

sequences. *Introduction of the R451G variant results in the generation of a restriction enzyme cut site for BstNI (CC^VWGG) that was utilized for genotyping. **(B)** Schematic for the generation of *Dsp*^{R451G/R451G} mice and control littermates after backcrossing is completed. **(C)** Embryonic isolations at time points E4 and E8 identified viable *Dsp*^{R451G/R451G} embryos. **(D)** Breakdown of timepoints and genotypes from isolated embryos from *Dsp*^{R451G/+} X *Dsp*^{R451G/+}, with no viable *Dsp*^{R451G/R451G} embryos isolated after E10.

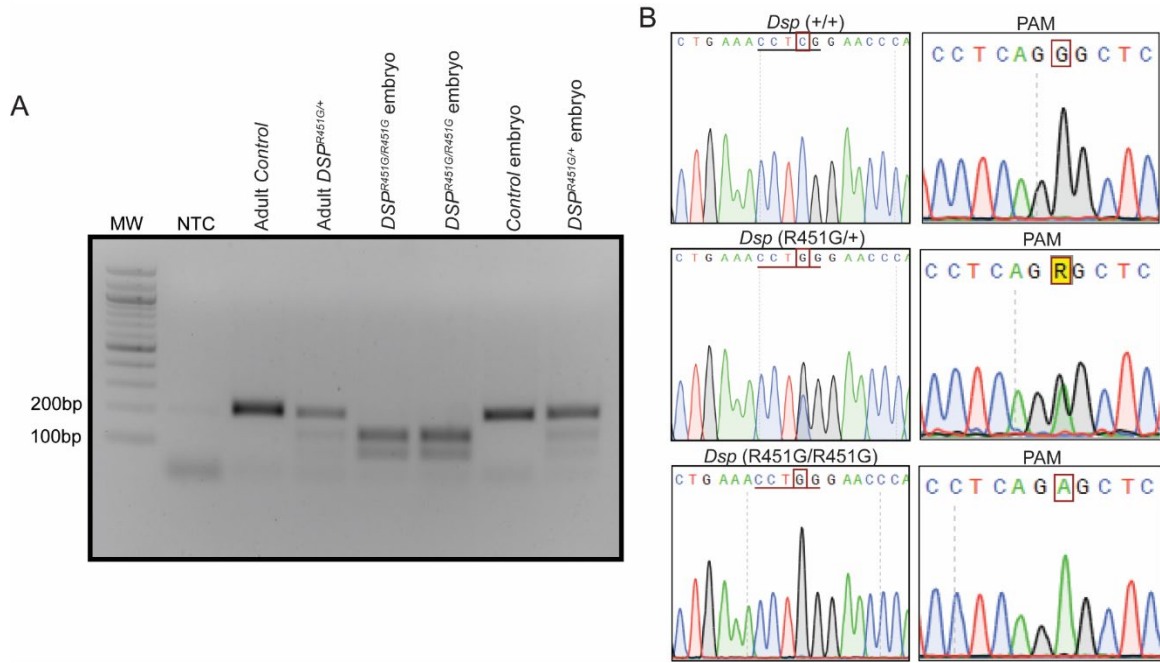


Figure 7: Genotyping analysis of the DSP R451G+ mouse model

(A) Representative genotyping of the DSP R451G+ embryo isolations, with no template control (NTC). Control and R451G+ positive controls previously confirmed with sequencing. Restriction enzyme digest using BstNI cleaves R451G+ DNA, but not control DNA. **(B)** Sequencing results verified both heterozygous and homozygous R451G+ mice at the mutation site and via the PAM sequence site.

Previous data from R451G human studies revealed a loss of full-length DSP protein that occurred post-translationally [76]. Heart lysates from control and *Dsp*^{R451G/+} littermates were analyzed at ~6 months of age. *Dsp*^{R451G/+} mice displayed an approximate 50% reduction of full-length DSP protein in comparison to control littermates (Figure 8A/B).

This was further confirmed in lysates from ~1 month and 3 month hearts. All lysates displayed a significant, near 50% reduction in DSP expression (Figure 9A/B). We did not observe any small fragments of DSP unique in the *Dsp*^{R451G/+} heart lysates. mRNA levels of *Dsp* were unchanged between *Dsp*^{R451G/+} and control hearts, indicating the reduction in DSP expression occurred post-translationally (Figure 8C). To ensure there were no potential dominant-negative effects from the R451G DSP variant, immunostaining of heart sections isolated at ~6 months of age was performed to analyze the localization of DSP. While *Dsp*^{R451G/+} heart tissue showed reduced DSP signal at the intercalated disc (ID) in relation to the control marker N-cadherin, we did not observe DSP mislocalization from the ID (Figure 8D). In summary, our findings support that DSP p.R451G is post-translationally unstable but does not impact the localization of DSP from the control allele.

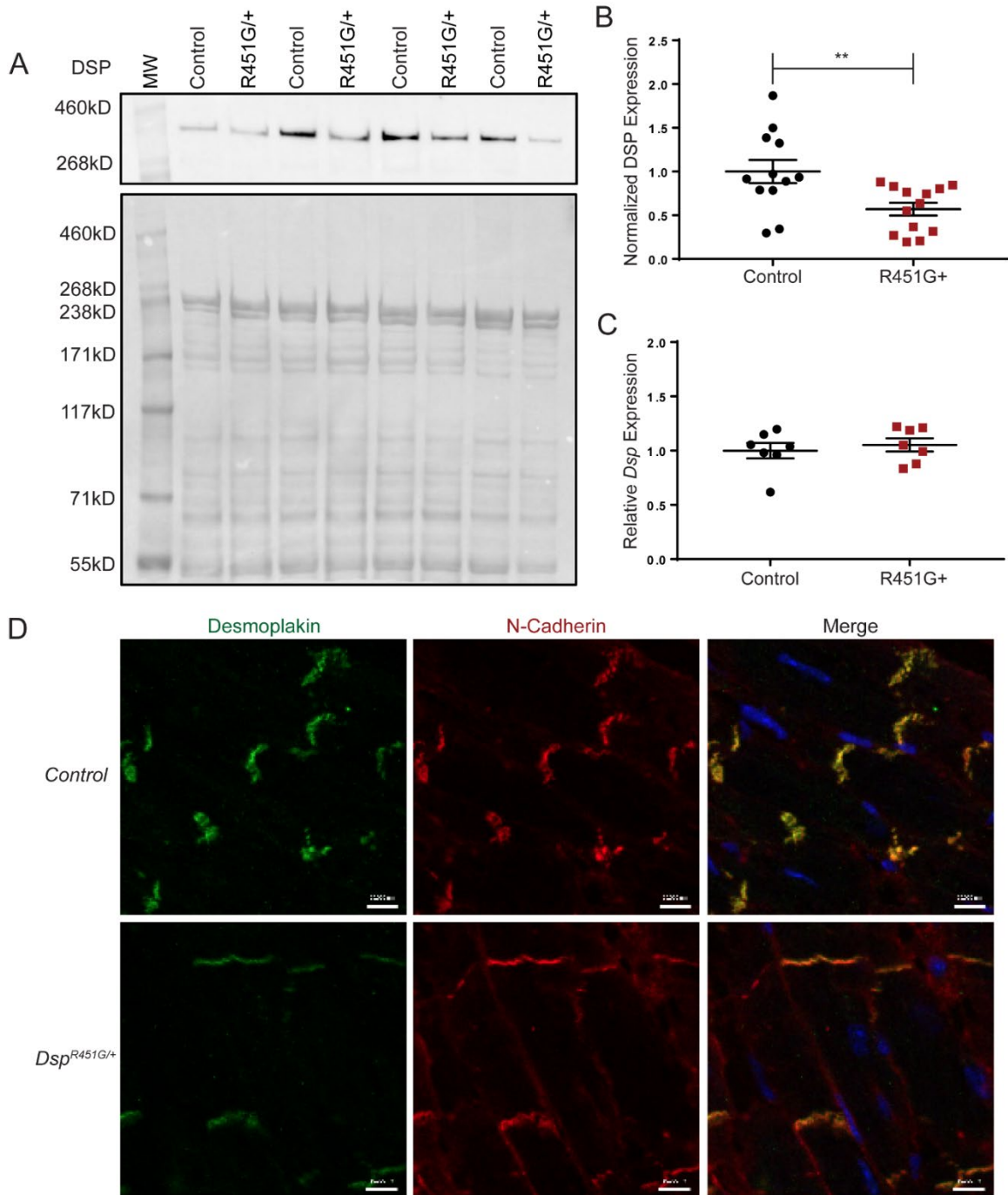


Figure 8: *Dsp*^{R451G/+} mice display a reduction in DSP protein expression
(A) Representative immunoblot of heart lysates from *Dsp*^{R451G/+} and control littermates isolated at 6 months of age, comparing full length DSP levels (control n=12, *Dsp*^{R451G/+} n=13). Ponceau staining included. **(B)** Quantification of immunoblotting of DSP normalized to Ponceau staining. **(C)** qPCR examining *Dsp* expression from isolated cDNA from *Dsp*^{R451G/+} and control littermates, normalized to *Hprt* (n=7 per group). **(D)**

Immunostaining of cardiac cryosections examining DSP localization and expression patterns at the intercalated disc, using N-Cadherin as a control marker (n=4 per genotype). Scale bars represent 10 μ m. ** p < 0.01.

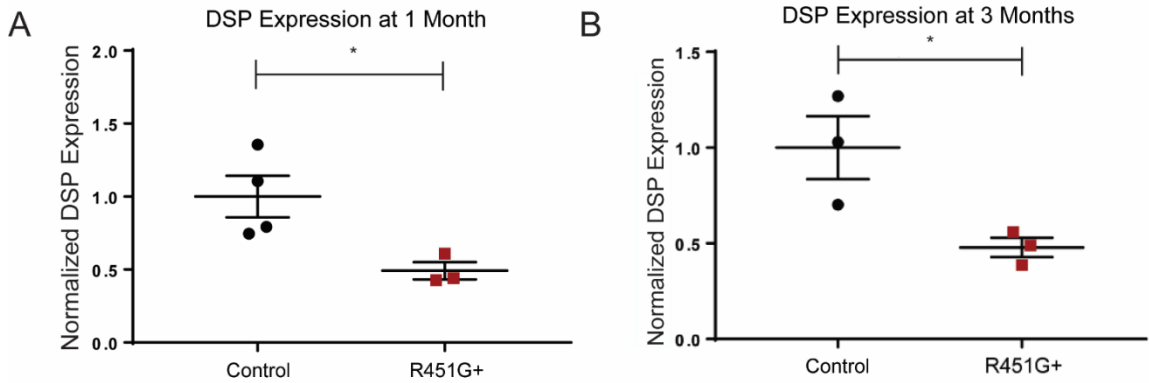


Figure 9: *Dsp*^{R451G/+} mice display a reduction in DSP protein expression at different timepoints

(A) Immunoblot quantification of DSP from heart lysates isolated at 1 month of age (Control n=4, *Dsp*^{R451G/+} n=3), (B) and 3 months of age (n=3 per group). * p < 0.05.

3.4.2 *Dsp*^{R451G/+} mice do not display changes in cardiac structure or function at baseline

Structural abnormalities have been previously observed in select individuals harboring the DSP p.R451G variant, where the majority of patients experience left or biventricular dysfunction [76]. We evaluated six-month *Dsp*^{R451G/+} mice for potential structural or functional cardiac phenotypes. We observed no changes in cardiac function as assessed by measuring fractional shortening (FS%), or left ventricular internal diameter (LVID; both systolic and diastolic; Figure 10A-D). A summary of all baseline echocardiographic data is noted in Table 2. We observed no signs of increased fibro-fatty infiltration in *Dsp*^{R451G/+} hearts (Figure 10E/F). Finally, *Dsp*^{R451G/+} mice displayed no changes in heart weight to tibia length ratio (Figure 10G).

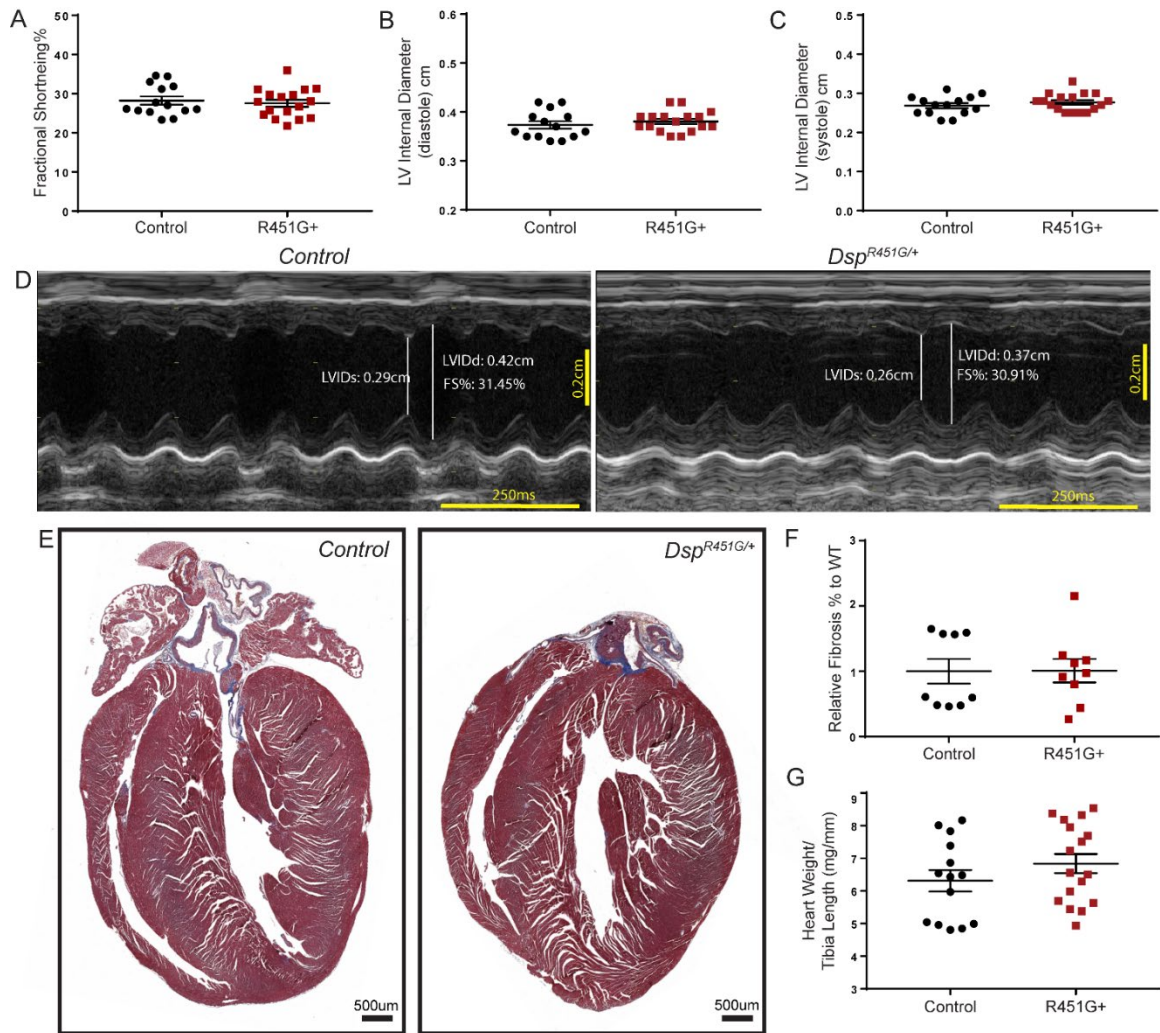


Figure 10: *Dsp*^{R451G/+} mice display no structural changes at baseline

(A) Baseline echocardiography measurements conducted on 6 month control and *Dsp*^{R451G/+} mice and littermates comparing fractional shortening, (B) LVIDd, (C) and LVIDs (control n=14, *Dsp*^{R451G/+} n=17). (D) Representative M-mode echocardiography recordings from control and *Dsp*^{R451G/+} mice performed at 6 months. (E) Masson's trichrome staining performed on 6 month old control and *DSP*^{R451G/+} mice littermates. (F) Relative fibrosis levels calculated from Masson's trichrome staining (n= 9 per genotype). (G) Heart weight to tibia length ratio isolated following echocardiography experiments (control n=14, *Dsp*^{R451G/+} n=17).

3.4.3 *Dsp*^{R451G/+} mice do not display electrical abnormalities at baseline

Electrical defects commonly precede structural abnormalities in ACM [44, 89]. Therefore, we evaluated *Dsp*^{R451G/+} mice for arrhythmia susceptibility in the absence of structural defects. Similar to control littermates, no baseline electrical abnormalities were noted in *Dsp*^{R451G/+} mice (Figure 11A). However, we observed trends toward a prolonged QTc (p= 0.0914) and T-peak to T-end (p=0.0609), with no changes in heart rate, suggesting potential defects in repolarization (Figure 11B/C, Table 3).

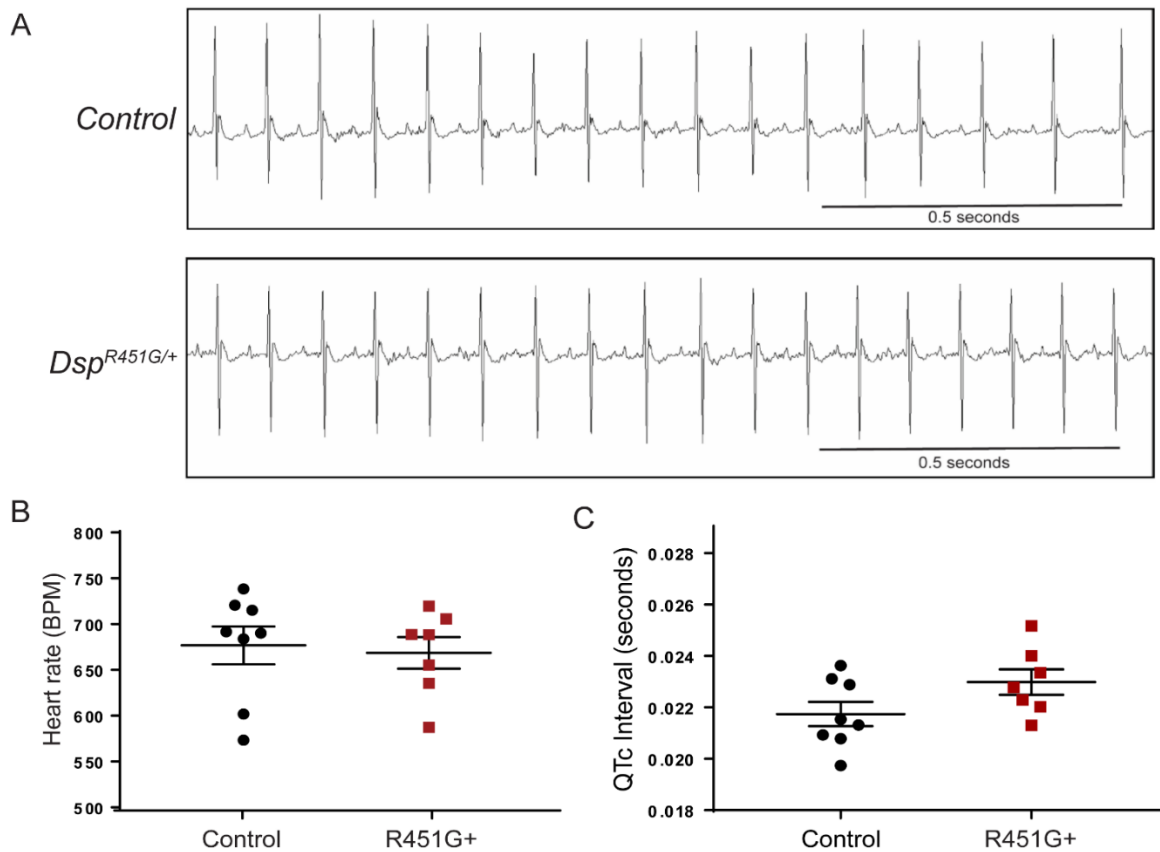


Figure 11: *Dsp*^{R451G/+} mice display no significant electrical abnormalities at baseline (A) Representative ECG trace in conscious mice at ~14 weeks of age displayed no signs of cardiac arrhythmias or abnormal ECG morphology. Scale bars represent 500ms. (B) Heart rate (C) and QTc (Mitchell et al. normalization) intervals calculated from telemetry mice at baseline. Stats performed using Student's t-test (control n=8, *Dsp*^{R451G/+} n=7).

3.4.4 *Dsp*^{R451G/+} mice display accelerated heart failure following pressure overload

To evaluate the response of cardiac output following chronic cardiac stress, transverse aortic constriction (TAC) surgeries were performed on *Dsp*^{R451G/+} mice to induce pressure overload. Surgeries were performed at ~12 weeks, and echocardiography measurements were acquired at baseline and every two weeks post-surgery for twelve weeks. Four weeks post-TAC, *Dsp*^{R451G/+} mice displayed a significant reduction in FS%

compared to control littermates (Figure 12A: Control FS%= 21.84%, $Dsp^{R451G/+}$ FS%= 15.77%; p= 0.0448). Interestingly, $Dsp^{R451G/+}$ mice also demonstrated an increase in LVIDs as early as four weeks post-TAC when compared to the control littermates (Figure 12B/C: Control LVIDs= 0.281cm, $Dsp^{R451G/+}$ LVIDs= 0.337cm; p= 0.0368). These parameters remained significant or trended towards significance throughout the study until the ending timepoint. Diastolic measurements at four weeks post-TAC, including LVIDd (p= 0.0520) and end diastolic volume (p= 0.0783) showed a trending increase in $Dsp^{R451G/+}$ mice (Figure 13A/B). There was a trending increase to end systolic volume in $Dsp^{R451G/+}$ mice 4 weeks post-surgery compared to control littermates (p= 0.0810, Figure 13C), with ejection fraction trending or significantly decreased in $Dsp^{R451G/+}$ mice at each timepoint starting at 4 weeks post-surgery (Figure 13D). No significant changes in overall survival or heart weight were observed (Figure 13E/F).

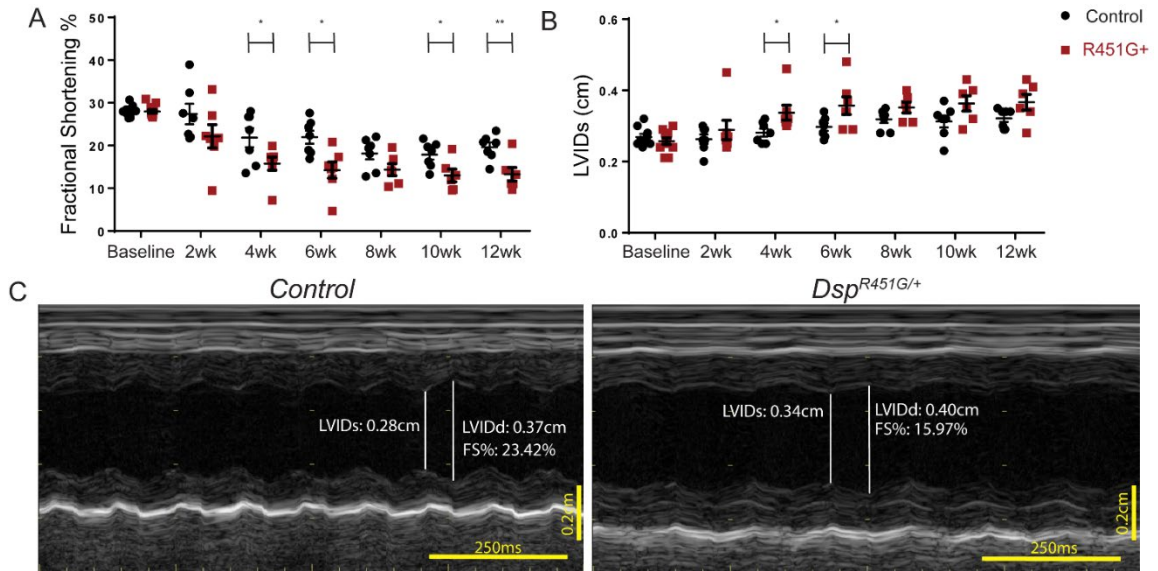


Figure 12: *Dsp*^{R451G/+} mice display structural changes post TAC surgery
(A) Comparison of fractional shortening **(B)** and LVIDs between *Dsp*^{R451G/+} mice and control littermates post TAC-surgery. Measurements taken every 2 weeks after surgery (n=7 per genotype post-surgery). * p <0.05, ** p <0.01. **(C)** Representative M-mode echocardiography recordings from *Dsp*^{R451G/+} and control littermates 4 weeks post-TAC surgery.

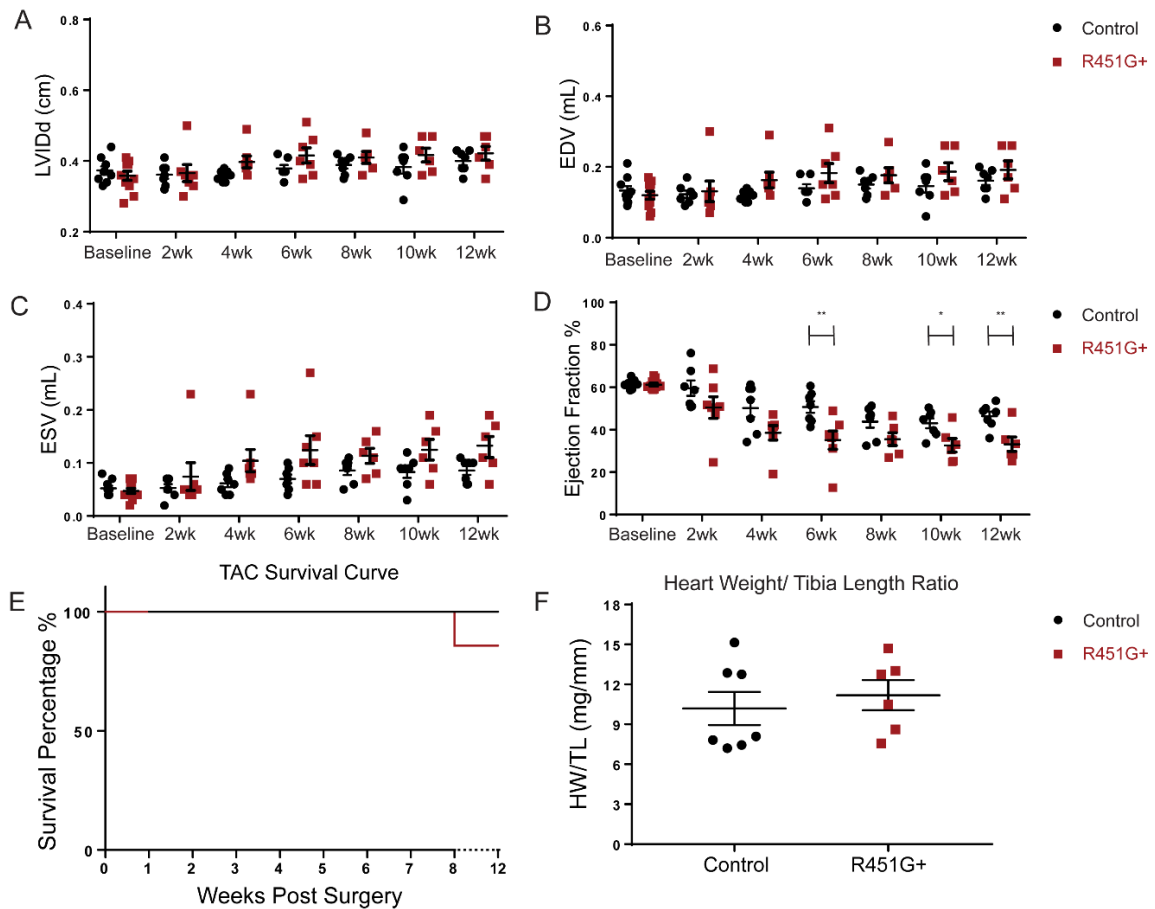


Figure 13: Structural changes in *Dsp*^{R451G/+} mice post TAC surgery

Structural changes in *Dsp*^{R451G/+} mice post TAC surgery. Quantification of additional LV parameters from *Dsp*^{R451G/+} and control littermates following TAC surgeries, including (A) left ventricular internal diameter at diastole, (B) end diastolic volume, (C) end systolic volume, (D) and ejection fraction. (E) Kaplan-Meier curve following TAC surgery. (F) Heart weight to tibia length ratio at endpoint experiments/heart isolations. (n=7 per genotype post-surgery). * p-value <0.05, ** p-value <0.01.

At baseline, *Dsp*^{R451G/+} mice displayed a trending, but not statistically significant increase in QTc interval as well as T-peak to T-end interval (Figure 11B/C, Table 3). To evaluate how this electrical phenotype was altered in response to pressure overload, ECG recordings were acquired from anesthetized mice every four weeks post-TAC. The QTc interval was significantly prolonged at four weeks post-TAC in *Dsp*^{R451G/+} mice, and the T-

peak to T-end showed a trending increase that did not reach significance ($p=0.0584$; Figure 14A-C). No other changes in electrical parameters were noted following surgery (Figure 14D-F). ECG morphological changes were also analyzed, and at four weeks post-TAC, control mice displayed minimal changes in the T-wave morphology, whereas $Dsp^{R451G/+}$ mice showed more severe T-wave inversion (Figure 15). Notably, T-wave inversion is a clinical diagnostic criterion of ACM and suggests a significant risk of SCD [317-318]. Lastly $Dsp^{R451G/+}$ mice displayed a fragmented pattern in the QRS (fQRS) structure, another diagnostic parameter for ACM, that was not observed in the control littermates (Figure 15). Taken together, $Dsp^{R451G/+}$ mice displayed no changes in cardiac structure or function at baseline. However, $Dsp^{R451G/+}$ mice exhibited reduced cardiac function, LV dilation, and signs of accelerated heart failure phenotypes following pressure overload.

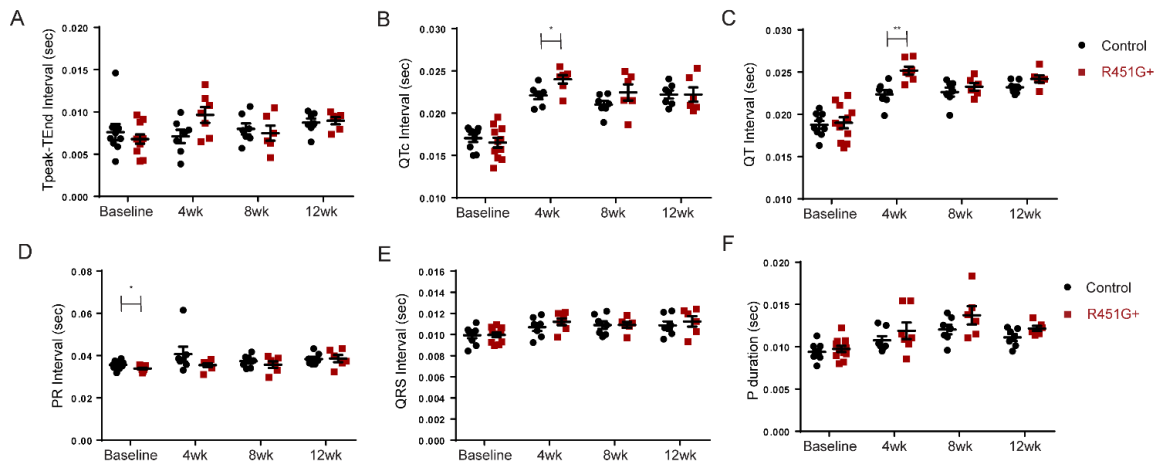


Figure 14: Surface ECG recordings from $Dsp^{R451G/+}$ mice and control littermates post-TAC surgery

Parameters analyzed include (A) T-peak to T-end duration, (B) QTc duration (Mitchell et al. normalization), (C) QT interval, (D) PR interval, (E) QRS interval, (F) and p duration. * $p<0.05$, ** $p<0.01$ ($n=7$ per genotype post-surgery).

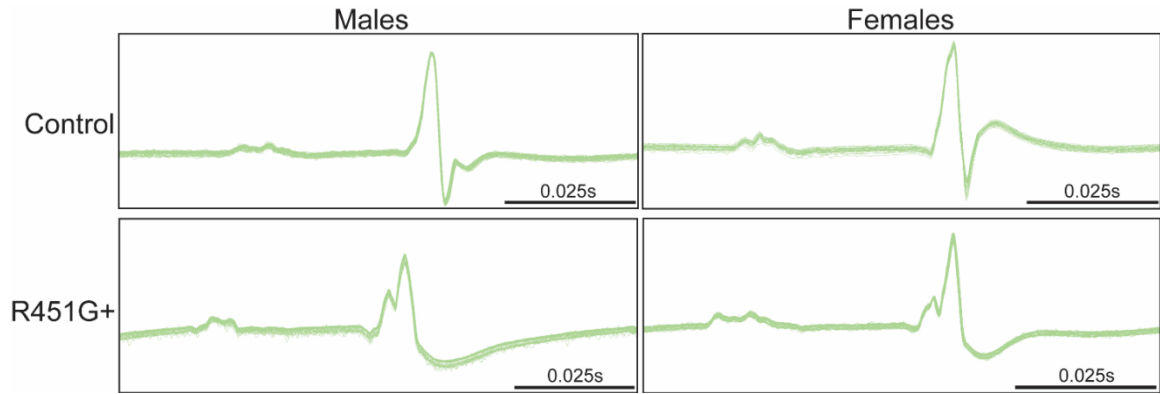


Figure 15: Representative ECG traces following TAC surgery
 Representative traces are average ECG morphology of $Dsp^{R451G/+}$ mice and control littermates at 4 weeks post-TAC. Scale bars represent 0.025 seconds.

3.4.5 $Dsp^{R451G/+}$ mice display stress-induced arrhythmias

To determine if $Dsp^{R451G/+}$ mice were prone to inducible arrhythmias prior to structural remodeling, we investigated the impact of catecholamines on cardiac electrical activity. As expected, following 2.0mg/kg epinephrine, control mice displayed limited arrhythmogenic events. In contrast, $Dsp^{R451G/+}$ mice displayed prolonged and severe arrhythmogenic events, including example traces of ventricular tachycardia (VT) and bigeminy (Figure 16A-C). Additionally, a greater proportion of $Dsp^{R451G/+}$ mice (71.4%) experienced arrhythmogenic events that exceeded two seconds compared to control littermates (12.5%, $p=0.0406$; Figure 16D-E). $Dsp^{R451G/+}$ mice also displayed a significant increase in atrioventricular block (AV) block events, as well as a trending increase in premature ventricular contractions (PVCs) ($p=0.144$; Figure 17A/B). No significant differences in rate of occurrence were observed in other types or arrhythmic events (Figure 17C/D). Taken together, $Dsp^{R451G/+}$ mice were prone to more frequent and prolonged

arrhythmias following catecholaminergic stimulation in the absence of a structural phenotype.

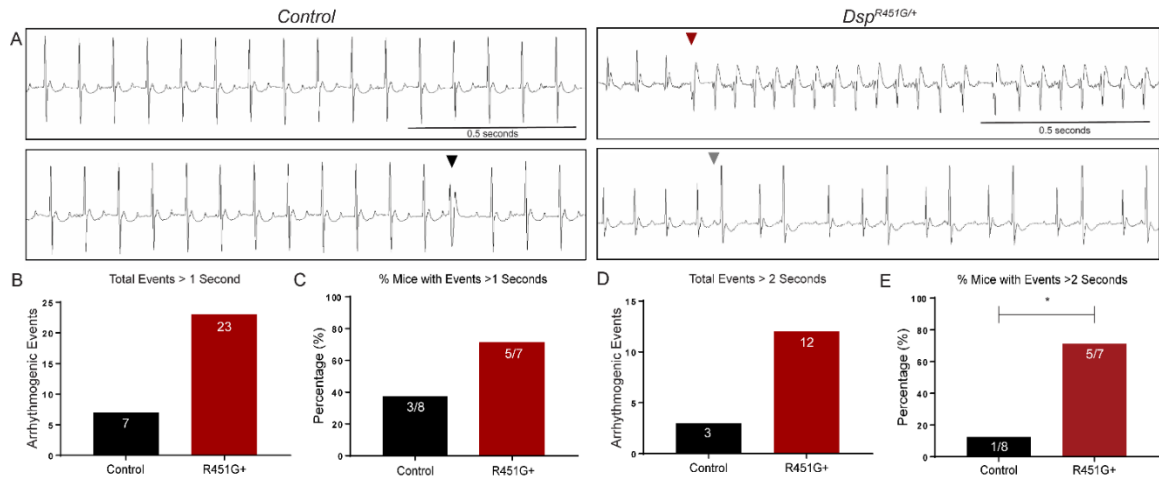


Figure 16: *Dsp*^{R451G/+} mice display arrhythmias following catecholaminergic challenge (A) Representative ECG recordings of control and *Dsp*^{R451G/+} mice littermates (~14 weeks of age) following 2mg/kg epinephrine. Arrowheads point to identified arrhythmic events, including isolated PVCs (Black), ventricular tachycardia (red), and bigeminy (gray). Scale bars represent 500ms. (B) Arrhythmic events that exceeded 1 second per group. (C) Percentage of mice in each genotype with at least 1 event that exceeded 1 second. (D) Total number of arrhythmic events longer than 2 seconds. (E) Percentage of mice in each genotype with at least 1 event that exceeded 2 seconds. * p < 0.05 (control n=8, *Dsp*^{R451G/+} n=7).

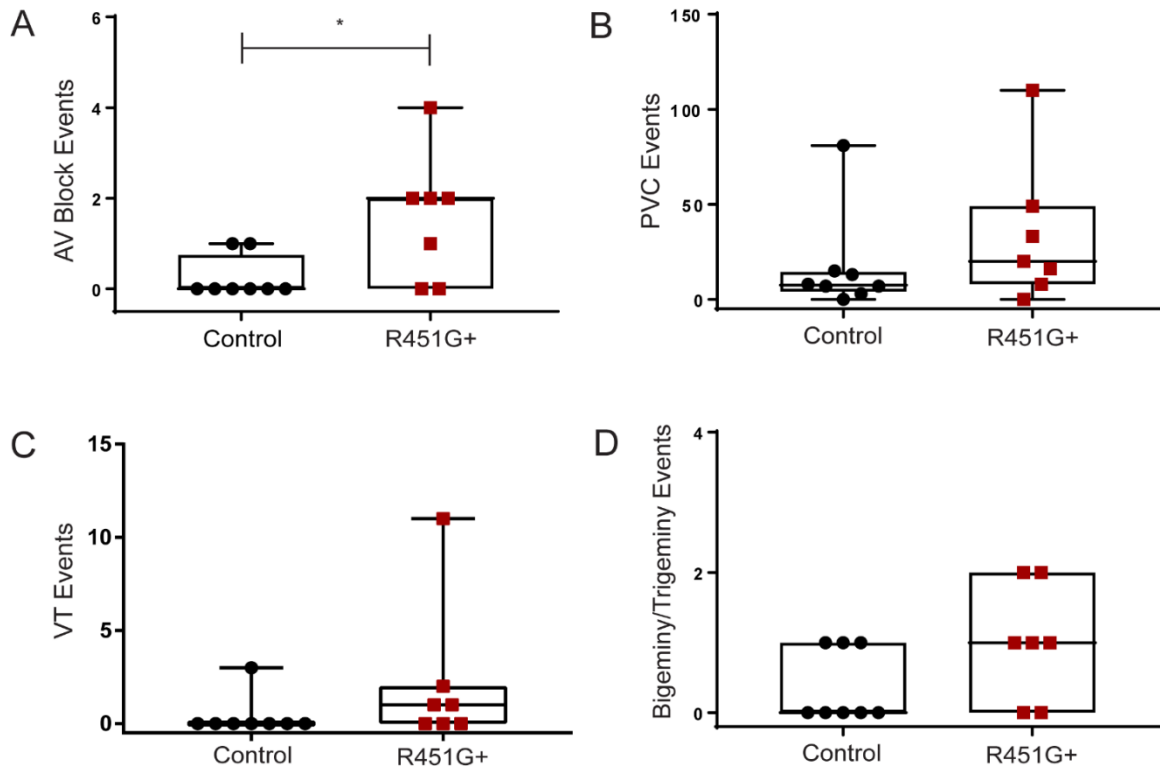


Figure 17: Electrocardiographic findings following catecholaminergic stimulation in telemeter mice

(A) Breakdown of different arrhythmia events in mice following epinephrine injections, including atrioventricular block, (B) premature ventricular contractions, (C) ventricular tachycardia, (D) and bi/trigeminy. Stats performed using Mann-Whitney non-parametric test. * $p < 0.05$ (control $n=8$, $Dsp^{R451G/+}$ $n=7$).

3.4.6 $Dsp^{R451G/+}$ mice display normal localization of key ID proteins but altered distribution of Cx43.

Based on the critical role of DSP in cardiac function, we hypothesized that the R451G missense variant would cause reduced expression and/or altered localization of key DSP binding partners in mice. Initial targets of interest included Cx43 and plakoglobin (PKG), as these proteins were shown to be frequently altered in ACM models and patients [90, 96, 110, 319-320]. R451G+ biopsy samples and human iPSCs previously identified

Cx43 mislocalization, decreased Cx43 protein expression, and increased phosphorylation at Cx43-S368 [76]. Expression levels of PKG and Cx43 were not different between *Dsp*^{R451G/+} mice and their control littermates (Figure 18A-C). Further, pCx43/Cx43 ratios were not altered as well (Figure 18D/E). We also examined additional targets including integrin-β1D, a protein reduced in many ACM cases with reduced DSP expression [321], as well as plakophilin-2 (PKP2) and β-catenin, ACM-linked proteins that localize at the ID [45, 87]. Notably, immunoblotting revealed no changes in expression patterns for integrin-β1D, PKP2, or β-Catenin (Figure 19A-C).

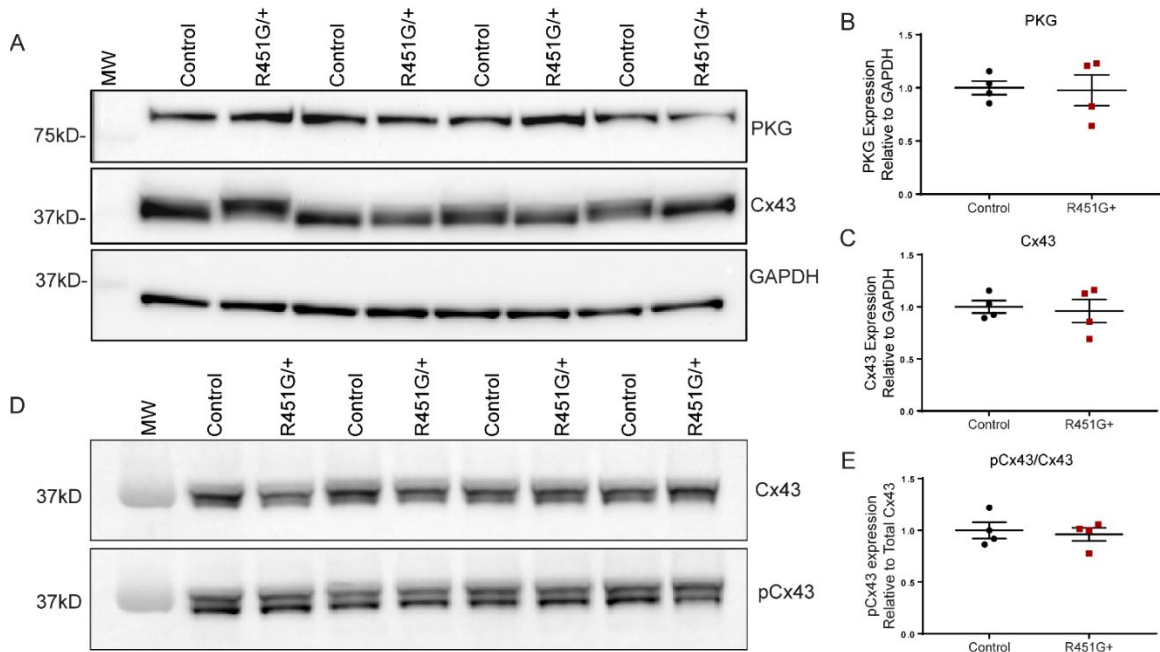


Figure 18: *Dsp*^{R451G/+} mice display no changes in expression of key ID proteins
(A) Immunoblots of heart lysates from *Dsp*^{R451G/+} mice and control littermates isolated at 3 months of age, evaluating key ID markers PKG and Cx43. **(B-C)** Quantification of PKG and Cx43 protein expression relative to GAPDH. **(D)** Immunoblot probing for pCx43 (Ser368) and Cx43. **(E)** Quantification of pCx43 protein expression compared to total Cx43. (N=4 per genotype).

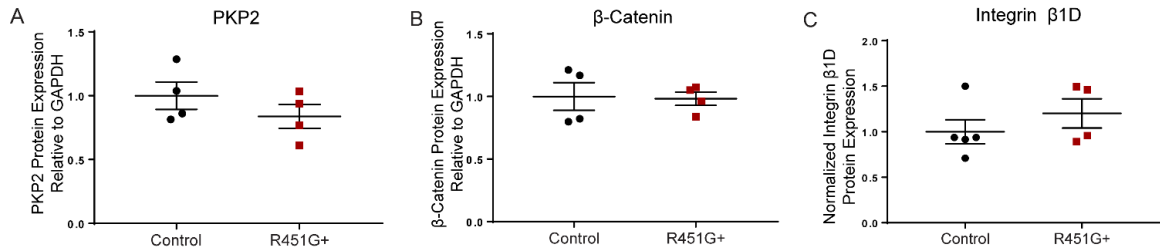


Figure 19: No changes in the expression of additional key ID proteins

(A) Immunoblots of heart lysates from *Dsp*^{R451G/+} and control littermates isolated at 3 months of age, evaluating expression of plakophilin-2, (B) and β-catenin (n=4 per genotype). Quantification of each target relative to appropriate GAPDH staining. (C) Immunoblot probing for Integrin β1D (Control n=5, *Dsp*^{R451G/+} n=4) quantified, relative to Ponceau staining.

Consistent with expression data, we observed no changes in PKG localization, as expression was uniform at the disc when compared to control marker N-cadherin (Figure 20A). However, we did observe minor, but consistent alterations of Cx43 at the ID when compared to the control heart tissue sections. Specifically, Cx43 displayed a pronounced punctate expression pattern in *Dsp*^{R451G/+} tissue when compared to control sections (Figure 20B). In summary, while displaying minor alterations in Cx43 localization, *Dsp*^{R451G/+} mice had normal expression and distribution of key DSP associated binding partners.

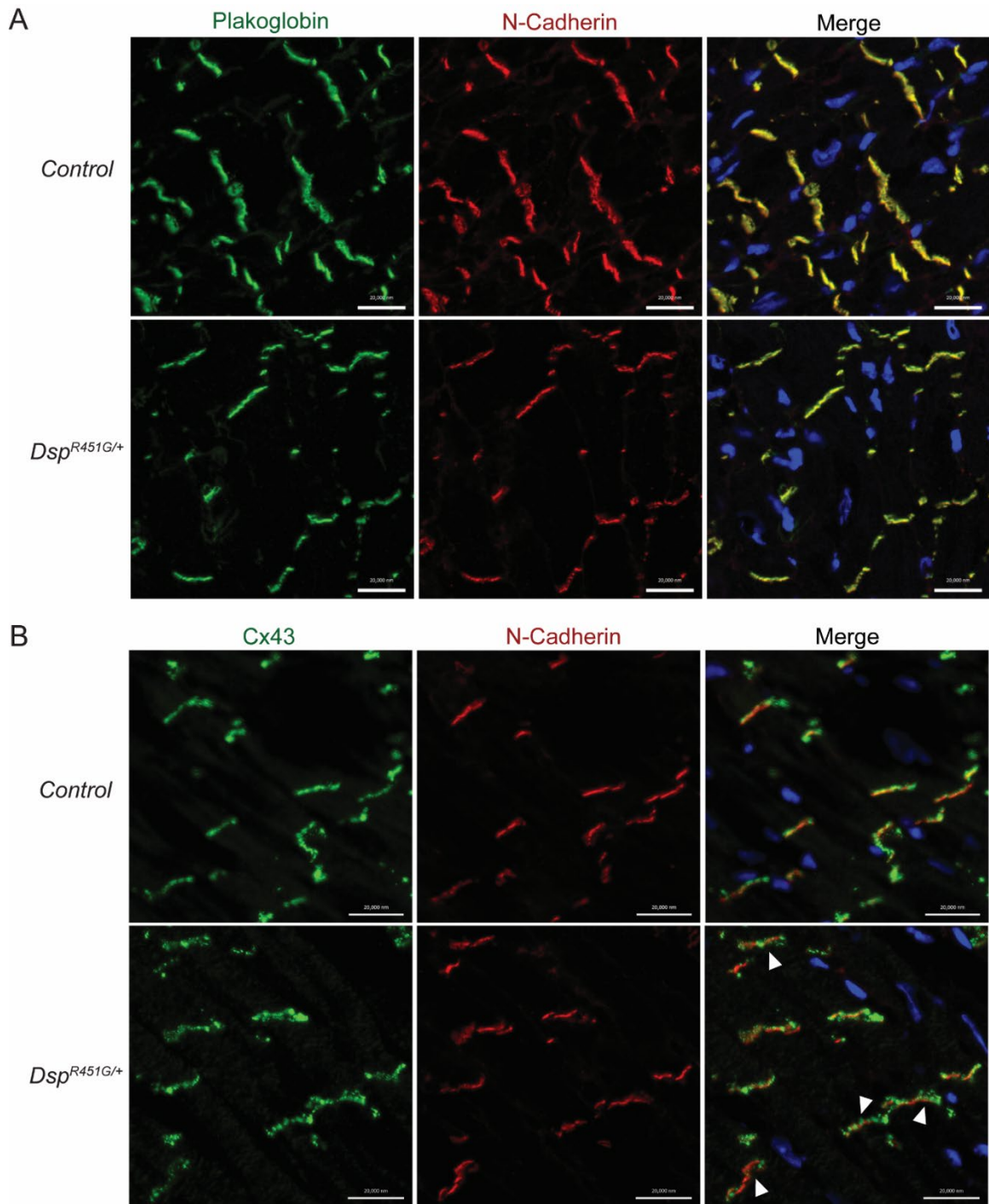


Figure 20: *Dsp*^{R451G/+} mice display changes in ID protein localization
(A) Immunofluorescent (IF) images of cardiac cryosections examining plakoglobin, N-cadherin co-stain used as a control marker. **(B)** Staining for Cx43 localization patterns at the ID, with arrowheads pointing to ID with punctate Cx43 expression at the disc in

comparison to control marker N-cadherin. Scale bars represent 20 μ m. n=4 per genotype, mix of male and female mice used for staining.

3.5 Discussion

The gap of knowledge on the progression of ACM phenotype and the molecular pathways of ACM pathogenicity makes therapeutic design and preventative treatment challenging. Therefore, developing models that better recapitulate the human phenotype is vital for the progression in ACM research. Our previous study utilized human cardiac biopsy tissues and iPSC-derived cardiomyocytes from an ACM family harboring a pathogenic *DSP* variant (DSP-p.R451G). Biopsy samples from heterozygous p.R451G patients displayed increased fibro-fatty infiltration, decreased DSP expression at the ID, and mislocalization of Cx43 from the ID. Additionally, iPSC-derived cardiomyocytes identified a reduced expression of Cx43 (including increased pCx43-S368, a degradation marker), as well as a decreased expression of DSP that was not connected to a loss of *DSP* mRNA. This post-translational reduction in DSP was ultimately attributed to an increase in calpain sensitivity, which was also linked to additional variants in this N-terminal mutational ‘hotspot’ using both *in silico* and *in vitro* techniques [76].

Desmoplakin is essential for proper embryonic development and plays a major role in the integrity of both cardiomyocytes and epithelial tissue [92]. Upon breeding heterozygous *Dsp*^{R451G/+} mice, no viable *Dsp*^{R451G/R451G} mice were detected, suggesting that homozygous expression of the R451G variant is embryonic lethal. Indeed, *Dsp*^{R451G/R451G} embryos were only identified in development prior to E10 (Figure 6C/D). While initially surprising, these results were not unexpected, as whole-body knock-out of *Dsp* is

embryonic lethal near E6.5 [92]. While we were unable to study *Dsp*^{R451G/R451G} mice, the heterozygous whole body *Dsp*^{R451G/+} model more accurately portrays the human population, as to date, all familial members in the p.R451G family are heterozygous for the variant [76].

Consistent with the incomplete penetrance found in humans, we observed no basal structural or electrical phenotypic changes in the *Dsp*^{R451G/+} mice (Figure 10-11, Tables 2-3). It is not uncommon for ACM models to lack a severe phenotype at baseline, where external stressors such as drug stimulation or exercise are required for a phenotypic development. Two separate studies used a plakoglobin heterozygous KO model, as well as a transgenic PKP2 p.R735X expressing mouse model. Interestingly, each showed no significant phenotype at six months of age, but following endurance exercise training, these models displayed RV abnormalities, spontaneous arrhythmias, and/or mis-localization of Cx43 [182, 273].

Both acute and chronic cardiac stressors were used in this study to fully understand the drivers that contribute towards ACM development in *Dsp*^{R451G/+} mice. We hypothesized that chronic cardiac stress might contribute to the progression of the ACM phenotype in the *Dsp*^{R451G/+} mice. Despite traditionally being considered a RV dominant disease, familial ACM cases with a DSP variant commonly show increased left or biventricular involvement [89], including the p.R451G family [76]. Additionally, LV dysfunction and/or dilation have been previously noted in heterozygous DSP knock-out mice at baseline [90, 96]. Therefore, we utilized a pressure overload model to examine the structural and functional changes of the LV of the heart post-TAC. Our model displayed a reduced LV functional

output (via fractional shortening %) and a dilated phenotype by 4 weeks post-TAC (Figure 12). Interestingly, ECG recordings displayed frequent fragmented QRS structures as well as inverted T-waves in *Dsp*^{R451G/+} mice that were not apparent in control littermates (Figure 15). fQRS is a feature reportedly indicative of fibrosis, ischemia, or scarring of the ventricles [322]. Importantly, fQRS has been linked to prolonged QT, and both fQRS and inverted T waves are considered diagnostic parameters for both myocardial scarring and ACM [323-324]. An early “concealed” phase is a significant problem in ACM diagnosis, as individuals that lack any apparent structural cardiac abnormalities are still vulnerable to life threatening arrhythmias and SCD [43-44, 146], a trait that was identified in the p.R451G patients [76]. The *Dsp*^{R451G/+} mice lacked a baseline electrical phenotype, however, an increase in prolonged arrhythmic events was noted following catecholaminergic challenge.

Overall, a multitude of pathways contribute towards the progression of ACM symptoms [111, 167, 268]. We aimed to study molecular changes in common ACM-associated proteins with disease development, including PKP2, β -Catenin, and Integrin- β 1D [179, 321]. We identified no changes in these targets (Figure 9). However, similar to what was seen in heart sections in the p.R451G family [76], altered localization patterns of Cx43 in *Dsp*^{R451G/+} mice were identified (Figure 20B). While the mislocalization was less significant in our mice, this could be attributed to the lack of a baseline phenotype in our model, as tissues from the human population were collected from an individual diagnosed with ACM following SCD. This is not surprising as Cx43 mislocalization is seen in other ACM models such as an inducible *Pkp2* KO line [75]. Cx43 plays a vital role in gap junction (GJ) formation and function at the ID and has been shown to be recruited to the

ID via DSP-EB1 interactions [71]. Desmosomes also stabilize GJ at the disc [325], so loss of DSP is expected to impact Cx43 localization. While we did not observe fibro-fatty infiltration, this is a feature that is not commonly identified in ACM mouse models.

We have successfully generated one of the first ACM mouse models that more accurately recapitulates human genetics by introducing the murine equivalent of the human DSP p.R451G variant endogenously. While punctate expression patterns of Cx43 may be linked to arrhythmia formation, *Dsp*^{R451G/+} mice displayed less significant mislocalization when compared to human studies. Future studies will focus on how different external stressors exacerbate this mislocalization, as well as identifying other molecular targets that may only be altered following prolonged stress. DSP plays a key role in protein recruitment to the ID, as well as providing structural support to the ID/desmosomes [5]. As desmosomes play a vital role in ID stability and membrane integrity, it is also important to consider the effects of this variant on ID stability. While beyond the scope of this initial study, future work will focus on potential morphological changes of the different ID structures (desmosomes, gap junctions, adherens junctions) with relationship to ID integrity.

Acknowledgments

The authors would like to acknowledge The Ohio State University's comparative pathology and mouse phenotyping core laboratory, as well as the Ohio State University's Wexner Medical Center human pathology/histology core, for assistance in cardiac sectioning and staining.

Conflict of Interests

The authors declare that they have no conflict of interest with the contents of this articles.

Funding

This research was funded by NIH grants R01HL156652 and R01HL135096 to TJH, R01HL149344 to FGA, R35HL135754 to PJM, R00HL146969 to MER, a grant from saving tiny hearts society (MAB), a grant from the Ohio State Frick Center for Heart Failure and Arrhythmia, the Leducq Foundation to PJM and the JB project.

Chapter 4. Calpain Sensitivity may be a Predictor of Disease for *DSP* Variants of Unknown Pathogenicity

Tyler L. Stevens^{1,2}, Micah Yoder³, Taylor Albertelli⁴, Heather R. Manring⁵, Nathan Wright⁴, Maegen A. Borzok³

¹Frick Center for Heart Failure and Arrhythmia Research, The Dorothy M. Davis Heart and Lung Research Institute, The Ohio State University Wexner Medical Center, Columbus, OH 43215, USA.

²Department of Physiology and Cellular Biology, The Ohio State University College of Medicine and Wexner Medical Center, Columbus, OH, 43215, USA

³Department of Natural Sciences, Mansfield University of Pennsylvania, Mansfield, PA 16933, USA.

⁴Department of Chemistry and Biochemistry, James Madison University, Harrisonburg, VA 22807, USA.

⁵Comprehensive Cancer Center, The Ohio State University College of Medicine and Wexner Medical Center, Columbus, OH 43215, USA.

4.1 Abstract

To date, heart disease remains to be the leading cause of death worldwide. A subset of heart disease associated with fibro-fatty infiltration and increased risk for sudden cardiac death, known as arrhythmogenic cardiomyopathy (ACM), is primarily associated with variants within desmosomal genes. A desmosomal gene of interest is desmoplakin (*DSP*), as select variants in a ‘hotspot’ of ACM-associated variants have been previously reported to increased sensitivity to calpain degradation. Despite past studies, the majority of variants in ACM patients have yet to be classified as pathogenic or benign. With over 75% of *DSP* variants classified under unknown pathogenicity (UP), improved molecular knowledge on these variants is necessary to improve appropriate diagnosis and treatment of familial ACM

patients. We examined 11 UP *DSP* variants within the mutational ‘hotspot’ to evaluate molecular modifications within the calpain sensitive region of each variant that may trigger calpain sensitivity. Molecular dynamic simulations identified 2 UP variants with disrupted exposure of the calpain target site. Surprisingly, nine variants had increased sensitivity to calpain *in vitro*, suggesting other factors may contribute to calpain-mediated degradation. Regardless, this reinforces understanding of the calpain sensitivity of DSP, and may aid in future personalized treatment for ACM patients with calpain sensitive variants.

4.2 Introduction

Heart disease remains as the leading cause of death worldwide and remains to be to be a significant economic burden worldwide, resulting in nearly 875,000 deaths in the U.S annually [326]. One subset of cardiac disease, arrhythmogenic cardiomyopathy (ACM), is a leading contributor to sudden cardiac death (SCD), the leading natural cause of death worldwide [2, 272, 307]. ACM is characterized by fibro-fatty infiltration of the ventricular myocardium, increased propensity of ventricular arrhythmias, and reduced cardiac functional output [88, 142]. More concerning, ACM patients or those with a disease-causing variant, are vulnerable to the formation of life-threatening arrhythmias prior to the onset of cardiac structural defects, known as the ‘concealed phase’ [43-44]. While a challenge to treat, most ACM cases are linked to a known genetic culprit that can aid in diagnosis of familial cases. Among a large pool of ACM-linked genes, genetic variants are most frequently identified (85%-90% of cases) with desmosomal genes [160, 164]. The desmosome is protein complex that lies at the intercellular junction between adjacent

cardiomyocytes known as the intercalated disc (ID), providing structural support through cytoskeletal linkage to ensure cells stay adhered during the mechanical stress generated from contractile forces [5]. Among desmosomal proteins, variants most frequently lie in plakophilin-2 (PKP2), desmoglein-2 (DSG2), and desmoplakin (DSP) [45, 85].

Among these, DSP is of particular interest for multiple reasons. ACM cases linked to *DSP* variants have a unique left/biventricular dominance with unique fibrotic patterns prior to systolic dysfunction, where some suggest should be referred to as a unique form of ACM [172]. While the majority of ACM-linked variants are associated with premature truncating or impacting splice sites (83%) [159], DSP has an increased proportion of missense variants (35%) [85, 113]. Additionally, there is a significantly disproportional upregulation of pathogenic missense variants at the N-terminus portion of DSP, referred to as a mutational ‘hotpot’ [85]. The N-terminus of DSP is comprised of multiple spectrin repeat (SR) with a Src homology 3 (SH3) domain [93]. This region has multiple functions, including mechanical stability/mechano-sensing [86, 93], linking the cytoskeletal network to the desmosome through plakoglobin (PKG) and PKP2 interactions [70, 94], as well as recruitment and stabilization of the essential gap junction (GJ) protein connexin-43 (Cx43) to the ID [71-72]. Based on the essential function, the connection of dysfunction of this SR/SH3 to ACM is not surprising.

Our group has previously studied the influences these ‘hotspot’ variants have on a calpain target site buried within the SH3 domain of DSP [76]. Calpain is a calcium expressed calcium-activated cysteine protease [115, 122]. It is expressed ubiquitously and has a multitude of functions, including cytoskeletal rearrangement, regulated protein

turnover, regulation of cellular signaling/gene expression, and apoptosis [115, 118, 123, 327-328]. However misregulation of calpain has been linked to multiple diseases, including Alzheimer's and muscular diseases [119-121, 130, 329]. We previously reported that select pathogenic variants at this 'hotspot' result in destabilization of this region from molecular dynamic (MD) stimulations. Ultimately DSP variants that resulted in a reduced stability and increased exposure of this target site displayed increased protein degradation following calpain incubation [76]. A strong correlation was identified when comparing the exposure of this calpain sensitive region to protein stability following calpain incubation, suggesting this may be a potential method of identifying additional pathogenic variants in the future.

As there are many subsets of ACM with unique symptoms from a variety of genetic causes, as well a growing pool of associated variants with unique mechanisms of action, it is essential to improve personalize management for patients in the clinical setting. However, this can be particularly challenging as a genetic culprit is not identified in each familial/idiopathic case [330]. Among a publicly accessible ACM database (<https://arvc.molgeniscloud.org/>; [113]), there is a significant number of identified variants that are not listed as pathogenic. Approximately 76% of reported *DSP* variants fail to be categorized as pathogenic or benign [113], creating a significant clinical burden for diagnosis and treatment. The need to categorize these variants of unknown pathogenicity, referred to as UP variants, is necessary to overcome this clinical obstacle.

Among the nine pathogenic variants in the mutational 'hotspot' of DSP, eleven additional UP variants exist within this site (residues 270-550). Based on our previous study, DSP expressed in iPSC-derived cardiomyocytes isolated from human patients (DSP

p.R451G) displayed reduced protein expression with unaltered mRNA levels [76]. Additional pathogenic variants were examined via *in silico* and *in vitro* approaches, where a tight correlation was found between the disrupted structure of a buried calpain target site when compared to DSP degradation levels following calpain incubation [76]. With this, we sought to examine these UP variants in the ‘hotspot’ to identify if they shared a similar mechanism as seen in pathogenic variants that may help categorize them as pathogenic. Molecular dynamic simulations determined that many of these variants primarily localized within the SR4 domain in close proximity to SH3 domain, the location of the buried calpain target site. Overall a small subset of DSP variants perturbed the molecular stability and environmental exposure of this region. Despite this, a larger subset of variants displayed increased sensitivity to calpain, indicating there may be additional molecular influence that determine calpain ability to interact and degrade DSP.

4.3 Materials and Methods

Site Directed Mutagenesis: The NH₂- terminus of human desmoplakin (residues 1-883; Addgene plasmid #32227) was directionally cloned into the pGEX-4T1 vector (insert citations) as previously described [76]. The Q271K, W285G, I305F, R315C, L392P, I399M, K401N, N408K, K449T, Y494F, and L547R mutations were individually introduced into the wildtype desmoplakin₁₋₈₈₃ using the QuikChange Site-directed mutagenesis Kit (Agilent Technologies, Santa Clara, CA) according to manufacturer’s instructions. Introduction of each mutation was confirmed via sequencing. Primers used are listed below.

Primers: A list of all primers utilized are provided below

Primer Name	Primer Sequence 5'-3'
SDM DSP Q271K-F	5'-gaggatggatcacctgcgaaagctgcagaacatcattca
SDM DSP Q271K-R	5'-tgaatgatgttctgcagcttgcaggtgatccatcctc
SDM DSP W285G-F	5'-ccagggagatcatggggatcaatgactgcgag
SDM DSP W285G-R	5'-ctcgcagtcattgatccccatgatccctgg
SDM DSP I305F-F	5'-gcgacaagaacaccaacttcgctcagaacagg
SDM DSP I305F-R	5'-cctgttctgagcgaagttggtgttctgtcgc
SDM DSP R315C-F	5'-ggaggccttctccatgatcatgagcaactggaag
SDM DSP R315C-R	5'-cttcagtgactcatgcatatggagaaggcctcc
SDM DSP L392P-F	5'-actgaagcataccgaaagggctccaggactc
SDM DSP L392P-R	5'-gagtcctggagccccttcgggtatgcttcagt
SDM DSP I399M-F	5'-gctccaggactccatgaggaagaagtaccctg
SDM DSP I399M-R	5'-caggggtacttctcctcatggagtctggagc
SDM DSP K401N-F	5'-ccaggactccatcaggaataagtaccctgcgac
SDM DSP K401N-R	5'-gtcgcaggggtacttattcctgatggagtctgg
SDM DSP N408K-F	5'-ctcgcacaagaaaatgccctgcagcacctg
SDM DSP N408K-R	5'-caggtgctgcaggggcatttctgtcgcag
SDM DSP K449T-F	5'-gaagattgtacagctgacgcctcgtaccagac
SDM DSP K449T-R	5'-gtctgggttacgagggcgtcagctgtacaatctc
SDM DSP Y494F-F	5'-agcgcagcaagtggttcgtgacgggccc
SDM DSP Y494F-R	5'-gggcccgtcacgaaccattgctgcgct
SDM DSP L547R-F	5'-tacatcaacatgaagagccgggtgtcctggcactac
SDM DSP L547R-R	5'-gtagtgccaggacaccggctctcatgttgatgta

Protein Purification: Wildtype and mutant desmoplakin₁₋₈₈₃ proteins were produced in bacteria (BL21 [DE3]) and purified GST-fusion proteins using the pGEX-4T1 vector system as previously described [76, 97].

Calpain Assays: Recombinant protein (5 ug) of each DSP variant was diluted in assay buffer (40 mM Trish HCl, 50 mM NaCl, 2 mM DTT, 10 mM CaCl₂) with and without calpain. Reactions were incubated at 37°C for 30 minutes. Reaction products were analyzed by SDS-PAGE followed by staining with Sypro Ruby total protein stain according to the manufacturer's instructions. Quantification of total amount of protein

remaining was calculated via densitometry obtained from ImageJ software (NIH) by comparing protein levels with calpain incubation to levels without calpain incubation. Values were normalized to wildtype calculations. Values for at least three independent replicates were averaged for each desmoplakin₁₋₈₈₃ protein.

Molecular Dynamics: Computational modeling was done using the human wildtype DSP residues 178–627 (PDB accession 3R6N) [331]. Models of each variant were generated with the “swap residue” command in YASARA using an AMBER14 forcefield and allowed to equilibrate for 60–200 ns in triplicate in explicit solvent at 37 °C, 150 mM NaCl, as previously described [76]. Simulations were surveyed every 100 ps, and the data were tabulated using YASARA macros. The exposed surface area of residues 447–451 was calculated every 2.5 ns for each variant as previously described [76, 97].

Statistics: Data are presented as mean \pm S.E.M. For the comparison of two groups, we performed unpaired two-tailed Student’s t-test when data passed normality test (Shapiro-Wilk normality test).

4.4 Results

4.4.1 Desmoplakin UP variants surround the calpain target site primarily in the SR4 domain

Previously we have examined pathogenic DSP variants using MD simulations to identify potential disruptions in the core stability of the calpain target site [76]. We sought to accomplish this in UP variants through the same process. Among the three major domains of DSP, most pathogenic variants lie with the N-terminal plakin domain,

specifically within the C-terminus of SR4 and throughout the SH3 domain (Figure 21A). The junction between the SR4 and SH3 domain encompasses the calpain target site that was previously studied among pathogenic variants (Figure 21B). Most pathogenic variants are within close proximity ($<20\text{\AA}$) of this target site (Table 4), even those that are distant in terms of linear sequence (i.e. S299R and N375I, Figure 21A/B). The majority of UP variants lie outside of the SH3 domain in the alpha helices of the SR4 domain (Figure 21A/B). Most UP variants lie more distal from the calpain target site, as only 27.3% of UP variants are within 20\AA of residue L448 as opposed to 77.8% of pathogenic variants (Figure 21B, Table 4). The four closest UP variants to the calpain target site (I305F, R315C K449T and Y494F) were analyzed to determine the potential impacts on intramolecular interactions. I305F and R315C localize in the SR4 domain near (R315C) or within a flexible hinge domain (I305F). Both R315 and I305 interact with an adjacent α -helix in this SR4 domain (Figure 21C/D). The hinge domain these residues directly interact with the calpain target site through interactions K449-D300, suggesting these UP variants, as well as K449T, may destabilize the stability of the target site (Figure 21C-E). Additionally, the Y494 residue is within the SH3 domain and is proximity to form interactions with an adjacent β -sheet (Figure 21F). Overall while these residues are typically further from the calpain target site compared to pathogenic variants, select variants still form key intramolecular interactions that may stabilize the SR4-SH3 junction.

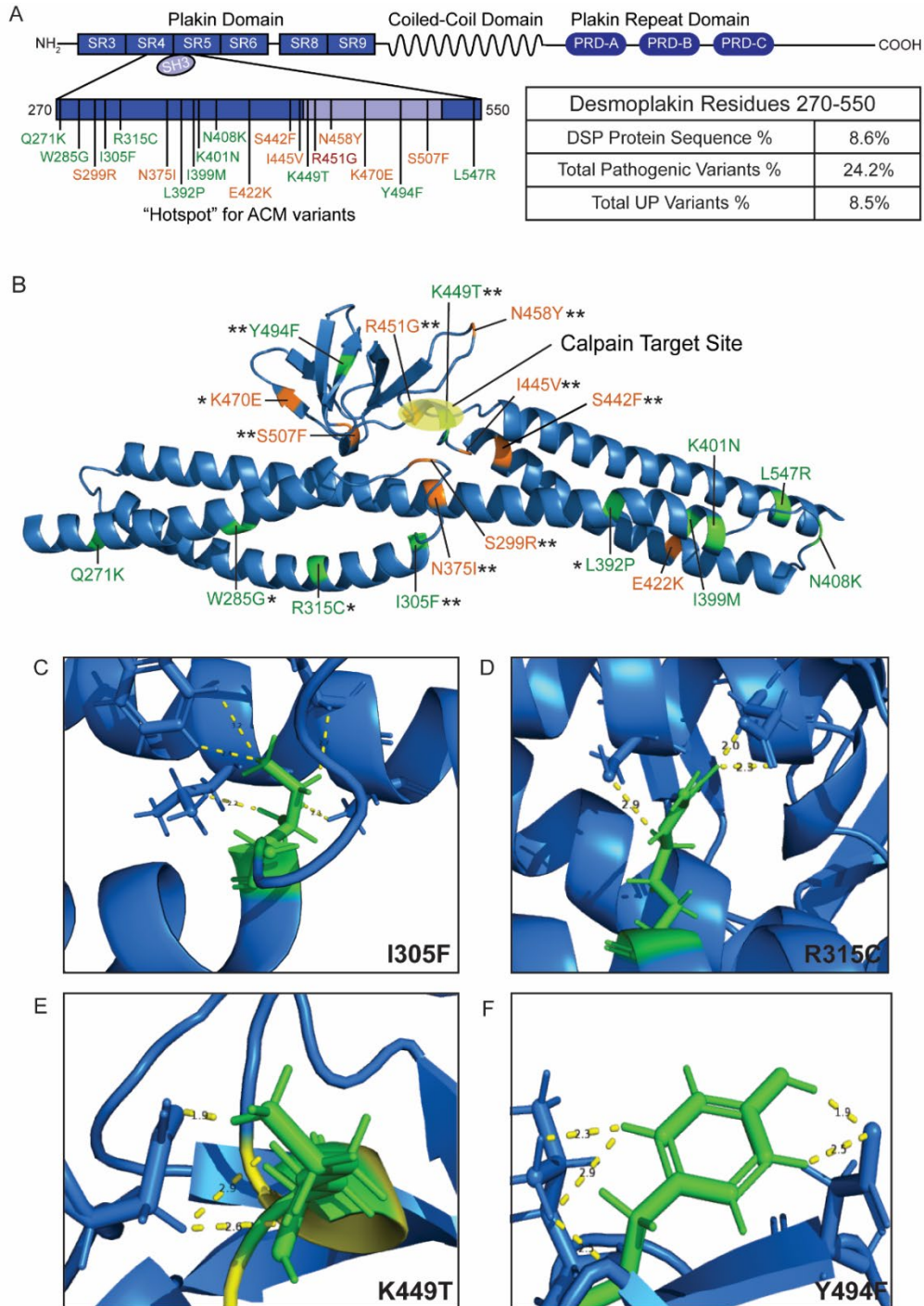


Figure 21: Stability of SH3/SR4 domains are maintained by the residues many UP variants reside

(A) 2D model of entire DSP protein with labeled domains. The mutational ‘hotspot’ is zoomed in (residues 270-550), and variants of pathogenicity (in orange) and unknown pathogenicity (in green) are labeled. The R451G pathogenic variant within the calpain target site is labeled in red. Distribution chart of the percentage of each variant in this ‘hotspot’ is provided. **(B)** Three dimensional model of N-terminal DSP (residues 265-554) labeled all pathogenic and UP variants. * Variant is within 30Å, ** or 20Å of the calpain target site, labeled in yellow. **(C)** Zoom in of residue I305 and its potential interactions (Y296, L372, N375, A376). **(D)** Zoom in of residue R315 and its potential interactions (C289, E292). **(E)** Zoom in of residue K449 and its interactions (D300). **(F)** Zoom in of residue Y494 and its interactions (D502, L504). All labeled interactions are under 3.5Å

4.4.2 Select UP variants disrupt important interactions within the calpain target site

To quantify the stability of this target site, we sought to analyze the intramolecular that stabilize the core region surrounding the calpain target site. MD simulations examined the structure of DSP following the introduction of each UP variant independently. Simulations revealed no variant resulted in protein unfolding or overt morphological changes when compared to WT DSP (Figure 22A). Previously we analyzed the stability and count of 11 interactions surrounding the target calpain target site, as pathogenic variants did not disrupt global protein structure [76]. Among the UP variants, two (R315C and K449T) displayed a statistically reduced interaction stability at this site compared to WT simulations (Figure 22B). Protein interactions are dynamic that allow flexibility and movement within protein domains, so changes in select interactions may be involved in determining overall stability of the SH3 domain. Histograms of the frequency of intramolecular interactions were generated to compare pathogenic and UP variants to WT DSP. Despite only two UP variants displayed a significant reduced interaction count, there are identifiable changes in additional UP variants. While WT simulations more frequently were measured to have 10 interactions, variants such as Q271K (8), W285G (8) and I399M

(9) displayed less interactions more frequently (Figure 22C). This suggests that while there is no statistical reduction in interaction count, select interactions may be disrupted by the introduction of a variety of these UP variants.

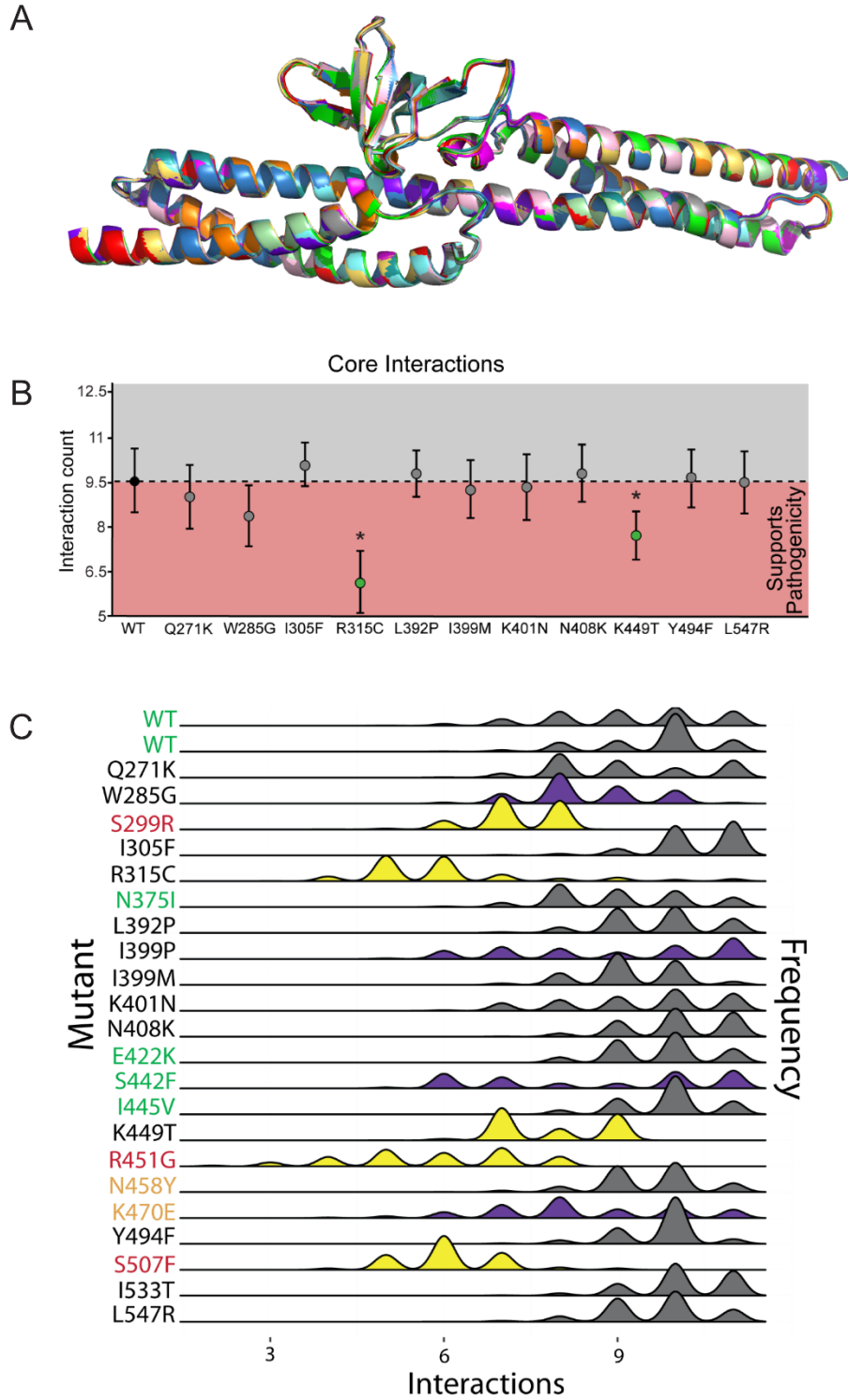


Figure 22: Select UP variants disrupt intra-molecular interactions surrounding the calpain target site

(A) Image of an alignment of all 11 UP variants compared to control DSP reveals no significant morphology changes or protein unfolding. **(B)** Calculation of the average number of intramolecular interactions surrounding the calpain target site. * p-value < 0.05. **(C)** Histograms showing the average number of interactions that surround the calpain target region in WT and each variant of DSP.

4.4.3 Exposure of the calpain target site is not influenced by most UP variants

As select UP variants resulted in perturbed interaction stability and count at the calpain target site, it is possible the protein stability is decreased resulting in an increased dynamic behavior of the protein. To evaluate this, we analyzed MD simulations by examining the surface area exposure of the target site to the exposed environment. Multiple measurements were recorded, representative images are provided (Figure 23A). Overall, only the K449T displayed a statistically reduced exposure of the target site compared to WT simulations (Figure 23B). While multiple other variants displayed a trending increase (R315C: p-value = 0.181) or decrease (N408K: p-value = 0.111; Y494F: p-value = 0.0780) in exposure, most UP variants did not display significant changes in exposure of the target site.

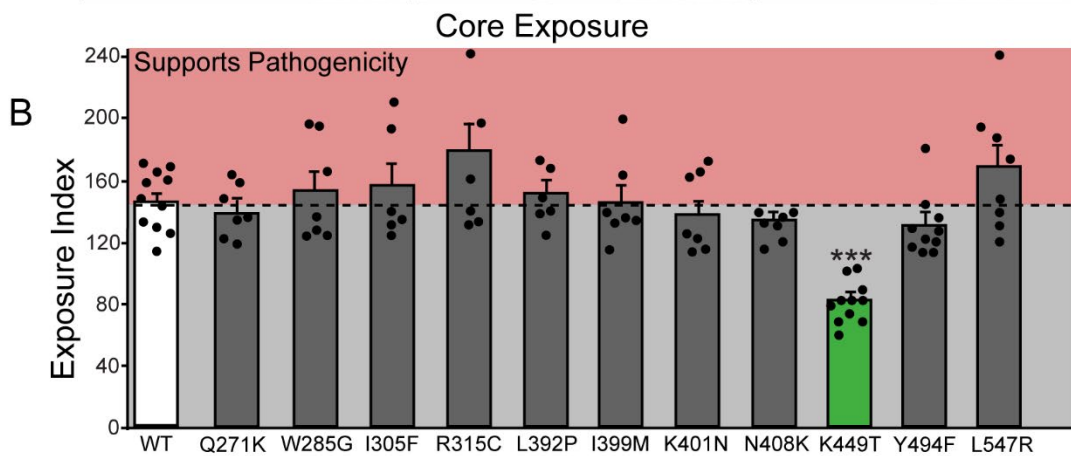
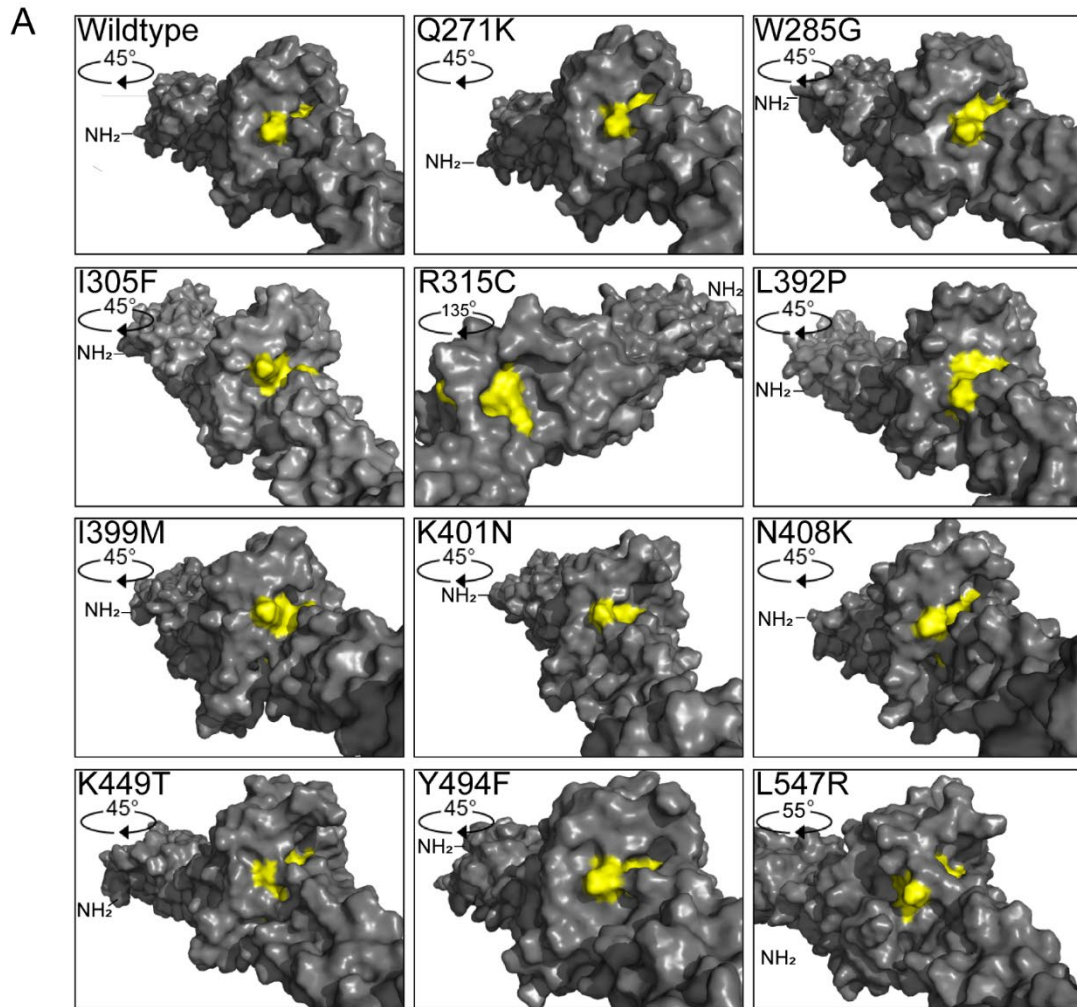


Figure 23: Core exposure of the calpain target site is uninfluenced by UP variants

(A) Representative MD images of the N-terminus of each UP variant examining the exposure of the calpain target site (labeled in yellow). (B) Quantification of the

environmental exposure (\AA^2) of the target site (residues 447-451) compared to WT simulations. *** p value <0.001.

4.4.4 Calpain sensitivity detected in the majority of UP variants *in vitro*

To determine if any of the UP variants that disrupted core integrity lead to increase calpain sensitivity *in vitro*, recombinant GST-tagged N-terminal DSP (residues 1-883) were produced. Each variant was incubated with calpain and protein levels were compared to samples without calpain by gel staining (Figure 24A). These values were normalized to WT DSP degradation. Interestingly, 9 of the 11 variants displayed increased sensitivity to calpain mediated degradation (Figure 24A), not anticipated as not all UP were predicted to alter DSP structure *in silico* (Figures 22-23). Previous work identified a strong correlation when comparing the values of core exposure to protein remaining after calpain incubation (normalized to WT) [76]. However, once all UP variants were added, this correlation became very weak (Figure 24C). There were multiple outliers in the data that could be excluded from this data. In our previous study, a pathogenic variant E422K was examined that resulted in significant degradation of DSP following the incubation of calpain despite having minimal influence to the target site [76]. Select variants displayed unexpected heightened sensitivity to calpain. It was identified that it modified an existing minor calpain target site to increase its sensitivity to calpain, and indeed the K401N and L547R lies directly on a calpain target site, and the Q271K, N408K and L392P variants influence the sensitivity of this site as well (Table 5). These values were therefore excluded from our correlation graphs, as well as K449T, a variant that manipulates the major calpain target site itself to be more sensitive despite decreasing its exposed site to the environment. It

also increased the sensitivity to Y455 to calpain, potentially making the target site involve more residues than other variants (Table 5). Overall, removing these variants resulted in a stronger correlation between the target site exposure and protein degradation (Figure 24D), although not as strong as the pathogenic variants themselves as previously reported [76]. This suggests that the calpain predictor model is a helpful tool that may help predict pathogenicity in variants of DSP, but other factors including additional minor calpain target sites must be considered during analysis.

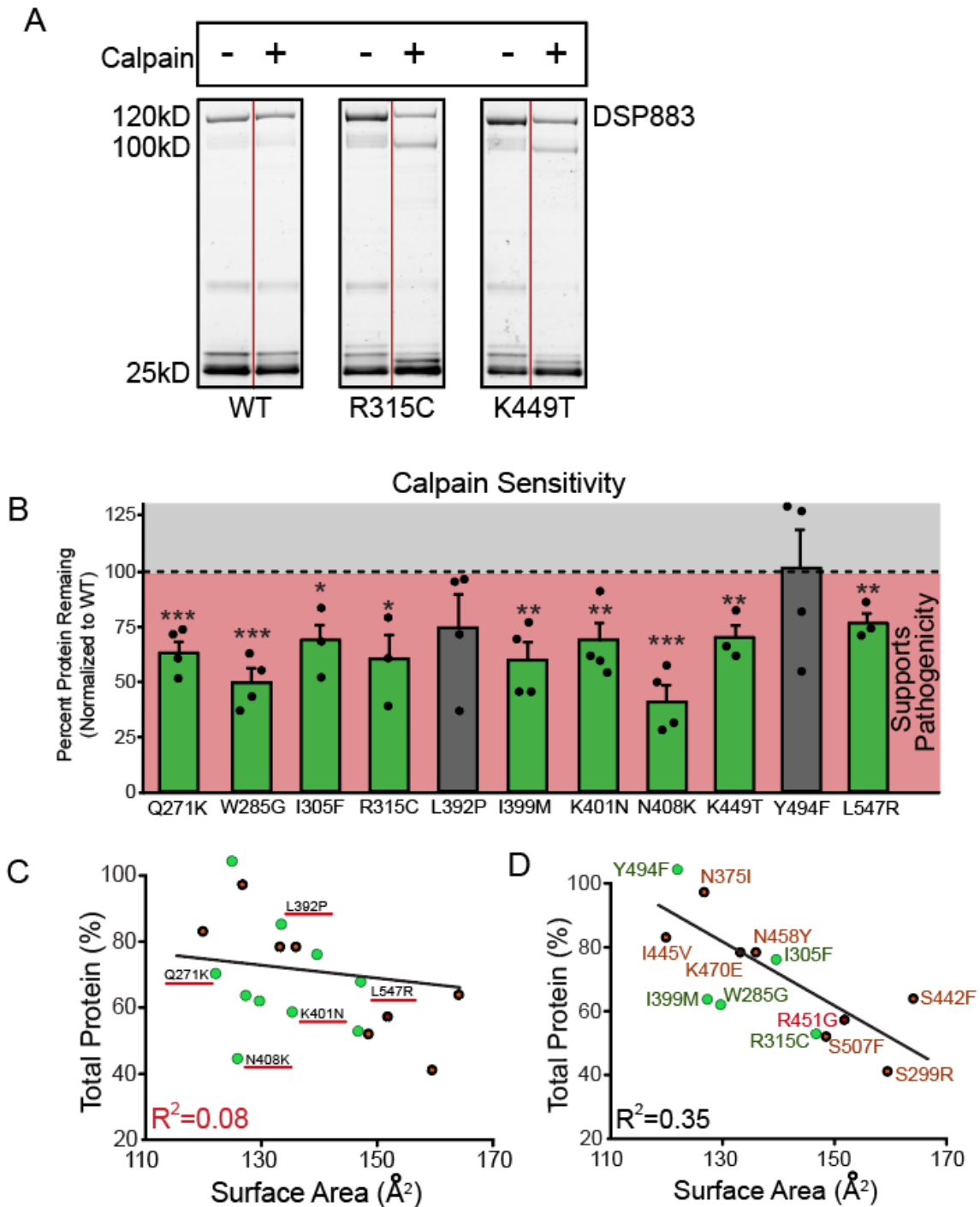


Figure 24: Increased sensitivity to calpain identified in most UP variants

(A) Representative sypro-ruby gel staining of GST-tagged DSP₈₈₃ before and after incubation of calpain of WT and UP variants. (B) Quantification of % protein remaining following calpain incubation when normalized to WT DSP. * p-value<0.05, ** p-value<0.01, *** p-value<0.001. (C) Correlation graph of all pathogenic variants and UP

variants comparing protein remaining after calpain incubation to surface area exposure of the target site. Excluded variants underlined in red. **(D)** Correlation graph of all variants after removing excluded variants.

4.5 Discussion

A significant number of genetic variants linked to ACM, and multiple studies have focused heavily on understanding the effects of loss of gene expression, as well as how each variant may contribute towards disease progression. This has led to significant progression in the clinical setting and improving scientific study design. Our previous work has identified a potential shared mechanism of pathogenicity with the N-terminal mutational ‘hotspot’ within *DSP*. While this a novel finding, there are a significant number of *DSP* variants within this ‘mutational’ hotspot that are labeled under unknown pathogenicity. Reclassifying these variants as pathogenic or benign is imperative to improve clinical diagnosis and personalized treatment of individuals with suspected ACM. *DSP* UP variants were of interest because of the mutational ‘hotspot’ in its N-terminus [85], where we have linked select variants in this region to increase sensitivity to the protease calpain [76]. With this, we aimed to evaluate the UP variants within this region to determine if any share this sensitivity.

We aimed to evaluate the properties of these variants via *in silico* and *in vitro* methods. Simulations via molecular dynamics revealed that none of the 11 variants resulted in significant destabilization of the N-terminus of *DSP* as a whole. However, interactions counts were significantly reduced in two variants (R315C and K449T), and additional variants had reduced stability of select interactions even if the average number was not

reduced. This is an important factor to consider, as the dynamic properties of these interactions result in significant fluctuations in protein the flexibility of the protein at the core of the SH3 domain. Variants may still be vulnerable to calpain degradation even if one of these interactions is disrupted. Exposure of the calpain target site to the environment was also compared to determine if this could be a useful model to predict sensitivity without an experimental model. Overall only one variant displayed a significant alteration to the environmental exposure, the K449T variant that is the center of this target site. Multiple variants did trend towards significance however. Like the interaction count, it is possible the maximal exposure of the site is more important than the average exposure. WT exposure of the target site fluctuated from 118 Å² to 172 Å², where UP variants such as W285G (197.2 Å²), I305F (211 Å²), R315C (244 Å²), I399M (198 Å²), and L547R (241 Å²) reached a higher maximum in core exposure. This suggests while the average exposure to the environment is not disrupted, these UP variants may spend more time exceeding a specific threshold of exposure they may make them more vulnerable to calpain targeting.

Using *in vitro* approaches through the production of recombinant DSP, nine of the eleven UP variants were identified to have increased sensitivity to calpain degradation when compared to control DSP. Some of these variants behaved unexpectedly based on MD simulations, however it was determined that multiple variants were within additional predicted calpain target sites, or within close proximity. This created variance in our previously generated predictor model using pathogenic variants previously discussed [45]. Once these variants were removed, we found there remained a correlation between exposure of the calpain target site and sensitivity to calpain-mediated degradation.

MD simulations were a useful tool in assisting in the prediction of these variants of UP that have been applied by multiple groups on DSP pathogenic variants previously. Previous research has identified that the N-terminus of DSP, specifically the SH3 and SR4-5 domains, are vital for providing mechanical strength to the protein [93], and different variants result in altered stiffness that resulted in decreased force required for rupture [95]. It is possible that variants may not only be influencing the SH3 structure, but the integrity of the SR domains. Supplemental biochemical analysis is essential to identifying calpain sensitive variants that are difficult to identify *in silico*, as evaluating the properties of every predicted calpain target site is not feasible. It is acknowledged that a limitation of this study was a lack of a cellular or *in vivo* model. While this will be a goal in future studies, a major premise of these techniques is to establish a rapid method to determine a shared mechanism to pathogenic variants that can be an effective predictor model of disease.

Overall we have determined that a multitude of UP DSP variants display increased calpain sensitivity as proximal pathogenic variants, indicative calpain sensitivity may be an indicator of disease pathogenicity. It is to be noted that multiple pathogenic variants did not display calpain sensitivity, indicating current and future UP variants stable following calpain incubation cannot be listed as benign. Additional studies by our group has focused on finding protective means to prevent DSP degradation in calpain-sensitive variants [97]. Recent studies have introduced a protective aromatic variant (L518Y) proximal to the calpain target site to protect calpain sensitive pathogenic variants. This variant showed effectiveness in mitigating protein degradation, suggesting the option to protect DSP is

viable [97]. Future studies will focus on further molecular characterization of these UP variants, and analyzing the properties of smaller predicted calpain target sites in relation to these calpain sensitive variants. Additional models, including cell lines, will also be generated with each UP variant to identify downstream physiological consequences.

Chapter 5. Discussion

Arrhythmogenic cardiomyopathy is a category of heart diseases with a strong genetic component with a variable phenotype that can be exacerbated by physical stress. Extensive work has been done on both of these topics to fully understand the mechanisms and drivers responsible for phenotypic progression of ACM. A genetic cause has been identified in nearly 60% of ACM cases, and among these, nearly 90% of genetic variants lie in proteins within the ID, specifically the desmosome [42, 45, 160, 164]. With desmosomal proteins playing a major role and ensuring proper function of the ID for electrical and mechanical signaling, as well as being involved in cell signaling, it is understood how variants in these proteins could result in an arrhythmic phenotype [5, 73]. What is less understood about the disease is the pathways that contribute towards disease development. Evidence has suggested that a variety of signaling pathways, including Wnt/ β -catenin [90, 106, 110], hippo [167, 268], and β -adrenergic [129, 155, 332] pathways are commonly disrupted that can induce the ACM phenotype. However, different disease-causing variant may contribute differently to the impacted pathways.

A large portion of familial ACM cases have no identified variant [42, 131, 134]. It is possible that a subset of these cases may be linked to undiscovered variants, related to understudied genes with no known role in the heart, or associated with oligogenic or polygenic genetic variants of unknown significance [158-159]. Despite this, the role of external stress and environmental factors is understood to be a significant variable in disease onset and prognosis of patients [135, 267, 271]. Among these, exercise is considered a leading contributor to disease progression, and poses a substantial risk factor

for inducing ventricular arrhythmias and SCD. Exercise restriction is universally recommended for all patients of ACM and asymptomatic individuals within a known disease causing variant, including individuals in families where the cause of disease is unknown [135, 287, 307, 330]. Between 40-60% of SCD cases in ACM patients occurred during exertion [150, 272]. One study of 202 SCD cases linked to ACM found that the 78% of cases had no reported symptoms prior to death, and competitive athletes were over represented among patients passing of SCD [150]. Aside from exercise, emotional distress is a frequent trigger for arrhythmias.

These variables make the clinical approach to treating ACM quite difficult, as there are many subclasses based on symptoms and associated genetic cause. Family members with the same pathogenic variant may experience drastically different phenotypes, and there are discrepancies in symptoms and disease severity among different variants within the same gene [172, 330, 333]. This emphasizes the need for personalized medicine to treat each individual uniquely based on their symptoms, external sources of stress, affected disease causing gene and even specific properties of the variant [330]. To achieve this, animal models that more accurately recapitulate the human are necessary to better understand the genotype-phenotype relationship and the influences of cardiac stress. As most mouse models currently focus on either transgenic or KO techniques, while information can be gathered on the manipulated gene might have in the heart function, they are less reliable examining disease progression [138-139]. With this, we sought to develop one of the first mouse models with an endogenous modification in *Dsp* meant to recapitulate a human variant. The R451G DSP variant was chosen because of its

involvement in a large ACM family, its extensive characterization in both human biopsy samples and iPSCs, and its potential shared mechanism of pathogenicity with other *DSP* variants in the mutational ‘hotspot’ [76].

The initial goals of the study including the development of a *Dsp*^{R451G/R451G} homozygous model to understand the consequences of this variant without the influence of the control allele. After sequencing multiple litters, it became apparent that homozygous mice were likely not viable, and indeed embryonic lethality was identified prior to E10 (Figures 6-7). This finding was significant for two major reasons. First, this suggests the single point variant of DSP has extreme detrimental effects, and the ramifications from its influences cannot be compensated. Second, this restricted us to proceed with the viable *Dsp*^{R451G/+} model, making our mouse model more recapitulative to the human genotype to improve the translatability of the research. When analyzing the molecular properties of these mice, we identified decreased DSP protein expression in the heart and at the ID without observing either degradation products or mislocalization patterns (Figure 8A/B/D). This loss of DSP occurred post-translationally, as *Dsp* levels were unchanged as seen from qPCR data (Figure 8C). Additionally, while not seen to the extent as in human biopsy samples, disrupted distribution of Cx43 at the ID was noted [76]. This connection in the molecular findings between human biopsy samples and the *Dsp*^{R451G/+} mouse cardiac tissue suggests we have successfully developed one of the first animal models to recapitulate properties of a human genetic variant. Despite this, the *Dsp*^{R451G/+} model develops no identifiable cardiac phenotype without the application of stress (Figure 10-11). This includes no chamber dilation, fibro-fatty infiltration, changes in cardiac output, or any

electrical defects, with the exception of a trending prolongation of QTc and T-peak and T-end (Table 2). Following acute stress through epinephrine injections to stimulate β -adrenergic signaling, *Dsp*^{R451G/+} mice experienced prolonged arrhythmias more frequently compared to control littermates (71.4% vs 12.5%; Figure 16). Additionally, chronic stress through pressure overload surgeries resulted in *Dsp*^{R451G/+} displaying signs of heart failure at 4 weeks post-surgery (Figure 15), ultimately linked to a reduction in cardiac output and increased chamber dilation (Figures 12-13).

Our model did not display a basal phenotype, but rather an inducible one through the application of multiple stressors. This concept has been previously shown in additional models of ACM, as well as other cardiac disorders including HCM. For ACM, a PKG heterozygous KO and R735X PKP2 transgenic mouse model was established by two separate groups [182, 273]. At baseline these models did not display a phenotype, but following exercise the development of electrical and structural defects were identified [182, 273]. A separate study produced a mouse model derived from a human DSC2 variant (G790del) [334]. While the human family was heterozygous for this variant, +/G790del mice displayed no phenotype, and homozygous G790del/G790del only displayed a slight chamber dilation and mild changes in intracellular calcium transients. No notable ID protein expression or localization were noted [334]. This suggests the DSC2 +/G790 variant, as is the heterozygous R451G variant based on our research, is not sufficient to drive the development of ACM without other stimuli. Yang et al. developed an HCM model using a truncated cardiac isoform of myosin binding protein C (cMyBP-C) identified in multiple individuals. This variant led to only a mild form of hypertrophy, however the

use of treadmill exercise reduced cardiac output, reduction in total exercise capacity, and increased mortality when compared to control mice [335]. As previously mentioned, two other groups have produced two ACM models through heterozygous KO of *DSP*, and while our novel model is not based on a KO method, it still shows a significant reduction in the expression of DSP. While it is possible the line each model was backcrossed into may play a role in disease severity, it is also possible that the *Dsp*^{R451G/+} model has enhanced integrity where the addition of stress is required to mediate this discrepancy. This significantly highlights the advantages of using endogenous variant models that recapitulate the human genome as opposed to traditional KO models.

While the findings from the novel *Dsp*^{R451G/+} were initially surprising, it lays the foundation for future studies to explore multiple avenues of ACM research. Future work on the molecular mechanisms that contribute towards the progression of the disease is vital. All targets evaluated have significant links towards ACM from other studies, including essential ID proteins that stabilize the desmosome [73, 75, 90], those involved in the formation of arrhythmias through perturbed sodium or calcium signaling [96, 321], or involved in Wnt/ β -catenin signaling pathways [90, 109, 336] (Figure 18-19). However, these were not analyzed without stress, and as our data shows cardiac stress was necessary to induce a phenotype, stress may be necessary to drive molecular changes. The only noted molecular change outside of DSP protein levels was slight disturbances in Cx43 localization at the ID (Figure 20), however this is not as severe as those found in biopsy samples positive for the R451G variant [76]. As these samples were originally obtained from late stage ACM samples following SCD, this only further supports the necessity of

external stress to result in molecular disturbances. While the additional of stress seems to be necessary, other molecular pathways remained to be explored. Epinephrine is an agonist of the β -adrenergic pathway, known to play a major role in calcium handling, contractility, and regulation of calpain through the activation of PKA and CaMKII [129]. Examining downstream targets of these pathways, including phosphorylation levels of essential calcium signaling proteins such PLN, RYR2, Cav1.2, and cMyBP-C, could provide important understanding the drivers of the arrhythmic phenotype without structural abnormalities. The hippo signaling pathway is strongly correlated with Wnt/ β -catenin signaling pathway through the activation of Yes-associated protein (YAP). YAP is capable of preventing β -cartenin localization to the nucleus [167], which may also be a driver that promotes ACM that can be further explored. Other pathways include the ERK pathway, previously shown to be activated following loss of DSP to trigger downstream phosphorylation and degradation of Cx43 [72], and has also been associated with the β -adrenergic pathway [129]. Cx43 also plays an important role in the localization and activity of $\text{Na}_v1.5$ [5], another key target to evaluate post-stress.

The sensitivity to structural remodeling using pressure overload supports the *Dsp*^{R451G/+} model has ACM like traits, however the timing of heart isolations posed as a limitation in our study. By the 12 week timepoint, control as well as *Dsp*^{R451G/+} mice displayed signs of heart failure, where no changes in fibrosis or HW/TL were identified (Figure 12-13 Figure 15). Four weeks post-surgery, *Dsp*^{R451G/+} showed clear signs of heart failure when compared to control littermates (Figure 15), including a dilated phenotype at systole that trended towards significance at diastole (Figures 12-13). This may be the ideal

age to examine global morphological changes (fibro-fatty infiltration), as well as molecular changes as previously described. Desmoplakin, being vital for desmosomal stability as the linker to the desmin cytoskeleton network, plays a significant role in the ultrastructure of the ID. While IF staining can reveal changes in protein localization, it cannot detect gross changes at the ID. Through TEM, the changes in ID integrity associated with the loss of DSP can be analyzed, and compared before and after the induction of stress. Alterations to desmosomal, GJ, and AJ measurements and morphology, each capable of being distinguished as seen in figure 2, can be evaluated after the administration of stress between groups as well.

It is acknowledged that TAC, while an easily regulated and consistent form of cardiac stress, may not be the most physiologically relevant towards an ACM model. As our model recapitulates a variant expressed in human ACM patients, it is important to utilize the appropriate stressor. As previously described, exercise is a strong inducer of the electrical phenotype that may be a contributor towards disease progression [135, 182, 272, 337], as the stimuli that trigger structural/fibro-fatty remodeling are not well characterized. Using exercise models as a stressor, as well as additional TAC studies could be beneficial in identifying which stressors lead to a more significant phenotype. Both treadmill and swimming exercise have been reported in mouse models previously [182, 273]. Swimming based exercise generally is considered more rigorous, it also requires training the mice and takes up considerable more time [338]. Treadmill exercise is an ideal starting point to identify the formation of arrhythmias as well as a structural phenotype, but swimming

experiments can be performed should treadmill exercise not induce a strong enough phenotype.

The goal of any disease model is to identify approaches to improve the diagnosis and treatments of patients. However a major limitation in the clinical setting is the lack of personalized treatment, due the variable nature of ACM between and within families with an identified genetic variant [330]. Analyzing potential effects of each disease causing variant is essential to administer the proper treatment plan, however this is difficult without proper identification of genetic variants. *DSP*'s N-terminus is a mutational hotspot with multiple pathogenic variants, but there are a host of variants of unknown pathogenicity at this site as well (Figure 3C) [113]. Determining if these variants are pathogenic or not is a difficult task if there is limited clinical information. However, as multiple DSP pathogenic variants share a similar mechanism to calpain sensitivity, identifying potential pathogenicity in these variants is plausible.

While these N-terminal pathogenic variants have been characterized in great detail, with further insights being enlightened by our novel mouse model, there remains a significant proportion of ACM variants labeled as unknown pathogenicity. Approximately 77% of *DSP* variants are classified as UP, making clinical diagnosis difficult [113]. By analyzing these UP variants, we have identified additional calpain sensitive variants by both *in silico* and *in vitro* techniques. It is important to note that more variants were determined to be calpain sensitive via biochemical techniques, suggesting additional factors are involved in determining degradation sensitivity outside of the interactions and exposure of the main calpain target site. It is important to consider that there additional,

poorly characterized calpain target sites outside of this main site linked ACM. Our previous research on pathogenic variants did determine one variant enhanced the sensitivity of a minor calpain target site [76], and select UP variants were determined to interact with, or directly lie in minor calpain sensitive sites (Table 5). These suggest that variants may still experience increased sensitivity to calpain despite minimal alterations to the major site, and novel/uncharacterized minor calpain target sites need to be examined in further detail. While the need to better understand these properties is imperative through MD studies, *in vitro* experiments are necessary to accurately determine the calpain sensitivity to each variant.

Approaches to treatment can vary greatly depending on the disease causing variant and the symptoms of each patient. Despite the shared mechanism of degradation via calpain in multiple DSP and PKP2 variants, calpain inhibitors are not physiologically viable due its essential role in muscle tissue as previously described. However, protecting DSP from calpain is a potential approach to explore in more detail. Using a large aromatic ring introduced by the L518Y variant in DSP, calpain sensitivity was mitigated when introduced in recombinant protein expressing select pathogenic variants as previously described [97]. This increased stability shows promise that calpain sensitivity can be overcome. Identifying large molecules or antibodies that can appropriately target DSP that remain continuously active without toxic effects may be challenging. However, this is a promising approach for a personalized treatment that may benefit multiple families with DSP/PKP2 sensitive variants [76, 97, 114]. Once developed, this could be administered into *Dsp*^{R451G/+} to potentially protect DSP protein levels, as well as prevent cardiac dysfunction following

stress induction. Beyond these novel therapeutic approaches, other therapeutic approaches can be evaluated independently or in conjunction. β -blockers are frequently prescribed to ACM patients as well as those with other arrhythmic disorders [45, 339-341]. By blocking the β -adrenergic pathway, PKA and CaMKII activity is restricted, preventing the phosphorylation of calcium handling proteins and preventing overactive calcium signaling [129]. This is particularly effective for preventing arrhythmias during physical exertion or emotional distress [341]. While no calcium defects have been identified to date in the *Dsp*^{R451G/+} model, calcium activates calpain activity and assists in translocating it to the ID via CaMKII [115, 127, 328], suggesting it may be beneficial to prevent arrhythmia formation in the *Dsp*^{R451G/+} mouse model. Additionally, GSK3 β inhibitors have been shown to be successful in multiple models of ACM [109, 197]. While this pertains more to Wnt/ β -catenin signaling, this is also an alternative approach if PKG/ β -catenin expression is found to be disrupted in *Dsp*^{R451G/+} mice following stress.

Murine models are acknowledged to have limitations in regards to the physiological representation to humans, specifically in terms of cardiac function. Firstly, the rodent model has significantly increased heart rate compared to humans, where the reliance on rapid contractions and filling is required for optimal cardiac output [342]. This results in mice only being able to have a minimal increase in heart rate during stress/exercise when compared to humans (~40% increase compared to ~170% increase) [343-346]. This results in humans having more regulatory ability to increase cardiac output through manipulation of stroke volume and heart rate [80]. Additionally, there is a significant reduction in AP duration, as well as AP morphology (rapid repolarization with an absent plateau phase) in

mice [80, 347-349]. Protein isoform and phosphorylation statuses can vary significantly between rodents and humans, where rodents display increased α MHC/ β MHC ratio [80, 350-352], increased N2B/N2BA titin ratios [353-355], and increased troponin I phosphorylation [356-358]. Calcium signaling also displays variabilities, where sarcoplasmic-reticulum calcium ATPase (SERCA) requesters more calcium in rodents, as the sodium calcium exchanger (NCX) plays a significantly reduced role [359-361]. Due to these alterations, the translatability of research conducted on murine disease models to human patients should be taken with caution, especially when studying therapeutic approaches.

The use of human derived iPSCs to produce EHT or other cardiac derived tissue has been an effective approach to overcome animal limitations. They have the most genotypic relevance towards humans, and has shown to be effective for identifying changes in gene/protein expression, changes in electrical conduction and contractility, and has even been implemented in pharmacological intervention studies [76, 362-363]. While an effective complementary model, there are limitations as this is not true cardiac tissue. EHT lacks the appropriate expression of other cells within the heart (epithelial, fibrotic, immune cells, neurons, etc.), each of which contributing significantly towards appropriate heart function and may be related to disease pathogenicity. Additionally, while electrical conductions can be observed, the global consequences of these defects on cardiac function cannot be determined in this model. Despite this, the use of EHT has been instrumental in improving our understanding of cardiac disorders, and is a useful model to use in conjunction with mouse studies.

Despite these limitations, this research addresses many gaps of knowledge in ACM research and aims to improve the development of more accurate ACM models in the future, as well as improved diagnosis and treatments of patients through personalized medical approaches. Molecular studies have also confirmed additional variants of unknown pathogenicity share increased sensitivity to calpain, suggesting this may be an effective risk factor for diagnosis of ACM, and may be a useful target to provide personalized care for patients with calpain sensitive variants. While these variants seem to have a gradient in terms of sensitivity to calpain, this may explain the differences in disease phenotypes among different familial variants, and external stress is a significant factor in the variance in phenotype within the same family.

References

1. Adabag, A. S.; Luepker, R. V.; Roger, V. L.; Gersh, B. J., Sudden cardiac death: epidemiology and risk factors. *Nat Rev Cardiol* **2010**, *7* (4), 216-25, DOI: 10.1038/nrcardio.2010.3
2. Srinivasan, N. T.; Schilling, R. J., Sudden Cardiac Death and Arrhythmias. *Arrhythm Electrophysiol Rev* **2018**, *7* (2), 111-117, DOI: 10.15420/aer.2018:15:2
3. Kennedy, A.; Finlay, D. D.; Guldenring, D.; Bond, R.; Moran, K.; McLaughlin, J., The Cardiac Conduction System: Generation and Conduction of the Cardiac Impulse. *Crit Care Nurs Clin North Am* **2016**, *28* (3), 269-79, DOI: 10.1016/j.cnc.2016.04.001
4. Burnstock, G., Purinergic Signaling in the Cardiovascular System. *Circ Res* **2017**, *120* (1), 207-228, DOI: 10.1161/CIRCRESAHA.116.309726
5. Vermij, S. H.; Abriel, H.; van Veen, T. A., Refining the molecular organization of the cardiac intercalated disc. *Cardiovasc Res* **2017**, *113* (3), 259-275, DOI: 10.1093/cvr/cvw259
6. Shih, H. T., Anatomy of the action potential in the heart. *Tex Heart Inst J* **1994**, *21* (1), 30-41,
7. Grant, A. O., Cardiac ion channels. *Circ Arrhythm Electrophysiol* **2009**, *2* (2), 185-94, DOI: 10.1161/CIRCEP.108.789081
8. Ather, S.; Respress, J. L.; Li, N.; Wehrens, X. H., Alterations in ryanodine receptors and related proteins in heart failure. *Biochim Biophys Acta* **2013**, *1832* (12), 2425-31, DOI: 10.1016/j.bbadis.2013.06.008
9. Wijesurendra, R. S.; Casadei, B., Mechanisms of atrial fibrillation. *Heart* **2019**, *105* (24), 1860-1867, DOI: 10.1136/heartjnl-2018-314267
10. Bhatt, H. V.; Fischer, G. W., Atrial Fibrillation: Pathophysiology and Therapeutic Options. *J Cardiothorac Vasc Anesth* **2015**, *29* (5), 1333-40, DOI: 10.1053/j.jvca.2015.05.058
11. Niebauer, M. J.; Chung, M. K., Management of atrial flutter. *Cardiol Rev* **2001**, *9* (5), 253-8, DOI: 10.1097/00045415-200109000-00004
12. Koplun, B. A.; Stevenson, W. G., Ventricular tachycardia and sudden cardiac death. *Mayo Clin Proc* **2009**, *84* (3), 289-97, DOI: 10.1016/S0025-6196(11)61149-X
13. Ludhwani, D.; Goyal, A.; Jagtap, M., Ventricular Fibrillation. In *StatPearls*, Treasure Island (FL), 2022,
14. Gourraud, J. B.; Barc, J.; Thollet, A.; Le Marec, H.; Probst, V., Brugada syndrome: Diagnosis, risk stratification and management. *Arch Cardiovasc Dis* **2017**, *110* (3), 188-195, DOI: 10.1016/j.acvd.2016.09.009
15. Hsiao, P. Y.; Tien, H. C.; Lo, C. P.; Juang, J. M.; Wang, Y. H.; Sung, R. J., Gene mutations in cardiac arrhythmias: a review of recent evidence in ion channelopathies. *Appl Clin Genet* **2013**, *6*, 1-13, DOI: 10.2147/TACG.S29676
16. Crotti, L.; Marcou, C. A.; Tester, D. J.; Castelletti, S.; Giudicessi, J. R.; Torchio, M.; Medeiros-Domingo, A.; Simone, S.; Will, M. L.; Dagradi, F.; Schwartz, P. J.; Ackerman, M. J., Spectrum and prevalence of mutations involving BrS1- through BrS12-susceptibility genes in a cohort of unrelated patients referred for Brugada syndrome

- genetic testing: implications for genetic testing. *J Am Coll Cardiol* **2012**, *60* (15), 1410-8, DOI: 10.1016/j.jacc.2012.04.037
17. Li, W.; Yin, L.; Shen, C.; Hu, K.; Ge, J.; Sun, A., SCN5A Variants: Association With Cardiac Disorders. *Front Physiol* **2018**, *9*, 1372, DOI: 10.3389/fphys.2018.01372
 18. Watanabe, H.; Koopmann, T. T.; Le Scouarnec, S.; Yang, T.; Ingram, C. R.; Schott, J. J.; Demolombe, S.; Probst, V.; Anselme, F.; Escande, D.; Wiesfeld, A. C.; Pfeufer, A.; Kaab, S.; Wichmann, H. E.; Hasdemir, C.; Aizawa, Y.; Wilde, A. A.; Roden, D. M.; Bezzina, C. R., Sodium channel beta1 subunit mutations associated with Brugada syndrome and cardiac conduction disease in humans. *J Clin Invest* **2008**, *118* (6), 2260-8, DOI: 10.1172/JCI33891
 19. Riuro, H.; Beltran-Alvarez, P.; Tarradas, A.; Selga, E.; Campuzano, O.; Verges, M.; Pagans, S.; Iglesias, A.; Brugada, J.; Brugada, P.; Vazquez, F. M.; Perez, G. J.; Scornik, F. S.; Brugada, R., A missense mutation in the sodium channel beta2 subunit reveals SCN2B as a new candidate gene for Brugada syndrome. *Hum Mutat* **2013**, *34* (7), 961-6, DOI: 10.1002/humu.22328
 20. Hu, D.; Barajas-Martinez, H.; Burashnikov, E.; Springer, M.; Wu, Y.; Varro, A.; Pfeiffer, R.; Koopmann, T. T.; Cordeiro, J. M.; Guerchicoff, A.; Pollevick, G. D.; Antzelevitch, C., A mutation in the beta 3 subunit of the cardiac sodium channel associated with Brugada ECG phenotype. *Circ Cardiovasc Genet* **2009**, *2* (3), 270-8, DOI: 10.1161/CIRCGENETICS.108.829192
 21. London, B.; Michalec, M.; Mehdi, H.; Zhu, X.; Kerchner, L.; Sanyal, S.; Viswanathan, P. C.; Pfahnl, A. E.; Shang, L. L.; Madhusudanan, M.; Baty, C. J.; Lagana, S.; Aleong, R.; Gutmann, R.; Ackerman, M. J.; McNamara, D. M.; Weiss, R.; Dudley, S. C., Jr., Mutation in glycerol-3-phosphate dehydrogenase 1 like gene (GPD1-L) decreases cardiac Na⁺ current and causes inherited arrhythmias. *Circulation* **2007**, *116* (20), 2260-8, DOI: 10.1161/CIRCULATIONAHA.107.703330
 22. Antzelevitch, C.; Nof, E., Brugada syndrome: recent advances and controversies. *Curr Cardiol Rep* **2008**, *10* (5), 376-83, DOI: 10.1007/s11886-008-0060-y
 23. Ishikawa, T.; Sato, A.; Marcou, C. A.; Tester, D. J.; Ackerman, M. J.; Crotti, L.; Schwartz, P. J.; On, Y. K.; Park, J. E.; Nakamura, K.; Hiraoka, M.; Nakazawa, K.; Sakurada, H.; Arimura, T.; Makita, N.; Kimura, A., A novel disease gene for Brugada syndrome: sarcolemmal membrane-associated protein gene mutations impair intracellular trafficking of hNav1.5. *Circ Arrhythm Electrophysiol* **2012**, *5* (6), 1098-107, DOI: 10.1161/CIRCEP.111.969972
 24. Antzelevitch, C.; Pollevick, G. D.; Cordeiro, J. M.; Casis, O.; Sanguinetti, M. C.; Aizawa, Y.; Guerchicoff, A.; Pfeiffer, R.; Oliva, A.; Wollnik, B.; Gelber, P.; Bonaros, E. P., Jr.; Burashnikov, E.; Wu, Y.; Sargent, J. D.; Schickel, S.; Oberheiden, R.; Bhatia, A.; Hsu, L. F.; Haissaguerre, M.; Schimpf, R.; Borggrefe, M.; Wolpert, C., Loss-of-function mutations in the cardiac calcium channel underlie a new clinical entity characterized by ST-segment elevation, short QT intervals, and sudden cardiac death. *Circulation* **2007**, *115* (4), 442-9, DOI: 10.1161/CIRCULATIONAHA.106.668392
 25. Burashnikov, E.; Pfeiffer, R.; Barajas-Martinez, H.; Delpon, E.; Hu, D.; Desai, M.; Borggrefe, M.; Haissaguerre, M.; Kanter, R.; Pollevick, G. D.; Guerchicoff, A.; Laino, R.; Marieb, M.; Nademanee, K.; Nam, G. B.; Robles, R.; Schimpf, R.; Stapleton,

- D. D.; Viskin, S.; Winters, S.; Wolpert, C.; Zimmern, S.; Veltmann, C.; Antzelevitch, C., Mutations in the cardiac L-type calcium channel associated with inherited J-wave syndromes and sudden cardiac death. *Heart Rhythm* **2010**, *7* (12), 1872-82, DOI: 10.1016/j.hrthm.2010.08.026
26. Ohno, S.; Zankov, D. P.; Ding, W. G.; Itoh, H.; Makiyama, T.; Doi, T.; Shizuta, S.; Hattori, T.; Miyamoto, A.; Naiki, N.; Hancox, J. C.; Matsuura, H.; Horie, M., KCNE5 (KCNE1L) variants are novel modulators of Brugada syndrome and idiopathic ventricular fibrillation. *Circ Arrhythm Electrophysiol* **2011**, *4* (3), 352-61, DOI: 10.1161/CIRCEP.110.959619
27. Giudicessi, J. R.; Ye, D.; Tester, D. J.; Crotti, L.; Mugione, A.; Nesterenko, V. V.; Albertson, R. M.; Antzelevitch, C.; Schwartz, P. J.; Ackerman, M. J., Transient outward current (I-to) gain-of-function mutations in the KCND3-encoded Kv4.3 potassium channel and Brugada syndrome. *Heart Rhythm* **2011**, *8* (7), 1024-1032, DOI: 10.1016/j.hrthm.2011.02.021
28. Barajas-Martinez, H.; Hu, D.; Ferrer, T.; Onetti, C. G.; Wu, Y.; Burashnikov, E.; Boyle, M.; Surman, T.; Urrutia, J.; Veltmann, C.; Schimpf, R.; Borggrefe, M.; Wolpert, C.; Ibrahim, B. B.; Sanchez-Chapula, J. A.; Winters, S.; Haissaguerre, M.; Antzelevitch, C., Molecular genetic and functional association of Brugada and early repolarization syndromes with S422L missense mutation in KCNJ8. *Heart Rhythm* **2012**, *9* (4), 548-55, DOI: 10.1016/j.hrthm.2011.10.035
29. Wang, Q. I.; Ohno, S.; Ding, W. G.; Fukuyama, M.; Miyamoto, A.; Itoh, H.; Makiyama, T.; Wu, J.; Bai, J.; Hasegawa, K.; Shinohara, T.; Takahashi, N.; Shimizu, A.; Matsuura, H.; Horie, M., Gain-of-function KCNH2 mutations in patients with Brugada syndrome. *J Cardiovasc Electrophysiol* **2014**, *25* (5), 522-530, DOI: 10.1111/jce.12361
30. Hu, D.; Barajas-Martinez, H.; Terzic, A.; Park, S.; Pfeiffer, R.; Burashnikov, E.; Wu, Y.; Borggrefe, M.; Veltmann, C.; Schimpf, R.; Cai, J. J.; Nam, G. B.; Deshmukh, P.; Scheinman, M.; Preminger, M.; Steinberg, J.; Lopez-Izquierdo, A.; Ponce-Balbuena, D.; Wolpert, C.; Haissaguerre, M.; Sanchez-Chapula, J. A.; Antzelevitch, C., ABCC9 is a novel Brugada and early repolarization syndrome susceptibility gene. *Int J Cardiol* **2014**, *171* (3), 431-42, DOI: 10.1016/j.ijcard.2013.12.084
31. Mercer, B. N.; Begg, G. A.; Page, S. P.; Bennett, C. P.; Tayebjee, M. H.; Mahida, S., Early Repolarization Syndrome; Mechanistic Theories and Clinical Correlates. *Front Physiol* **2016**, *7*, 266, DOI: 10.3389/fphys.2016.00266
32. Gussak, I.; Antzelevitch, C., Early repolarization syndrome: a decade of progress. *J Electrocardiol* **2013**, *46* (2), 110-3, DOI: 10.1016/j.jelectrocard.2012.12.002
33. Pereira, R.; Campuzano, O.; Sarquella-Brugada, G.; Cesar, S.; Iglesias, A.; Brugada, J.; Cruz, F. E. S.; Brugada, R., Short QT syndrome in pediatrics. *Clinical Research in Cardiology* **2017**, *106* (6), 393-400, DOI: 10.1007/s00392-017-1094-1
34. Wallace, E.; Howard, L.; Liu, M.; O'Brien, T.; Ward, D.; Shen, S.; Prendiville, T., Long QT Syndrome: Genetics and Future Perspective. *Pediatr Cardiol* **2019**, *40* (7), 1419-1430, DOI: 10.1007/s00246-019-02151-x
35. Schwartz, P. J.; Crotti, L.; Insolia, R., Long-QT syndrome: from genetics to management. *Circ Arrhythm Electrophysiol* **2012**, *5* (4), 868-77, DOI: 10.1161/CIRCEP.111.962019

36. Schwartz, P. J.; Crotti, L., QTc behavior during exercise and genetic testing for the long-QT syndrome. *Circulation* **2011**, *124* (20), 2181-4, DOI: 10.1161/CIRCULATIONAHA.111.062182
37. Killeen, M. J.; Sabir, I. N.; Grace, A. A.; Huang, C. L., Dispersions of repolarization and ventricular arrhythmogenesis: lessons from animal models. *Prog Biophys Mol Biol* **2008**, *98* (2-3), 219-29, DOI: 10.1016/j.pbiomolbio.2008.10.008
38. Dewi, I. P.; Dharmadjati, B. B., Short QT syndrome: The current evidences of diagnosis and management. *J Arrhythm* **2020**, *36* (6), 962-966, DOI: 10.1002/joa3.12439
39. Abriel, H.; Zaklyazminskaya, E. V., Cardiac channelopathies: genetic and molecular mechanisms. *Gene* **2013**, *517* (1), 1-11, DOI: 10.1016/j.gene.2012.12.061
40. Napolitano, C.; Priori, S. G.; Bloise, R., Catecholaminergic Polymorphic Ventricular Tachycardia. In *GeneReviews((R))*, Adam, M. P.; Ardinger, H. H.; Pagon, R. A.; Wallace, S. E.; Bean, L. J. H.; Gripp, K. W.; Mirzaa, G. M.; Amemiya, A., Eds. Seattle (WA), 1993,
41. Bezzerides, V. J.; Caballero, A.; Wang, S.; Ai, Y.; Hyland, R. J.; Lu, F.; Heims-Waldron, D. A.; Chambers, K. D.; Zhang, D.; Abrams, D. J.; Pu, W. T., Gene Therapy for Catecholaminergic Polymorphic Ventricular Tachycardia by Inhibition of Ca(2+)/Calmodulin-Dependent Kinase II. *Circulation* **2019**, *140* (5), 405-419, DOI: 10.1161/CIRCULATIONAHA.118.038514
42. Calore, M.; Lorenzon, A.; De Bortoli, M.; Poloni, G.; Rampazzo, A., Arrhythmogenic cardiomyopathy: a disease of intercalated discs. *Cell Tissue Res* **2015**, *360* (3), 491-500, DOI: 10.1007/s00441-014-2015-5
43. Sen-Chowdhry, S.; Syrris, P.; McKenna, W. J., Role of genetic analysis in the management of patients with arrhythmogenic right ventricular dysplasia/cardiomyopathy. *J Am Coll Cardiol* **2007**, *50* (19), 1813-21, DOI: 10.1016/j.jacc.2007.08.008
44. Basso, C.; Corrado, D.; Marcus, F. I.; Nava, A.; Thiene, G., Arrhythmogenic right ventricular cardiomyopathy. *Lancet* **2009**, *373* (9671), 1289-300, DOI: 10.1016/S0140-6736(09)60256-7
45. Stevens, T. L.; Wallace, M. J.; Refaey, M. E.; Roberts, J. D.; Koenig, S. N.; Mohler, P. J., Arrhythmogenic Cardiomyopathy: Molecular Insights for Improved Therapeutic Design. *J Cardiovasc Dev Dis* **2020**, *7* (2), DOI: 10.3390/jcdd7020021
46. Kleber, A. G.; Saffitz, J. E., Role of the intercalated disc in cardiac propagation and arrhythmogenesis. *Front Physiol* **2014**, *5*, 404, DOI: 10.3389/fphys.2014.00404
47. Moise, N.; Struckman, H. L.; Dagher, C.; Veeraraghavan, R.; Weinberg, S. H., Intercalated disk nanoscale structure regulates cardiac conduction. *J Gen Physiol* **2021**, *153* (8), DOI: 10.1085/jgp.202112897
48. Shimada, T.; Kawazato, H.; Yasuda, A.; Ono, N.; Sueda, K., Cytoarchitecture and intercalated disks of the working myocardium and the conduction system in the mammalian heart. *Anat Rec A Discov Mol Cell Evol Biol* **2004**, *280* (2), 940-51, DOI: 10.1002/ar.a.20109
49. Vanslebrouck, B.; Kremer, A.; Pavie, B.; van Roy, F.; Lippens, S.; van Hengel, J., Three-dimensional reconstruction of the intercalated disc including the intercellular junctions by applying volume scanning electron microscopy. *Histochem Cell Biol* **2018**, *149* (5), 479-490, DOI: 10.1007/s00418-018-1657-x

50. Raisch, T. B.; Yanoff, M. S.; Larsen, T. R.; Farooqui, M. A.; King, D. R.; Veeraghavan, R.; Gourdie, R. G.; Baker, J. W.; Arnold, W. S.; AlMahameed, S. T.; Poelzing, S., Intercalated Disk Extracellular Nanodomain Expansion in Patients With Atrial Fibrillation. *Front Physiol* **2018**, *9*, 398, DOI: 10.3389/fphys.2018.00398
51. Sheikh, F.; Ross, R. S.; Chen, J., Cell-cell connection to cardiac disease. *Trends Cardiovasc Med* **2009**, *19* (6), 182-90, DOI: 10.1016/j.tcm.2009.12.001
52. Luo, Y.; Ferreira-Cornwell, M.; Baldwin, H.; Kostetskii, I.; Lenox, J.; Lieberman, M.; Radice, G., Rescuing the N-cadherin knockout by cardiac-specific expression of N- or E-cadherin. *Development* **2001**, *128* (4), 459-69, DOI: 10.1242/dev.128.4.459
53. Wang, Q.; Lin, J. L.; Wu, K. H.; Wang, D. Z.; Reiter, R. S.; Sinn, H. W.; Lin, C. I.; Lin, C. J., Xin proteins and intercalated disc maturation, signaling and diseases. *Front Biosci (Landmark Ed)* **2012**, *17* (7), 2566-93, DOI: 10.2741/4072
54. Yonemura, S.; Wada, Y.; Watanabe, T.; Nagafuchi, A.; Shibata, M., alpha-Catenin as a tension transducer that induces adherens junction development. *Nat Cell Biol* **2010**, *12* (6), 533-42, DOI: 10.1038/ncb2055
55. Chopra, A.; Tabdanov, E.; Patel, H.; Janmey, P. A.; Kresh, J. Y., Cardiac myocyte remodeling mediated by N-cadherin-dependent mechanosensing. *Am J Physiol Heart Circ Physiol* **2011**, *300* (4), H1252-66, DOI: 10.1152/ajpheart.00515.2010
56. le Duc, Q.; Shi, Q.; Blonk, I.; Sonnenberg, A.; Wang, N.; Leckband, D.; de Rooij, J., Vinculin potentiates E-cadherin mechanosensing and is recruited to actin-anchored sites within adherens junctions in a myosin II-dependent manner. *J Cell Biol* **2010**, *189* (7), 1107-15, DOI: 10.1083/jcb.201001149
57. Ehler, E.; Horowitz, R.; Zuppinger, C.; Price, R. L.; Perriard, E.; Leu, M.; Caroni, P.; Sussman, M.; Eppenberger, H. M.; Perriard, J. C., Alterations at the intercalated disk associated with the absence of muscle LIM protein. *J Cell Biol* **2001**, *153* (4), 763-72, DOI: 10.1083/jcb.153.4.763
58. Janssens, B.; Mohapatra, B.; Vatta, M.; Goossens, S.; Vanpoucke, G.; Kools, P.; Montoye, T.; van Hengel, J.; Bowles, N. E.; van Roy, F.; Towbin, J. A., Assessment of the CTNNA3 gene encoding human alpha T-catenin regarding its involvement in dilated cardiomyopathy. *Hum Genet* **2003**, *112* (3), 227-36, DOI: 10.1007/s00439-002-0857-5
59. Li, J.; Levin, M. D.; Xiong, Y.; Petrenko, N.; Patel, V. V.; Radice, G. L., N-cadherin haploinsufficiency affects cardiac gap junctions and arrhythmic susceptibility. *J Mol Cell Cardiol* **2008**, *44* (3), 597-606, DOI: 10.1016/j.yjmcc.2007.11.013
60. Ferreira-Cornwell, M. C.; Luo, Y.; Narula, N.; Lenox, J. M.; Lieberman, M.; Radice, G. L., Remodeling the intercalated disc leads to cardiomyopathy in mice misexpressing cadherins in the heart. *J Cell Sci* **2002**, *115* (Pt 8), 1623-34, DOI: 10.1242/jcs.115.8.1623
61. Olson, T. M.; Illenberger, S.; Kishimoto, N. Y.; Huttelmaier, S.; Keating, M. T.; Jockusch, B. M., Metavinculin mutations alter actin interaction in dilated cardiomyopathy. *Circulation* **2002**, *105* (4), 431-7, DOI: 10.1161/hc0402.102930
62. Gemel, J.; Levy, A. E.; Simon, A. R.; Bennett, K. B.; Ai, X.; Akhter, S.; Beyer, E. C., Connexin40 abnormalities and atrial fibrillation in the human heart. *J Mol Cell Cardiol* **2014**, *76*, 159-68, DOI: 10.1016/j.yjmcc.2014.08.021

63. Barker, R. J.; Price, R. L.; Gourdie, R. G., Increased association of ZO-1 with connexin43 during remodeling of cardiac gap junctions. *Circ Res* **2002**, *90* (3), 317-24, DOI: 10.1161/hh0302.104471
64. Noorman, M.; van der Heyden, M. A.; van Veen, T. A.; Cox, M. G.; Hauer, R. N.; de Bakker, J. M.; van Rijen, H. V., Cardiac cell-cell junctions in health and disease: Electrical versus mechanical coupling. *J Mol Cell Cardiol* **2009**, *47* (1), 23-31, DOI: 10.1016/j.yjmcc.2009.03.016
65. Toyofuku, T.; Yabuki, M.; Otsu, K.; Kuzuya, T.; Hori, M.; Tada, M., Direct association of the gap junction protein connexin-43 with ZO-1 in cardiac myocytes. *J Biol Chem* **1998**, *273* (21), 12725-31, DOI: 10.1074/jbc.273.21.12725
66. El Refaey, M.; Coles, S.; Musa, H.; Stevens, T. L.; Wallace, M. J.; Murphy, N. P.; Antwi-Boasiako, S.; Young, L. J.; Manring, H. R.; Curran, J.; Makara, M. A.; Sas, K.; Han, M.; Koenig, S. N.; Skaf, M.; Kline, C. F.; Janssen, P. M. L.; Accornero, F.; Borzok, M. A.; Mohler, P. J., Altered Expression of Zonula occludens-1 Affects Cardiac Na(+) Channels and Increases Susceptibility to Ventricular Arrhythmias. *Cells* **2022**, *11* (4), DOI: 10.3390/cells11040665
67. Harmon, R. M.; Green, K. J., Structural and functional diversity of desmosomes. *Cell Commun Adhes* **2013**, *20* (6), 171-87, DOI: 10.3109/15419061.2013.855204
68. Delmar, M.; McKenna, W. J., The cardiac desmosome and arrhythmogenic cardiomyopathies: from gene to disease. *Circ Res* **2010**, *107* (6), 700-14, DOI: 10.1161/CIRCRESAHA.110.223412
69. Schinner, C.; Erber, B. M.; Yeruva, S.; Schlipp, A.; Rotzer, V.; Kempf, E.; Kant, S.; Leube, R. E.; Mueller, T. D.; Waschke, J., Stabilization of desmoglein-2 binding rescues arrhythmia in arrhythmogenic cardiomyopathy. *JCI Insight* **2020**, *5* (9), DOI: 10.1172/jci.insight.130141
70. Kowalczyk, A. P.; Bornslaeger, E. A.; Borgwardt, J. E.; Palka, H. L.; Dhaliwal, A. S.; Corcoran, C. M.; Denning, M. F.; Green, K. J., The amino-terminal domain of desmoplakin binds to plakoglobin and clusters desmosomal cadherin-plakoglobin complexes. *J Cell Biol* **1997**, *139* (3), 773-84, DOI: 10.1083/jcb.139.3.773
71. Patel, D. M.; Dubash, A. D.; Kreitzer, G.; Green, K. J., Disease mutations in desmoplakin inhibit Cx43 membrane targeting mediated by desmoplakin-EB1 interactions. *J Cell Biol* **2014**, *206* (6), 779-97, DOI: 10.1083/jcb.201312110
72. Kam, C. Y.; Dubash, A. D.; Magistrati, E.; Polo, S.; Satchell, K. J. F.; Sheikh, F.; Lampe, P. D.; Green, K. J., Desmoplakin maintains gap junctions by inhibiting Ras/MAPK and lysosomal degradation of connexin-43. *J Cell Biol* **2018**, *217* (9), 3219-3235, DOI: 10.1083/jcb.201710161
73. Cerrone, M.; Montnach, J.; Lin, X.; Zhao, Y. T.; Zhang, M.; Agullo-Pascual, E.; Leo-Macias, A.; Alvarado, F. J.; Dolgalev, I.; Karathanos, T. V.; Malkani, K.; Van Opbergen, C. J. M.; van Bavel, J. J. A.; Yang, H. Q.; Vasquez, C.; Tester, D.; Fowler, S.; Liang, F.; Rothenberg, E.; Heguy, A.; Morley, G. E.; Coetzee, W. A.; Trayanova, N. A.; Ackerman, M. J.; van Veen, T. A. B.; Valdivia, H. H.; Delmar, M., Plakophilin-2 is required for transcription of genes that control calcium cycling and cardiac rhythm. *Nat Commun* **2017**, *8* (1), 106, DOI: 10.1038/s41467-017-00127-0

74. Cerrone, M.; Noorman, M.; Lin, X.; Chkourko, H.; Liang, F. X.; van der Nagel, R.; Hund, T.; Birchmeier, W.; Mohler, P.; van Veen, T. A.; van Rijen, H. V.; Delmar, M., Sodium current deficit and arrhythmogenesis in a murine model of plakophilin-2 haploinsufficiency. *Cardiovasc Res* **2012**, *95* (4), 460-8, DOI: 10.1093/cvr/cvs218
75. Kim, J. C.; Perez-Hernandez, M.; Alvarado, F. J.; Maurya, S. R.; Montnach, J.; Yin, Y.; Zhang, M.; Lin, X.; Vasquez, C.; Heguy, A.; Liang, F. X.; Woo, S. H.; Morley, G. E.; Rothenberg, E.; Lundby, A.; Valdivia, H. H.; Cerrone, M.; Delmar, M., Disruption of Ca(2+)i Homeostasis and Connexin 43 Hemichannel Function in the Right Ventricle Precedes Overt Arrhythmogenic Cardiomyopathy in Plakophilin-2-Deficient Mice. *Circulation* **2019**, *140* (12), 1015-1030, DOI: 10.1161/CIRCULATIONAHA.119.039710
76. Ng, R.; Manring, H.; Papoutsidakis, N.; Albertelli, T.; Tsai, N.; See, C. J.; Li, X.; Park, J.; Stevens, T. L.; Bobbili, P. J.; Riaz, M.; Ren, Y.; Stoddard, C. E.; Janssen, P. M.; Bunch, T. J.; Hall, S. P.; Lo, Y. C.; Jacoby, D. L.; Qyang, Y.; Wright, N.; Ackermann, M. A.; Campbell, S. G., Patient mutations linked to arrhythmogenic cardiomyopathy enhance calpain-mediated desmoplakin degradation. *JCI Insight* **2019**, *5*, DOI: 10.1172/jci.insight.128643
77. Kaplan, S. R.; Gard, J. J.; Protonotarios, N.; Tsatsopoulou, A.; Spiliopoulou, C.; Anastasakis, A.; Squarcioni, C. P.; McKenna, W. J.; Thiene, G.; Basso, C.; Brousse, N.; Fontaine, G.; Saffitz, J. E., Remodeling of myocyte gap junctions in arrhythmogenic right ventricular cardiomyopathy due to a deletion in plakoglobin (Naxos disease). *Heart Rhythm* **2004**, *1* (1), 3-11, DOI: 10.1016/j.hrthm.2004.01.001
78. Kaplan, S. R.; Gard, J. J.; Carvajal-Huerta, L.; Ruiz-Cabezas, J. C.; Thiene, G.; Saffitz, J. E., Structural and molecular pathology of the heart in Carvajal syndrome. *Cardiovasc Pathol* **2004**, *13* (1), 26-32, DOI: 10.1016/S1054-8807(03)00107-8
79. Agullo-Pascual, E.; Reid, D. A.; Keegan, S.; Sidhu, M.; Fenyo, D.; Rothenberg, E.; Delmar, M., Super-resolution fluorescence microscopy of the cardiac connexome reveals plakophilin-2 inside the connexin43 plaque. *Cardiovasc Res* **2013**, *100* (2), 231-40, DOI: 10.1093/cvr/cvt191
80. Jansen, J. A.; Noorman, M.; Musa, H.; Stein, M.; de Jong, S.; van der Nagel, R.; Hund, T. J.; Mohler, P. J.; Vos, M. A.; van Veen, T. A.; de Bakker, J. M.; Delmar, M.; van Rijen, H. V., Reduced heterogeneous expression of Cx43 results in decreased Nav1.5 expression and reduced sodium current that accounts for arrhythmia vulnerability in conditional Cx43 knockout mice. *Heart Rhythm* **2012**, *9* (4), 600-7, DOI: 10.1016/j.hrthm.2011.11.025
81. Sato, P. Y.; Coombs, W.; Lin, X.; Nekrasova, O.; Green, K. J.; Isom, L. L.; Taffet, S. M.; Delmar, M., Interactions between ankyrin-G, Plakophilin-2, and Connexin43 at the cardiac intercalated disc. *Circ Res* **2011**, *109* (2), 193-201, DOI: 10.1161/CIRCRESAHA.111.247023
82. Leo-Macias, A.; Agullo-Pascual, E.; Delmar, M., The cardiac connexome: Non-canonical functions of connexin43 and their role in cardiac arrhythmias. *Semin Cell Dev Biol* **2016**, *50*, 13-21, DOI: 10.1016/j.semcdb.2015.12.002
83. Palatinus, J. A.; O'Quinn, M. P.; Barker, R. J.; Harris, B. S.; Jourdan, J.; Gourdie, R. G., ZO-1 determines adherens and gap junction localization at intercalated disks. *Am J Physiol Heart Circ Physiol* **2011**, *300* (2), H583-94, DOI: 10.1152/ajpheart.00999.2010

84. Agullo-Pascual, E.; Cerrone, M.; Delmar, M., Arrhythmogenic cardiomyopathy and Brugada syndrome: diseases of the connexome. *FEBS Lett* **2014**, *588* (8), 1322-30, DOI: 10.1016/j.febslet.2014.02.008
85. Kapplinger, J. D.; Landstrom, A. P.; Salisbury, B. A.; Callis, T. E.; Pollevick, G. D.; Tester, D. J.; Cox, M. G.; Bhuiyan, Z.; Bikker, H.; Wiesfeld, A. C.; Hauer, R. N.; van Tintelen, J. P.; Jongbloed, J. D.; Calkins, H.; Judge, D. P.; Wilde, A. A.; Ackerman, M. J., Distinguishing arrhythmogenic right ventricular cardiomyopathy/dysplasia-associated mutations from background genetic noise. *J Am Coll Cardiol* **2011**, *57* (23), 2317-27, DOI: 10.1016/j.jacc.2010.12.036
86. Al-Jassar, C.; Bikker, H.; Overduin, M.; Chidgey, M., Mechanistic basis of desmosome-targeted diseases. *J Mol Biol* **2013**, *425* (21), 4006-22, DOI: 10.1016/j.jmb.2013.07.035
87. Yuan, Z. Y.; Cheng, L. T.; Wang, Z. F.; Wu, Y. Q., Desmoplakin and clinical manifestations of desmoplakin cardiomyopathy. *Chin Med J (Engl)* **2021**, *134* (15), 1771-1779, DOI: 10.1097/CM9.0000000000001581
88. Bennett, R. G.; Haqqani, H. M.; Berruezo, A.; Della Bella, P.; Marchlinski, F. E.; Hsu, C. J.; Kumar, S., Arrhythmogenic Cardiomyopathy in 2018-2019: ARVC/ALVC or Both? *Heart Lung Circ* **2019**, *28* (1), 164-177, DOI: 10.1016/j.hlc.2018.10.013
89. Sen-Chowdhry, S.; Syrris, P.; Ward, D.; Asimaki, A.; Sevdalis, E.; McKenna, W. J., Clinical and genetic characterization of families with arrhythmogenic right ventricular dysplasia/cardiomyopathy provides novel insights into patterns of disease expression. *Circulation* **2007**, *115* (13), 1710-20, DOI: 10.1161/CIRCULATIONAHA.106.660241
90. Garcia-Gras, E.; Lombardi, R.; Giocondo, M. J.; Willerson, J. T.; Schneider, M. D.; Khoury, D. S.; Marian, A. J., Suppression of canonical Wnt/beta-catenin signaling by nuclear plakoglobin recapitulates phenotype of arrhythmogenic right ventricular cardiomyopathy. *J Clin Invest* **2006**, *116* (7), 2012-21, DOI: 10.1172/JCI27751
91. Lai Cheong, J. E.; Wessagowit, V.; McGrath, J. A., Molecular abnormalities of the desmosomal protein desmoplakin in human disease. *Clin Exp Dermatol* **2005**, *30* (3), 261-6, DOI: 10.1111/j.1365-2230.2005.01736.x
92. Gallicano, G. I.; Bauer, C.; Fuchs, E., Rescuing desmoplakin function in extra-embryonic ectoderm reveals the importance of this protein in embryonic heart, neuroepithelium, skin and vasculature. *Development* **2001**, *128* (6), 929-41,
93. Daday, C.; Kolsek, K.; Grater, F., The mechano-sensing role of the unique SH3 insertion in plakin domains revealed by Molecular Dynamics simulations. *Sci Rep* **2017**, *7* (1), 11669, DOI: 10.1038/s41598-017-11017-2
94. Kowalczyk, A. P.; Hatzfeld, M.; Bornslaeger, E. A.; Kopp, D. S.; Borgwardt, J. E.; Corcoran, C. M.; Settler, A.; Green, K. J., The head domain of plakophilin-1 binds to desmoplakin and enhances its recruitment to desmosomes - Implications for cutaneous disease. *Journal of Biological Chemistry* **1999**, *274* (26), 18145-18148, DOI: DOI 10.1074/jbc.274.26.18145
95. Daday, C.; Mateyka, L. M.; Grater, F., How ARVC-Related Mutations Destabilize Desmoplakin: An MD Study. *Biophys J* **2019**, *116* (5), 831-835, DOI: 10.1016/j.bpj.2019.01.023

96. Gomes, J.; Finlay, M.; Ahmed, A. K.; Ciaccio, E. J.; Asimaki, A.; Saffitz, J. E.; Quarta, G.; Nobles, M.; Syrris, P.; Chaubey, S.; McKenna, W. J.; Tinker, A.; Lambiase, P. D., Electrophysiological abnormalities precede overt structural changes in arrhythmogenic right ventricular cardiomyopathy due to mutations in desmoplakin-A combined murine and human study. *Eur Heart J* **2012**, *33* (15), 1942-53, DOI: 10.1093/eurheartj/ehr472
97. Hoover, C. A.; Ott, K. L.; Manring, H. R.; Dew, T.; Borzok, M. A.; Wright, N. T., Creating a 'Molecular Band-Aid'; Blocking an Exposed Protease Target Site in Desmoplakin. *J Pers Med* **2021**, *11* (5), DOI: 10.3390/jpm11050401
98. Green, K. J.; Stappenbeck, T. S.; Parry, D. A.; Virata, M. L., Structure of desmoplakin and its association with intermediate filaments. *J Dermatol* **1992**, *19* (11), 765-9, DOI: 10.1111/j.1346-8138.1992.tb03777.x
99. Hatsell, S.; Cowin, P., Deconstructing desmoplakin. *Nat Cell Biol* **2001**, *3* (12), E270-2, DOI: 10.1038/ncb1201-e270
100. Mason, J. M.; Arndt, K. M., Coiled coil domains: stability, specificity, and biological implications. *Chembiochem* **2004**, *5* (2), 170-6, DOI: 10.1002/cbic.200300781
101. Bar, H.; Fischer, D.; Goudeau, B.; Kley, R. A.; Clemen, C. S.; Vicart, P.; Herrmann, H.; Vorgerd, M.; Schroder, R., Pathogenic effects of a novel heterozygous R350P desmin mutation on the assembly of desmin intermediate filaments in vivo and in vitro. *Hum Mol Genet* **2005**, *14* (10), 1251-60, DOI: 10.1093/hmg/ddi136
102. Choi, H. J.; Weis, W. I., Purification and Structural Analysis of Desmoplakin. *Methods Enzymol* **2016**, *569*, 197-213, DOI: 10.1016/bs.mie.2015.05.006
103. Norgett, E. E.; Hatsell, S. J.; Carvajal-Huerta, L.; Cabezas, J. C.; Common, J.; Purkis, P. E.; Whittock, N.; Leigh, I. M.; Stevens, H. P.; Kelsell, D. P., Recessive mutation in desmoplakin disrupts desmoplakin-intermediate filament interactions and causes dilated cardiomyopathy, woolly hair and keratoderma. *Hum Mol Genet* **2000**, *9* (18), 2761-6, DOI: 10.1093/hmg/9.18.2761
104. Albrecht, L. V.; Zhang, L.; Shabanowitz, J.; Purevjav, E.; Towbin, J. A.; Hunt, D. F.; Green, K. J., GSK3- and PRMT-1-dependent modifications of desmoplakin control desmoplakin-cytoskeleton dynamics. *J Cell Biol* **2015**, *208* (5), 597-612, DOI: 10.1083/jcb.201406020
105. Yang, Z.; Bowles, N. E.; Scherer, S. E.; Taylor, M. D.; Kearney, D. L.; Ge, S.; Nadvoretzkiy, V. V.; DeFreitas, G.; Carabello, B.; Brandon, L. I.; Godsel, L. M.; Green, K. J.; Saffitz, J. E.; Li, H.; Danieli, G. A.; Calkins, H.; Marcus, F.; Towbin, J. A., Desmosomal dysfunction due to mutations in desmoplakin causes arrhythmogenic right ventricular dysplasia/cardiomyopathy. *Circ Res* **2006**, *99* (6), 646-55, DOI: 10.1161/01.RES.0000241482.19382.c6
106. Lorenzon, A.; Calore, M.; Poloni, G.; De Windt, L. J.; Braghetta, P.; Rampazzo, A., Wnt/beta-catenin pathway in arrhythmogenic cardiomyopathy. *Oncotarget* **2017**, *8* (36), 60640-60655, DOI: 10.18632/oncotarget.17457
107. Giuliodori, A.; Beffagna, G.; Marchetto, G.; Fornetto, C.; Vanzi, F.; Toppo, S.; Facchinello, N.; Santimaria, M.; Vettori, A.; Rizzo, S., Loss of cardiac Wnt/ β -catenin signalling in Desmoplakin-deficient AC8 zebrafish models is rescuable by genetic and pharmacological intervention. *Cardiovascular research* **2018**, *114* (8), 1082-1097,

108. Oxford, E. M.; Danko, C. G.; Fox, P. R.; Kornreich, B. G.; Moise, N. S., Change in beta-catenin localization suggests involvement of the canonical Wnt pathway in Boxer dogs with arrhythmogenic right ventricular cardiomyopathy. *J Vet Intern Med* **2014**, *28* (1), 92-101, DOI: 10.1111/jvim.12238
109. Roberts, J. D.; Murphy, N. P.; Hamilton, R. M.; Lubbers, E. R.; James, C. A.; Kline, C. F.; Gollob, M. H.; Krahn, A. D.; Sturm, A. C.; Musa, H.; El-Refaey, M.; Koenig, S.; Aneq, M. A.; Hoorntje, E. T.; Graw, S. L.; Davies, R. W.; Rafiq, M. A.; Koopmann, T. T.; Aafaqi, S.; Fatah, M.; Chiasson, D. A.; Taylor, M. R.; Simmons, S. L.; Han, M.; van Opbergen, C. J.; Wold, L. E.; Sinagra, G.; Mittal, K.; Tichnell, C.; Murray, B.; Codima, A.; Nazer, B.; Nguyen, D. T.; Marcus, F. I.; Sobriera, N.; Lodder, E. M.; van den Berg, M. P.; Spears, D. A.; Robinson, J. F.; Ursell, P. C.; Green, A. K.; Skanes, A. C.; Tang, A. S.; Gardner, M. J.; Hegele, R. A.; van Veen, T. A.; Wilde, A. A.; Healey, J. S.; Janssen, P. M.; Mestroni, L.; van Tintelen, J. P.; Calkins, H.; Judge, D. P.; Hund, T. J.; Scheinman, M. M.; Mohler, P. J., Ankyrin-B dysfunction predisposes to arrhythmogenic cardiomyopathy and is amenable to therapy. *J Clin Invest* **2019**, *129* (8), 3171-3184, DOI: 10.1172/JCI125538
110. Lombardi, R.; da Graca Cabreira-Hansen, M.; Bell, A.; Fromm, R. R.; Willerson, J. T.; Marian, A. J., Nuclear plakoglobin is essential for differentiation of cardiac progenitor cells to adipocytes in arrhythmogenic right ventricular cardiomyopathy. *Circ Res* **2011**, *109* (12), 1342-53, DOI: 10.1161/CIRCRESAHA.111.255075
111. Li, J.; Swope, D.; Raess, N.; Cheng, L.; Muller, E. J.; Radice, G. L., Cardiac tissue-restricted deletion of plakoglobin results in progressive cardiomyopathy and activation of β -catenin signaling. *Mol Cell Biol* **2011**, *31* (6), 1134-44, DOI: 10.1128/MCB.01025-10
112. Fidler, L. M.; Wilson, G. J.; Liu, F.; Cui, X.; Scherer, S. W.; Taylor, G. P.; Hamilton, R. M., Abnormal connexin43 in arrhythmogenic right ventricular cardiomyopathy caused by plakophilin-2 mutations. *J Cell Mol Med* **2009**, *13* (10), 4219-28, DOI: 10.1111/j.1582-4934.2008.00438.x
113. van der Velde, K. J.; Imhann, F.; Charbon, B.; Pang, C.; van Enkevort, D.; Slofstra, M.; Barbieri, R.; Alberts, R.; Hendriksen, D.; Kelpin, F.; de Haan, M.; de Boer, T.; Haakma, S.; Stroomberg, C.; Scholtens, S.; van de Geijn, G. J.; Festen, E. A. M.; Weersma, R. K.; Swertz, M. A., MOLGENIS research: advanced bioinformatics data software for non-bioinformaticians. *Bioinformatics* **2019**, *35* (6), 1076-1078, DOI: 10.1093/bioinformatics/bty742
114. Kirchner, F.; Schuetz, A.; Boldt, L. H.; Martens, K.; Dittmar, G.; Haverkamp, W.; Thierfelder, L.; Heinemann, U.; Gerull, B., Molecular insights into arrhythmogenic right ventricular cardiomyopathy caused by plakophilin-2 missense mutations. *Circ Cardiovasc Genet* **2012**, *5* (4), 400-11, DOI: 10.1161/CIRCGENETICS.111.961854
115. Goll, D. E.; Thompson, V. F.; Li, H.; Wei, W.; Cong, J., The calpain system. *Physiol Rev* **2003**, *83* (3), 731-801, DOI: 10.1152/physrev.00029.2002
116. Portbury, A. L.; Willis, M. S.; Patterson, C., Tearin' up my heart: proteolysis in the cardiac sarcomere. *J Biol Chem* **2011**, *286* (12), 9929-34, DOI: 10.1074/jbc.R110.170571

117. Cong, J.; Goll, D. E.; Peterson, A. M.; Kapprell, H. P., The role of autolysis in activity of the Ca²⁺-dependent proteinases (mu-calpain and m-calpain). *J Biol Chem* **1989**, *264* (17), 10096-103,
118. Hyatt, H. W.; Powers, S. K., The Role of Calpains in Skeletal Muscle Remodeling with Exercise and Inactivity-induced Atrophy. *Int J Sports Med* **2020**, *41* (14), 994-1008, DOI: 10.1055/a-1199-7662
119. Potz, B. A.; Abid, M. R.; Sellke, F. W., Role of Calpain in Pathogenesis of Human Disease Processes. *J Nat Sci* **2016**, *2* (9),
120. Sorimachi, H.; Ono, Y., Regulation and physiological roles of the calpain system in muscular disorders. *Cardiovasc Res* **2012**, *96* (1), 11-22, DOI: 10.1093/cvr/cvs157
121. Letavernier, E.; Zafrani, L.; Perez, J.; Letavernier, B.; Haymann, J. P.; Baud, L., The role of calpains in myocardial remodelling and heart failure. *Cardiovasc Res* **2012**, *96* (1), 38-45, DOI: 10.1093/cvr/cvs099
122. Gil-Parrado, S.; Popp, O.; Knoch, T. A.; Zahler, S.; Bestvater, F.; Felgentrager, M.; Holloschi, A.; Fernandez-Montalvan, A.; Auerswald, E. A.; Fritz, H.; Fuentes-Prior, P.; Machleidt, W.; Spiess, E., Subcellular localization and in vivo subunit interactions of ubiquitous mu-calpain. *J Biol Chem* **2003**, *278* (18), 16336-46, DOI: 10.1074/jbc.M208657200
123. Li, Y.; Bondada, V.; Joshi, A.; Geddes, J. W., Calpain 1 and Calpastatin expression is developmentally regulated in rat brain. *Exp Neurol* **2009**, *220* (2), 316-9, DOI: 10.1016/j.expneurol.2009.09.004
124. Yamato, S.; Tanaka, K.; Murachi, T., The appearance of a 34,000-dalton inhibitor of calpain (Ca²⁺-dependent cysteine proteinase) in rat liver after the administration of phenylhydrazine. *Biochem Biophys Res Commun* **1983**, *115* (2), 715-21, DOI: 10.1016/s0006-291x(83)80203-4
125. Aversa, M.; De Tullio, R.; Capini, P.; Salamino, F.; Pontremoli, S.; Melloni, E., Changes in calpastatin localization and expression during calpain activation: a new mechanism for the regulation of intracellular Ca(2+)-dependent proteolysis. *Cell Mol Life Sci* **2003**, *60* (12), 2669-78, DOI: 10.1007/s00018-003-3288-0
126. Aversa, M.; de Tullio, R.; Passalacqua, M.; Salamino, F.; Pontremoli, S.; Melloni, E., Changes in intracellular calpastatin localization are mediated by reversible phosphorylation. *Biochem J* **2001**, *354* (Pt 1), 25-30, DOI: 10.1042/0264-6021:3540025
127. Lu, H. T.; Feng, R. Q.; Tang, J. K.; Zhou, J. J.; Gao, F.; Ren, J., CaMKII/calpain interaction mediates ischemia/reperfusion injury in isolated rat hearts. *Cell Death Dis* **2020**, *11* (5), 388, DOI: 10.1038/s41419-020-2605-y
128. Kong, L. H.; Gu, X. M.; Wu, F.; Jin, Z. X.; Zhou, J. J., CaMKII inhibition mitigates ischemia/reperfusion-elicited calpain activation and the damage to membrane skeleton proteins in isolated rat hearts. *Biochem Biophys Res Commun* **2017**, *491* (3), 687-692, DOI: 10.1016/j.bbrc.2017.07.128
129. Lohse, M. J.; Engelhardt, S.; Eschenhagen, T., What is the role of beta-adrenergic signaling in heart failure? *Circ Res* **2003**, *93* (10), 896-906, DOI: 10.1161/01.RES.0000102042.83024.CA

130. Heysieattalab, S.; Lee, K. H.; Liu, Y.; Wang, Y.; Foy, M. R.; Bi, X.; Baudry, M., Impaired cerebellar plasticity and eye-blink conditioning in calpain-1 knock-out mice. *Neurobiol Learn Mem* **2020**, *170*, 106995, DOI: 10.1016/j.nlm.2019.02.005
131. Herren, T.; Gerber, P. A.; Duru, F., Arrhythmogenic right ventricular cardiomyopathy/dysplasia: a not so rare "disease of the desmosome" with multiple clinical presentations. *Clin Res Cardiol* **2009**, *98* (3), 141-58, DOI: 10.1007/s00392-009-0751-4
132. Silvano, M.; Mastella, G.; Zorzi, A.; Migliore, F.; Pilichou, K.; Bauce, B.; Rigato, I.; Perazzolo Marra, M.; Iliceto, S.; Thiene, G.; Basso, C.; Corrado, D., Management of arrhythmogenic right ventricular cardiomyopathy. *Minerva Med* **2016**, *107* (4), 194-216,
133. Rigato, I.; Corrado, D.; Basso, C.; Zorzi, A.; Pilichou, K.; Bauce, B.; Thiene, G., Pharmacotherapy and Other Therapeutic Modalities for Managing Arrhythmogenic Right Ventricular Cardiomyopathy. *Cardiovasc. Drugs Ther.* **2015**, *29* (2), 171-177, DOI: 10.1007/s10557-015-6583-8
134. Hoorntje, E. T.; Te Rijdt, W. P.; James, C. A.; Pilichou, K.; Basso, C.; Judge, D. P.; Bezzina, C. R.; van Tintelen, J. P., Arrhythmogenic cardiomyopathy: pathology, genetics, and concepts in pathogenesis. *Cardiovasc Res* **2017**, *113* (12), 1521-1531, DOI: 10.1093/cvr/cvx150
135. Wang, W.; Tichnell, C.; Murray, B. A.; Agafonova, J.; Cadrin-Tourigny, J.; Chelko, S.; Tandri, H.; Calkins, H.; James, C. A., Exercise restriction is protective for genotype-positive family members of arrhythmogenic right ventricular cardiomyopathy patients. *Europace* **2020**, *22* (8), 1270-1278, DOI: 10.1093/europace/euaa105
136. Tabib, A.; Loire, R.; Chalabreysse, L.; Meyronnet, D.; Miras, A.; Malicier, D.; Thivolet, F.; Chevalier, P.; Bouvagnet, P., Circumstances of death and gross and microscopic observations in a series of 200 cases of sudden death associated with arrhythmogenic right ventricular cardiomyopathy and/or dysplasia. *Circulation* **2003**, *108* (24), 3000-5, DOI: 10.1161/01.CIR.0000108396.65446.21
137. La Gerche, A.; Robberecht, C.; Kuiperi, C.; Nuyens, D.; Willems, R.; de Ravel, T.; Matthijs, G.; Heidbuchel, H., Lower than expected desmosomal gene mutation prevalence in endurance athletes with complex ventricular arrhythmias of right ventricular origin. *Heart* **2010**, *96* (16), 1268-74, DOI: 10.1136/hrt.2009.189621
138. Lodder, E. M.; Rizzo, S., Mouse models in arrhythmogenic right ventricular cardiomyopathy. *Front Physiol* **2012**, *3*, 221, DOI: 10.3389/fphys.2012.00221
139. Padron-Barthe, L.; Dominguez, F.; Garcia-Pavia, P.; Lara-Pezzi, E., Animal models of arrhythmogenic right ventricular cardiomyopathy: what have we learned and where do we go? Insight for therapeutics. *Basic Res Cardiol* **2017**, *112* (5), 50, DOI: 10.1007/s00395-017-0640-3
140. Marcus, F. I.; McKenna, W. J.; Sherrill, D.; Basso, C.; Bauce, B.; Bluemke, D. A.; Calkins, H.; Corrado, D.; Cox, M. G.; Daubert, J. P.; Fontaine, G.; Gear, K.; Hauer, R.; Nava, A.; Picard, M. H.; Protonotarios, N.; Saffitz, J. E.; Sanborn, D. M.; Steinberg, J. S.; Tandri, H.; Thiene, G.; Towbin, J. A.; Tsatsopoulou, A.; Wichter, T.; Zareba, W., Diagnosis of arrhythmogenic right ventricular cardiomyopathy/dysplasia: proposed modification of the task force criteria. *Circulation* **2010**, *121* (13), 1533-41, DOI: 10.1161/CIRCULATIONAHA.108.840827

141. Corrado, D.; Fontaine, G.; Marcus, F. I.; McKenna, W. J.; Nava, A.; Thiene, G.; Wichter, T., Arrhythmogenic right ventricular dysplasia/cardiomyopathy: need for an international registry. Study Group on Arrhythmogenic Right Ventricular Dysplasia/Cardiomyopathy of the Working Groups on Myocardial and Pericardial Disease and Arrhythmias of the European Society of Cardiology and of the Scientific Council on Cardiomyopathies of the World Heart Federation. *Circulation* **2000**, *101* (11), E101-6, DOI: 10.1161/01.cir.101.11.e101
142. Akdis, D.; Brunckhorst, C.; Duru, F.; Saguner, A. M., Arrhythmogenic Cardiomyopathy: Electrical and Structural Phenotypes. *Arrhythm Electrophysiol Rev* **2016**, *5* (2), 90-101, DOI: 10.15420/AER.2016.4.3
143. McRae, A. T., 3rd; Chung, M. K.; Asher, C. R., Arrhythmogenic right ventricular cardiomyopathy: a cause of sudden death in young people. *Cleve Clin J Med* **2001**, *68* (5), 459-67, DOI: 10.3949/ccjm.68.5.459
144. Tavora, F.; Zhang, M.; Franco, M.; Oliveira, J. B.; Li, L.; Fowler, D.; Zhao, Z.; Cresswell, N.; Burke, A., Distribution of biventricular disease in arrhythmogenic cardiomyopathy: an autopsy study. *Hum Pathol* **2012**, *43* (4), 592-6, DOI: 10.1016/j.humpath.2011.06.014
145. Shen, W. K.; Edwards, W. D.; Hammill, S. C.; Bailey, K. R.; Ballard, D. J.; Gersh, B. J., Sudden unexpected nontraumatic death in 54 young adults: a 30-year population-based study. *Am J Cardiol* **1995**, *76* (3), 148-52, DOI: 10.1016/s0002-9149(99)80047-2
146. Cho, Y., Arrhythmogenic right ventricular cardiomyopathy. *J Arrhythm* **2018**, *34* (4), 356-368, DOI: 10.1002/joa3.12012
147. Nava, A.; Bauce, B.; Basso, C.; Muriago, M.; Rampazzo, A.; Villanova, C.; Daliento, L.; Buja, G.; Corrado, D.; Danieli, G. A.; Thiene, G., Clinical profile and long-term follow-up of 37 families with arrhythmogenic right ventricular cardiomyopathy. *J Am Coll Cardiol* **2000**, *36* (7), 2226-33, DOI: 10.1016/s0735-1097(00)00997-9
148. Sen-Chowdhry, S.; Syrris, P.; McKenna, W. J., Genetics of right ventricular cardiomyopathy. *J Cardiovasc Electrophysiol* **2005**, *16* (8), 927-35, DOI: 10.1111/j.1540-8167.2005.40842.x
149. Saguner, A. M.; Brunckhorst, C.; Duru, F., Arrhythmogenic ventricular cardiomyopathy: A paradigm shift from right to biventricular disease. *World J Cardiol* **2014**, *6* (4), 154-74, DOI: 10.4330/wjc.v6.i4.154
150. Miles, C.; Finocchiaro, G.; Papadakis, M.; Gray, B.; Westaby, J.; Ensam, B.; Basu, J.; Parry-Williams, G.; Papatheodorou, E.; Paterson, C.; Malhotra, A.; Robertus, J. L.; Ware, J. S.; Cook, S. A.; Asimaki, A.; Witney, A.; Ster, I. C.; Tome, M.; Sharma, S.; Behr, E. R.; Sheppard, M. N., Sudden Death and Left Ventricular Involvement in Arrhythmogenic Cardiomyopathy. *Circulation* **2019**, *139* (15), 1786-1797, DOI: 10.1161/CIRCULATIONAHA.118.037230
151. Corrado, D.; Basso, C.; Thiene, G.; McKenna, W. J.; Davies, M. J.; Fontaliran, F.; Nava, A.; Silvestri, F.; Blomstrom-Lundqvist, C.; Wlodarska, E. K.; Fontaine, G.; Camerini, F., Spectrum of clinicopathologic manifestations of arrhythmogenic right ventricular cardiomyopathy/dysplasia: a multicenter study. *J Am Coll Cardiol* **1997**, *30* (6), 1512-20, DOI: 10.1016/s0735-1097(97)00332-x

152. Forleo, C.; Carmosino, M.; Resta, N.; Rampazzo, A.; Valecce, R.; Sorrentino, S.; Iacoviello, M.; Pisani, F.; Procino, G.; Gerbino, A.; Scardapane, A.; Simone, C.; Calore, M.; Torretta, S.; Svelto, M.; Favale, S., Clinical and functional characterization of a novel mutation in lamin a/c gene in a multigenerational family with arrhythmogenic cardiac laminopathy. *PLoS One* **2015**, *10* (4), e0121723, DOI: 10.1371/journal.pone.0121723
153. van der Zwaag, P. A.; van Rijsingen, I. A.; Asimaki, A.; Jongbloed, J. D.; van Veldhuisen, D. J.; Wiesfeld, A. C.; Cox, M. G.; van Lochem, L. T.; de Boer, R. A.; Hofstra, R. M.; Christiaans, I.; van Spaendonck-Zwarts, K. Y.; Lekanne dit Deprez, R. H.; Judge, D. P.; Calkins, H.; Suurmeijer, A. J.; Hauer, R. N.; Saffitz, J. E.; Wilde, A. A.; van den Berg, M. P.; van Tintelen, J. P., Phospholamban R14del mutation in patients diagnosed with dilated cardiomyopathy or arrhythmogenic right ventricular cardiomyopathy: evidence supporting the concept of arrhythmogenic cardiomyopathy. *Eur J Heart Fail* **2012**, *14* (11), 1199-207, DOI: 10.1093/eurjhf/hfs119
154. Pieperhoff, S., Gene Mutations Resulting in the Development of ARVC/D Could Affect Cells of the Cardiac Conduction System. *Front Physiol* **2012**, *3*, 22, DOI: 10.3389/fphys.2012.00022
155. Corrado, D.; Wichter, T.; Link, M. S.; Hauer, R. N.; Marchlinski, F. E.; Anastasakis, A.; Bauce, B.; Basso, C.; Brunckhorst, C.; Tsatsopoulou, A.; Tandri, H.; Paul, M.; Schmied, C.; Pelliccia, A.; Duru, F.; Protonotarios, N.; Estes, N. M., 3rd; McKenna, W. J.; Thiene, G.; Marcus, F. I.; Calkins, H., Treatment of Arrhythmogenic Right Ventricular Cardiomyopathy/Dysplasia: An International Task Force Consensus Statement. *Circulation* **2015**, *132* (5), 441-53, DOI: 10.1161/CIRCULATIONAHA.115.017944
156. Migliore, F.; Zorzi, A.; Silvano, M.; Rigato, I.; Basso, C.; Thiene, G.; Corrado, D., Clinical management of arrhythmogenic right ventricular cardiomyopathy: an update. *Curr Pharm Des* **2010**, *16* (26), 2918-28, DOI: 10.2174/138161210793176491
157. Marcus, G. M.; Glidden, D. V.; Polonsky, B.; Zareba, W.; Smith, L. M.; Cannom, D. S.; Estes, N. A., 3rd; Marcus, F.; Scheinman, M. M.; Multidisciplinary Study of Right Ventricular Dysplasia, I., Efficacy of antiarrhythmic drugs in arrhythmogenic right ventricular cardiomyopathy: a report from the North American ARVC Registry. *J Am Coll Cardiol* **2009**, *54* (7), 609-15, DOI: 10.1016/j.jacc.2009.04.052
158. Gandjbakhch, E.; Redheuil, A.; Pousset, F.; Charron, P.; Frank, R., Clinical Diagnosis, Imaging, and Genetics of Arrhythmogenic Right Ventricular Cardiomyopathy/Dysplasia: JACC State-of-the-Art Review. *J Am Coll Cardiol* **2018**, *72* (7), 784-804, DOI: 10.1016/j.jacc.2018.05.065
159. Bhonsale, A.; Groeneweg, J. A.; James, C. A.; Dooijes, D.; Tichnell, C.; Jongbloed, J. D.; Murray, B.; te Riele, A. S.; van den Berg, M. P.; Bikker, H.; Atsma, D. E.; de Groot, N. M.; Houweling, A. C.; van der Heijden, J. F.; Russell, S. D.; Doevendans, P. A.; van Veen, T. A.; Tandri, H.; Wilde, A. A.; Judge, D. P.; van Tintelen, J. P.; Calkins, H.; Hauer, R. N., Impact of genotype on clinical course in arrhythmogenic right ventricular dysplasia/cardiomyopathy-associated mutation carriers. *Eur Heart J* **2015**, *36* (14), 847-55, DOI: 10.1093/eurheartj/ehu509
160. van Lint, F. H. M.; Murray, B.; Tichnell, C.; Zwart, R.; Amat, N.; Lekanne Deprez, R. H.; Dittmann, S.; Stallmeyer, B.; Calkins, H.; van der Smagt, J. J.; van den

- Wijngaard, A.; Dooijes, D.; van der Zwaag, P. A.; Schulze-Bahr, E.; Judge, D. P.; Jongbloed, J. D. H.; van Tintelen, J. P.; James, C. A., Arrhythmogenic Right Ventricular Cardiomyopathy-Associated Desmosomal Variants Are Rarely De Novo. *Circ Genom Precis Med* **2019**, *12* (8), e002467, DOI: 10.1161/CIRCGEN.119.002467
161. Akdis, D.; Saguner, A. M.; Shah, K.; Wei, C.; Medeiros-Domingo, A.; von Eckardstein, A.; Luscher, T. F.; Brunckhorst, C.; Chen, H. S. V.; Duru, F., Sex hormones affect outcome in arrhythmogenic right ventricular cardiomyopathy/dysplasia: from a stem cell derived cardiomyocyte-based model to clinical biomarkers of disease outcome. *Eur Heart J* **2017**, *38* (19), 1498-1508, DOI: 10.1093/eurheartj/ehx011
162. Protonotarios, N.; Tsatsopoulou, A., Naxos disease and Carvajal syndrome: cardiocutaneous disorders that highlight the pathogenesis and broaden the spectrum of arrhythmogenic right ventricular cardiomyopathy. *Cardiovasc Pathol* **2004**, *13* (4), 185-94, DOI: 10.1016/j.carpath.2004.03.609
163. Karmouch, J.; Protonotarios, A.; Syrris, P., Genetic basis of arrhythmogenic cardiomyopathy. *Curr Opin Cardiol* **2018**, *33* (3), 276-281, DOI: 10.1097/HCO.0000000000000509
164. Groeneweg, J. A.; Bhonsale, A.; James, C. A.; te Riele, A. S.; Dooijes, D.; Tichnell, C.; Murray, B.; Wiesfeld, A. C.; Sawant, A. C.; Kassamali, B.; Atsma, D. E.; Volders, P. G.; de Groot, N. M.; de Boer, K.; Zimmerman, S. L.; Kamel, I. R.; van der Heijden, J. F.; Russell, S. D.; Jan Cramer, M.; Tedford, R. J.; Doevendans, P. A.; van Veen, T. A.; Tandri, H.; Wilde, A. A.; Judge, D. P.; van Tintelen, J. P.; Hauer, R. N.; Calkins, H., Clinical Presentation, Long-Term Follow-Up, and Outcomes of 1001 Arrhythmogenic Right Ventricular Dysplasia/Cardiomyopathy Patients and Family Members. *Circ Cardiovasc Genet* **2015**, *8* (3), 437-46, DOI: 10.1161/CIRCGENETICS.114.001003
165. Rampazzo, A.; Calore, M.; van Hengel, J.; van Roy, F., Intercalated discs and arrhythmogenic cardiomyopathy. *Circ Cardiovasc Genet* **2014**, *7* (6), 930-40, DOI: 10.1161/CIRCGENETICS.114.000645
166. Chen, S.; Guttridge, D. C.; You, Z.; Zhang, Z.; Fribley, A.; Mayo, M. W.; Kitajewski, J.; Wang, C. Y., Wnt-1 signaling inhibits apoptosis by activating beta-catenin/T cell factor-mediated transcription. *J Cell Biol* **2001**, *152* (1), 87-96, DOI: 10.1083/jcb.152.1.87
167. Chen, S. N.; Gurha, P.; Lombardi, R.; Ruggiero, A.; Willerson, J. T.; Marian, A. J., The hippo pathway is activated and is a causal mechanism for adipogenesis in arrhythmogenic cardiomyopathy. *Circ Res* **2014**, *114* (3), 454-68, DOI: 10.1161/CIRCRESAHA.114.302810
168. Rigato, I.; Bauce, B.; Rampazzo, A.; Zorzi, A.; Pilichou, K.; Mazzotti, E.; Migliore, F.; Marra, M. P.; Lorenzon, A.; De Bortoli, M.; Calore, M.; Nava, A.; Daliento, L.; Gregori, D.; Iliceto, S.; Thiene, G.; Basso, C.; Corrado, D., Compound and digenic heterozygosity predicts lifetime arrhythmic outcome and sudden cardiac death in desmosomal gene-related arrhythmogenic right ventricular cardiomyopathy. *Circ Cardiovasc Genet* **2013**, *6* (6), 533-42, DOI: 10.1161/CIRCGENETICS.113.000288
169. Cheung, C. C.; Healey, J. S.; Hamilton, R.; Spears, D.; Gollob, M. H.; Mellor, G.; Steinberg, C.; Sanatani, S.; Laksman, Z. W.; Krahn, A. D., Phospholamban

- cardiomyopathy: a Canadian perspective on a unique population. *Neth Heart J* **2019**, *27* (4), 208-213, DOI: 10.1007/s12471-019-1247-0
170. Merner, N. D.; Hodgkinson, K. A.; Haywood, A. F.; Connors, S.; French, V. M.; Drenckhahn, J. D.; Kupprion, C.; Ramadanova, K.; Thierfelder, L.; McKenna, W.; Gallagher, B.; Morris-Larkin, L.; Bassett, A. S.; Parfrey, P. S.; Young, T. L., Arrhythmogenic right ventricular cardiomyopathy type 5 is a fully penetrant, lethal arrhythmic disorder caused by a missense mutation in the TMEM43 gene. *Am J Hum Genet* **2008**, *82* (4), 809-21, DOI: 10.1016/j.ajhg.2008.01.010
171. Hall, C. L.; Akhtar, M. M.; Sabater-Molina, M.; Futema, M.; Asimaki, A.; Protonotarios, A.; Dalageorgou, C.; Pittman, A. M.; Suarez, M. P.; Aguilera, B.; Molina, P.; Zorio, E.; Hernandez, J. P.; Pastor, F.; Gimeno, J. R.; Syrris, P.; McKenna, W. J., Filamin C variants are associated with a distinctive clinical and immunohistochemical arrhythmogenic cardiomyopathy phenotype. *Int J Cardiol* **2019**, DOI: 10.1016/j.ijcard.2019.09.048
172. Smith, E. D.; Lakdawala, N. K.; Papoutsidakis, N.; Aubert, G.; Mazzanti, A.; McCanta, A. C.; Agarwal, P. P.; Arscott, P.; Dellefave-Castillo, L. M.; Vorovich, E. E.; Nutakki, K.; Wilsbacher, L. D.; Priori, S. G.; Jacoby, D. L.; McNally, E. M.; Helms, A. S., Desmoplakin Cardiomyopathy, a Fibrotic and Inflammatory Form of Cardiomyopathy Distinct from Typical Dilated or Arrhythmogenic Right Ventricular Cardiomyopathy. *Circulation* **2020**, DOI: 10.1161/CIRCULATIONAHA.119.044934
173. van der Zwaag, P. A.; Jongbloed, J. D.; van den Berg, M. P.; van der Smagt, J. J.; Jongbloed, R.; Bikker, H.; Hofstra, R. M.; van Tintelen, J. P., A genetic variants database for arrhythmogenic right ventricular dysplasia/cardiomyopathy. *Hum Mutat* **2009**, *30* (9), 1278-83, DOI: 10.1002/humu.21064
174. McKoy, G.; Protonotarios, N.; Crosby, A.; Tsatsopoulou, A.; Anastasakis, A.; Coonar, A.; Norman, M.; Baboonian, C.; Jeffery, S.; McKenna, W. J., Identification of a deletion in plakoglobin in arrhythmogenic right ventricular cardiomyopathy with palmoplantar keratoderma and woolly hair (Naxos disease). *Lancet* **2000**, *355* (9221), 2119-24, DOI: 10.1016/S0140-6736(00)02379-5
175. Fressart, V.; Duthoit, G.; Donal, E.; Probst, V.; Deharo, J. C.; Chevalier, P.; Klug, D.; Dubourg, O.; Delacretaz, E.; Cosnay, P.; Scanu, P.; Extramiana, F.; Keller, D.; Hidden-Lucet, F.; Simon, F.; Bessirard, V.; Roux-Buisson, N.; Hebert, J. L.; Azarine, A.; Casset-Senon, D.; Rouzet, F.; Lecarpentier, Y.; Fontaine, G.; Coirault, C.; Frank, R.; Hainque, B.; Charron, P., Desmosomal gene analysis in arrhythmogenic right ventricular dysplasia/cardiomyopathy: spectrum of mutations and clinical impact in practice. *Europace* **2010**, *12* (6), 861-8, DOI: 10.1093/europace/euq104
176. Quarta, G.; Syrris, P.; Ashworth, M.; Jenkins, S.; Zuborne Alapi, K.; Morgan, J.; Muir, A.; Pantazis, A.; McKenna, W. J.; Elliott, P. M., Mutations in the Lamin A/C gene mimic arrhythmogenic right ventricular cardiomyopathy. *Eur Heart J* **2012**, *33* (9), 1128-36, DOI: 10.1093/eurheartj/ehr451
177. Bao, J. R.; Wang, J. Z.; Yao, Y.; Wang, Y. L.; Fan, X. H.; Sun, K.; Zhang, S.; Hui, R. T.; Song, L., Screening of pathogenic genes in Chinese patients with arrhythmogenic right ventricular cardiomyopathy. *Chin Med J (Engl)* **2013**, *126* (22), 4238-41,

178. Bass-Zubek, A. E.; Hobbs, R. P.; Amargo, E. V.; Garcia, N. J.; Hsieh, S. N.; Chen, X.; Wahl, J. K., 3rd; Denning, M. F.; Green, K. J., Plakophilin 2: a critical scaffold for PKC alpha that regulates intercellular junction assembly. *J Cell Biol* **2008**, *181* (4), 605-13, DOI: 10.1083/jcb.200712133
179. Chen, X.; Bonne, S.; Hatzfeld, M.; van Roy, F.; Green, K. J., Protein binding and functional characterization of plakophilin 2. Evidence for its diverse roles in desmosomes and beta -catenin signaling. *J Biol Chem* **2002**, *277* (12), 10512-22, DOI: 10.1074/jbc.M108765200
180. Hall, C.; Li, S.; Li, H.; Creason, V.; Wahl, J. K., 3rd, Arrhythmogenic right ventricular cardiomyopathy plakophilin-2 mutations disrupt desmosome assembly and stability. *Cell Commun Adhes* **2009**, *16* (1-3), 15-27, DOI: 10.1080/15419060903009329
181. Grossmann, K. S.; Grund, C.; Huelsken, J.; Behrend, M.; Erdmann, B.; Franke, W. W.; Birchmeier, W., Requirement of plakophilin 2 for heart morphogenesis and cardiac junction formation. *J Cell Biol* **2004**, *167* (1), 149-60, DOI: 10.1083/jcb.200402096
182. Cruz, F. M.; Sanz-Rosa, D.; Roche-Molina, M.; Garcia-Prieto, J.; Garcia-Ruiz, J. M.; Pizarro, G.; Jimenez-Borreguero, L. J.; Torres, M.; Bernad, A.; Ruiz-Cabello, J.; Fuster, V.; Ibanez, B.; Bernal, J. A., Exercise triggers ARVC phenotype in mice expressing a disease-causing mutated version of human plakophilin-2. *J Am Coll Cardiol* **2015**, *65* (14), 1438-50, DOI: 10.1016/j.jacc.2015.01.045
183. Moncayo-Arlandi, J.; Guasch, E.; Sanz-de la Garza, M.; Casado, M.; Garcia, N. A.; Mont, L.; Sitges, M.; Knoll, R.; Buyandelger, B.; Campuzano, O.; Diez-Juan, A.; Brugada, R., Molecular disturbance underlies to arrhythmogenic cardiomyopathy induced by transgene content, age and exercise in a truncated PKP2 mouse model. *Hum Mol Genet* **2016**, *25* (17), 3676-3688, DOI: 10.1093/hmg/ddw213
184. Agarwal, U.; Ghalayini, W.; Dong, F.; Weber, K.; Zou, Y. R.; Rabbany, S. Y.; Rafii, S.; Penn, M. S., Role of cardiac myocyte CXCR4 expression in development and left ventricular remodeling after acute myocardial infarction. *Circ Res* **2010**, *107* (5), 667-76, DOI: 10.1161/CIRCRESAHA.110.223289
185. Lyon, R. C.; Mezzano, V.; Wright, A. T.; Pfeiffer, E.; Chuang, J.; Banares, K.; Castaneda, A.; Ouyang, K.; Cui, L.; Contu, R.; Gu, Y.; Evans, S. M.; Omens, J. H.; Peterson, K. L.; McCulloch, A. D.; Sheikh, F., Connexin defects underlie arrhythmogenic right ventricular cardiomyopathy in a novel mouse model. *Hum Mol Genet* **2014**, *23* (5), 1134-50, DOI: 10.1093/hmg/ddt508
186. Asimaki, A.; Tandri, H.; Huang, H.; Halushka, M. K.; Gautam, S.; Basso, C.; Thiene, G.; Tsatsopoulou, A.; Protonotarios, N.; McKenna, W. J.; Calkins, H.; Saffitz, J. E., A new diagnostic test for arrhythmogenic right ventricular cardiomyopathy. *N Engl J Med* **2009**, *360* (11), 1075-84, DOI: 10.1056/NEJMoa0808138
187. Dieding, M.; Debus, J. D.; Kerkhoff, R.; Gaertner-Rommel, A.; Walhorn, V.; Milting, H.; Anselmetti, D., Arrhythmogenic cardiomyopathy related DSG2 mutations affect desmosomal cadherin binding kinetics. *Sci Rep* **2017**, *7* (1), 13791, DOI: 10.1038/s41598-017-13737-x
188. Christensen, A. H.; Andersen, C. B.; Wassilew, K.; Svendsen, J. H.; Bundgaard, H.; Brand, S. M.; Schmitz, B., Rare non-coding Desmoglein-2 variant contributes to

- Arrhythmogenic right ventricular cardiomyopathy. *J Mol Cell Cardiol* **2019**, *131*, 164-170, DOI: 10.1016/j.yjmcc.2019.04.029
189. Bauce, B.; Nava, A.; Beffagna, G.; Basso, C.; Lorenzon, A.; Smaniotto, G.; De Bortoli, M.; Rigato, I.; Mazzotti, E.; Steriotis, A., Multiple mutations in desmosomal proteins encoding genes in arrhythmogenic right ventricular cardiomyopathy/dysplasia. *Heart rhythm* **2010**, *7* (1), 22-29,
190. Nakajima, T.; Kaneko, Y.; Irie, T.; Takahashi, R.; Kato, T.; Iijima, T.; Iso, T.; Kurabayashi, M., Compound and digenic heterozygosity in desmosome genes as a cause of arrhythmogenic right ventricular cardiomyopathy in Japanese patients. *Circ J* **2012**, *76* (3), 737-43, DOI: 10.1253/circj.cj-11-0927
191. Xu, T.; Yang, Z.; Vatta, M.; Rampazzo, A.; Beffagna, G.; Pilichou, K.; Scherer, S. E.; Saffitz, J.; Kravitz, J.; Zareba, W.; Danieli, G. A.; Lorenzon, A.; Nava, A.; Bauce, B.; Thiene, G.; Basso, C.; Calkins, H.; Gear, K.; Marcus, F.; Towbin, J. A.; Multidisciplinary Study of Right Ventricular Dysplasia, I., Compound and digenic heterozygosity contributes to arrhythmogenic right ventricular cardiomyopathy. *J Am Coll Cardiol* **2010**, *55* (6), 587-97, DOI: 10.1016/j.jacc.2009.11.020
192. Lin, Y.; Zhang, Q.; Zhong, Z. A.; Xu, Z.; He, S.; Rao, F.; Liu, Y.; Tang, J.; Wang, F.; Liu, H.; Xie, J.; Wu, H.; Wang, S.; Li, X.; Shan, Z.; Deng, C.; Liao, Z.; Deng, H.; Liao, H.; Xue, Y.; Chen, W.; Zhan, X.; Zhang, B.; Wu, S., Whole Genome Sequence Identified a Rare Homozygous Pathogenic Mutation of the DSG2 Gene in a Familial Arrhythmogenic Cardiomyopathy Involving Both Ventricles. *Cardiology* **2017**, *138* (1), 41-54, DOI: 10.1159/000462962
193. Hermida, A.; Fressart, V.; Hidden-Lucet, F.; Donal, E.; Probst, V.; Deharo, J. C.; Chevalier, P.; Klug, D.; Mansencal, N.; Delacretaz, E.; Cosnay, P.; Scanu, P.; Extramiana, F.; Keller, D. I.; Rouanet, S.; Charron, P.; Gandjbakhch, E., High risk of heart failure associated with desmoglein-2 mutations compared to plakophilin-2 mutations in arrhythmogenic right ventricular cardiomyopathy/dysplasia. *Eur J Heart Fail* **2019**, *21* (6), 792-800, DOI: 10.1002/ejhf.1423
194. Eshkind, L.; Tian, Q.; Schmidt, A.; Franke, W. W.; Windoffer, R.; Leube, R. E., Loss of desmoglein 2 suggests essential functions for early embryonic development and proliferation of embryonal stem cells. *Eur J Cell Biol* **2002**, *81* (11), 592-8, DOI: 10.1078/0171-9335-00278
195. Krusche, C. A.; Holthofer, B.; Hofe, V.; van de Sandt, A. M.; Eshkind, L.; Bockamp, E.; Merx, M. W.; Kant, S.; Windoffer, R.; Leube, R. E., Desmoglein 2 mutant mice develop cardiac fibrosis and dilation. *Basic Res Cardiol* **2011**, *106* (4), 617-33, DOI: 10.1007/s00395-011-0175-y
196. Kant, S.; Krull, P.; Eisner, S.; Leube, R. E.; Krusche, C. A., Histological and ultrastructural abnormalities in murine desmoglein 2-mutant hearts. *Cell Tissue Res* **2012**, *348* (2), 249-59, DOI: 10.1007/s00441-011-1322-3
197. Chelko, S. P.; Asimaki, A.; Andersen, P.; Bedja, D.; Amat-Alarcon, N.; DeMazumder, D.; Jasti, R.; MacRae, C. A.; Leber, R.; Kleber, A. G.; Saffitz, J. E.; Judge, D. P., Central role for GSK3beta in the pathogenesis of arrhythmogenic cardiomyopathy. *JCI Insight* **2016**, *1* (5), DOI: 10.1172/jci.insight.85923

198. Pilichou, K.; Remme, C. A.; Basso, C.; Campian, M. E.; Rizzo, S.; Barnett, P.; Scicluna, B. P.; Bauce, B.; van den Hoff, M. J.; de Bakker, J. M.; Tan, H. L.; Valente, M.; Nava, A.; Wilde, A. A.; Moorman, A. F.; Thiene, G.; Bezzina, C. R., Myocyte necrosis underlies progressive myocardial dystrophy in mouse *dsg2*-related arrhythmogenic right ventricular cardiomyopathy. *J Exp Med* **2009**, *206* (8), 1787-802, DOI: 10.1084/jem.20090641
199. Rizzo, S.; Lodder, E. M.; Verkerk, A. O.; Wolswinkel, R.; Beekman, L.; Pilichou, K.; Basso, C.; Remme, C. A.; Thiene, G.; Bezzina, C. R., Intercalated disc abnormalities, reduced Na(+) current density, and conduction slowing in desmoglein-2 mutant mice prior to cardiomyopathic changes. *Cardiovasc Res* **2012**, *95* (4), 409-18, DOI: 10.1093/cvr/cvs219
200. Christensen, A. H.; Benn, M.; Bundgaard, H.; Tybjaerg-Hansen, A.; Haunso, S.; Svendsen, J. H., Wide spectrum of desmosomal mutations in Danish patients with arrhythmogenic right ventricular cardiomyopathy. *J Med Genet* **2010**, *47* (11), 736-44, DOI: 10.1136/jmg.2010.077891
201. Beffagna, G.; De Bortoli, M.; Nava, A.; Salamon, M.; Lorenzon, A.; Zaccolo, M.; Mancuso, L.; Sigalotti, L.; Bauce, B.; Occhi, G.; Basso, C.; Lanfranchi, G.; Towbin, J. A.; Thiene, G.; Danieli, G. A.; Rampazzo, A., Missense mutations in desmocollin-2 N-terminus, associated with arrhythmogenic right ventricular cardiomyopathy, affect intracellular localization of desmocollin-2 in vitro. *BMC Med Genet* **2007**, *8*, 65, DOI: 10.1186/1471-2350-8-65
202. Gehmlich, K.; Asimaki, A.; Cahill, T. J.; Ehler, E.; Syrris, P.; Zachara, E.; Re, F.; Avella, A.; Monserrat, L.; Saffitz, J. E.; McKenna, W. J., Novel missense mutations in exon 15 of desmoglein-2: role of the intracellular cadherin segment in arrhythmogenic right ventricular cardiomyopathy? *Heart Rhythm* **2010**, *7* (10), 1446-53, DOI: 10.1016/j.hrthm.2010.08.007
203. Tan, B. Y.; Jain, R.; den Haan, A. D.; Chen, Y.; Dalal, D.; Tandri, H.; Amat-Alarcon, N.; Daly, A.; Tichnell, C.; James, C.; Calkins, H.; Judge, D. P., Shared desmosome gene findings in early and late onset arrhythmogenic right ventricular dysplasia/cardiomyopathy. *J Cardiovasc Transl Res* **2010**, *3* (6), 663-73, DOI: 10.1007/s12265-010-9224-4
204. Bhuiyan, Z. A.; Jongbloed, J. D.; van der Smagt, J.; Lombardi, P. M.; Wiesfeld, A. C.; Nelen, M.; Schouten, M.; Jongbloed, R.; Cox, M. G.; van Wolferen, M.; Rodriguez, L. M.; van Gelder, I. C.; Bikker, H.; Suurmeijer, A. J.; van den Berg, M. P.; Mannens, M. M.; Hauer, R. N.; Wilde, A. A.; van Tintelen, J. P., Desmoglein-2 and desmocollin-2 mutations in dutch arrhythmogenic right ventricular dysplasia/cardiomyopathy patients: results from a multicenter study. *Circ Cardiovasc Genet* **2009**, *2* (5), 418-27, DOI: 10.1161/CIRCGENETICS.108.839829
205. Gehmlich, K.; Syrris, P.; Peskett, E.; Evans, A.; Ehler, E.; Asimaki, A.; Anastasakis, A.; Tsatsopoulou, A.; Vouliotis, A. I.; Stefanadis, C.; Saffitz, J. E.; Protonotarios, N.; McKenna, W. J., Mechanistic insights into arrhythmogenic right ventricular cardiomyopathy caused by desmocollin-2 mutations. *Cardiovasc Res* **2011**, *90* (1), 77-87, DOI: 10.1093/cvr/cvq353

206. Brodehl, A.; Belke, D. D.; Garnett, L.; Martens, K.; Abdelfatah, N.; Rodriguez, M.; Diao, C.; Chen, Y. X.; Gordon, P. M.; Nygren, A.; Gerull, B., Transgenic mice overexpressing desmocollin-2 (DSC2) develop cardiomyopathy associated with myocardial inflammation and fibrotic remodeling. *PLoS One* **2017**, *12* (3), e0174019, DOI: 10.1371/journal.pone.0174019
207. Heuser, A.; Plovie, E. R.; Ellinor, P. T.; Grossmann, K. S.; Shin, J. T.; Wichter, T.; Basson, C. T.; Lerman, B. B.; Sasse-Klaassen, S.; Thierfelder, L.; MacRae, C. A.; Gerull, B., Mutant desmocollin-2 causes arrhythmogenic right ventricular cardiomyopathy. *Am J Hum Genet* **2006**, *79* (6), 1081-8, DOI: 10.1086/509044
208. Hariharan, V.; Asimaki, A.; Michaelson, J. E.; Plovie, E.; MacRae, C. A.; Saffitz, J. E.; Huang, H., Arrhythmogenic right ventricular cardiomyopathy mutations alter shear response without changes in cell-cell adhesion. *Cardiovasc Res* **2014**, *104* (2), 280-9, DOI: 10.1093/cvr/cvu212
209. Kant, S.; Krusche, C. A.; Gaertner, A.; Milting, H.; Leube, R. E., Loss of plakoglobin immunoreactivity in intercalated discs in arrhythmogenic right ventricular cardiomyopathy: protein mislocalization versus epitope masking. *Cardiovasc Res* **2016**, *109* (2), 260-71, DOI: 10.1093/cvr/cvv270
210. Ross, S. E.; Hemati, N.; Longo, K. A.; Bennett, C. N.; Lucas, P. C.; Erickson, R. L.; MacDougald, O. A., Inhibition of adipogenesis by Wnt signaling. *Science* **2000**, *289* (5481), 950-3, DOI: 10.1126/science.289.5481.950
211. Ruiz, P.; Brinkmann, V.; Ledermann, B.; Behrend, M.; Grund, C.; Thalhammer, C.; Vogel, F.; Birchmeier, C.; Gunthert, U.; Franke, W. W.; Birchmeier, W., Targeted mutation of plakoglobin in mice reveals essential functions of desmosomes in the embryonic heart. *J Cell Biol* **1996**, *135* (1), 215-25, DOI: 10.1083/jcb.135.1.215
212. Li, D.; Liu, Y.; Maruyama, M.; Zhu, W.; Chen, H.; Zhang, W.; Reuter, S.; Lin, S. F.; Haneline, L. S.; Field, L. J.; Chen, P. S.; Shou, W., Restrictive loss of plakoglobin in cardiomyocytes leads to arrhythmogenic cardiomyopathy. *Hum Mol Genet* **2011**, *20* (23), 4582-96, DOI: 10.1093/hmg/ddr392
213. Swope, D.; Cheng, L.; Gao, E.; Li, J.; Radice, G. L., Loss of cadherin-binding proteins beta-catenin and plakoglobin in the heart leads to gap junction remodeling and arrhythmogenesis. *Mol Cell Biol* **2012**, *32* (6), 1056-67, DOI: 10.1128/MCB.06188-11
214. Beffagna, G.; Occhi, G.; Nava, A.; Vitiello, L.; Ditadi, A.; Basso, C.; Bauce, B.; Carraro, G.; Thiene, G.; Towbin, J. A.; Danieli, G. A.; Rampazzo, A., Regulatory mutations in transforming growth factor-beta3 gene cause arrhythmogenic right ventricular cardiomyopathy type 1. *Cardiovasc Res* **2005**, *65* (2), 366-73, DOI: 10.1016/j.cardiores.2004.10.005
215. Roux-Buisson, N.; Gandjbakhch, E.; Donal, E.; Probst, V.; Deharo, J. C.; Chevalier, P.; Klug, D.; Mansencal, N.; Delacretaz, E.; Cosnay, P.; Scanu, P.; Extramiana, F.; Keller, D.; Hidden-Lucet, F.; Trapani, J.; Fouret, P.; Frank, R.; Fressart, V.; Faure, J.; Lunardi, J.; Charron, P., Prevalence and significance of rare RYR2 variants in arrhythmogenic right ventricular cardiomyopathy/dysplasia: results of a systematic screening. *Heart Rhythm* **2014**, *11* (11), 1999-2009, DOI: 10.1016/j.hrthm.2014.07.020
216. Tiso, N.; Stephan, D. A.; Nava, A.; Bagattin, A.; Devaney, J. M.; Stanchi, F.; Larderet, G.; Brahmabhatt, B.; Brown, K.; Bauce, B.; Muriago, M.; Basso, C.; Thiene, G.;

- Danieli, G. A.; Rampazzo, A., Identification of mutations in the cardiac ryanodine receptor gene in families affected with arrhythmogenic right ventricular cardiomyopathy type 2 (ARVD2). *Hum Mol Genet* **2001**, *10* (3), 189-94, DOI: 10.1093/hmg/10.3.189
217. Milting, H.; Lukas, N.; Klauke, B.; Korfer, R.; Perrot, A.; Osterziel, K. J.; Vogt, J.; Peters, S.; Thieleczek, R.; Varsanyi, M., Composite polymorphisms in the ryanodine receptor 2 gene associated with arrhythmogenic right ventricular cardiomyopathy. *Cardiovasc Res* **2006**, *71* (3), 496-505, DOI: 10.1016/j.cardiores.2006.04.004
218. van Hengel, J.; Calore, M.; Bauce, B.; Dazzo, E.; Mazzotti, E.; De Bortoli, M.; Lorenzon, A.; Li Mura, I. E.; Beffagna, G.; Rigato, I.; Vleeschouwers, M.; Tyberghein, K.; Hulpiau, P.; van Hamme, E.; Zaglia, T.; Corrado, D.; Basso, C.; Thiene, G.; Daliento, L.; Nava, A.; van Roy, F.; Rampazzo, A., Mutations in the area composita protein alphaT-catenin are associated with arrhythmogenic right ventricular cardiomyopathy. *Eur Heart J* **2013**, *34* (3), 201-10, DOI: 10.1093/eurheartj/ehs373
219. Otten, E.; Asimaki, A.; Maass, A.; van Langen, I. M.; van der Wal, A.; de Jonge, N.; van den Berg, M. P.; Saffitz, J. E.; Wilde, A. A.; Jongbloed, J. D.; van Tintelen, J. P., Desmin mutations as a cause of right ventricular heart failure affect the intercalated disks. *Heart Rhythm* **2010**, *7* (8), 1058-64, DOI: 10.1016/j.hrthm.2010.04.023
220. Klauke, B.; Kossmann, S.; Gaertner, A.; Brand, K.; Stork, I.; Brodehl, A.; Dieding, M.; Walhorn, V.; Anselmetti, D.; Gerdes, D.; Bohms, B.; Schulz, U.; Zu Knyphausen, E.; Vorgerd, M.; Gummert, J.; Milting, H., De novo desmin-mutation N116S is associated with arrhythmogenic right ventricular cardiomyopathy. *Hum Mol Genet* **2010**, *19* (23), 4595-607, DOI: 10.1093/hmg/ddq387
221. Te Rijdt, W. P.; van Tintelen, J. P.; Vink, A.; van der Wal, A. C.; de Boer, R. A.; van den Berg, M. P.; Suurmeijer, A. J., Phospholamban p.Arg14del cardiomyopathy is characterized by phospholamban aggregates, aggresomes, and autophagic degradation. *Histopathology* **2016**, *69* (4), 542-50, DOI: 10.1111/his.12963
222. Bar, H.; Goudeau, B.; Walde, S.; Casteras-Simon, M.; Mucke, N.; Shatunov, A.; Goldberg, Y. P.; Clarke, C.; Holton, J. L.; Eymard, B.; Katus, H. A.; Fardeau, M.; Goldfarb, L.; Vicart, P.; Herrmann, H., Conspicuous involvement of desmin tail mutations in diverse cardiac and skeletal myopathies. *Hum Mutat* **2007**, *28* (4), 374-86, DOI: 10.1002/humu.20459
223. Lorenzon, A.; Beffagna, G.; Bauce, B.; De Bortoli, M.; Li Mura, I. E.; Calore, M.; Dazzo, E.; Basso, C.; Nava, A.; Thiene, G.; Rampazzo, A., Desmin mutations and arrhythmogenic right ventricular cardiomyopathy. *Am J Cardiol* **2013**, *111* (3), 400-5, DOI: 10.1016/j.amjcard.2012.10.017
224. van Tintelen, J. P.; Van Gelder, I. C.; Asimaki, A.; Suurmeijer, A. J.; Wiesfeld, A. C.; Jongbloed, J. D.; van den Wijngaard, A.; Kuks, J. B.; van Spaendonck-Zwarts, K. Y.; Notermans, N.; Boven, L.; van den Heuvel, F.; Veenstra-Knol, H. E.; Saffitz, J. E.; Hofstra, R. M.; van den Berg, M. P., Severe cardiac phenotype with right ventricular predominance in a large cohort of patients with a single missense mutation in the DES gene. *Heart Rhythm* **2009**, *6* (11), 1574-83, DOI: 10.1016/j.hrthm.2009.07.041
225. Park, K. Y.; Dalakas, M. C.; Goebel, H. H.; Ferrans, V. J.; Semino-Mora, C.; Litvak, S.; Takeda, K.; Goldfarb, L. G., Desmin splice variants causing cardiac and skeletal myopathy. *J Med Genet* **2000**, *37* (11), 851-7, DOI: 10.1136/jmg.37.11.851

226. Ariza, A.; Coll, J.; Fernandez-Figueras, M. T.; Lopez, M. D.; Mate, J. L.; Garcia, O.; Fernandez-Vasalo, A.; Navas-Palacios, J. J., Desmin myopathy: a multisystem disorder involving skeletal, cardiac, and smooth muscle. *Hum Pathol* **1995**, *26* (9), 1032-7, DOI: 10.1016/0046-8177(95)90095-0
227. Liang, J. J.; Grogan, M.; Ackerman, M. J.; Goodsell, K., LMNA-Mediated Arrhythmogenic Right Ventricular Cardiomyopathy and Charcot-Marie-Tooth Type 2B1: A Patient-Discovered Unifying Diagnosis. *J Cardiovasc Electrophysiol* **2016**, *27* (7), 868-71, DOI: 10.1111/jce.12984
228. Petillo, R.; D'Ambrosio, P.; Torella, A.; Taglia, A.; Picillo, E.; Testori, A.; Ergoli, M.; Nigro, G.; Piluso, G.; Nigro, V.; Politano, L., Novel mutations in LMNA A/C gene and associated phenotypes. *Acta Myol* **2015**, *34* (2-3), 116-9,
229. Kato, K.; Takahashi, N.; Fujii, Y.; Umehara, A.; Nishiuchi, S.; Makiyama, T.; Ohno, S.; Horie, M., LMNA cardiomyopathy detected in Japanese arrhythmogenic right ventricular cardiomyopathy cohort. *J Cardiol* **2016**, *68* (4), 346-51, DOI: 10.1016/j.jjcc.2015.10.013
230. van Rijsingen, I. A.; van der Zwaag, P. A.; Groeneweg, J. A.; Nannenbergh, E. A.; Jongbloed, J. D.; Zwinderman, A. H.; Pinto, Y. M.; Dit Deprez, R. H.; Post, J. G.; Tan, H. L.; de Boer, R. A.; Hauer, R. N.; Christiaans, I.; van den Berg, M. P.; van Tintelen, J. P.; Wilde, A. A., Outcome in phospholamban R14del carriers: results of a large multicentre cohort study. *Circ Cardiovasc Genet* **2014**, *7* (4), 455-65, DOI: 10.1161/CIRCGENETICS.113.000374
231. Haghghi, K.; Kolokathis, F.; Gramolini, A. O.; Waggoner, J. R.; Pater, L.; Lynch, R. A.; Fan, G. C.; Tsiapras, D.; Parekh, R. R.; Dorn, G. W., 2nd; MacLennan, D. H.; Kremastinos, D. T.; Kranias, E. G., A mutation in the human phospholamban gene, deleting arginine 14, results in lethal, hereditary cardiomyopathy. *Proc Natl Acad Sci U S A* **2006**, *103* (5), 1388-93, DOI: 10.1073/pnas.0510519103
232. Te Rijdt, W. P.; Asimaki, A.; Jongbloed, J. D. H.; Hoorntje, E. T.; Lazzarini, E.; van der Zwaag, P. A.; de Boer, R. A.; van Tintelen, J. P.; Saffitz, J. E.; van den Berg, M. P.; Suurmeijer, A. J. H., Distinct molecular signature of phospholamban p.Arg14del arrhythmogenic cardiomyopathy. *Cardiovasc Pathol* **2019**, *40*, 2-6, DOI: 10.1016/j.carpath.2018.12.006
233. Franke, W. W.; Dorflinger, Y.; Kuhn, C.; Zimbelmann, R.; Winter-Simanowski, S.; Frey, N.; Heid, H., Protein LUMA is a cytoplasmic plaque constituent of various epithelial adherens junctions and composite junctions of myocardial intercalated disks: a unifying finding for cell biology and cardiology. *Cell Tissue Res* **2014**, *357* (1), 159-72, DOI: 10.1007/s00441-014-1865-1
234. Padron-Barthe, L.; Villalba-Orero, M.; Gomez-Salinerio, J. M.; Dominguez, F.; Roman, M.; Larrasa-Alonso, J.; Ortiz-Sanchez, P.; Martinez, F.; Lopez-Olaneta, M.; Bonzon-Kulichenko, E.; Vazquez, J.; Marti-Gomez, C.; Santiago, D. J.; Prados, B.; Giovino, G.; Gomez-Gavero, M. V.; Priori, S.; Garcia-Pavia, P.; Lara-Pezzi, E., Severe Cardiac Dysfunction and Death Caused by Arrhythmogenic Right Ventricular Cardiomyopathy Type 5 Are Improved by Inhibition of Glycogen Synthase Kinase-3beta. *Circulation* **2019**, *140* (14), 1188-1204, DOI: 10.1161/CIRCULATIONAHA.119.040366

235. AbdelWahab, A.; Gardner, M.; Parkash, R.; Gray, C.; Sapp, J., Ventricular tachycardia ablation in arrhythmogenic right ventricular cardiomyopathy patients with TMEM43 gene mutations. *J Cardiovasc Electrophysiol* **2018**, *29* (1), 90-97, DOI: 10.1111/jce.13353
236. Hodgkinson, K. A.; Connors, S. P.; Merner, N.; Haywood, A.; Young, T. L.; McKenna, W. J.; Gallagher, B.; Curtis, F.; Bassett, A. S.; Parfrey, P. S., The natural history of a genetic subtype of arrhythmogenic right ventricular cardiomyopathy caused by a p.S358L mutation in TMEM43. *Clin Genet* **2013**, *83* (4), 321-31, DOI: 10.1111/j.1399-0004.2012.01919.x
237. Aalbaek Kjaergaard, K.; Kristensen, J.; Molgaard, H.; Cosedis Nielsen, J.; Jensen, H. K., Failure of ICD therapy in lethal arrhythmogenic right ventricular cardiomyopathy type 5 caused by the TMEM43 p.Ser358Leu mutation. *HeartRhythm Case Rep* **2016**, *2* (3), 217-222, DOI: 10.1016/j.hrcr.2015.12.009
238. Taylor, M.; Graw, S.; Sinagra, G.; Barnes, C.; Slavov, D.; Brun, F.; Pinamonti, B.; Salcedo, E. E.; Sauer, W.; Pyxaras, S.; Anderson, B.; Simon, B.; Bogomolovas, J.; Labeit, S.; Granzier, H.; Mestroni, L., Genetic variation in titin in arrhythmogenic right ventricular cardiomyopathy-overlap syndromes. *Circulation* **2011**, *124* (8), 876-85, DOI: 10.1161/CIRCULATIONAHA.110.005405
239. Brun, F.; Barnes, C. V.; Sinagra, G.; Slavov, D.; Barbati, G.; Zhu, X.; Graw, S. L.; Spezzacatene, A.; Pinamonti, B.; Merlo, M.; Salcedo, E. E.; Sauer, W. H.; Taylor, M. R.; Mestroni, L.; Familial Cardiomyopathy, R., Titin and desmosomal genes in the natural history of arrhythmogenic right ventricular cardiomyopathy. *J Med Genet* **2014**, *51* (10), 669-76, DOI: 10.1136/jmedgenet-2014-102591
240. Bogomolovas, J.; Fleming, J. R.; Anderson, B. R.; Williams, R.; Lange, S.; Simon, B.; Khan, M. M.; Rudolf, R.; Franke, B.; Bullard, B.; Rigden, D. J.; Granzier, H.; Labeit, S.; Mayans, O., Exploration of pathomechanisms triggered by a single-nucleotide polymorphism in titin's I-band: the cardiomyopathy-linked mutation T2580I. *Open Biol* **2016**, *6* (9), DOI: 10.1098/rsob.160114
241. Gigli, M.; Begay, R. L.; Morea, G.; Graw, S. L.; Sinagra, G.; Taylor, M. R.; Granzier, H.; Mestroni, L., A Review of the Giant Protein Titin in Clinical Molecular Diagnostics of Cardiomyopathies. *Front Cardiovasc Med* **2016**, *3*, 21, DOI: 10.3389/fcvm.2016.00021
242. Franaszczyk, M.; Chmielewski, P.; Truszkowska, G.; Stawinski, P.; Michalak, E.; Rydzanicz, M.; Sobieszczanska-Malek, M.; Pollak, A.; Szczygiel, J.; Kosinska, J.; Parulski, A.; Stoklosa, T.; Tarnowska, A.; Machnicki, M. M.; Foss-Nieradko, B.; Szperl, M.; Sioma, A.; Kusmierczyk, M.; Grzybowski, J.; Zielinski, T.; Ploski, R.; Bilinska, Z. T., Titin Truncating Variants in Dilated Cardiomyopathy - Prevalence and Genotype-Phenotype Correlations. *PLoS One* **2017**, *12* (1), e0169007, DOI: 10.1371/journal.pone.0169007
243. Corrado, D.; Zorzi, A., Filamin C: A New Arrhythmogenic Cardiomyopathy-Causing Gene? *JACC Clin Electrophysiol* **2018**, *4* (4), 515-517, DOI: 10.1016/j.jacep.2018.01.004
244. van der Flier, A.; Sonnenberg, A., Structural and functional aspects of filamins. *Biochim Biophys Acta* **2001**, *1538* (2-3), 99-117, DOI: 10.1016/s0167-4889(01)00072-6

245. Ortiz-Genga, M. F.; Cuenca, S.; Dal Ferro, M.; Zorio, E.; Salgado-Aranda, R.; Climent, V.; Padron-Barthe, L.; Duro-Aguado, I.; Jimenez-Jaimez, J.; Hidalgo-Olivares, V. M.; Garcia-Campo, E.; Lanzillo, C.; Suarez-Mier, M. P.; Yonath, H.; Marcos-Alonso, S.; Ochoa, J. P.; Santome, J. L.; Garcia-Giustiniani, D.; Rodriguez-Garrido, J. L.; Dominguez, F.; Merlo, M.; Palomino, J.; Pena, M. L.; Trujillo, J. P.; Martin-Vila, A.; Stolfo, D.; Molina, P.; Lara-Pezzi, E.; Calvo-Iglesias, F. E.; Nof, E.; Calo, L.; Barriales-Villa, R.; Gimeno-Blanes, J. R.; Arad, M.; Garcia-Pavia, P.; Monserrat, L., Truncating FLNC Mutations Are Associated With High-Risk Dilated and Arrhythmogenic Cardiomyopathies. *J Am Coll Cardiol* **2016**, *68* (22), 2440-2451, DOI: 10.1016/j.jacc.2016.09.927
246. Brodehl, A.; Ferrier, R. A.; Hamilton, S. J.; Greenway, S. C.; Brundler, M. A.; Yu, W.; Gibson, W. T.; McKinnon, M. L.; McGillivray, B.; Alvarez, N.; Giuffre, M.; Schwartzenuber, J.; Consortium, F. C.; Gerull, B., Mutations in FLNC are Associated with Familial Restrictive Cardiomyopathy. *Hum Mutat* **2016**, *37* (3), 269-79, DOI: 10.1002/humu.22942
247. Begay, R. L.; Graw, S. L.; Sinagra, G.; Asimaki, A.; Rowland, T. J.; Slavov, D. B.; Gowan, K.; Jones, K. L.; Brun, F.; Merlo, M.; Miani, D.; Sweet, M.; Devaraj, K.; Wartchow, E. P.; Gigli, M.; Puggia, I.; Salcedo, E. E.; Garrity, D. M.; Ambardekar, A. V.; Buttrick, P.; Reece, T. B.; Bristow, M. R.; Saffitz, J. E.; Mestroni, L.; Taylor, M. R. G., Filamin C Truncation Mutations Are Associated With Arrhythmogenic Dilated Cardiomyopathy and Changes in the Cell-Cell Adhesion Structures. *JACC Clin Electrophysiol* **2018**, *4* (4), 504-514, DOI: 10.1016/j.jacep.2017.12.003
248. Yu, J.; Hu, J.; Dai, X.; Cao, Q.; Xiong, Q.; Liu, X.; Liu, X.; Shen, Y.; Chen, Q.; Hua, W.; Hong, K., SCN5A mutation in Chinese patients with arrhythmogenic right ventricular dysplasia. *Herz* **2014**, *39* (2), 271-5, DOI: 10.1007/s00059-013-3998-5
249. Ge, J.; Sun, A.; Paajanen, V.; Wang, S.; Su, C.; Yang, Z.; Li, Y.; Wang, S.; Jia, J.; Wang, K.; Zou, Y.; Gao, L.; Wang, K.; Fan, Z., Molecular and clinical characterization of a novel SCN5A mutation associated with atrioventricular block and dilated cardiomyopathy. *Circ Arrhythm Electrophysiol* **2008**, *1* (2), 83-92, DOI: 10.1161/CIRCEP.107.750752
250. Te Riele, A. S.; Agullo-Pascual, E.; James, C. A.; Leo-Macias, A.; Cerrone, M.; Zhang, M.; Lin, X.; Lin, B.; Sobreira, N. L.; Amat-Alarcon, N.; Marsman, R. F.; Murray, B.; Tichnell, C.; van der Heijden, J. F.; Dooijes, D.; van Veen, T. A.; Tandri, H.; Fowler, S. J.; Hauer, R. N.; Tomaselli, G.; van den Berg, M. P.; Taylor, M. R.; Brun, F.; Sinagra, G.; Wilde, A. A.; Mestroni, L.; Bezzina, C. R.; Calkins, H.; Peter van Tintelen, J.; Bu, L.; Delmar, M.; Judge, D. P., Multilevel analyses of SCN5A mutations in arrhythmogenic right ventricular dysplasia/cardiomyopathy suggest non-canonical mechanisms for disease pathogenesis. *Cardiovasc Res* **2017**, *113* (1), 102-111, DOI: 10.1093/cvr/cvw234
251. McNair, W. P.; Sinagra, G.; Taylor, M. R.; Di Lenarda, A.; Ferguson, D. A.; Salcedo, E. E.; Slavov, D.; Zhu, X.; Caldwell, J. H.; Mestroni, L.; Familial Cardiomyopathy Registry Research, G., SCN5A mutations associate with arrhythmic dilated cardiomyopathy and commonly localize to the voltage-sensing mechanism. *J Am Coll Cardiol* **2011**, *57* (21), 2160-8, DOI: 10.1016/j.jacc.2010.09.084

252. Erkapic, D.; Neumann, T.; Schmitt, J.; Sperzel, J.; Berkowitsch, A.; Kuniss, M.; Hamm, C. W.; Pitschner, H. F., Electrical storm in a patient with arrhythmogenic right ventricular cardiomyopathy and SCN5A mutation. *Europace* **2008**, *10* (7), 884-7, DOI: 10.1093/europace/eun065
253. Roberts, J. D., TJP1 Mutations in Arrhythmogenic Cardiomyopathy. *Circ Genom Precis Med* **2018**, *11* (10), e002337, DOI: 10.1161/CIRCGEN.118.002337
254. Turkowski, K. L.; Tester, D. J.; Bos, J. M.; Haugaa, K. H.; Ackerman, M. J., Whole exome sequencing with genomic triangulation implicates CDH2-encoded N-cadherin as a novel pathogenic substrate for arrhythmogenic cardiomyopathy. *Congenit Heart Dis* **2017**, *12* (2), 226-235, DOI: 10.1111/chd.12462
255. Mayosi, B. M.; Fish, M.; Shaboodien, G.; Mastantuono, E.; Kraus, S.; Wieland, T.; Kotta, M. C.; Chin, A.; Laing, N.; Ntusi, N. B.; Chong, M.; Horsfall, C.; Pimstone, S. N.; Gentilini, D.; Parati, G.; Strom, T. M.; Meitinger, T.; Pare, G.; Schwartz, P. J.; Crotti, L., Identification of Cadherin 2 (CDH2) Mutations in Arrhythmogenic Right Ventricular Cardiomyopathy. *Circ Cardiovasc Genet* **2017**, *10* (2), DOI: 10.1161/CIRCGENETICS.116.001605
256. Gessner, G.; Runge, S.; Koenen, M.; Heinemann, S. H.; Koenen, M.; Haas, J.; Meder, B.; Thomas, D.; Katus, H. A.; Schweizer, P. A., ANK2 functionally interacts with KCNH2 aggravating long QT syndrome in a double mutation carrier. *Biochem Biophys Res Commun* **2019**, *512* (4), 845-851, DOI: 10.1016/j.bbrc.2019.03.162
257. Cunha, S. R.; Hund, T. J.; Hashemi, S.; Voigt, N.; Li, N.; Wright, P.; Koval, O.; Li, J.; Gudmundsson, H.; Gumina, R. J.; Karck, M.; Schott, J. J.; Probst, V.; Le Marec, H.; Anderson, M. E.; Dobrev, D.; Wehrens, X. H.; Mohler, P. J., Defects in ankyrin-based membrane protein targeting pathways underlie atrial fibrillation. *Circulation* **2011**, *124* (11), 1212-22, DOI: 10.1161/CIRCULATIONAHA.111.023986
258. Le Scouarnec, S.; Bhasin, N.; Vieyres, C.; Hund, T. J.; Cunha, S. R.; Koval, O.; Marionneau, C.; Chen, B.; Wu, Y.; Demolombe, S.; Song, L. S.; Le Marec, H.; Probst, V.; Schott, J. J.; Anderson, M. E.; Mohler, P. J., Dysfunction in ankyrin-B-dependent ion channel and transporter targeting causes human sinus node disease. *Proc Natl Acad Sci U S A* **2008**, *105* (40), 15617-22, DOI: 10.1073/pnas.0805500105
259. Asano, Y.; Takashima, S.; Asakura, M.; Shintani, Y.; Liao, Y.; Minamino, T.; Asanuma, H.; Sanada, S.; Kim, J.; Ogai, A.; Fukushima, T.; Oikawa, Y.; Okazaki, Y.; Kaneda, Y.; Sato, M.; Miyazaki, J.; Kitamura, S.; Tomoike, H.; Kitakaze, M.; Hori, M., Lamr1 functional retroposon causes right ventricular dysplasia in mice. *Nat Genet* **2004**, *36* (2), 123-30, DOI: 10.1038/ng1294
260. Asimaki, A.; Kapoor, S.; Plovie, E.; Arndt, A. K.; Adams, E.; Liu, Z.; James, C. A.; Judge, D. P.; Calkins, H.; Churko, J., Identification of a new modulator of the intercalated disc in a zebrafish model of arrhythmogenic cardiomyopathy. *Science translational medicine* **2014**, *6* (240), 240ra74-240ra74,
261. Basso, C.; Fox, P. R.; Meurs, K. M.; Towbin, J. A.; Spier, A. W.; Calabrese, F.; Maron, B. J.; Thiene, G., Arrhythmogenic right ventricular cardiomyopathy causing sudden cardiac death in boxer dogs: a new animal model of human disease. *Circulation* **2004**, *109* (9), 1180-5, DOI: 10.1161/01.CIR.0000118494.07530.65

262. Fox, P. R.; Maron, B. J.; Basso, C.; Liu, S. K.; Thiene, G., Spontaneously occurring arrhythmogenic right ventricular cardiomyopathy in the domestic cat: A new animal model similar to the human disease. *Circulation* **2000**, *102* (15), 1863-70, DOI: 10.1161/01.cir.102.15.1863
263. Sommariva, E.; Stadiotti, I.; Perrucci, G. L.; Tondo, C.; Pompilio, G., Cell models of arrhythmogenic cardiomyopathy: advances and opportunities. *Dis Model Mech* **2017**, *10* (7), 823-835, DOI: 10.1242/dmm.029363
264. Wlodarska, E. K.; Konka, M.; Zaleska, T.; Ploski, R.; Cedro, K.; Pucilowska, B.; Bekiesinska-Figatowska, M.; Rydlewska-Sadowska, W.; Ruzylo, W.; Hoffman, P., Arrhythmogenic right ventricular cardiomyopathy in two pairs of monozygotic twins. *Int J Cardiol* **2005**, *105* (2), 126-33, DOI: 10.1016/j.ijcard.2004.11.016
265. Furlanello, F.; Bertoldi, A.; Dallago, M.; Furlanello, C.; Fernando, F.; Inama, G.; Pappone, C.; Chierchia, S., Cardiac arrest and sudden death in competitive athletes with arrhythmogenic right ventricular dysplasia. *Pacing Clin Electrophysiol* **1998**, *21* (1 Pt 2), 331-5, DOI: 10.1111/j.1540-8159.1998.tb01116.x
266. Gemayel, C.; Pelliccia, A.; Thompson, P. D., Arrhythmogenic right ventricular cardiomyopathy. *J Am Coll Cardiol* **2001**, *38* (7), 1773-81, DOI: 10.1016/s0735-1097(01)01654-0
267. Saberniak, J.; Hasselberg, N. E.; Borgquist, R.; Platonov, P. G.; Sarvari, S. I.; Smith, H. J.; Ribe, M.; Holst, A. G.; Edvardsen, T.; Haugaa, K. H., Vigorous physical activity impairs myocardial function in patients with arrhythmogenic right ventricular cardiomyopathy and in mutation positive family members. *Eur J Heart Fail* **2014**, *16* (12), 1337-44, DOI: 10.1002/ejhf.181
268. Austin, K. M.; Trembley, M. A.; Chandler, S. F.; Sanders, S. P.; Saffitz, J. E.; Abrams, D. J.; Pu, W. T., Molecular mechanisms of arrhythmogenic cardiomyopathy. *Nat Rev Cardiol* **2019**, *16* (9), 519-537, DOI: 10.1038/s41569-019-0200-7
269. Huang, H.; Asimaki, A.; Lo, D.; McKenna, W.; Saffitz, J., Disparate effects of different mutations in plakoglobin on cell mechanical behavior. *Cell Motil Cytoskeleton* **2008**, *65* (12), 964-78, DOI: 10.1002/cm.20319
270. Schlipp, A.; Schinner, C.; Spindler, V.; Vielmuth, F.; Gehmlich, K.; Syrris, P.; McKenna, W. J.; Dendorfer, A.; Hartlieb, E.; Waschke, J., Desmoglein-2 interaction is crucial for cardiomyocyte cohesion and function. *Cardiovasc Res* **2014**, *104* (2), 245-57, DOI: 10.1093/cvr/cvu206
271. James, C. A.; Bhonsale, A.; Tichnell, C.; Murray, B.; Russell, S. D.; Tandri, H.; Tedford, R. J.; Judge, D. P.; Calkins, H., Exercise increases age-related penetrance and arrhythmic risk in arrhythmogenic right ventricular dysplasia/cardiomyopathy-associated desmosomal mutation carriers. *J Am Coll Cardiol* **2013**, *62* (14), 1290-1297, DOI: 10.1016/j.jacc.2013.06.033
272. Finocchiaro, G.; Papadakis, M.; Robertus, J. L.; Dhutia, H.; Steriotis, A. K.; Tome, M.; Mellor, G.; Merghani, A.; Malhotra, A.; Behr, E.; Sharma, S.; Sheppard, M. N., Etiology of Sudden Death in Sports: Insights From a United Kingdom Regional Registry. *J Am Coll Cardiol* **2016**, *67* (18), 2108-2115, DOI: 10.1016/j.jacc.2016.02.062
273. Kirchhof, P.; Fabritz, L.; Zwiener, M.; Witt, H.; Schafers, M.; Zellerhoff, S.; Paul, M.; Athai, T.; Hiller, K. H.; Baba, H. A.; Breithardt, G.; Ruiz, P.; Wichter, T.; Levkau,

- B., Age- and training-dependent development of arrhythmogenic right ventricular cardiomyopathy in heterozygous plakoglobin-deficient mice. *Circulation* **2006**, *114* (17), 1799-806, DOI: 10.1161/CIRCULATIONAHA.106.624502
274. Mitchell, J. H.; Haskell, W.; Snell, P.; Van Camp, S. P., Task Force 8: classification of sports. *J Am Coll Cardiol* **2005**, *45* (8), 1364-7, DOI: 10.1016/j.jacc.2005.02.015
275. Taggart, P.; Boyett, M. R.; Logantha, S.; Lambiase, P. D., Anger, emotion, and arrhythmias: from brain to heart. *Front Physiol* **2011**, *2*, 67, DOI: 10.3389/fphys.2011.00067
276. Cox, M. G.; van der Zwaag, P. A.; van der Werf, C.; van der Smagt, J. J.; Noorman, M.; Bhuiyan, Z. A.; Wiesfeld, A. C.; Volders, P. G.; van Langen, I. M.; Atsma, D. E., Arrhythmogenic right ventricular dysplasia/cardiomyopathy: pathogenic desmosome mutations in index-patients predict outcome of family screening: Dutch arrhythmogenic right ventricular dysplasia/cardiomyopathy genotype-phenotype follow-up study. *Circulation* **2011**, *123* (23), 2690-2700,
277. Basso, C.; Corrado, D.; Bauce, B.; Thiene, G., Arrhythmogenic right ventricular cardiomyopathy. *Circ Arrhythm Electrophysiol* **2012**, *5* (6), 1233-46, DOI: 10.1161/CIRCEP.111.962035
278. Corrado, D.; Link, M. S.; Calkins, H., Arrhythmogenic Right Ventricular Cardiomyopathy. *N Engl J Med* **2017**, *376* (15), 1489-90, DOI: 10.1056/NEJMc1701400
279. Thiene, G.; Nava, A.; Corrado, D.; Rossi, L.; Pennelli, N., Right ventricular cardiomyopathy and sudden death in young people. *New England Journal of Medicine* **1988**, *318* (3), 129-133,
280. Corrado, D.; van Tintelen, P. J.; McKenna, W. J.; Hauer, R. N.; Anastakis, A.; Asimaki, A.; Basso, C.; Bauce, B.; Brunckhorst, C.; Bucciarelli-Ducci, C., Arrhythmogenic right ventricular cardiomyopathy: evaluation of the current diagnostic criteria and differential diagnosis. *Eur. Heart J.* **2020**, *41* (14), 1414-1429,
281. Haugaa, K. H.; Basso, C.; Badano, L. P.; Bucciarelli-Ducci, C.; Cardim, N.; Gaemperli, O.; Galderisi, M.; Habib, G.; Knuuti, J.; Lancellotti, P., Comprehensive multi-modality imaging approach in arrhythmogenic cardiomyopathy—an expert consensus document of the European Association of Cardiovascular Imaging. *European Heart Journal-Cardiovascular Imaging* **2017**, *18* (3), 237-253,
282. Towbin, J. A.; McKenna, W. J.; Abrams, D. J.; Ackerman, M. J.; Calkins, H.; Darrieux, F. C. C.; Daubert, J. P.; de Chillou, C.; DePasquale, E. C.; Desai, M. Y.; Estes, N. A. M.; Hua, W.; Indik, J. H.; Ingles, J.; James, C. A.; John, R. M.; Judge, D. P.; Keegan, R.; Krahn, A. D.; Link, M. S.; Marcus, F. I.; McLeod, C. J.; Mestroni, L.; Priori, S. G.; Saffitz, J. E.; Sanatani, S.; Shimizu, W.; van Tintelen, J. P.; Wilde, A. A. M.; Zareba, W., 2019 HRS expert consensus statement on evaluation, risk stratification, and management of arrhythmogenic cardiomyopathy. *Heart Rhythm* **2019**, *16* (11), E301-+, DOI: 10.1016/j.hrthm.2019.05.007
283. McNally, E.; MacLeod, H.; Dellefave-Castillo, L., Arrhythmogenic right ventricular cardiomyopathy. In *GeneReviews®*, University of Washington, Seattle: 2017,
284. Cadrin-Tourigny, J.; Bosman, L. P.; Nozza, A.; Wang, W. J.; Tadros, R.; Bhonsale, A.; Bourfiss, M.; Fortier, A.; Lie, O. H.; Saguner, A. M.; Svensson, A.;

- Andorin, A.; Tichnell, C.; Murray, B.; Zeppenfeld, K.; van den Berg, M. P.; Asselbergs, F. W.; Wilde, A. A. M.; Krahn, A. D.; Talajic, M.; Rivard, L.; Chelko, S.; Zimmerman, S. L.; Kamel, I. R.; Crosson, J. E.; Judge, D. P.; Yap, S. C.; van der Heijden, J. F.; Tandri, H.; Jongbloed, J. D. H.; Guertin, M. C.; van Tintelen, J. P.; Platonov, P. G.; Duru, F.; Haugaa, K. H.; Khairy, P.; Hauer, R. N. W.; Calkins, H.; te Riele, A.; James, C. A., A new prediction model for ventricular arrhythmias in arrhythmogenic right ventricular cardiomyopathy. *Eur. Heart J.* **2019**, *40* (23), 1850-1858, DOI: 10.1093/eurheartj/ehz103
285. Orgeron, G. M.; Te Riele, A.; Tichnell, C.; Wang, W.; Murray, B.; Bhonsale, A.; Judge, D. P.; Kamel, I. R.; Zimmerman, S. L.; Tandri, H., Performance of the 2015 International Task Force Consensus Statement risk stratification algorithm for implantable cardioverter-defibrillator placement in arrhythmogenic right ventricular dysplasia/cardiomyopathy. *Circulation: Arrhythmia and Electrophysiology* **2018**, *11* (2), e005593,
286. Sagawa, Y.; Nagata, Y.; Yamaguchi, T.; Mitsui, K.; Nagamine, T.; Yamaguchi, J.; Hijikata, S.; Watanabe, K.; Masuda, R.; Miyazaki, R.; Kaneko, M.; Miwa, N.; Sekigawa, M.; Hara, N.; Nozato, T.; Ashikaga, T.; Goya, M.; Sasano, T.; Hirao, K., Long-Term Performance of Right Ventricular Implantable Cardioverter-Defibrillator Leads in Arrhythmogenic Right Ventricular Cardiomyopathy and Hypertrophic Cardiomyopathy. *Int. Heart J.* **2020**, *61* (1), 39-45, DOI: 10.1536/ihj.19-279
287. Wang, W.; Orgeron, G.; Tichnell, C.; Murray, B.; Crosson, J.; Monfredi, O.; Cadrin-Tourigny, J.; Tandri, H.; Calkins, H.; James, C. A., Impact of exercise restriction on arrhythmic risk among patients with arrhythmogenic right ventricular cardiomyopathy. *Journal of the American Heart Association* **2018**, *7* (12), e008843,
288. Corrado, D.; Leoni, L.; Link, M. S.; Bella, P. D.; Gaita, F.; Curnis, A.; Salerno, J. U.; Igidbashian, D.; Raviele, A.; Disertori, M., Implantable cardioverter-defibrillator therapy for prevention of sudden death in patients with arrhythmogenic right ventricular cardiomyopathy/dysplasia. *Circulation* **2003**, *108* (25), 3084-3091,
289. Hodgkinson, K. A.; Howes, A. J.; Boland, P.; Shen, X. S.; Stuckless, S.; Young, T. L.; Curtis, F.; Collier, A.; Parfrey, P. S.; Connors, S. P., Long-Term Clinical Outcome of Arrhythmogenic Right Ventricular Cardiomyopathy in Individuals With a p.S358L Mutation in TMEM43 Following Implantable Cardioverter Defibrillator Therapy. *Circ.-Arrhythmia Electrophysiol.* **2016**, *9* (3), 9, DOI: 10.1161/circep.115.003589
290. Ermakov, S.; Gerstenfeld, E. P.; Svetlichnaya, Y.; Scheinman, M. M., Use of flecainide in combination antiarrhythmic therapy in patients with arrhythmogenic right ventricular cardiomyopathy. *Heart Rhythm* **2017**, *14* (4), 564-569, DOI: 10.1016/j.hrthm.2016.12.010
291. Echt, D. S.; Liebson, P. R.; Mitchell, L. B.; Peters, R. W.; Obias-Manno, D.; Barker, A. H.; Arensberg, D.; Baker, A.; Friedman, L.; Greene, H. L., Mortality and morbidity in patients receiving encainide, flecainide, or placebo: the Cardiac Arrhythmia Suppression Trial. *New England journal of medicine* **1991**, *324* (12), 781-788,
292. Zareba, W., Clinical Trial: Pilot Randomized Trial With Flecainide in ARVC Patients, NCT03685149, currently ongoing (unpublished). University of Rochester 2018, Estimated completion August 2021. URL: <https://clinicaltrials.gov/ct2/show/NCT03685149#contacts>

293. Mahida, S.; Venlet, J.; Saguner, A. M.; Kumar, S.; Baldinger, S. H.; AbdelWahab, A.; Tedrow, U. B.; Castelletti, S.; Pantazis, A.; John, R. M.; McKenna, W. J.; Lambiase, P. D.; Duru, F.; Sapp, J. L.; Zeppenfeld, K.; Stevenson, W. G., Ablation compared with drug therapy for recurrent ventricular tachycardia in arrhythmogenic right ventricular cardiomyopathy: Results from a multicenter study. *Heart Rhythm* **2019**, *16* (4), 536-543, DOI: 10.1016/j.hrthm.2018.10.016
294. Santangeli, P.; Zado, E. S.; Supple, G. E.; Haqqani, H. M.; Garcia, F. C.; Tschabrunn, C. M.; Callans, D. J.; Lin, D.; Dixit, S.; Hutchinson, M. D.; Riley, M. P.; Marchlinski, F. E., Long-Term Outcome With Catheter Ablation of Ventricular Tachycardia in Patients With Arrhythmogenic Right Ventricular Cardiomyopathy. *Circ.-Arrhythmia Electrophysiol.* **2015**, *8* (6), 1413-1421, DOI: 10.1161/circep.115.003562
295. Christiansen, M. K.; Haugaa, K. H.; Svensson, A.; Gilljam, T.; Madsen, T.; Hansen, J.; Holst, A. G.; Bundgaard, H.; Edvardsen, T.; Svendsen, J. H., Incidence, Predictors, and Success of Ventricular Tachycardia Catheter Ablation in Arrhythmogenic Right Ventricular Cardiomyopathy (from the Nordic ARVC Registry). *The American Journal of Cardiology* **2020**, *125* (5), 803-811,
296. Bourke, T.; Vaseghi, M.; Michowitz, Y.; Sankhla, V.; Shah, M.; Swapna, N.; Boyle, N. G.; Mahajan, A.; Narasimhan, C.; Lokhandwala, Y.; Shivkumar, K., Neuraxial Modulation for Refractory Ventricular Arrhythmias Value of Thoracic Epidural Anesthesia and Surgical Left Cardiac Sympathetic Denervation. *Circulation* **2010**, *121* (21), 2255-2262, DOI: 10.1161/circulationaha.109.929703
297. te Riele, A.; Ajijola, O. A.; Shivkumar, K.; Tandri, H., Role of Bilateral Sympathectomy in the Treatment of Refractory Ventricular Arrhythmias in Arrhythmogenic Right Ventricular Dysplasia/Cardiomyopathy. *Circ.-Arrhythmia Electrophysiol.* **2016**, *9* (4), 5, DOI: 10.1161/circep.115.003713
298. Assis, F. R.; Krishnan, A.; Zhou, X.; James, C. A.; Murray, B.; Tichnell, C.; Berger, R.; Calkins, H.; Tandri, H.; Mandal, K., Cardiac sympathectomy for refractory ventricular tachycardia in arrhythmogenic right ventricular cardiomyopathy. *Heart Rhythm* **2019**, *16* (7), 1003-1010, DOI: 10.1016/j.hrthm.2019.01.019
299. Ajijola, O. A.; Lellouche, N.; Bourke, T.; Tung, R.; Ahn, S.; Mahajan, A.; Shivkumar, K., Bilateral cardiac sympathetic denervation for the management of electrical storm. *Journal of the American College of Cardiology* **2012**, *59* (1), 91-92,
300. Vaseghi, M.; Gima, J.; Kanaan, C.; Ajijola, O. A.; Marmureanu, A.; Mahajan, A.; Shivkumar, K., Cardiac sympathetic denervation in patients with refractory ventricular arrhythmias or electrical storm: Intermediate and long-term follow-up. *Heart Rhythm* **2014**, *11* (3), 360-366, DOI: 10.1016/j.hrthm.2013.11.028
301. Vaseghi, M.; Barwad, P.; Corrales, F. J. M.; Tandri, H.; Mathuria, N.; Shah, R.; Sorg, J. M.; Gima, J.; Mandal, K.; Morales, L. C. S., Cardiac sympathetic denervation for refractory ventricular arrhythmias. *Journal of the American College of Cardiology* **2017**, *69* (25), 3070-3080,
302. Kumar, S.; Tedrow, U. B.; Stevenson, W. G., Adjunctive interventional techniques when percutaneous catheter ablation for drug refractory ventricular arrhythmias fail: a contemporary review. *Circulation: Arrhythmia and Electrophysiology* **2017**, *10* (2), e003676,

303. Saffitz, J. E., Molecular mechanisms in the pathogenesis of arrhythmogenic cardiomyopathy. *Cardiovasc. Pathol.* **2017**, *28*, 51-58, DOI: 10.1016/j.carpath.2017.02.005
304. Coghlan, M. P.; Culbert, A. A.; Cross, D. A.; Corcoran, S. L.; Yates, J. W.; Pearce, N. J.; Rausch, O. L.; Murphy, G. J.; Carter, P. S.; Cox, L. R., Selective small molecule inhibitors of glycogen synthase kinase-3 modulate glycogen metabolism and gene transcription. *Chemistry & biology* **2000**, *7* (10), 793-803,
305. Yue, Y. P.; Binalsheikh, I. M.; Leach, S. B.; Domeier, T. L.; Duan, D. S., Prospect of gene therapy for cardiomyopathy in hereditary muscular dystrophy. *Exp. Opin. Orphan Drugs* **2016**, *4* (2), 169-183, DOI: 10.1517/21678707.2016.1124039
306. Peña, J. R.; Szkudlarek, A. C.; Warren, C. M.; Heinrich, L. S.; Gaffin, R. D.; Jagatheesan, G.; del Monte, F.; Hajjar, R. J.; Goldspink, P. H.; Solaro, R. J., Neonatal gene transfer of Serca2a delays onset of hypertrophic remodeling and improves function in familial hypertrophic cardiomyopathy. *Journal of molecular and cellular cardiology* **2010**, *49* (6), 993-1002,
307. Goff, Z. D.; Calkins, H., Sudden death related cardiomyopathies - Arrhythmogenic right ventricular cardiomyopathy, arrhythmogenic cardiomyopathy, and exercise-induced cardiomyopathy. *Prog Cardiovasc Dis* **2019**, *62* (3), 217-226, DOI: 10.1016/j.pcad.2019.04.002
308. Pilichou, K.; Bezzina, C. R.; Thiene, G.; Basso, C., Arrhythmogenic cardiomyopathy: transgenic animal models provide novel insights into disease pathobiology. *Circ Cardiovasc Genet* **2011**, *4* (3), 318-26, DOI: 10.1161/CIRCGENETICS.110.959031
309. Lubbers, E. R.; Murphy, N. P.; Musa, H.; Huang, C. Y.; Gupta, R.; Price, M. V.; Han, M.; Daoud, E.; Gratz, D.; El Refaey, M.; Xu, X.; Hoeflinger, N. K.; Friel, E. L.; Lancione, P.; Wallace, M. J.; Cavus, O.; Simmons, S. L.; Williams, J. L.; Skaf, M.; Koenig, S. N.; Janssen, P. M. L.; Rasband, M. N.; Hund, T. J.; Mohler, P. J., Defining new mechanistic roles for alphaII spectrin in cardiac function. *J Biol Chem* **2019**, *294* (24), 9576-9591, DOI: 10.1074/jbc.RA119.007714
310. Mitchell, G. F.; Jeron, A.; Koren, G., Measurement of heart rate and Q-T interval in the conscious mouse. *Am J Physiol* **1998**, *274* (3), H747-51, DOI: 10.1152/ajpheart.1998.274.3.H747
311. Albrecht, A.; Porthun, J.; Eucker, J.; Coats, A. J. S.; von Haehling, S.; Pezzutto, A.; Karakas, M.; Riess, H.; Keller, U.; Landmesser, U.; Haverkamp, W.; Anker, S. D.; Anker, M. S., Spontaneous Non-Sustained Ventricular Tachycardia and Premature Ventricular Contractions and Their Prognostic Relevance in Patients with Cancer in Routine Care. *Cancers (Basel)* **2021**, *13* (10), DOI: 10.3390/cancers13102303
312. Alvarado, F. J.; Bos, J. M.; Yuchi, Z.; Valdivia, C. R.; Hernandez, J. J.; Zhao, Y. T.; Henderlong, D. S.; Chen, Y.; Booher, T. R.; Marcou, C. A.; Van Petegem, F.; Ackerman, M. J.; Valdivia, H. H., Cardiac hypertrophy and arrhythmia in mice induced by a mutation in ryanodine receptor 2. *JCI Insight* **2019**, *5*, DOI: 10.1172/jci.insight.126544
313. Mohler, P. J.; Schott, J.-J.; Gramolini, A. O.; Dilly, K. W.; Guatimosim, S.; Song, L.-S.; Haurogné, K.; Kyndt, F.; Ali, M. E.; Rogers, T. B., Ankyrin-B mutation causes

- type 4 long-QT cardiac arrhythmia and sudden cardiac death. *Nature* **2003**, *421* (6923), 634-639,
314. Hund, T. J.; Wright, P. J.; Dun, W.; Snyder, J. S.; Boyden, P. A.; Mohler, P. J., Regulation of the ankyrin-B-based targeting pathway following myocardial infarction. *Cardiovasc Res* **2009**, *81* (4), 742-9, DOI: 10.1093/cvr/cvn348
315. Gratz, D.; Winkle, A. J.; Dalic, A.; Unudurthi, S. D.; Hund, T. J., Computational tools for automated histological image analysis and quantification in cardiac tissue. *MethodsX* **2020**, *7*, 22-34, DOI: 10.1016/j.mex.2019.11.028
316. El Refaey, M.; Musa, H.; Murphy, N. P.; Lubbers, E. R.; Skaf, M.; Han, M.; Cavus, O.; Koenig, S. N.; Wallace, M. J.; Gratz, D.; Bradley, E.; Alsina, K. M.; Wehrens, X. H. T.; Hund, T. J.; Mohler, P. J., Protein Phosphatase 2A Regulates Cardiac Na(+) Channels. *Circ Res* **2019**, *124* (5), 737-746, DOI: 10.1161/CIRCRESAHA.118.314350
317. Aro, A. L.; Anttonen, O.; Tikkanen, J. T.; Junttila, M. J.; Kerola, T.; Rissanen, H. A.; Reunanen, A.; Huikuri, H. V., Prevalence and prognostic significance of T-wave inversions in right precordial leads of a 12-lead electrocardiogram in the middle-aged subjects. *Circulation* **2012**, *125* (21), 2572-7, DOI: 10.1161/CIRCULATIONAHA.112.098681
318. Morin, D. P.; Mauer, A. C.; Gear, K.; Zareba, W.; Markowitz, S. M.; Marcus, F. I.; Lerman, B. B., Usefulness of precordial T-wave inversion to distinguish arrhythmogenic right ventricular cardiomyopathy from idiopathic ventricular tachycardia arising from the right ventricular outflow tract. *Am J Cardiol* **2010**, *105* (12), 1821-4, DOI: 10.1016/j.amjcard.2010.01.365
319. Chen, X.; Chen, L.; Chen, Z.; Chen, X.; Song, J., Remodelling of myocardial intercalated disc protein connexin 43 causes increased susceptibility to malignant arrhythmias in ARVC/D patients. *Forensic Sci Int* **2017**, *275*, 14-22, DOI: 10.1016/j.forsciint.2017.02.020
320. Oxford, E. M.; Pariaut, R.; Tursi, M.; Fox, P. R.; Santilli, R. A., Immunofluorescent Localization of Plakoglobin Is Altered in Endomyocardial Biopsy Samples from Dogs with Clinically Relevant Arrhythmogenic Right Ventricular Cardiomyopathy (ARVC). *Vet Sci* **2021**, *8* (11), DOI: 10.3390/vetsci8110248
321. Wang, Y.; Li, C.; Shi, L.; Chen, X.; Cui, C.; Huang, J.; Chen, B.; Hall, D. D.; Pan, Z.; Lu, M.; Hong, J.; Song, L. S.; Zhao, S., Integrin beta1D Deficiency-Mediated RyR2 Dysfunction Contributes to Catecholamine-Sensitive Ventricular Tachycardia in Arrhythmogenic Right Ventricular Cardiomyopathy. *Circulation* **2020**, *141* (18), 1477-1493, DOI: 10.1161/CIRCULATIONAHA.119.043504
322. Steger, A.; Sinnecker, D.; Berkefeld, A.; Muller, A.; Gebhardt, J.; Dommasch, M.; Huster, K. M.; Barthel, P.; Schmidt, G., [Fragmented QRS. Relevance in clinical practice]. *Herzschrittmacherther Elektrophysiol* **2015**, *26* (3), 235-41, DOI: 10.1007/s00399-015-0390-6
323. Peters, S.; Trummel, M.; Koehler, B., QRS fragmentation in standard ECG as a diagnostic marker of arrhythmogenic right ventricular dysplasia-cardiomyopathy. *Heart Rhythm* **2008**, *5* (10), 1417-21, DOI: 10.1016/j.hrthm.2008.07.012
324. Haraoka, K.; Morita, H.; Saito, Y.; Toh, N.; Miyoshi, T.; Nishii, N.; Nagase, S.; Nakamura, K.; Kohno, K.; Kusano, K. F.; Kawaguchi, K.; Ohe, T.; Ito, H., Fragmented

- QRS is associated with torsades de pointes in patients with acquired long QT syndrome. *Heart Rhythm* **2010**, *7* (12), 1808-14, DOI: 10.1016/j.hrthm.2010.09.008
325. Green, K. J.; Jaiganesh, A.; Broussard, J. A., Desmosomes: Essential contributors to an integrated intercellular junction network. *F1000Res* **2019**, *8*, DOI: 10.12688/f1000research.20942.1
326. Tsao, C. W.; Aday, A. W.; Almarzooq, Z. I.; Alonso, A.; Beaton, A. Z.; Bittencourt, M. S.; Boehme, A. K.; Buxton, A. E.; Carson, A. P.; Commodore-Mensah, Y.; Elkind, M. S. V.; Evenson, K. R.; Eze-Nliam, C.; Ferguson, J. F.; Generoso, G.; Ho, J. E.; Kalani, R.; Khan, S. S.; Kissela, B. M.; Knutson, K. L.; Levine, D. A.; Lewis, T. T.; Liu, J.; Loop, M. S.; Ma, J.; Mussolino, M. E.; Navaneethan, S. D.; Perak, A. M.; Poudel, R.; Rezk-Hanna, M.; Roth, G. A.; Schroeder, E. B.; Shah, S. H.; Thacker, E. L.; VanWagner, L. B.; Virani, S. S.; Voecks, J. H.; Wang, N. Y.; Yaffe, K.; Martin, S. S., Heart Disease and Stroke Statistics-2022 Update: A Report From the American Heart Association. *Circulation* **2022**, *145* (8), e153-e639, DOI: 10.1161/CIR.0000000000001052
327. Taneike, M.; Mizote, I.; Morita, T.; Watanabe, T.; Hikoso, S.; Yamaguchi, O.; Takeda, T.; Oka, T.; Tamai, T.; Oyabu, J.; Murakawa, T.; Nakayama, H.; Nishida, K.; Takeda, J.; Mochizuki, N.; Komuro, I.; Otsu, K., Calpain protects the heart from hemodynamic stress. *J Biol Chem* **2011**, *286* (37), 32170-7, DOI: 10.1074/jbc.M111.248088
328. Raynaud, F.; Marcilhac, A.; Chebli, K.; Benyamin, Y.; Rossel, M., Calpain 2 expression pattern and sub-cellular localization during mouse embryogenesis. *Int J Dev Biol* **2008**, *52* (4), 383-8, DOI: 10.1387/ijdb.072448fr
329. Vainzof, M.; de Paula, F.; Tsanaclis, A. M.; Zatz, M., The effect of calpain 3 deficiency on the pattern of muscle degeneration in the earliest stages of LGMD2A. *J Clin Pathol* **2003**, *56* (8), 624-6, DOI: 10.1136/jcp.56.8.624
330. James, C. A.; Calkins, H., Arrhythmogenic Right Ventricular Cardiomyopathy: Progress Toward Personalized Management. *Annu Rev Med* **2019**, *70*, 1-18, DOI: 10.1146/annurev-med-041217-010932
331. Manring, H. R.; Dorn, L. E.; Ex-Willey, A.; Accornero, F.; Ackermann, M. A., At the heart of inter- and intracellular signaling: the intercalated disc. *Biophys Rev* **2018**, *10* (4), 961-971, DOI: 10.1007/s12551-018-0430-7
332. Beffagna, G.; Sommariva, E.; Bellin, M., Mechanotransduction and Adrenergic Stimulation in Arrhythmogenic Cardiomyopathy: An Overview of in vitro and in vivo Models. *Front Physiol* **2020**, *11*, 568535, DOI: 10.3389/fphys.2020.568535
333. Xu, Z.; Zhu, W.; Wang, C.; Huang, L.; Zhou, Q.; Hu, J.; Cheng, X.; Hong, K., Genotype-phenotype relationship in patients with arrhythmogenic right ventricular cardiomyopathy caused by desmosomal gene mutations: A systematic review and meta-analysis. *Sci Rep* **2017**, *7*, 41387, DOI: 10.1038/srep41387
334. Hamada, Y.; Yamamoto, T.; Nakamura, Y.; Sufu-Shimizu, Y.; Nanno, T.; Fukuda, M.; Ono, M.; Oda, T.; Okuda, S.; Ueyama, T.; Kobayashi, S.; Yano, M., G790del mutation in DSC2 alone is insufficient to develop the pathogenesis of ARVC in a mouse model. *Biochem Biophys Res Commun* **2020**, *21*, 100711, DOI: 10.1016/j.bbrep.2019.100711

335. Yang, Q.; Osinska, H.; Klevitsky, R.; Robbins, J., Phenotypic deficits in mice expressing a myosin binding protein C lacking the titin and myosin binding domains. *J Mol Cell Cardiol* **2001**, *33* (9), 1649-58, DOI: 10.1006/jmcc.2001.1417
336. Calore, M.; Lorenzon, A.; Vitiello, L.; Poloni, G.; Khan, M. A. F.; Beffagna, G.; Dazzo, E.; Sacchetto, C.; Polishchuk, R.; Sabatelli, P.; Doliana, R.; Carnevale, D.; Lembo, G.; Bonaldo, P.; De Windt, L.; Braghetta, P.; Rampazzo, A., A novel murine model for arrhythmogenic cardiomyopathy points to a pathogenic role of Wnt signalling and miRNA dysregulation. *Cardiovasc Res* **2019**, *115* (4), 739-751, DOI: 10.1093/cvr/cvy253
337. Wang, W.; Orgeron, G.; Tichnell, C.; Murray, B.; Crosson, J.; Monfredi, O.; Cadrin-Tourigny, J.; Tandri, H.; Calkins, H.; James, C. A., Impact of Exercise Restriction on Arrhythmic Risk Among Patients With Arrhythmogenic Right Ventricular Cardiomyopathy. *J Am Heart Assoc* **2018**, *7* (12), DOI: 10.1161/JAHA.118.008843
338. Poole, D. C.; Copp, S. W.; Colburn, T. D.; Craig, J. C.; Allen, D. L.; Sturek, M.; O'Leary, D. S.; Zucker, I. H.; Musch, T. I., Guidelines for animal exercise and training protocols for cardiovascular studies. *Am J Physiol Heart Circ Physiol* **2020**, *318* (5), H1100-H1138, DOI: 10.1152/ajpheart.00697.2019
339. Lampert, R.; Burg, M. M.; Jamner, L. D.; Dziura, J.; Brandt, C.; Li, F.; Donovan, T.; Soufer, R., Effect of beta-blockers on triggering of symptomatic atrial fibrillation by anger or stress. *Heart Rhythm* **2019**, *16* (8), 1167-1173, DOI: 10.1016/j.hrthm.2019.03.004
340. Abriel, H.; Rougier, J. S., beta-blockers in congenital short-QT syndrome as ion channel blockers. *J Cardiovasc Electrophysiol* **2013**, *24* (10), 1172-4, DOI: 10.1111/jce.12204
341. Marcus, G. M.; Glidden, D. V.; Polonsky, B.; Zareba, W.; Smith, L. M.; Cannom, D. S.; Estes, N. A. M.; Marcus, F.; Scheinman, M. M.; Multidisciplinary Study Right, V., Efficacy of Antiarrhythmic Drugs in Arrhythmogenic Right Ventricular Cardiomyopathy A Report From the North American ARVC Registry. *Journal of the American College of Cardiology* **2009**, *54* (7), 609-615, DOI: 10.1016/j.jacc.2009.04.052
342. Milani-Nejad, N.; Janssen, P. M., Small and large animal models in cardiac contraction research: advantages and disadvantages. *Pharmacol Ther* **2014**, *141* (3), 235-49, DOI: 10.1016/j.pharmthera.2013.10.007
343. Flamm, S. D.; Taki, J.; Moore, R.; Lewis, S. F.; Keech, F.; Maltais, F.; Ahmad, M.; Callahan, R.; Dragotakes, S.; Alpert, N.; et al., Redistribution of regional and organ blood volume and effect on cardiac function in relation to upright exercise intensity in healthy human subjects. *Circulation* **1990**, *81* (5), 1550-9, DOI: 10.1161/01.cir.81.5.1550
344. Stratton, J. R.; Levy, W. C.; Cerqueira, M. D.; Schwartz, R. S.; Abrass, I. B., Cardiovascular responses to exercise. Effects of aging and exercise training in healthy men. *Circulation* **1994**, *89* (4), 1648-55, DOI: 10.1161/01.cir.89.4.1648
345. Desai, K. H.; Sato, R.; Schauble, E.; Barsh, G. S.; Kobilka, B. K.; Bernstein, D., Cardiovascular indexes in the mouse at rest and with exercise: new tools to study models of cardiac disease. *Am J Physiol* **1997**, *272* (2 Pt 2), H1053-61, DOI: 10.1152/ajpheart.1997.272.2.H1053

346. Lujan, H. L.; Janbaih, H.; Feng, H. Z.; Jin, J. P.; DiCarlo, S. E., Ventricular function during exercise in mice and rats. *Am J Physiol Regul Integr Comp Physiol* **2012**, *302* (1), R68-74, DOI: 10.1152/ajpregu.00340.2011
347. Glukhov, A. V.; Flagg, T. P.; Fedorov, V. V.; Efimov, I. R.; Nichols, C. G., Differential K(ATP) channel pharmacology in intact mouse heart. *J Mol Cell Cardiol* **2010**, *48* (1), 152-60, DOI: 10.1016/j.yjmcc.2009.08.026
348. Fedorov, V. V.; Glukhov, A. V.; Ambrosi, C. M.; Kostecki, G.; Chang, R.; Janks, D.; Schuessler, R. B.; Moazami, N.; Nichols, C. G.; Efimov, I. R., Effects of KATP channel openers diazoxide and pinacidil in coronary-perfused atria and ventricles from failing and non-failing human hearts. *J Mol Cell Cardiol* **2011**, *51* (2), 215-25, DOI: 10.1016/j.yjmcc.2011.04.016
349. Glukhov, A. V.; Fedorov, V. V.; Lou, Q.; Ravikumar, V. K.; Kalish, P. W.; Schuessler, R. B.; Moazami, N.; Efimov, I. R., Transmural dispersion of repolarization in failing and nonfailing human ventricle. *Circ Res* **2010**, *106* (5), 981-91, DOI: 10.1161/CIRCRESAHA.109.204891
350. Alpert, N. R.; Brosseau, C.; Federico, A.; Krenz, M.; Robbins, J.; Warshaw, D. M., Molecular mechanics of mouse cardiac myosin isoforms. *Am J Physiol Heart Circ Physiol* **2002**, *283* (4), H1446-54, DOI: 10.1152/ajpheart.00274.2002
351. Krenz, M.; Sanbe, A.; Bouyer-Dalloz, F.; Gulick, J.; Klevitsky, R.; Hewett, T. E.; Osinska, H. E.; Lorenz, J. N.; Brosseau, C.; Federico, A.; Alpert, N. R.; Warshaw, D. M.; Perryman, M. B.; Helmke, S. M.; Robbins, J., Analysis of myosin heavy chain functionality in the heart. *J Biol Chem* **2003**, *278* (19), 17466-74, DOI: 10.1074/jbc.M210804200
352. Miyata, S.; Minobe, W.; Bristow, M. R.; Leinwand, L. A., Myosin heavy chain isoform expression in the failing and nonfailing human heart. *Circ Res* **2000**, *86* (4), 386-90, DOI: 10.1161/01.res.86.4.386
353. Cazorla, O.; Freiburg, A.; Helmes, M.; Centner, T.; McNabb, M.; Wu, Y.; Trombitas, K.; Labeit, S.; Granzier, H., Differential expression of cardiac titin isoforms and modulation of cellular stiffness. *Circ Res* **2000**, *86* (1), 59-67, DOI: 10.1161/01.res.86.1.59
354. Nagueh, S. F.; Shah, G.; Wu, Y.; Torre-Amione, G.; King, N. M.; Lahmers, S.; Witt, C. C.; Becker, K.; Labeit, S.; Granzier, H. L., Altered titin expression, myocardial stiffness, and left ventricular function in patients with dilated cardiomyopathy. *Circulation* **2004**, *110* (2), 155-62, DOI: 10.1161/01.CIR.0000135591.37759.AF
355. Opitz, C. A.; Linke, W. A., Plasticity of cardiac titin/connectin in heart development. *J Muscle Res Cell Motil* **2005**, *26* (6-8), 333-42, DOI: 10.1007/s10974-005-9040-7
356. Ayaz-Guner, S.; Zhang, J.; Li, L.; Walker, J. W.; Ge, Y., In vivo phosphorylation site mapping in mouse cardiac troponin I by high resolution top-down electron capture dissociation mass spectrometry: Ser22/23 are the only sites basally phosphorylated. *Biochemistry* **2009**, *48* (34), 8161-70, DOI: 10.1021/bi900739f
357. Taglieri, D. M.; Monasky, M. M.; Knezevic, I.; Sheehan, K. A.; Lei, M.; Wang, X.; Chernoff, J.; Wolska, B. M.; Ke, Y.; Solaro, R. J., Ablation of p21-activated kinase-1 in mice promotes isoproterenol-induced cardiac hypertrophy in association with

activation of Erk1/2 and inhibition of protein phosphatase 2A. *J Mol Cell Cardiol* **2011**, *51* (6), 988-96, DOI: 10.1016/j.yjmcc.2011.09.016

358. van der Velden, J.; Papp, Z.; Boontje, N. M.; Zaremba, R.; de Jong, J. W.; Janssen, P. M.; Hasenfuss, G.; Stienen, G. J., The effect of myosin light chain 2 dephosphorylation on Ca²⁺ -sensitivity of force is enhanced in failing human hearts. *Cardiovasc Res* **2003**, *57* (2), 505-14, DOI: 10.1016/s0008-6363(02)00662-4

359. Piacentino, V., 3rd; Weber, C. R.; Chen, X.; Weisser-Thomas, J.; Margulies, K. B.; Bers, D. M.; Houser, S. R., Cellular basis of abnormal calcium transients of failing human ventricular myocytes. *Circ Res* **2003**, *92* (6), 651-8, DOI: 10.1161/01.RES.0000062469.83985.9B

360. Li, L.; Chu, G.; Kranias, E. G.; Bers, D. M., Cardiac myocyte calcium transport in phospholamban knockout mouse: relaxation and endogenous CaMKII effects. *Am J Physiol* **1998**, *274* (4), H1335-47, DOI: 10.1152/ajpheart.1998.274.4.H1335

361. Bassani, J. W.; Bassani, R. A.; Bers, D. M., Relaxation in rabbit and rat cardiac cells: species-dependent differences in cellular mechanisms. *J Physiol* **1994**, *476* (2), 279-93, DOI: 10.1113/jphysiol.1994.sp020130

362. Goldfracht, I.; Protze, S.; Shiti, A.; Setter, N.; Gruber, A.; Shaheen, N.; Nartiss, Y.; Keller, G.; Gepstein, L., Generating ring-shaped engineered heart tissues from ventricular and atrial human pluripotent stem cell-derived cardiomyocytes. *Nat Commun* **2020**, *11* (1), 75, DOI: 10.1038/s41467-019-13868-x

363. Nguyen, A. H.; Marsh, P.; Schmiess-Heine, L.; Burke, P. J.; Lee, A.; Lee, J.; Cao, H., Cardiac tissue engineering: state-of-the-art methods and outlook. *J Biol Eng* **2019**, *13*, 57, DOI: 10.1186/s13036-019-0185-0

364. Bao, J.; Wang, J.; Yao, Y.; Wang, Y.; Fan, X.; Sun, K.; He, D. S.; Marcus, F. I.; Zhang, S.; Hui, R.; Song, L., Correlation of ventricular arrhythmias with genotype in arrhythmogenic right ventricular cardiomyopathy. *Circ Cardiovasc Genet* **2013**, *6* (6), 552-6, DOI: 10.1161/CIRCGENETICS.113.000122

365. De Bortoli, M.; Postma, A. V.; Poloni, G.; Calore, M.; Minervini, G.; Mazzotti, E.; Rigato, I.; Ebert, M.; Lorenzon, A.; Vazza, G.; Cipriani, A.; Bariani, R.; Perazzolo Marra, M.; Husser, D.; Thiene, G.; Daliento, L.; Corrado, D.; Basso, C.; Tosatto, S. C. E.; Bauce, B.; van Tintelen, J. P.; Rampazzo, A., Whole-Exome Sequencing Identifies Pathogenic Variants in TJP1 Gene Associated With Arrhythmogenic Cardiomyopathy. *Circ Genom Precis Med* **2018**, *11* (10), e002123, DOI: 10.1161/CIRCGEN.118.002123

Appendix A. Chapter 2 Tables

Gene	Protein	Structure or Location	Pathogenic Variants*	ACM Prevalence**	Phenotype	References
<i>PKP2</i>	Plakophilin-2	ID/desmosome	171	23.4–57.6%	RV dominant ACM	[85, 159-160, 164, 175-177]
<i>DSP</i>	Desmoplakin	ID/desmosome	86	1.6–15.7%	RV, LV, and biventricular ACM, DCM, Carvajal syndrome (recessive), palmoplantar keratoderma, additional cutaneous diseases.	[85, 159-160, 164, 175-177]
<i>DSG2</i>	Desmoglein-2	ID/desmosome	50	4.0–20.4%	RV and biventricular ACM	[85, 159-160, 164, 175-177]
<i>DSC2</i>	Desmocollin-2	ID/desmosome	42	1.0–8.3%	RV, LV, and biventricular ACM	[85, 159-160, 164, 175-177]
<i>JUP</i>	Junction plakoglobin (PKG)	ID/desmosome	15	<1–3.0%	RV dominant ACM, Naxos disease (recessive), palmoplantar keratoderma, woolly hair disease	[85, 159, 164, 177]
<i>CTNNA3</i>	α -T-catenin	ID/area composita	2	<2.6% (among ACM cases without common mutation)	RV dominant ACM	[218]
<i>DES</i>	Desmin	Intermediate filaments/cytoskeleton	11	<1–2.2%	RV and biventricular dominant ACM. DCM, HCM, DRM, muscular dystrophy	[177, 219-220, 223]
<i>LMNA</i>	Lamin A/C	Nuclear envelope	16	3.5–3.7%	RV and biventricular dominant ACM. DCM, HCM, muscular dystrophy	[176-177, 229]
<i>PLN</i>	Phospholamban	Sarcoplasmic reticulum	4	2.2–12.4%	RV, LV, and biventricular dominant ACM, DCM	[153, 159-160, 164]
<i>TMEM43</i>	Transmembrane protein 43 (LUMA)	Nuclear envelope/ID	3	<1–2.2%	RV, LV, and biventricular dominant ACM, DCM, muscular dystrophy	[159-160, 164, 177, 364]

Continued

Table 1: A list of all genes linked to ACM/ARVC.

Table 1 Continued

Gene	Protein	Structure or Location	Pathogenic Variants*	ACM Prevalence**	Phenotype	References
<i>TTN</i>	Titin	Sarcomere	10	<1% (18.4% of ACM cases negative for variants in common genes)	RV and biventricular dominant ACM, DCM, HCM, muscular dystrophy	[238-239]
<i>FLNC</i>	Filamin C	Sarcomere/I D		<1% (7.5% of ACM cases negative for variants in common genes)	RV, LV, and biventricular dominant ACM, DCM, restrictive cardiomyopathy	[171, 245, 247]
<i>SCN5A</i>	Sodium channel Na _v 1.5	Cell membrane		<1–1.8%	RV dominant ACM, DCM, HCM, Brugada syndrome, long QT syndrome	[160, 215, 250]
<i>TJP1</i>	Zonula occludens 1 (ZO1)	ID/tight junction		<1% (<5% of ACM cases negative for variants in common genes)	RV, LV, and biventricular dominant ACM	[160, 250, 253, 365]
<i>CDH2</i>	N-Cadherin	ID/adherens junction		<1% (2.7% of ACM cases negative for variants in common genes)	RV and biventricular ACM	[253-255, 365]
<i>ANK2</i>	Ankyrin B (AnkB)	Z-lines/T-tubules		Unknown	RV dominant ACM, long QT-syndrome, atrial Fibrillation, ankyrin-B syndrome	[109, 254-255]

Table provides information of the localization of each gene product in the cell, along with the count of ACM linked variants and associated phenotype. *Variant count determined by those listed within the ARVC database [113, 173]. **Prevalence calculated by the percentage of ACM cases with an identified mutation in the gene of interest vs. total ACM cases). Abbreviations: RV, right ventricle; LV, left ventricle; ACM, arrhythmogenic cardiomyopathy; ARVC, arrhythmogenic right ventricular cardiomyopathy; DCM, dilated cardiomyopathy; HCM, hypertrophic cardiomyopathy; DRM, desmin related myopathy.

Appendix B. Chapter 3 Tables

Sex	Genotype	IVSd (cm)	LVIDd (cm)	EDV (mL)	LVPWd (cm)	IVSs (cm)	LVIDs (cm)	ESV (mL)	EF%	FS%	LVPWs (cm)
Male	Control	0.04	0.41	0.17	0.05	0.05	0.3	0.07	56.75	25.31	0.07
Male	Control	0.05	0.39	0.15	0.04	0.07	0.28	0.06	60.69	27.71	0.07
Male	Control	0.05	0.35	0.11	0.06	0.06	0.23	0.03	70.75	34.62	0.07
Male	Control	0.04	0.39	0.15	0.06	0.05	0.29	0.06	58.10	26.09	0.06
Male	Control	0.05	0.37	0.13	0.06	0.06	0.28	0.06	57.47	25.68	0.07
Male	Control	0.04	0.42	0.18	0.05	0.05	0.29	0.06	65.82	31.17	0.07
Male	Control	0.04	0.42	0.19	0.05	0.06	0.31	0.08	57.84	26.00	0.06
Female	Control	0.04	0.34	0.1	0.06	0.05	0.26	0.05	53.89	23.50	0.09
Female	Control	0.03	0.34	0.1	0.05	0.05	0.25	0.04	59.76	27.00	0.06
Female	Control	0.04	0.36	0.12	0.05	0.05	0.25	0.04	67.01	31.87	0.06
Female	Control	0.04	0.35	0.11	0.05	0.06	0.23	0.03	70.53	34.45	0.07
Female	Control	0.05	0.35	0.11	0.06	0.06	0.27	0.05	53.51	23.30	0.07
Female	Control	0.04	0.36	0.12	0.05	0.05	0.27	0.05	57.56	25.70	0.06
Female	Control	0.05	0.38	0.14	0.06	0.08	0.25	0.04	68.56	33.04	0.09
	Mean ± SEM	0.0429 ± 0.00163	0.374 ± 0.00760	0.134 ± 0.00796	0.0536 ± 0.00169	0.0571 ± 0.00244	0.269 ± 0.00662	0.0514 ± 0.00390	61.30 ± 1.61	28.25 ± 1.06	0.0693 ± 0.00267
Male	R451G+	0.05	0.42	0.19	0.06	0.07	0.3	0.07	63.49	29.60	0.07
Male	R451G+	0.04	0.39	0.15	0.05	0.06	0.25	0.04	72.31	35.93	0.07
Male	R451G+	0.05	0.42	0.18	0.06	0.06	0.33	0.09	50.53	21.77	0.09
Male	R451G+	0.04	0.39	0.15	0.06	0.05	0.3	0.07	53.49	23.38	0.07
Male	R451G+	0.04	0.35	0.11	0.06	0.05	0.25	0.04	63.04	29.13	0.09
Male	R451G+	0.05	0.36	0.12	0.05	0.06	0.25	0.04	63.89	29.72	0.08
Male	R451G+	0.04	0.35	0.11	0.06	0.06	0.25	0.04	61.33	28.02	0.07
Male	R451G+	0.04	0.39	0.15	0.06	0.05	0.28	0.06	60.98	27.90	0.08
Male	R451G+	0.03	0.37	0.13	0.06	0.06	0.28	0.06	57.11	25.45	0.08
Male	R451G+	0.04	0.4	0.16	0.06	0.05	0.29	0.06	59.05	26.69	0.08
Female	R451G+	0.03	0.37	0.13	0.07	0.06	0.28	0.06	55.78	24.66	0.08
Female	R451G+	0.04	0.39	0.14	0.05	0.05	0.3	0.07	53.28	23.25	0.05
Female	R451G+	0.03	0.37	0.13	0.04	0.05	0.26	0.04	66.04	31.22	0.06

Continued

Table 2: Full list of echocardiographic findings from *Dsp*^{R451G/+} mice and control littermates.

Table 2 Continued

Sex	Genotype	IVSd (cm)	LVIDd (cm)	EDV (mL)	LVPWd (cm)	IVSs (cm)	LVIDs (cm)	ESV (mL)	EF%	FS%	LVPWs (cm)
Female	R451G+	0.04	0.37	0.13	0.06	0.05	0.26	0.04	65.80	31.05	0.08
Female	R451G+	0.04	0.38	0.13	0.05	0.05	0.29	0.06	54.22	23.77	0.06
Female	R451G+	0.04	0.36	0.12	0.05	0.05	0.27	0.05	57.56	25.70	0.06
Female	R451G+	0.03	0.39	0.15	0.05	0.07	0.27	0.05	65.70	31.03	0.07
	Mean ± SEM	0.0394 ± 0.00160	0.381 ± 0.00511	0.140 ± 0.00542	0.0559 ± 0.00173	0.0559 ± 0.00173	0.277 ± 0.00554	0.0553 ± 0.00355	60.21 ± 1.40	27.55 ± 0.900	0.0729 ± 0.00268
	p-value	0.145	0.437	0.547	0.353	0.669	0.330	0.470	0.612	0.616	0.346

Sex	Genotype	RR Interval (s)	Heart Rate (BPM)	PR Interval (s)	P Duration (s)	QRS Interval (s)	QT Interval (s)	QTc (s)	Tpeak Tend Interval (s)
Male	Control	0.0841	715.1	0.0311	0.00830	0.00996	0.0197	0.0215	0.00790
Male	Control	0.105	573.4	0.0316	0.0103	0.0117	0.0202	0.0197	0.00595
Male	Control	0.101	601.8	0.0320	0.00953	0.0108	0.0210	0.0209	0.00815
Male	Control	0.0871	691.7	0.0315	0.00940	0.0110	0.0220	0.0236	0.00990
Female	Control	0.0871	690.0	0.0320	0.00843	0.0112	0.0213	0.0229	0.00675
Female	Control	0.0881	683.8	0.0340	0.00880	0.00987	0.0195	0.0208	0.00664
Female	Control	0.0834	720.5	0.0336	0.00940	0.00942	0.0194	0.0213	0.00872
Female	Control	0.0813	738.3	0.0329	0.00940	0.00998	0.0208	0.0231	0.00682
	Mean ± SEM	0.0896 ± 0.00305	676.8 ± 20.7	0.0323 ± 0.000376	0.00919 ± 0.000229	0.0105 ± 0.000285	0.0205 ± 0.000334	0.0217 ± 0.000473	0.00760 ± 0.000461
Male	R451G+	0.0852	705.7	0.0326	0.0103	0.0101	0.0215	0.0234	0.00972
Male	R451G+	0.0952	635.4	0.0325	0.00848	0.0117	0.0234	0.0240	0.0105
Male	R451G+	0.103	587.4	0.0319	0.00825	0.0117	0.0223	0.0220	0.00834
Male	R451G+	0.0923	655.3	0.0334	0.00868	0.0115	0.0214	0.0223	0.00819
Female	R451G+	0.0836	719.6	0.0327	0.00988	0.0097	0.0208	0.0228	0.00630
Female	R451G+	0.0874	688.5	0.0309	0.00889	0.0098	0.0235	0.0252	0.01173
Female	R451G+	0.0876	688.3	0.0330	0.00876	0.0089	0.0199	0.0213	0.00988
	Mean± SEM	0.0905 ± 0.00251	668.6 ± 17.3	0.0324± 0.000302	0.00903 ± 0.000285	0.0105 ± 0.000428	0.0218 ± 0.000499	0.0230 ± 0.000493	0.00924 ± 0.000674
	p-value	0.829	0.769	0.859	0.672	0.947	*0.0429	0.0914	0.0609

Table 3: ECG findings from conscious mice without anesthetic or catecholaminergic stimulation.

Appendix C. Chapter 4 Tables

DSP Variants	Pathogenicity	Distance (Å) from calpain target site (Residue 448)
Q271K	Unknown	47.5
W285G	Unknown	27
S299R	Pathogenic	3.7
I305F	Unknown	8.6
R315C	Unknown	21.7
N375I	Pathogenic	5.2
L392P	Unknown	24.4
I399M	Unknown	34.8
K401N	Unknown	38.6
N408K	Unknown	54.1
E422K	Pathogenic	40.8
S442F	Pathogenic	12.4
I445V	Pathogenic	7.6
K449T	Unknown	2.5
R451G	Pathogenic	3.5
N458Y	Pathogenic	15.4
K470E	Pathogenic	23.4
Y494F	Unknown	16.1
S507F	Pathogenic	10.5
L547R	Unknown	51.7

Table 4: DSP variant distance from calpain target site

		Wildtype		Q271K		R315C		L392P		I399M		K401N		N408K		E422K	
Position	AA	CC	GPS	CC	GPS	CC	GPS	CC	GPS	CC	GPS	CC	GPS	CC	GPS	CC	GPS
273	Q		0.791		0.685		0.791		0.791		0.791		0.791		0.791		0.791
277	Q		0.630		0.630		0.630		0.630		0.630		0.630		0.630		0.630
280	S		0.715		0.606		0.715		0.715		0.715		0.715		0.715		0.715
315	R		0.693		0.693		0.427		0.693		0.693		0.693		0.693		0.693
316	M		0.658		0.658		0.541		0.658		0.658		0.658		0.658		0.658
323	E		0.622		0.622		0.356		0.622		0.622		0.622		0.622		0.622
327	N		0.606		0.606		0.606		0.606		0.606		0.606		0.606		0.606
330	K		0.954		0.954		0.954		0.954		0.954		0.954		0.954		0.954
338	L		0.565		0.565		0.565		0.565		0.565		0.565		0.565		0.565
339	N	18.24	0.717	18.24	0.717	18.24	0.717	18.24	0.717	18.24	0.717	18.24	0.717	18.24	0.717	18.24	0.717
389	E		0.601		0.601		0.601	17.87	0.935		0.601		0.601		0.601		0.601
393	K		0.622		0.622		0.622		0.310		0.622		0.622		0.622		0.622
394	G								0.568								
400	R	15.27		15.27		15.27		15.27		14.86		14.59		15.27		15.27	
401	K	15.32		15.32		15.32		15.32		14.59		13.13		16.11		15.32	
422	E		0.745		0.745		0.745		0.745		0.745		0.745		0.745		0.886
429	L																0.568
430	E		0.584		0.584		0.584		0.584		0.584		0.584		0.584		0.671
432	K		0.709		0.709		0.709		0.709		0.709		0.709		0.709		0.709
439	V		0.880		0.880		0.880		0.880		0.880		0.880		0.880		0.880
440	N		0.660		0.660		0.660		0.660		0.660		0.660		0.660		0.660
441	K	16.05		16.05		16.05		16.05		16.05		16.05		16.05		16.05	
447	Q	17.60	0.565	17.60	0.565	17.60	0.565	17.60	0.565	17.60	0.565	17.60	0.565	17.60	0.565	17.60	0.565
448	L		0.568		0.568		0.568		0.568		0.568		0.568		0.568		0.568
449	K	15.59	0.774	15.59	0.774	15.59	0.774	15.59	0.774	15.59	0.774	15.59	0.774	15.59	0.774	15.59	0.774
450	P	16.15		16.15		16.15		16.15		16.15		16.15		16.15		16.15	
455	Y	15	0.595	15	0.595	15	0.595	15	0.595	15	0.595	15	0.595	15	0.595	15	0.595
456	R		0.573		0.573		0.573		0.573		0.573		0.573		0.573		0.573
490	R	17.29		17.29		17.29		17.29		17.29		17.29		17.29		17.29	
495	V	17.11		17.11		17.11		17.11		17.11		17.11		17.11		17.11	
503	M	15.22		15.22		15.22		15.22		15.22		15.22		15.22		15.22	
509	G	15.69		15.69		15.69		15.69		15.69		15.69		15.69		15.69	
510	L	17.12		17.12		17.12		17.12		17.12		17.12		17.12		17.12	
511	I	21.25		21.25		21.25		21.25		21.25		21.25		21.25		21.25	
512	I	15.68		15.68		15.68		15.68		15.68		15.68		15.68		15.68	
547	L	15.69		15.69		15.69		15.69		15.69		15.69		15.69		15.69	

Table 5: Calpain targeting prediction values for each pathogenic and UP DSP variants.

Continued

Table 5 Continued

Position	AA	S442F		I445V		K449T		R451G		N458Y		Y494F		S507F		L547R	
		CC	GPS														
273	Q		0.791		0.791		0.791		0.791		0.791		0.791		0.791		0.791
277	Q		0.630		0.630		0.630		0.630		0.630		0.630		0.630		0.630
280	S		0.715		0.715		0.715		0.715		0.715		0.715		0.715		0.715
315	R		0.693		0.693		0.693		0.693		0.693		0.693		0.693		0.693
316	M		0.658		0.658		0.658		0.658		0.658		0.658		0.658		0.658
323	E		0.622		0.622		0.622		0.622		0.622		0.622		0.622		0.622
327	N		0.606		0.606		0.606		0.606		0.606		0.606		0.606		0.606
330	K		0.954		0.954		0.954		0.954		0.954		0.954		0.954		0.954
338	L		0.565		0.565		0.565		0.565		0.565		0.565		0.565		0.565
339	N	18.24	0.717	18.24	0.717	18.24	0.717	18.24	0.717	18.24	0.717	18.24	0.717	18.24	0.717	18.24	0.717
389	E		0.601		0.601		0.601		0.601		0.601		0.601		0.601		0.601
393	K		0.622		0.622		0.622		0.622		0.622		0.622		0.622		0.622
394	G																
400	R	15.27		15.27		15.27		15.27		15.27		15.27		15.27		15.27	
401	K	15.32		15.32		15.32		15.32		15.32		15.32		15.32		15.32	
422	E		0.745		0.745		0.745		0.745		0.745		0.745		0.745		0.745
429	L																
430	E		0.584		0.584		0.584		0.584		0.584		0.584		0.584		0.584
432	K		0.709		0.709		0.709		0.709		0.709		0.709		0.709		0.709
439	V		0.880		0.880		0.880		0.880		0.880		0.880		0.880		0.880
440	N		0.660		0.660		0.660		0.660		0.660		0.660		0.660		0.660
441	K	16.05		16.05		16.05		16.05		16.05		16.05		16.05		16.05	
447	Q	17.60	0.424	18.04	0.625	16.86	0.598	18.3	0.677	17.60	0.565	17.60	0.565	17.60	0.565	17.60	0.565
448	L		0.315		0.617		0.582		0.453		0.568		0.568		0.568		0.568
449	K	15.59	0.609	15.59	0.815	14.61	0.821	16.47	0.747	15.59	0.774	15.59	0.774	15.59	0.774	15.59	0.774
450	P	16.15		16.15	0.543	18.39	0.611	15.02		16.15		16.15		16.15		16.15	
455	Y	15	0.595	15	0.595	15	0.674	15	0.484	14.95	0.508	15	0.595	15	0.595	15	0.595
456	R		0.573		0.573		0.530		0.443		0.440		0.573		0.573		0.573
490	R	17.29		17.29		17.29		17.29		17.29		18.08		17.29		17.29	
495	V	17.11		17.11		17.11		17.11		17.11		17.04		17.11		17.11	
503	M	15.22		15.22		15.22		15.22		15.22		15.22		15.53		15.22	
509	G	15.69		15.69		15.69		15.69		15.69		15.69		14.32		15.69	
510	L	17.12		17.12		17.12		17.12		17.12		17.12		16.15		17.12	
511	I	21.25		21.25		21.25		21.25		21.25		21.25		21.25		21.25	
512	I	15.68		15.68		15.68		15.68		15.68		15.68		15.68		15.68	
547	L	15.69		15.69		15.69		15.69		15.69		15.69		15.69		17.64	

Continued

CALPCLEAV (CC) and GPS-CCD 1.0 software prediction of DSP residues 270-550. Threshold of 15 for CC and 0.537 for GPS used to determine likely target sites. Values smaller and larger than wild type are indicated in blue and red respectively